

https://dspace.org/

Design of a depot formulation for disulfiram

Mia, Fatema

2016
http://hdl.handle.net/10539/23145

Downloaded from a DSpace repository. https://dspace.org/

DESIGN OF A DEPOT FORMULATION FOR DISULFIRAM

FATEMA MIA

A dissertation submitted to the Faculty of Health Sciences, University of the Witwatersrand, in fulfilment of the requirements for the degree of Master of Pharmacy

Supervisor:

Professor Viness Pillay

Department of Pharmacy and Pharmacology, Faculty of Health Sciences, University of the Witwatersrand, South Africa

Co-Supervisors:

Professor Yahya E. Choonara

Professor Lisa C. du Toit

Mr Pradeep Kumar

Department of Pharmacy and Pharmacology, Faculty of Health Sciences, University of the Witwatersrand, South Africa

Johannesburg, 2016

DECLARATION

I, Fatema Mia, declare that this Dissertation is my own, unaided work. It is being submitted for the degree of Master of Pharmacy in the Faculty of Health Sciences at the University of the Witwatersrand, Johannesburg, South Africa. It has not been submitted before for any degree or examination at this or any other University.

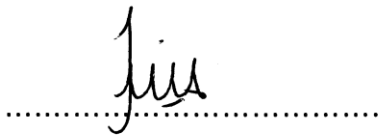

Signed this 21st day of December 2016

RESEARCH OUTPUTS

1. Review Paper

A Review of the Trends and Advances in Drug Delivery Technologies for the Treatment of Substance Abuse and Drug Addiction. Fatema Mia, Yahya E. Choonara, Charu Tyagi, Lomas Kumar Tomar, Lisa C. du Toit, Pradeep Kumar and Viness Pillay. (abstract in Appendix A). *To be submitted to Journal.*

2. Research Papers

2.1 Design fabrication, statistical optimization and in vitro characterization of disulfiram-loaded TPGS nanomicelles. Fatema Mia, Yahya E. Choonara, Lisa C. du Toit, Pradeep Kumar and Viness Pillay. (abstract in Appendix B). *To be submitted to Journal.*

2.2 The influence of the degree of gellan gum acetylation on the rheological properties of Pluronic F127-gellan gum gels. Fatema Mia, Yahya E. Choonara, Pradeep Kumar, Lisa C. du Toit, Pierre P.D. Kondiah, Viness Pillay. (abstract in Appendix C). *To be submitted to Journal.*

2.3 A disulfiram-loaded nano-enclatherated-gel-composite for the treatment of alcohol abuse and addiction: physicochemical characterization and *in vitro, in vivo* studies. Fatema Mia, Yahya E. Choonara, Lisa C. du Toit, Pradeep Kumar and Viness Pillay. (abstract in Appendix D). *To be submitted to Journal.*

DEDICATION

This dissertation is dedicated to my three greatest gifts from the Almighty; my dearest parents, Salim and Salma Mia and my beloved husband, Adnaan Nana. You are my life, my love, my happiness. I will cherish you forever.

ACKNOWLEDGEMENTS

It brings me great pleasure to acknowledge the countless number of individuals whose invaluable contribution assisted in the completion of this study.

All praise and gratitude is due, first and foremost, to the Almighty for His infinite mercy, blessings, and guidance throughout this journey.

I would like to express my sincere gratitude to my supervisor, Professor Viness Pillay, for the opportunity to complete my masters degree under his experienced guidance. Being a part of an esteemed academic research platform such as the Wits Advanced Drug Delivery Platform has been a great honour. His expertise in Pharmaceutical Sciences and Drug Delivery combined with his superb leadership and financial support has been a huge contribution to the completion of this degree. I would like to thank him for imparting valuable knowledge and skills to me which will hold great value in pursuing my future goals.

Thank you to Associate Professor Yahya Choonara for his valuable input throughout this research study. His critical analysis was of great benefit in the completion of this dissertation.

My deepest gratitude goes to Associate Professor Lisa du Toit for her immeasurable kindness, expertise and assistance. Thank you for all the time and effort you invested in my work, without which I would not have succeeded. You have been a beacon of hope and a guiding star throughout this voyage. I wish you the very best for your future as you are most deserving of it.

A tremendous contributor to the completion of this work is Mr Pradeep Kumar. He is truly a genius amongst us, one I am very fortunate to have had the pleasure of meeting. His humble nature, passion and devotion to science, and unwavering willingness to help cannot go unrecognized. Thank you for the priceless knowledge and precious time you have shared with me. You are an indispensable asset to the academic world and I have no doubt that you are destined for greatness.

I would like to extend my heartfelt appreciation to my wonderful parents, Salim and Salma Mia. Thank you for all the sacrifices you have made and for providing me with the opportunities which allowed me to reach this stage. It is through your encouragement, support, and prayers that I am here today. Your unconditional love, patience and belief in me have been an infinite source of inspiration always. Thank you for teaching me that with hard

work and honesty, anything is possible. I know that this research took priority over family many a time and I am filled with appreciation at your understanding and support of this. I am truly honoured to share this accomplishment with you and I hope I have made you proud. With parents like you, the world is my oyster.

I am eternally indebted to my best friend and darling husband, Adnaan Nana, for his inexhaustible patience and encouragement. From the bottom of my heart, I thank you for having faith in me when I had none. Your confidence in my ability to complete this pulled me through the many times when I felt that the end would never come. You have been my greatest comfort, a shoulder to cry on and a pillar of strength. Thank you for lifting my spirits and motivating me to persevere. I would not have completed this odyssey without you. I look forward to sharing with you the many adventures that lay ahead.

I am thankful to my family; my brothers, Ebrahim and Muhammad, and my sisters-in-law, Saajida and Farhanah, for the moral support and words of encouragement over the years. I am truly fortunate to be blessed with four such amazing siblings. Thank you for all your help, it means the world to me.

A special thank you to my two little bears, Yusuf and Haaniya, for bringing so much of joy to my life and for being my rays of sunshine on the gloomy days.

I would like to wholeheartedly say thank you to my new family; my mother-in-law, Zohra Minty, and siblings-in-law, Zeenat, Muhammad Zain and Shahistha, for all their support. You have given me a warm welcome into your home and have made it so easy for me to adjust and settle into my new life. Your kindness has played a vital role in the completion of this degree.

I would also like to express my gratitude to the University of the Witwatersrand and the staff of the Department of Pharmacy and Pharmacology, Professor Paul Danckwerts, Mrs Neelaveni Padayachee, Ms Shirona Naidoo and Ms Nompumelelo Damane. To Mr David Bayever, thank you very much for all the advice and motivation; it is tremendously appreciated.

To the many post-docs who have kindly assisted and encouraged me over the years: Dr Lomas Kumar Tomar, Dr Charu Tyagi, Dr Divya Bijukumar, Dr Thashree Marimuthu, Dr Dharmesh Chejara, Dr Ravindra Badhe and Dr Mostafa Mabrouk, I extend my deepest thanks.

My sincere appreciation goes to our excellent lab technicians, Mr Kleinbooi Mohlabi and Mr Bafana Temba as well as Professor Sandy van Vuuren and Phumzile Madondo for their immense help. Thank you also to Mr Sello Ramarumo and Ms Pride Mothobi.

Many thanks to the Animal Ethics Screening Committee and Professor Kennedy Erlwanger for the ethics approval. My appreciation also extends to the staff of the Central Animal Services at the University of the Witwatersrand, Ms Kershnee Chetty, Sr. Amelia Rammekwa, Ms Lorraine Setimo, Sr. Mary-Ann Costello, Mr Patrick Selahle, Mr Nico Douths and others for their expert advice and *in vivo* assistance.

Thank you to Mr Deran Reddy, Mr Jacques Gerber and Ms Pamela Sharp of the MMU for their help.

Many genuine thanks to my friends and colleagues, both past and present; Bibi Fatima Choonara, Margaret Siyawamwaya, Zikhona Hayiyana, Karmani Murugan, Poornima Ramburrun, Olufemi Akilo, Felix Mashingaidze, Famida Ghulam-Hoosain, Naeema Mayet, Pierre Kondiah, Mduduzi Sithole, Pakama Mahlumba, Simphiwe Mavuso, Samson Adayemi, Gretta Mbitsi-Ibouily, Miles Braithwaite, Angus Hibbins, Mpho Ngoepe, Steven Mufamadi, Ahmed Seedat, Derusha Frank, Kealeboga Mokolobate, Az-Zamakshariy Zardad, Teboho Kgesa, Martina Manyikana, Mandla Mcunu, Thiresen Govender, Ameena Wadee, Rubina Shaikh, Yusuf Dawood, Ane van der Merwe, Tasneem Suleman, Zelna Hubsch, Stephanie de Rapper, Unathi Mabona and Gillian Mahumane, for their help and friendship.

My sincere gratitude goes to Sunaina Indermun and Mershen Govender for their invaluable friendship. Your beneficial knowledge and helpful nature were of immense benefit during this study. Words cannot adequately capture my appreciation to both of you. May our friendship see many more years.

To the new friends I made during my postgraduate years; Tasneem Rajan, Dimitris Georgiou, Raeesa Moosa, Khadija Rhoda, Khuphukile Madida, Zamanzima Mazibuko, Jonathan Pantshwa and Nonhlanhla Masina, thank you for the years of support, encouragement and most importantly, laughter.

During my postgraduate studies I have had the privilege of meeting my closest friend Latavia Singh. You have been there for me through all my triumphs and trials. The support you have afforded me throughout the last few years has been instrumental in my completion of this project. I can't think of anyone else I would have wanted to share this rollercoaster

experience with. Your pure, kind heart and gentle, caring nature will undoubtedly take you far in life.

Thank you to the NRF, PSSA and Department of Education for lightening the financial burden and making this opportunity possible. However, opinions expressed are those of the author and are not necessarily to be attributed to the NRF, PSSA or Department of Education.

This list is wholly incomplete. There have been countless other individuals who have aided in some or other special manner. Thank you to everyone that I may have unintentionally left out.

"Acquire knowledge: it enables its possessor to distinguish right from wrong;
it lights the way to heaven; it is our friend in the desert, our society in solitude,
our companion when friendless; it guides us to happiness; it sustains us in misery;
it is an ornament among friends and an armour against enemies."

- Prophet Muhammad (Peace Be Upon Him) -

ABSTRACT

Drug addiction and abuse, specifically relating to alcohol, is a globally calamitous mental illness. An important facet of treating this destructive health issue is pharmacological intervention. The current treatment options and their limitations were reviewed as well as the advances that have been made in drug delivery technologies for combating addiction and abuse. The current treatment of addiction, and alcohol abuse in particular, is a large scale concern. Whilst treatment is available in the form of disulfiram, naltrexone and acamprosate; these too possess many short-comings. The greatest of which is poor compliance which results in relapse. This can be successfully averted by the utilisation of a feasible depot system to deliver the medication. Incorporation of disulfiram, an FDA-approved active with promising clinical potential, into a modified depot system comprising a dual delivery system yields a prospective solution to the drawbacks of current treatment regimes. The dual system is made up of nanomicelles dispersed within a thermosensitive gel. Immediate and sustained release is controlled by free disulfiram released into the gel and then the tissue and encapsulated disulfiram released from the nanomicelles into the gel and then the tissue, respectively. The thermosensitive gel is a carrier for the disulfiram-loaded nanomicelles and the free disulfiram. It also serves as a vehicle which allows ease of administration by maintaining a liquid state prior to intramuscular injection and thereafter solidifying into a solid gel-depot inside the muscle tissue. Polymers were selected based on the suitability to the desired outcome as well as compatibility with disulfiram. d-α-tocopheryl polyethylene glycol 1000 succinate (TPGS) was used for nanomicelle formulation whilst Pluronic F127 (PF127) and high acyl gellan gum (HAGG) was chosen for the thermosensitive gel. A Face-Centred Central Composite Design was utilised for statistical optimization of the nanomicelles. The design consisted of two variables, 1) stirring time of the formulation (hours) and 2) the amount of TPGS used (mg), both of which were crucial to the success of the formation of the nanomicelles. Response surface and contour plots were generated for the variable effects on selected responses (i.e. drug entrapment efficiency, drug loading efficiency and drug release). Statistical optimization computed a single optimized formulation composed of 500mg TPGS and 1 hour of stirring. The optimized nanomicelles were then incorporated into the rheologically selected PF127-HAGG gel. The final nano-enclatherated-gel-composite (NEGC) underwent *in vitro* release testing, physicochemical characterization and physicomechanical characterization. Results displayed sustained release over 28 days with positive physicochemical and physicomechanical outcomes. Ex vivo results confirmed the release of disulfiram from the NEGC into the tissue as well as established the safety of the system through myotoxicity analysis. Administration of the NEGC to the Sprague-Dawley rat model determined the effectiveness and safety of the delivery system *in vivo*. Ultra Performance Liquid Chromatography was carried out on plasma to ascertain the level of disulfiram in the plasma. The NEGC yielded a maximum plasma level of 27.33μg/mL which is above values previously reported. Ultrasound imaging confirmed the presence of the NEGC within the muscle over 28 days. Myotoxicity studies disclosed an increase in Creatine Kinase after administration with a return to normal levels within 24 hours indicating that permanent muscle damage did not occur. Histopathological lesions were symptomatic of injury and repair of tissue due to intramuscular needle insertion and the decline in lesion severity is indicative of mild, acute toxicity and repairable injury. The results obtained in this study revealed the therapeutic potential of the NEGC to treat not only alcohol addiction but perhaps other conditions as well due to the versatility of this dual delivery system.

ANIMAL ETHICS DECLARATION

I, Fatema Mia, hereby confirm that the study entitled “Design Of A Depot Formulation For Disulfiram” received approval by the Animal Ethics Screening Committee of the University of the Witwatersrand. Ethics Clearance Number 2014/43/C (Appendix E).

TABLE OF CONTENTS

DECLARATION i
RESEARCH OUTPUTS ii
DEDICATION iii
ACKNOWLEDGEMENTS iv
ABSTRACT viii
ANIMAL ETHICS DECLARATION ix
TABLE OF CONTENTS x
LIST OF COMMONLY-USED ABBREVIATIONS xxii
LIST OF EQUATIONS xxiv
LIST OF FIGURES xxv
LIST OF TABLES xxxi

CHAPTER 1

INTRODUCTION

1.1 Background to this Study 1

1.2 Rationale and Motivation for the Study 3

1.3 Aims and Objectives 5

1.4 Novelty of the Study 5

1.5 A Nano-Enclatherated-Gel-Composite System: Concept and Outline 5

1.6 Overview of this Dissertation 8

CHAPTER 2

A REVIEW OF THE TRENDS AND ADVANCES IN DRUG DELIVERY TECHNOLOGIES FOR THE TREATMENT OF SUBSTANCE ABUSE AND DRUG ADDICTION

2.1 Introduction 10
2.2 Drugs of Abuse and Their Existing Treatments 11
2.2.1 Alcohol 13
2.2.2 Nicotine 13
2.2.3 Opioids 14
2.2.4 Stimulants 14
2.3 Overcoming Addiction Through Formulation Manipulation 15
2.4 Multiparticulate Drug Delivery Technology 16
2.4.1 Microparticulates 17
2.4.2 Nanoparticulates 18
2.4.2.1 Polymeric nanoparticles 18
2.4.2.2 Polymer-drug nanoconjugates 19
2.4.2.3 Liposomes 19
2.4.2.4 Solid lipid nanoparticles and nano-structured lipid carriers 19
2.4.2.5 Drug nanocrystals and nanosuspensions 20
2.4.2.6 Nanogels 20
2.5 Preparation of Multiparticulate Systems 22
2.6 Comparison of Microsystems and Nanosystems 23
2.7 Challenges of Multiparticulate Systems 24
2.8 Selection of Polymers for Multiparticulate Systems 25
2.9 Drug Delivery to the Brain 27
2.10 Reformulation of Anti-Addiction Drugs into Multiparticulates 28
2.10.1 Disulfiram 28
2.10.2 Naltrexone 29
2.10.3 Nicotine Replacement Therapy 30
2.10.4 Bupropion 31
2.10.5 Varenicline 31

2.10.6 Methadone 31
2.10.7 Buprenorphine 32
2.10.8 Naloxone 33
2.11 Other Potential Treatment Options for Drug Addiction 35
2.11.1 Glial Cell Line-Derived Neurotrophic Factor 35
2.11.2 Topiramate Microparticles and Nanoparticles 36
2.11.3 Risperidone Microspheres 36
2.11.4 Immunopharmacology 36
2.11.5 Gene Silencing Nanotechnology 37
2.12 Concluding Remarks 38

CHAPTER 3

DESIGN FABRICATION, OPTIMIZATION AND *IN VITRO* CHARACTERIZATION OF DISULFIRAM-LOADED d-α-TOCOPHERYL POLYETHYLENE GLYCOL 1000 SUCCINATE NANOMICELLES

3.1 Introduction 39

3.2 Materials and Methods 42

3.2.1 Materials 42

3.2.2 Design criteria and considerations for the disulfiram-loaded TPGS nanomicelles 42

3.2.3 Construction of a randomized Central Composite Design for the optimization of the TPGS nanomicelles 42

3.2.4 Fabrication of disulfiram-loaded self-assembled TPGS nanomicelles utilising the solvent casting method 43

3.2.5 Particle size determination by Dynamic Light Scattering (DLS) 44

3.2.6 Preparation of simulated body fluid 44

3.2.7 Acetone-buffer solution preparation..... 45

3.2.8 Drug entrapment efficiency and drug loading capacity of the nanomicelles 45

3.2.9 Calibration curve construction for the quantification of disulfiram 46

3.2.10 *In vitro* dissolution studies of disulfiram-loaded nanomicelles 46

3.2.11 Statistical analysis of the Face-Centred Central Composite Design 46

3.2.12 Constraint optimization of formulation responses 46

3.2.13 Preparation of the optimized nanomicelles 47

3.2.14 Experimental responses of the optimized nanomicelles 47

3.2.15 Characterization of the optimal TPGS-nanomicelle system 47

3.2.15.1 Morphological characterization of nanomicelles using Transmission Electron Microscopy (TEM) 47

3.2.15.2 Determination of the Critical Micelle Concentration (CMC) of the TPGS nanomicelles 47

3.2.15.3 Redispersability studies to determine the effect of lyophilisation on the nanomicelles 48

3.2.15.4 Characterization of the molecular vibrational transitions using Fourier Transform Infrared Spectroscopy 48

3.2.15.5 Characterization of thermal transitions using Differential Scanning Calorimetry 48

3.2.15.6 Determination of the degree of crystallinity using X-Ray Diffraction analysis .. 49

3.3 Results and Discussion 49

3.3.1 Assessment of particle size using DLS 49

3.3.2 Morphological characterization of the TPGS nanomicelles 50

3.3.3 A calibration curve for the quantification of disulfiram 50

3.3.4 Assessment of the drug loading and drug entrapment of the design formulations 51

3.3.5 *In vitro* drug release profiles of design formulations 52

3.3.6 Statistical analysis of the FCCCD 53

3.3.6.1 Residual error plot analysis 53

3.3.6.2 Response surface and contour plot analysis 56

3.3.7 Constraint optimization of formulation responses 59

3.3.8 Experimental responses of the optimized system 60

3.3.9 Analysis of particle size and zeta potential of TPGS nanomicelles 65

3.3.10 Morphological analysis of the TPGS nanomicelles using Transmission Electron Microscopy 68

3.3.11 Confirmation of the Critical Micelle Concentration (CMC) of TPGS nanomicelles... 68

3.3.12 Redispersability of the optimized TPGS nanomicelles 69

3.3.13 Investigation of structural variation via Fourier Transform Infrared spectroscopy analysis 70

3.3.14 Thermal profile analysis of the nanomicelles 72

3.3.15 Analysis of the degree of crystallinity of nanomicelles 74

3.4 Concluding Remarks 76

CHAPTER 4

THE INFLUENCE OF THE DEGREE OF GELLAN GUM ACETYLATION ON THE RHEOLOGICAL PROPERTIES OF PLURONIC F127-GELLAN GUM GELS

4.1 Introduction 77

4.2 Materials and Methods 77

4.2.1 Materials 79

4.2.2 Preparation of the gel systems 80

4.2.3 Rheological analysis of the gel systems 81

4.2.3.1 Amplitude sweep 82

4.2.3.2 Temperature sweep 83

4.2.3.3 Frequency sweep, time sweep and flow analysis 83

4.3 Results and Discussion 84

4.3.1 Temperature sweep 84

4.3.1.1 Effect of PF127 concentration on different concentrations of GG 85

4.3.1.1.1 Effect of PF127 concentration on different concentrations of HAGG 85

4.3.1.1.2 Effect of PF127 concentration on different concentrations of LAGG 88

4.3.1.2 Comparison of temperature sweep data for HAGG and LAGG 90

4.3.1.3 Effect of GG concentration and PF127 concentration on storage modulus (G'), loss modulus (G") and complex viscosity (η)* 97

4.3.2 Frequency sweep 98

4.3.3 Time sweep 101

4.3.4 Flow analysis using rheological models 102

4.3.5 Mechanism of gelation and analysis of trends 105

4.4 Concluding Remarks 107

CHAPTER 5

SYNTHESIS, PHYSICOCHEMICAL AND PHYSICOMECHANICAL CHARACTERIZATION OF NANOMICELLE-ENCLATHERATED-GEL-COMPOSITE

5.1 Introduction 108

5.2 Materials and Methods 109

5.2.1 Materials 109

5.2.2 Amalgamation of the various gel composites 109

5.2.3 Flash freezing of the various gel composites 110

5.2.4 Macroscopic evaluation of the gel 111

5.2.5 *In vitro* drug release of the various gel composites 111

5.2.6 Rheological analysis of the various gel composites 111

5.2.7 Characterization of the molecular vibrational transitions of the various gel composites using Fourier Transform Infrared Spectroscopy 111

5.2.8 Characterization of thermal transitions of the various gel composites using Differential Scanning Calorimetry 111

5.2.9 Determination of the degree of crystallinity of the various gel composites employing X-Ray Diffraction analysis 111

5.2.10 Evaluation of the surface morphology of the gel composites using Scanning Electron Microscopy (SEM) 112

5.3 Results and Discussion 112

5.3.1 Macroscopic examination of the gel 112

5.3.2 *In vitro* drug release from the various drug-loaded gel composites 112

5.3.3 Rheological analysis of the gel composites 114

5.3.4 Investigation of structural variation via Fourier Transform Infrared spectroscopy analysis 116

5.3.5 Thermal profile analysis of the gel polymers and gel composites 118

5.3.6 Analysis of the degree of crystallinity of the gel polymers and gel composites 122

5.3.7 Surface morphology exploration of the various gel composites using Scanning Electron Microscopy (SEM) 126

5.4 Concluding Remarks 128

CHAPTER 6

EX VIVO AND _IN VIVO_ EVALUATION OF THE NANOMICELLE-ENCLATHERATED-GEL-COMPOSITE

6.1 Introduction 129

Part I - *Ex Vivo* Studies 131

6.2 Materials and Methods 131

6.2.1 Materials 131

6.2.2 Preparation of the NEGC 131

6.2.3 Preparation of the rat muscle tissue samples 131

6.2.4 Simulated organ bath 131

6.2.5 *Ex vivo* drug release study 132

6.2.6 *Ex vivo* myotoxicity study 132

6.3 Results and Discussion 133

6.3.1 *Ex vivo* drug release 133

6.3.2 *Ex vivo* myotoxicity 133

Part II - *In Vivo* Studies 134

6.4 Materials and Methods 134

6.4.1 Materials 134

6.4.2 Preparation of *in vivo* formulations 135

6.4.2.1 Preparation of oral disulfiram formulation for comparison group 135

6.4.2.2 Preparation of the test group NEGC and placebo group NEGC for IM injection into the rat 135

6.4.3 Animal ethics clearance 135

6.4.4 Animal husbandry 135

6.4.5 *In vivo* experimental design and procedure 136

6.4.6 Animal welfare and humane endpoints 138

6.4.7 High frequency ultra sound imaging 138

6.4.8 Blood sampling 139

6.4.9 Muscle tissue sampling 139

6.4.10 Quantitative chromatographic determination of drug in plasma and tissue 139

6.4.11 UPLC conditions analysis: solvents, mobile phases and parameter conditions for chromatographic separation 140

6.4.11.1 *Preparation of diluent and calibration standards* 140

6.4.11.2 *Sample preparation utilising liquid-liquid extraction* 140

6.4.11.3 *Validation of the liquid-liquid extraction procedure* 141

6.4.11.4 *Construction of a calibration curve for the quantification of disulfiram in blood plasma* 141

6.4.12 Histomorphological analysis of muscle tissue post-IM injection 141

6.4.13 *In vivo* myotoxicity study 142

6.5 Results and Discussion 142

6.5.1 High frequency ultra sound imaging 142

6.5.2 Validation of the liquid-liquid extraction procedure 146

6.5.3 Elution times of disulfiram and internal standard 147

6.5.4 A calibration curve for the quantification of disulfiram concentration in plasma .. 148

6.5.5 *In vivo* profiles of the comparison group, test group and placebo group 148

6.5.6 *In vivo* myotoxicity 153

6.5.7 Histopathological evaluation of muscle tissue 154

6.6 Concluding Remarks 159

CHAPTER 7

CONCLUSION AND RECOMMENDATIONS

7.1 Conclusion 160

7.2 Recommendations 161

7.2.1 Determination of the DER 161

7.2.2 Overcome the inconsistencies of disulfiram research 162

7.2.3 Pertinence of disulfiram to other diseases 163

7.2.4 Refine *ex vivo* myotoxicity assessment 163

7.2.5 Applicability of alternative animal model 163

7.2.6 Correlation of tissue concentration with plasma concentration 163

REFERENCES AND APPENDICES

REFERENCES

References 164

APPENDICES

Appendix A

Abstract of Review Paper..... 194

Appendix B

Abstract of Research Paper 1 195

Appendix C

Abstract of Research Paper 2 196

Appendix D

Abstract of Research Paper 3 197

Appendix E

Animal Ethics Clearance Certificate 198

LIST OF COMMONLY-USED ABBREVIATIONS

ABS- acetone-buffer solution
AESC- Animal Ethics Screening Committee
ALDH- Aldehyde Dehydrogenase
BBB- Blood-Brain-Barrier
CAS- Central Animal Services
CCD- Central Composite Design
CK- creatine kinase
CMC- Critical Micelle Concentration
CNS- Central Nervous System
DER- Disulfiram Ethanol Reaction
DIMF- Depot Intramuscular Formulation
DLS- Dynamic Light Scattering
DoE- Design of Experiments
DR- drug loading
DSC- Differential Scanning Calorimetry
EE- entrapment efficiency
FCCCD- Face Centred Central Composite Design
FDA- Food and Drug Administration
FTIR- Fourier Transform Infrared Spectroscopy
GG- gellan gum
Gt- gelation time
HAGG- high acyl gellan gum
IM- intramuscular
IS- internal standard
KP- Kairotic Point
LAGG- low acyl gellan gum
LVER- Linear Visco-Elastic Region
NEGC- nano-enclatherated gel composite
PCL- polycaprolactone
PDI- Poly Dispersity Index
PF127- Pluronic F127
PF127-HAGG- Pluronic F127-High Acyl Gellan Gum
PLA- polylactic acid
PLGA- poly (lactic-co-glycolic acid)

RES- Reticulo-Endothelial System

RSD- Relative Standard Deviation

RSM- Response Surface Methodology

SBF- simulated body fluid

SD- standard deviation

SEM- Scanning Electron Microscopy

TEM- Transmission Electron Microscopy

TPGS- d-α-tocopheryl polyethylene glycol 1000 succinate (vitamin E TPGS)

TRP- Thermorigidity Phenomena

UPLC- Ultra Performance Liquid Chromatography

UV - ultraviolet

XRD- X-Ray Diffraction

LIST OF EQUATIONS

Equation 3.1: Polynomial equation 43
Equation 3.2: Percentage entrapment efficiency 45
Equation 3.3: Percentage drug loading 45
Equation 3.4: CMC equation 47
Equation 3.5: Redispersability ratio 48
Equation 3.6: Entrapment efficiency regression equation 54
Equation 3.7: Drug loading regression equation 54
Equation 3.8: Drug release at 2 hours regression equation 54
Equation 3.9: Drug release at 7 days regression equation 54
Equation 4.1: Storage modulus 81
Equation 4.2: Loss modulus 82
Equation 4.3: Viscosity 82
Equation 4.4: Complex viscosity 82
Equation 4.5: Gelation time 83
Equation 4.6: Bingham model 102
Equation 4.7: Casson model 102
Equation 4.8: Cross model 102
Equation 4.9: Herschel-Bulkley model 102
Equation 4.10: Ostwald–de Waele model 102
Equation 6.1: Creatine kinase activity 132
Equation 6.2: Percentage extraction yield 141
Equation 6.3: Percentage relative standard deviation 141

LIST OF FIGURES

Figure 1.1: Componential configuration of the dyadic delivery system: a nano-enclatherated-gel-composite system 7

Figure 2.1: Various positive effects of an innovative drug delivery system 16

Figure 2.2: The difference between microspheres and microcapsules 17

Figure 2.3: The different types of nanosystems..... 21

Figure 2.4: Confocal microscopy image of blank PLGA microspheres prepared with Nile red dye. Reproduced with permission from Checa-Casalengua and co-workers (2011)..... 26

Figure 2.5: Photomicrographs of a) methadone-PLA and b) methadone-PLGA microspheres. Reproduced with permission from Negrin and co-workers (2001) 26

Figure 3.1: Chemical structure of disulfiram 39

Figure 3.2: Chemical structure of TPGS..... 40

Figure 3.3: Transmission electron micrograph of disulfiram-loaded nanomicelles at 50000x magnification (a=F3, b=F7) 50

Figure 3.4: Calibration curve of disulfiram at λ_{262}..... 51

Figure 3.5: Drug loading % for each formulation of the FCCD..... 52

Figure 3.6: Entrapment efficiency % for each formulation of the FCCD..... 52

Figure 3.7: Cumulative disulfiram release from F1-F13 over 28 days..... 53

Figure 3.8: Residual plots for the responses a) drug loading %, b) drug entrapment %, c) drug release % at 2 hours and d) drug release % at 7 days 56

Figure 3.9: Response surface and contour plots illustrating the effects of stirring time (hours) and TPGS amount (mg) on drug loading %..... 57

Figure 3.10: Response surface and contour plots illustrating the effects of stirring time (hours) and TPGS amount (mg) on entrapment efficiency % 58

Figure 3.11: Response surface and contour plots illustrating the effects of stirring time (hours) and TPGS amount (mg) on % drug release at 2 hours..... 59

Figure 3.12: Response surface and contour plots illustrating the effects of stirring time (hours) and TPGS amount (mg) on % drug release at 7 days 59

Figure 3.13: Desirability plots representing the level of TPGS and the stirring time required to synthesize the optimized formulation 60

Figure 3.14: a) *In vitro* drug release from the optimized disulfiram-loaded TPGS nanomicelles over 28 days and b) enlarged inset depicting *in vitro* drug release from the optimized disulfiram-loaded TPGS nanomicelles over the first 24 hours 64

Figure 3.15: Size distribution profile for optimized disulfiram-loaded TPGS nanomicelles. 66

Figure 3.16: Size distribution profile for optimized drug free TPGS nanomicelles..... 66

Figure 3.17: Zeta potential distribution profile for optimized disulfiram-loaded TPGS nanomicelles..... 67

Figure 3.18: Zeta potential distribution profile for optimized drug free TPGS nanomicelles 67

Figure 3.19: Electron micrographs of a) disulfiram-loaded nanomicelles and b) drug free nanomicelles at 50 000x magnification..... 68

Figure 3.20: The determination of the CMC value for TPGS nanomicelles..... 69

Figure 3.21: Comparison of particle size before and after lyophilisation for disulfiram-loaded nanomicelles and drug free nanomicelles (SD ≤ 1.09 in all cases, n=3)..... 70

Figure 3.22: FTIR spectra of a) disulfiram, b) disulfiram-loaded nanomicelles, c) drug-free nanomicelles and d) TPGS 71

Figure 3.23: Thermograms of a) TPGS, b) drug-free nanomicelles, c) disulfiram-loaded nanomicelles and d) pure disulfiram..... 73

Figure 3.24: Diffractograms of a) TPGS, b) disulfiram, c) disulfiram-loaded nanomicelles and d) drug free nanomicelles..... 75

Figure 4.1: Chemical structure of PF127..... 78

Figure 4.2: Chemical structure of a) LAGG and b) HAGG..... 79

Figure 4.3: Typical amplitude sweep curve showing the LVER 83

Figure 4.4: KP values for varying concentrations of PF127 at: a) 0.1% GG, b) 0.2% GG, c) 0.3% GG and d) 0.4% GG 86

Figure 4.5: Schematic illustrating the effect of PF127 concentration with 0.1% HAGG..... 87

Figure 4.6: Schematic illustrating the effect of PF127 concentration with 0.2% HAGG..... 87

Figure 4.7: Schematic illustrating the effect of PF127 concentration with 0.3% HAGG..... 87

Figure 4.8: Schematic illustrating the effect of PF127 concentration with 0.4% HAGG..... 88

Figure 4.9: The effect of concentration of PF127 and HAGG on the KP..... 88

Figure 4.10: Schematic illustrating the effect of PF127 concentration with 0.1% LAGG 89

Figure 4.11: Schematic illustrating the effect of PF127 concentration with 0.2% LAGG 89

Figure 4.12: Schematic illustrating the effect of PF127 concentration with 0.3% LAGG 89

Figure 4.13: Schematic illustrating the effect of PF127 concentration with 0.4% LAGG 90

Figure 4.14: The effect of concentration of PF127 and LAGG on the KP 90

Figure 4.15: Temperature sweeps of H1 - H4 (left) and L1 - L4 (right) 91

Figure 4.16: Temperature sweeps of H5 - H8 (left) and L5 - L8 (right) 92

Figure 4.17: Temperature sweeps of H9 - H12 (left) and L9 - L12 (right)..... 93

Figure 4.18: Temperature sweeps of H13 - H16 (left) and L13 - L16 (right)..... 94

Figure 4.19: Temperature sweeps of H17 - H20 (left) and L17 - L20 (right)..... 95

Figure 4.20: Temperature sweeps of H21 - H24 (left) and L21 - L24 (right)..... 96

Figure 4.21.1: Frequency Sweep of H3 and L3 at 10°C (right HAGG, left LAGG) 98

Figure 4.21.2: Frequency Sweep of H3 and L3 at 36.5°C (right HAGG, left LAGG) 99

Figure 4.22.1: Frequency Sweep of H6 and L6 at 10°C (right HAGG, left LAGG) 99

Figure 4.22.2: Frequency Sweep of H6 and L6 at 36.5°C (right HAGG, left LAGG) 99

Figure 4.23.1: Frequency Sweep of H15 and L15 at 10 °C (right HAGG, left LAGG) ... 99

Figure 4.23.2: Frequency Sweep of H15 and L15 at 36.5 °C (right HAGG, left LAGG)..... 100

Figure 4.24: Mechanical spectra for a) an entanglement network and b) a gel system (Source: adapted from Picout et al., 2003)..... 101

Figure 5.1: Advantages of *in situ* depot systems..... 108

Figure 5.2: Various gel composites formed for further characterization and *in vitro* testing 110

Figure 5.3: PF127-HAGG formulation at 10°C (A), 25°C (B) and 37.5°C (C)..... 112

Figure 5.4: Drug release from various gel composites (SD ≤ 0.7 in all cases, n=3) 113

Figure 5.5: Temperature Sweep of a) drug free nanomicelles in gel, b) free disulfiram in gel, c) free disulfiram with disulfiram-loaded nanomicelles in gel and d) disulfiram-loaded nanomicelle in gel 114

Figure 5.6: FTIR spectra of a) LAGG and b) HAGG 117

Figure 5.7: FTIR spectra of the native components of the NEGC as well as the combined NEGC its variations..... 118

Figure 5.8: Thermograms of a) LAGG and b) HAGG..... 119

Figure 5.9: Thermogram of PF127 119

Figure 5.10: Thermograms of various combinations of gel, nanomicelles and disulfiram at 36.5°C (top row) and 10°C (bottom row) 121

Figure 5.11: Diffractograms of a) LAGG and b) HAGG..... 123

Figure 5.12: Diffractogram of PF127 123

Figure 5.13: Diffractograms of various combinations of gel, nanomicelles and disulfiram at 36.5°C (top row) and 10°C (bottom row) 125

Figure 5.14: Photomicrographs of a) Composite 5 at 10°C, b) Composite 5 at 37.5 °C, c) Composite 1 at 10°C, d) Composite 1 at 37.5°C, e) Composite 2 at 10°C, f) Composite 2 at 37.5°C, g) Composite 3 at 10°C, h) Composite 3 at 37.5°C, i) Composite 4 at 10°C and j) Composite 4 at 37.5°C..... 126

Figure 6.1: Setup of the modified simulated organ bath 132

Figure 6.2: *Ex vivo* % drug release..... 133

Figure 6.3: Flow- chart summary of the *in vivo* experimental design procedure..... 137

Figure 6.4: Rat undergoing High Frequency Ultra-Sound Imaging 139

Figure 6.5a: NEGC in placebo (left) and test group (right) at 1 hour after administration... 143

Figure 6.5b: NEGC in placebo (left) and test group (right) at 2 hour after administration... 143

Figure 6.5c: NEGC in placebo (left) and test group (right) at 6 hour after administration ... 144

Figure 6.5d: NEGC in placebo (left) and test group (right) at 24 hour after administration. 144

Figure 6.5e: NEGC in placebo (left) and test group (right) at 2 days after administration .. 144

Figure 6.5f: NEGC in placebo (left) and test group (right) at 3 days after administration ... 144

Figure 6.5g: NEGC in placebo (left) and test group (right) at 7 days after administration .. 145

Figure 6.5h: NEGC in placebo (left) and test group (right) at 14 days after administration 145

Figure 6.5i: NEGC in placebo (left) and test group (right) at 21 days after administration.. 145

Figure 6.5j: NEGC in placebo (left) and test group (right) at 28 days after administration.. 145

Figure 6.6: Ultrasound images displaying healthy muscle fibres (left) and the *in situ* gel system (right) 146

Figure 6.7: Digital photograph displaying the presence of the *in situ* gel in the rat muscle (circled in red) 146

Figure 6.8a: 2D chromatogram plot of disulfiram (left peak) and diclofenac (right peak).... 147

Figure 6.8b: 3D PDA plot of disulfiram (left peak) and diclofenac (right peak) 147

Figure 6.9: UPLC calibration curve of known plasma disulfiram concentrations 148

Figure 6.10: *In vivo* disulfiram profiles of the various groups tested..... 149

Figure 6.11**:** Chromatogram of placebo group showing peak for IS only 149

Figure 6.12: *In vivo* CK levels for the test group and placebo group..... 154

Figure 6.13a: Light microscopy histological image of healthy muscle tissue..... 157

Figure 6.13b: Light microscopy histological image of muscle tissue with minimal histopathological lesions (A: test group, B: placebo group) 157

Figure 6.13c: Light microscopy histological image of muscle tissue with mild histopathological lesions (A: test group, B: placebo group) 157

Figure 6.13d: Light microscopy histological image of muscle tissue with moderate histopathological lesions (A: test group, B: placebo group) 158

LIST OF TABLES

Table 2.1: Substances of addiction and their approved treatment protocols 11

Table 2.2: Comparison of microsystems and nanosystems in drug delivery (Kohane, 2006) 23

Table 2.3: Summary of FDA approved treatments formulated as nanosystems and/or microsystems 33

Table 3.1: Advantages of nanomicelles 39

Table 3.2: Variables to be employed for incorporation into the Face Centred Central Composite statistical design 43

Table 3.3: Formulations generated using a Face Centred Central Composite statistical design for the optimization of disulfiram-loaded nanomicelles 44

Table 3.4: Reagents used for preparation of 1L of SBF 45

Table 3.5: Particle sizes and PDI values for F1-F13 49

Table 3.6: Formulation constraints utilised for response optimization 60

Table 3.7: Predicted, experimental and desirability values of the disulfiram- loaded TPGS based nanomicelle formulation 61

Table 3.8: drug loading values for various TPGS-containing nano-sized formulations.. 61

Table 3.9: Particle size, PDI and zeta potential for disulfiram-loaded and drug free nanomicelles 65

Table 4.1: Combination of PF127 with HAGG to yield 24 different gels 80

Table 4.2: Combination of PF127 with LAGG to yield 24 different gels 81

Table 4.3: Experimental setup for rheological tests 84

Table 4.4: Breakdown of temperature sweep graphs 97

Table 4.5: Gelation times for PF127 + HAGG gels and PF127 + LAGG gels 101

Table 4.6.1: R^2 and Chi^2 values for 15% PF127 with 0.3% HAGG and 15% PF127 with 0.3% LAGG 103

Table 4.6.2: R^2 and Chi^2 values for 16% PF127 with 0.2% HAGG and 16% PF127 with 0.2% LAGG 103

Table 4.6.3: R^2 and Chi^2 values for 18% PF127 with 0.3% HAGG and 18% PF127 with 0.3% LAGG 103

Table 4.7: Flow behaviour index (n) values for gels fitting the Herschel-Bulkley model 104

Table 5.1: Summary of gelation temperature, gelation time and flow curve behaviour of the various composites 115

Table 5.2: Flow behaviour index for composites displaying Herschel-Bulkley flow behaviour 116

CHAPTER 1
INTRODUCTION

1.1 Background to this Study

The abuse of alcohol and its consequences are a predicament of epidemic proportions. World-wide 2.5 million deaths per year are alcohol-related (WHO, 2005). Alcohol is recognised as a global leading risk factor for death and disability (Parry and Rehm, 2011). The adverse effects of alcohol addiction are four-fold: physical/ physiological effects, psychological effects, social effects and financial/economical effects (Swift, 1999; Patel, 2009). The severity of this recognised psychological illness, at both national and international levels, and its devastating impact not only on the individual affected, but also on society as a whole, provides a strong argument for the need for an effective treatment option.

A successful treatment plan for alcohol abuse includes a non-pharmacological as well as a pharmacological component (Swift, 1999). The two components are co-dependent and their effects are synergistic when used in combination. The Food and Drug Administration (FDA) has approved three drugs for the pharmacological treatment of alcohol dependence; these include acamprosate, naltrexone and disulfiram (Center for Substance Abuse Treatment, 2009). These drugs are also approved for use in South Africa by the Medicines Control Council.

Acamprosate is available as Campral® (Forest Pharmaceuticals Inc, Darmstadt, Germany), a 333mg enteric coated tablet (Williams, 2005). Acamprosate is thought to correct the GABA-glutamate imbalance caused by alcohol consumption (Pettinati and Rabinowitz, 2005). The recommended dosage is two tablets three times daily (Williams, 2005). Campral has a bioavailability of 11% (FDA, 2004). Consequently the dosing regimen requires that a total of six tablets be taken daily. The tedious nature of the regimen leads to poor patient compliance.

Naltrexone, a reversible opioid receptor antagonist, reduces alcohol cravings (Patel, 2009). There are two FDA-approved dosage forms; an oral tablet and an extended-release intramuscular injection (Center for Substance Abuse Treatment, 2009). Oral naltrexone, marketed as Revia® (Duramed, New York, USA), is available as a 50mg film coated tablet (Pettinati and Rabinowitz, 2005). The dosing schedule is one tablet daily (Williams, 2005). This dosing is simpler than that of Campral® but Revia® has an erratic bioavailability which

ranges from 5-40%. The dose will have to be tailored to suit the patient and this gives rise to complications. Oral naltrexone has a 'black-box' warning regarding its hepatotoxic effects (Center for Substance Abuse Treatment, 2009).

Vivitrol® (Alkermes Inc., Waltham, Massachusetts, USA) is a depot injection containing 380mg of naltrexone in a microsphere formulation (FDA, 2010). It is administered every four weeks (FDA, 2010). Despite improved adherence compared to Revia®, from a formulation perspective it has limitations. Injections are associated with pain and anxiety which hinders patient acceptance (Hogan et al., 2010). Another concern is the affordability of the injection. The polymer employed for the formulation is poly (lactic-co-glycolic acid) (PLGA) which is FDA approved (FDA, 2010). While PLGA is beneficial in research, incorporation of it into marketable formulations results in a significant increase in cost. Thus it may be clinically useful, but it is not affordable. Alcohol dependence is not class specific and it affects people at both ends of the financial scale. This implies that the true efficacy of this treatment option is questionable.

A naltrexone implant is also available. However this is not approved by the FDA for use in alcoholics. It consists of the biodegradable polymer poly (D,L-lactide). Implants allow extended release up to one year but they are costly and administration is complex and more invasive than injections (Herrmann et al., 2007). Implants limit the quantity of drug that can be delivered. This influences the duration of action and consequently increases the frequency of implant replacement (Herrmann et al., 2007).

Disulfiram is an alcohol deterrent that inhibits aldehyde dehydrogenase (ALDH) causing an accumulation of acetaldehyde (Patel, 2009). This produces what is known as the disulfiram-ethanol reaction (DER) (Pettinati and Rabinowitz, 2005). This reaction results in the unpleasant effects that serve as an effective deterrent to alcohol consumption. The DER is attributed to the high absorption of disulfiram and its rapid conversion to the active metabolite.

Disulfiram is available in an oral form and as an implant. The oral form, marketed as Antabuse® (Odyssey Pharmaceuticals, New Jersey, USA) is approved by the FDA for use in alcohol dependence (Pettinati and Rabinowitz, 2005). Antabuse® is available as tablets (250mg or 500mg) and effervescent tablets or dispergettes (200mg and 400mg) (Andersen, 1992). The daily dosage range is 250-500mg (Williams, 2005). The oral route has positive outcomes but is dependent on the patient adhering to the therapy (Pettinati and Rabinowitz,

2005). The physical and mental status of alcoholic patients has significant influence on treatment adherence.

The implant is a subcutaneous preparation containing 1g of disulfiram (Cid et al., 1991). It is marketed as Esperal® and it consists of ten 100mg disulfiram pellets. As stated previously, the amount of drug that can be incorporated into an implant is limited. The DER only occurs at a certain dosage; anything below this amount will fail to produce a reaction. As a result, the absorption of disulfiram is insufficient to consistently produce a proper DER (Kline and Kingstone, 1977). An allergic reaction to the implant has also been reported (Black, 1979). Additionally, extrusion of the implant may occur (Kline and Kingstone, 1977). The implant is rarely used and not easily available. In South Africa, the Medicines Control Council does not approve the use of the implant (Cassimjee, 2012). It can only be used for experimental purposes.

It is evident that the large scale of the problem and the various shortcomings of available formulations provide a great universal need for an improved and effective treatment formulation.

1.2 Rationale and Motivation for the Study

Acamprosate, naltrexone and disulfiram have shown clinical efficacy (Center for Substance Abuse Treatment, 2009). In a comparison of disulfiram and naltrexone, disulfiram produced a better result overall (De Sousa et al. 2004). Disulfiram was also shown to be more effective than acamprosate (Diehl et al. 2010). Thus, due to the aforementioned statement, the rationale to reformulate disulfiram as opposed to naltrexone or acamprosate stems from the fact that of these three drugs disulfiram is the key pharmacological option with efficacy exceeding the other two. Reformulating an FDA approved active rather than an active without regulatory approval eliminates the uncertainty related to newer treatment options.

The usage of depot formulations is not very popular when compared to other routes of administration. However, depots hold many advantages and are able to overcome the limitations facing current treatment options. The current choices do not provide any long-term guarantee of adherence and relapse prevention. These two issues are critical aspects that challenge successful abstinence (Jaeger and Rossler, 2010). Non-adherence stems largely from inadequate and costly delivery systems. These systems depend on the patient for therapeutic success. It is an unfortunate truth that, in a condition where the effects of addiction negatively affect one's ability to make rational decisions, expecting such a person to choose the long-term benefits of therapy over the short-term pleasure of alcohol is overly

ambitious. Administration of a depot which will consistently release drug over a period of 1-3 months eliminates the need of this reliance. A study comparing the efficacy of long term injections versus oral preparations for the treatment of psychiatric disorders has shown that depots possess several advantages since depots implement blood concentration stability (Jaeger and Rossler, 2010). This positively influences side-effect profiles and the therapeutic efficacy of the bioactive (Jaeger and Rossler, 2010). This is particularly relevant as the tablet and effervescent tablet of disulfiram lack bioequivalence when compared to each other (Andersen, 1992). A depot can assist in overcoming this unpredictable trait of disulfiram. Furthermore, the need to monitor adherence becomes unnecessary. There is no need for invasive surgical procedures.

Although depot formulations of drugs are not new, it provides a solid, proven dependable platform to begin as it limits the number of unknown formulation concerns, it possesses confirmed ability to be manufactured on a large scale and it has an established position in clinical practice (Tice, 2004). Modification of the depot system by using advanced carrier systems and incorporating improved excipients creates a novel drug delivery system with untapped potential. This Depot Intramuscular Formulation (DIMF) will overcome the challenges facing conventional depot formulations. Currently there are no FDA approved sustained release formulations of disulfiram. Employing biodegradable and biocompatible polymers the depot makes certain that the formulation poses no toxic harm to the body. Utilising viable alternate polymers that are cost-effective establishes the affordability of the injection.

Advances in drug delivery over the years have provided a selection of optimal formulation techniques. Employing advanced formulation procedures such as microtechnology (microspheres) or nanotechnology (nanosuspensions or nanoparticles) has immense pharmaceutical and therapeutic benefits. Microspheres, nanosuspensions and nanoparticles allow incorporation of a variety of drugs (Kim and Pack, 2006). They are biocompatible and biodegradable and they greatly improve bioavailability (Kim and Pack, 2006). They also allow for sustained and controlled release as well as being versatile and not specific to a particular route of administration (Kim and Pack, 2006). Furthermore, they possess improved physical stability (Kim and Pack, 2006). Nanoparticles and nanosuspensions decrease tissue irritation and pain on injection as well as protect the active from enzymatic degradation (Tiyaboonchai, 2003). The preparation of microspheres, nanosuspensions and nanoparticles share a basic methodology which is then modified depending on the particles being formulated. Figure 1 in appendix A schematically depicts the common steps involved in each method as well as the completed DIMF.

Motivating factors to support the design of the DIMF include the following: 1) Easy administration of the active through IM injection. Skeletal muscle is highly vascular allowing the drug to enter the systemic circulation easily. Formulation as a depot results in slow diffusion of the drug. It also allows for the administration of several millilitres of drug with minimal discomfort to the patient. These two characteristics produce sustained release of drug over a prolonged time period. 2) The DIMF will promote adherence. The sustained release properties of depot formulations will allow for monthly (as opposed to daily) dosing. The patient is not expected to remember to take the medication daily neither can they stop their therapy at their own will. 4) Side-effects will be decreased with the DIMF. The slow release of the drug ensures that drug-blood levels are not too high to cause adverse effects. A common side effect associated with disulfiram is the metallic-garlic aftertaste in the mouth. This will be eliminated through parenteral administration. 5) The DIMF will improve bioavailability. Disulfiram undergoes approximately 90% liver metabolism. An intramuscular formulation will bypass the first pass effect and improve bioavailability. 6) The DIMF will be cost-effective. By formulating the depot using cost-effective excipients the cost of treatment will decrease or be comparable to the current therapy.

1.3 Aims and Objectives

The aim of this investigation is to design a depot injection of disulfiram for intramuscular administration. The above aim was achieved with the following objectives:

1. Identification of a suitable formulation approach as well as suitable materials for use as polymers and other excipients.
2. Adjustment of the variables involved in order to obtain an optimized formulation.
3. Elucidation of the physicochemical parameters such as particle size, surface morphology, drug-polymer interactions and physicomechanical parameters such as viscosity.
4. Evaluation of the drug entrapment and release using *in vitro* testing and analysis as well as ensuring that the depot is successful at this stage so that it is eligible for *in vivo* analysis.
5. Evaluation of the depot system at a clinical level using *in vivo* studies in a suitable animal model. This objective was fulfilled in accordance with ethical laws and regulations.

1.4 Novelty of the Study

The design of a novel system for the delivery of disulfiram (i.e. the DIMF) is achieved through a dyadic delivery system comprising a nano-enclatherated-gel-composite (NEGC).

1.5 A Nano-Enclatherated-Gel-Composite System: Concept and Outline

The dyadic composite was to be fabricated from disulfiram-loaded self-assembling nanomicelles uniformly embedded in a thermosensitive *in situ* gel which would be

administered via intramuscular injection in a liquid state and morph into a solid depot post-injection. The gel matrix would contain both free drug, for first phase release, and disulfiram-loaded nanomicelles for sustained release. Drug would diffuse out of the systems into the surrounding tissue and thereafter into the blood supply of the tissue. The polymers employed will allow sustained and controlled release as well as a suitable carrier for the highly hydrophobic disulfiram (Figure 1.1).

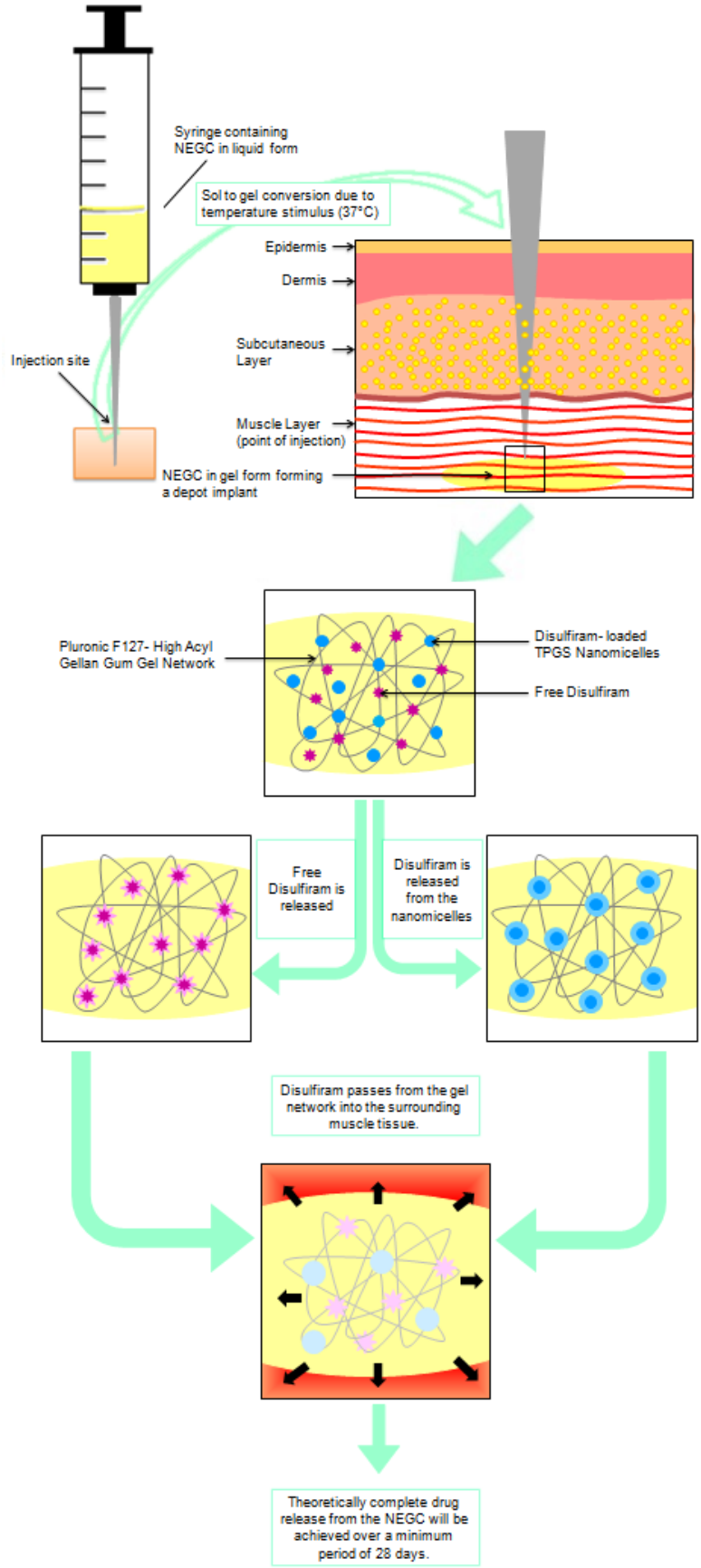

Figure 1.1: Componential configuration of the dyadic delivery system: a nano-enclatherated-gel-composite system.

1.6 Overview of this Dissertation

Chapter 1 presents a summary of the dissertation. It contains a brief introduction to the current approved treatment options for alcohol abuse and their shortcomings. The rationale and motivation for the study are also delineated. In addition the novelty of the study and potential benefits of the system are highlighted.

Chapter 2 is a review of the literature relating to the trends and advances in drug delivery technologies in the treatment of substance abuse and drug addiction. The review focuses on the role of multiparticulate delivery systems in addiction. It includes an in-depth discussion on addiction treatment, types of multiparticulate preparations, as well as comparison of multiparticulate systems and challenges faced with these. It also covers reformulation of anti-addiction drugs into multiparticulate systems and other potential treatments for substance abuse.

Chapter 3 provides details on the fabrication of the nanomicellar component of the delivery system. Development was based on a design of experiments which was obtained through a Face Centred Central Composite Design. This allowed determination of the optimal levels of constituent and process variables. Responses studied included entrapment efficiency, drug loading and drug release followed by which optimization of the nanomicelles was conducted utilising response surface methodology. Further physicochemical and physicomechanical characterization and *in vitro* drug release studies were conducted to obtain a complete report of the nanomicelles. This included particle size and morphology, thermal profiling, and chemical and structural configuration amongst others.

Chapter 4 evaluates the rheological properties of the gel aspect of the system. It is a detailed comparison of the two strains of gellan gum in conjunction with Pluronic F127. The chapter thoroughly investigates the rheological, and consequently, the overall superiority of the various gels formulated and concludes on a deliberately chosen gel formulation for inclusion in the depot delivery system.

Chapter 5 describes the incorporation and assimilation of the optimized nanomicelle formulation of chapter 3 into the rheologically appropriate gel in order to assemble the depot-like composite. *In vitro* release, physicochemical and physicomechanical characterization and analysis was performed on various combinations of the two components as well as the final system- the nano-enclatherated-gel-composite (NEGC).

Chapter 6 comprehensively details the *ex vivo* and *in vivo* analysis of the NEGC in the Sprague Dawley rat model. *Ex vivo* studies included drug release and myotoxicity studies. *In vivo* studies included the comparison of plasma levels due to oral conventional therapy and the NEGC utilising a modified, established method of quantitative, chromatographic determination. Biocompatibility was also determined by investigating myotoxicity due to IM administration through plasma analysis and histopathology of muscle tissue. High frequency ultrasound imaging was undertaken to confirm administration and presence of the depot *in vivo*.

Chapter 7 concludes this dissertation. Limitations of the study and recommendations for future investigations are included in this chapter.

CHAPTER 2

A REVIEW OF THE TRENDS AND ADVANCES IN DRUG DELIVERY TECHNOLOGIES FOR THE TREATMENT OF SUBSTANCE ABUSE AND DRUG ADDICTION

2.1 Introduction

One of the world's dominant health issues is that of substance abuse. The data released by the United Nations Office on Drugs and Crime in 2016 revealed shocking statistics. In 2014 the number of people (between the ages of 15-64) who had utilised a prohibited substance was estimated to be a quarter of a billion people and this equates to 1 in 20 adults (United Nations Office on Drugs and Crime, 2016). Drug dependence and addiction, apart from posing serious health hazards, has severe financial effects as well. The cost to society due to illicit drug use is valued at $180.9 billion per annum (Paterson, 2011). Substance abuse treatment has various positive effects such as reduction in drug abuse, decreased criminal behaviour, lower risk of blood-borne virus transmission and an overall improvement in social, physical and mental wellbeing.

A common misconception in society is that addiction is a voluntary habit. However, only the initial misuse of a substance is voluntary. When the person engages in it repeatedly the neural pathways are altered in such a way that the behaviour then becomes involuntary. This signifies that addiction is not merely a personal choice but rather a Central Nervous System (CNS) disease governed by three primal traits. These traits are compulsive intake of the substance, engaging in drug-seeking behaviour and chronic relapses due to irrepressible craving, all of which occur despite awareness of the harmful consequences (Yahyavi-Firouz-Abadi and See, 2009). Withdrawal of a drug is a negative reinforcement of drug abuse and the effects are so strong that the addict engages in drug use to avoid the unpleasant emotions generated. Due to the complexity of the disease the treatment is seldom easy and straight forward. The greatest challenge hindering the recovery process is the risk of relapse. Treatment of withdrawal of a substance has great clinical success, but as far as gaining complete control over cravings and relapse is concerned, the therapies are limited or non-existent. An overall treatment regimen should involve pharmacological and psychosocial plans. Long-term therapy is imperative in order to obtain complete abstinence.

The various substances of abuse have diverse mechanisms of action. However, due to a better understanding of the pathway of addiction it is now clear that they are similar in their target area (the reward system of the brain) and shared neural path exists for addiction to most drugs (Melichar, 2001). Majority of the drugs abused, such as alcohol, opioids and

stimulants, exert their effects by stimulating this pathway in one way or another. Consequently there exists an overlap and thus treatment of one abused substance may be applicable to treatment of other drug addictions too. Instead of attempting to discover new treatments which will have to be tested for efficacy, it is a feasible option to reformulate current tested treatments such that their limitations are surmounted. The key fundamentals of addiction treatment relevant to the pharmaceutical aspect are as follows (National Institute on Drug Abuse):

- Addiction is treatable. This is important as drug delivery systems can be created or modified to target the main area affected which is the brain.
- Treatment is not generalised. Every individual is affected differently so every treatment regimen has to be suited to the patient in question. This means that the drug delivery system must be flexible in order to accommodate patient individuality.
- The patient must remain in treatment for an adequate time period. While it differs from patient to patient the average time for treatment to be effective is estimated at three months and the longer the duration, the better the outcome. This is why sustained-release preparations will be useful to assist in this regard.
- Medications are crucial especially when used in combination with psychosocial therapies.
- Many addicts have co-morbid CNS disorders (such as depression, bipolar, psychosis). This also needs to be treated for complete recovery.

2.2 Drugs of Abuse and their Existing Treatments

The four major classes of abused substances are alcohol, nicotine, opioids and stimulants (cocaine and methamphetamine). Table 2.1 lists the drugs and the products available to treat addiction of these substances.

Table 2.1. Substances of addiction and their approved treatment protocols.

Substance of Abuse	Treatment	Dosage Form	Dosage
Alcohol	Acamprosate (Campral®)	333mg EC tablets	2 tablets thrice daily
	Disulfiram (Antabuse®)	250mg tablets 500mg tablets 200mg dispergettes 400mg dispergettes	250-500mg daily
	Naltrexone (Revia®)	50mg FC tablets	1 tablet daily
	Naltrexone IM (Vivitrol®)	380mg IM injection	Monthly
Nicotine	Nicotine Replacement Therapy (NRT): -Gum (Nicorette®) -Inhaler (Nicorette® Inhaler) -Nasal spray -Lozenge (Commit®) -Transdermal patch (Nicoderm CQ®)	Gum: 2mg, 4mg Lozenge: 2mg, 4mg Patch: 5mg/day, 7mg/day, 10mg/day, 14mg/day, 15mg/day, 21mg/day	Varies depending on the dosage form Tailored to suit the patient Treatment occurs for 10-12 weeks
	Bupropion(Zyban®)	75mg, 100mg, 150mg tablets	150mg daily for 3 days then 150mg twice daily
	Varenicline (Chantix®)	0.5mg and 1mg tablets	0.5mg daily for 3 days, then 0.5mg twice daily for 4 days, then 1mg twice daily for 11 weeks
Opioids: (illicit: heroin, opium Codeine)	Methadone (Methadose®)	5mg,10mg, 40mg tablets	15-40mg daily then reduce by 20% daily
	Buprenorphine (Subutex®)	2mg and 8mg SL tablets	Day 1 induction: 8mg Day 2 induction: 16mg Continue over 3-4 days with maintenance 12-16mg
	Buprenorphine/naloxone (Suboxone®)	2mg/0.5mg and 8mg/2mg SL tablets 2mg/0.5mg and 8mg/2mg SL films	Same as Subutex®.
	Naltrexone oral (Revia®)	Same as above	Same as above
	Naltrexone IM (Vivitrol®)	Same as above	Same as above

Stimulants: (cocaine and amphetamines)	No approved treatment for stimulant dependence.

2.2.1 Alcohol

The consumption of alcohol is one of the top three risk factors for disease and disability. It is responsible for 4.5% of the burden of disease and injury and 4% of deaths worldwide (World Health Organisation, 2011). The FDA has approved three drugs for the pharmacological treatment of alcohol dependence: acamprosate (Campral®), naltrexone orally and intramuscularly (Revia® and Vivitrol® respectively) and disulfiram (Antabuse®). The dosing regimen for Campral® requires a total of six tablets to be taken daily and this tedious nature of the regimen leads to poor patient compliance. Revia® on the other hand has an erratic and low bioavailability; as such the dose will have to be tailored to suit the patient and this gives rise to complications (Wall et al., 1981). Revia® further has a 'black-box' warning regarding its hepatotoxic effects. Vivitrol® is an intramuscular (IM) depot injection containing 380mg of naltrexone in a microsphere formulation. Despite improved adherence compared to Revia®, from a formulation perspective it has limitations as injections are associated with pain and anxiety which influences patient acceptance. Another concern is the affordability of the injection. Disulfiram has positive outcomes but its success relies on the patients adherence to the therapy (Pettinati and Rabinowitz, 2005). The physical and mental status of alcoholic patients has significant influence on treatment adherence. The rate of medication compliance is poor in alcoholics.

2.2.2 Nicotine

Death related to smoking is a leading preventable cause of death (Strasinger et al., 2009). The first therapeutic agent for smoking cessation was a reservoir transdermal patch that released nicotine. Advances have led to the formulation of gums, lozenges, inhalers, matrix systems and nasal sprays. Nicotine Replacement Therapy (NRT) is the term given to these treatments and it has two effects; firstly it replaces the addictive nicotine with a pharmaceutical alternative eliminating the poisonous chemicals associated with smoking, secondly it stops withdrawal symptoms from occurring so that the patient does not experience any cravings. There are three FDA approved treatments for smoking cessation; NRT, bupropion (Zyban®) and varenicline (Chantix®). Varenicline is the first medication approved only for nicotine dependence that does not contain nicotine. All forms of NRT have comparable efficacy and are relatively safe. On the whole the rate of efficacy of NRT and Zyban® is sub-standard (Heidbreder, 2005). Unfortunately, within a year the relapse rate

reaches 80% (Cryan et al., 2003). The poor success rate of NRT is due to its inability to truly achieve the rapid high nicotine plasma level that is induced by cigarette smoking. Thus the success rate of smoking cessation therapy is a poor 19% after one year of treatment (Wills, 2005). The other treatments that have been tested for nicotine addiction include naltrexone, risperidone, pergolide, amantidine, methylphenidate, methadone, buprenorphine but have not been successful (Heidbreder, 2005).

2.2.3 Opioids

Opioid therapy includes methadone, buprenorphine, naloxone and naltrexone which are effective but these formulations can be improved with regards to safety and efficacy (Heidbreder, 2005). Initial methadone therapy involved daily visits to clinics in order to receive treatment however this was inconvenient and led to poor compliance. To overcome this, a long acting preparation was formulated but this did not sustain release for required time periods (Negrın et al., 2001). The current slow release preparations of buprenorphine allow dosing to extend from daily to less-than-daily dosing but the issue with this is that multiples of the daily dose have to be administered. It is formulated as a sublingual tablet due to its poor oral bioavailability. While conventional tablets do hold some advantages such as accurate unit dosing and increased stability, they have a potential for abuse; they can be crushed, dissolved and injected (Gross et al., 2001). This was overcome by formulation of a sublingual tablet containing buprenorphine and naloxone in a 1:4 ratio (Chiang and Hawks, 2003). If this is injected it results in withdrawal symptoms. It is important to note that this therapy is a daily regimen. Tripling the daily dose will increase the amount of buprenorphine allowing the patient to remain dose free for up to three days (Gross et al., 2001). This is too short a time period and can still result in poor adherence.

2.2.4 Stimulants

Psychostimulant addiction is rife but specific approved treatment options are not available. Pharmaceutical actives that have shown potential in clinical trials for treating relapse in cocaine addicts include topiramate, baclofen, vigabatrin, tiagabine, bupropion, aripiprazole, disulfiram, modafinil, buprenorphine and desipramine. All exert varying efficacy depending on the patient's profile of substance abuse but each has shown promise in cocaine addiction and are currently undergoing further evaluation (Yahyavi-Firouz-Abadi and See, 2009). It is evident that the large scale problems and the various shortcomings of available treatments provide a great universal need for an improved and effective treatment formulation.

2.3 Overcoming Addiction Through Formulation Manipulation

The chronic nature of addiction treatment results in non-compliance which has a negative effect on the overall health of the patient and on the economy as a whole (Frijlink, 2003). A new approach therefore needs to be devised to overcome non-compliance associated with long-term treatment of addiction. Currently most preparations can afford a 3-5 day interval between dosing (National Institute on Drug Abuse Research Monographs Series, 1976). However this is not a long enough time for the patient to become detached from their addictive behaviour. The rate of recovery varies per individual and is largely dependent on the patients' determination and willpower. Recovering addicts, particularly those in the initial stages of treatment, are vulnerable. As such, the possibility of a relapse cannot be overlooked. Relying on the patient to take the medication is unadvisable as there is no guarantee that he/she is following the regimen as it should be. A patient is more likely to adhere to a treatment plan that is uncomplicated. A covetable element is a long-acting preparation which will decrease dosing to monthly or at least bi-monthly. There are two means by which this desired drug delivery system can be obtained, mechanically by using an implant system or chemically by using compounds that possess sustained release properties. In the latter, a compatible chemical carrier, together with the pharmaceutical active, will deliver the drug consistently over a prolonged time period (National Institute on Drug Abuse Research Monographs Series, 1976). Advanced drug delivery systems that allow a reduction in the number of administrations and the amount of drug to be administered are advantageous. Improved dosage forms, particularly those that have controlled/sustained release, have had great success for treatment of various conditions. Drug release can be managed by time-dependent sustained drug delivery systems which simplify the treatment regimen as it is easier for the patient to use; this improves compliance and simultaneously ensures the plasma concentrations are at the ideal therapeutic level. These factors all come together to decrease costs directly and indirectly. The effects of such an innovative drug delivery system are summarised in Figure 2.1.

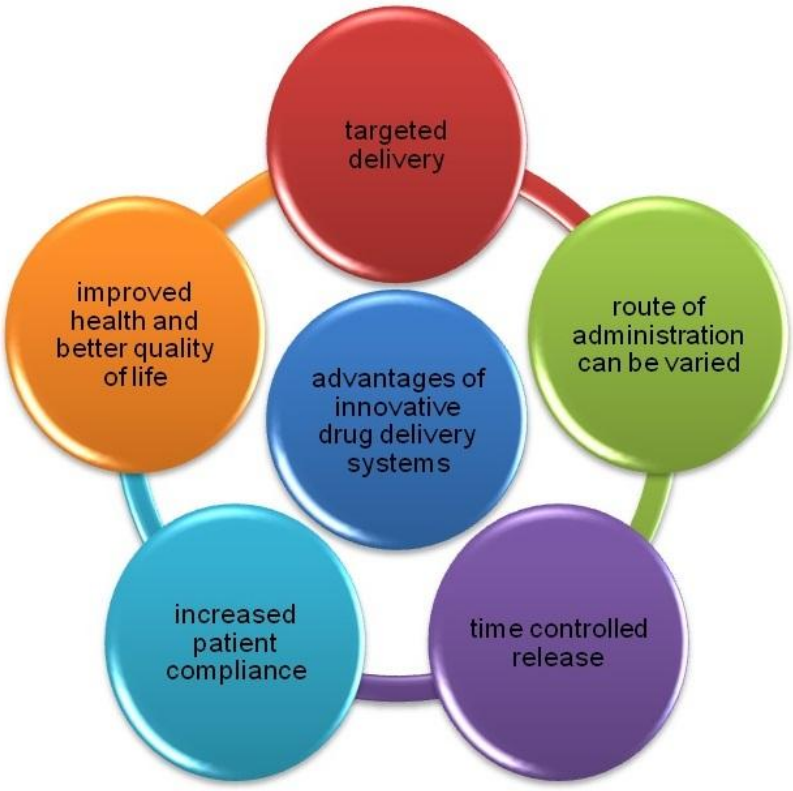

Figure 2.1: Various positive effects of an innovative drug delivery system.

A discerning advent in drug delivery is the use of carrier mediated delivery systems. This technology involves the pairing of the drug or the active component to a carrier which can comprise of a host of particles such as nanoparticles, microparticles and the like. The development of optimal drug delivery systems is based on three broad categories. These are the carrier system to be employed, the biomaterials that will be used and the properties of the active ingredient. All three categories are inter-linked and compatibility between the three will result in an optimized formulation. Multiparticulate systems are model systems that combine these three requirements in an absolute manner. They include granules, pellets, nanoparticles and microparticles. Many marketed preparations consist of microspheres. In addition to this, nanosystems offer distinct advantages as well. It is important to note that a high drug loading is essential for drug carriers in order to obtain a therapeutic effect which can be well-achieved by multiparticulate systems.

2.4 Multiparticulate Drug Delivery Technology

The poor solubility and poor chemical stability of a significant number of potentially active pharmaceutical ingredients for substance abuse results in suboptimal performance. Formulation-related issues that may arise include inadequate oral bioavailability, absence of proportionality of doses, and a slow onset of action. The appealing attributes of

nanoparticles and microparticles can overcome these challenges and may provide an exclusive niche in advancing the management of drug addiction.

2.4.1 Microparticulates

A microparticulate system comprises of a microparticle matrix of natural or synthetic polymers containing the active ingredient in either of these forms: entrapped, attached, dissolved or encapsulated. Regardless of a particles interior and exterior architecture, if the diameter lies between 1µm and 1000µm, the particle is termed a microparticle. The active leaves the microsystem either through melting, diffusion, dissolution or rupturing of the particle. Microencapsulation offers numerous advantages. It protects volatile drugs from vaporisation as well as protects sensitive drugs from heat, moisture, light and oxidation. It allows for reduction in side effects as only the necessary amount of drug is delivered. This has a two-fold effect as it decreases toxicity and irritant effects of certain actives and enhances therapeutic efficacy. Additional advantages of micro-based carrier systems are increased bioavailability, controlled release, reduced frequency of dosing, enhanced patient compliance and continuous and extended release of the active. Polymeric microparticles have good stability, reproducibility and dosage form versatility thus having an application in a broad area of therapeutics (Vilos and Velasquez, 2012). There are two types of particles that can be obtained through microencapsulation: microspheres and microcapsules (Agnihotri et al., 2012). Microspheres consist of uniformly dispersed drug within a polymeric matrix. Microcapsules refers to those microparticles which consist of a core, containing the active, surrounded by a layer of a material different to that of the core; usually this membrane is composed of a polymeric substance (Padalkar et al., 2011). Figure 2.2 depicts the difference between microspheres and microcapsules.

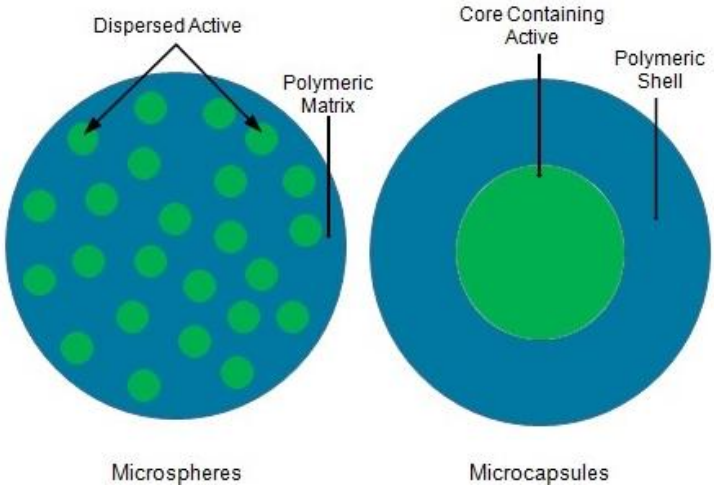

Figure 2.2: The difference between microspheres and microcapsules.

It is important to consider the following when formulating microparticles:

- The particles must be able to embody a high concentration of the active.
- The final formulation must be stable.
- Particle size must be constant and it must be maintained.
- In the event of parenteral administration, the powder must be easily dispersed in aqueous vehicles.
- The active must be released consistently and in a controlled manner (no burst release).
- The formulation must be biocompatible and biodegradable.

2.4.2 Nanoparticulates

A recent important pharmaceutical milestone has been the lucrative development and commercialisation of a nano drug delivery system. The advent of nano drug delivery systems has broadened the drug delivery and development horizon. It is a logical thought that if a chemical with a problematic profile could be modified to be perfect and blemish-free then there would be no need for complex drug delivery systems. Thus far, this has yet to be accomplished. Nanoparticulate systems possess unique physical as well as biological traits that can rise above the difficulties of current options. Consequently, nanoparticulate systems are the ideal solution to overcome the pharmacokinetic and biodistribution challenges of those drugs that are poorly soluble, unstable or too toxic. Nanoparticles have a greater surface area (compared to macro and micro particles) which can enhance the efficiency of drug delivery. Nanoparticle-based drug delivery mostly includes the use of liposomes or polymers as a carrier. The advantages of using these is higher drug loading capacity and improved solubility and delivery of poorly water soluble drugs. They allow targeted delivery of drugs which leads to increased efficiency and decreased side effects. The successful conversion of stable nanoparticles into suitable dosage forms is a primary concern. Types of nano carriers investigated include polymeric nanoparticles, polymer-drug conjugates, solid lipid nanoparticles (SLN), nano-structured lipid carriers (NLC), liposomes, nanosuspensions, nanocrystals and nanogels. The type of drug, delivery periods, stability, permeability and drug release will influence the modification of the surface, synthesis and type of nanoparticle system to be employed.

2.4.2.1 Polymeric nanoparticles

Drug is usually incorporated into the nanoparticle by dissolving, entrapment, encapsulation or attachment to the polymeric matrix. While polymeric nanoparticles have greater storage stability, the hydrophobic polymers used must be dissolved in organic solvents which can be harmful. The first commercial polymeric nanoparticle product was Abraxane® (Celgene

Corporation, Summit, NJ, United States of America) which consists of albumin bound to paclitaxel in a nanoparticle system.

2.4.2.2 Polymer-drug nanoconjugates

Polymer therapeutics include nano-sized compounds which are composed of the bioactive material linked via a chemical covalent bond to a biocompatible, water soluble polymeric carrier. In the polymer-drug conjugate the active is not encapsulated. Current research is exploring the viability of polymer-drug conjugates in neurodegenerative disorders (Canal et al., 2011) which are often employed in the diagnosis and treatment of cancer. The polymer N-(2-hydroxypropyl)methacrylamide (HPMA) has been conjugated to various chemotherapeutic agents such as doxorubicin (HPMA copolymer-DOX and HPMA copolymer-DOX-galactosamine), camptothecan (HPMA copolymer-camptothecan), paclitaxel (HPMA copolymer-paclitaxel) and the platinates (HPMA copolymer-platinates). Furthermore HPMA copolymer drug conjugates have also shown success in other diseases such as musculoskeletal diseases (HPMA copolymer conjugated to prostaglandin E) and inflammatory and infectious diseases (HPMA copolymer conjugated to Amphotericin B) (Kopeček, 2013).

2.4.2.3 Liposomes

Liposomes are nano carriers consisting of an aqueous core surrounded by amphiphilic bilayers. LipoBridge®, a lipid based technology developed by Genzyme Pharmaceuticals (Cambridge, Massachusetts, United States), is thought to be able to deliver large amounts of bioactives to the brain by temporarily opening the Blood-Brain-Barrier (BBB). The company has developed technology that formulates the active with short chain oligoglycerolipids. This briefly opens up the tight junctions in the barrier thus allowing the active to enter the CNS. LipoBridge® overcomes the major disadvantage of many CNS active compounds that is their inability to cross the BBB which is the cause of poor therapeutic outcome. By only opening the BBB for a limited period of time the risk of harmful and unnecessary substances passing through is minimised. LipoBridge® can be used for hydrophobic and hydrophilic actives making it suitable for a large variety of CNS drugs.

2.4.2.4 Solid lipid nanoparticles and nano-structured lipid carriers

As with most lipophillic drugs parenteral formulation is challenging due to a low aqueous solubility. An alternative to emulsions and liposomes as drug carriers are solid lipid nanoparticles (SLN) and nano-structured lipid carriers (NLC) which differ in the structure of the solid particle matrices. A SLN consists of a solid lipid dispersed in an aqueous medium which is stabilised with a surfactant (Pardeike et al., 2009). Preparation of these particles

using lipids that are biodegradable or physiological allows these systems to be well tolerated for various routes of administration such as ocular, peroral, dermal, pulmonary and parenteral. The drug is dispersed in the solid hydrophobic core. Brain uptake of SLN is safe and toxicity is low (Blasi et al., 2007). Acceptable size range for SLN transport across the BBB is 10-100nm. Drug entrapment and drug stability in SLN systems are both high; additionally they exhibit controlled release for a number of weeks. A hydrophilic coating can further be beneficial to improve the bioavailability of the drug (Mishra et al., 2010). SLN are favoured because of their ability to protect chemically labile constituents, modulate the release of drug and are less cytotoxic compared to polymeric nanoparticles. Nanobase®, an injection for the treatment of Hepatitis C, is an FDA approved SLN formulation (Wang et al., 2009). Modified SLN wherein the lipid phase consists of a blend of solid and liquid lipids are known as NLC (Pardeike et al., 2009). NLCs have a higher drug loading capacity, a lower water content in the suspension and they have a lower risk of active being expelled during storage (Mehnert and Mäder, 2001).

2.4.2.5 Drug nanocrystals and nanosuspensions

Drug nanocrystals are crystalline nano-sized pure drug particles (Junghanns and Müller, 2008). The difference between a drug nanocrystal (also known as a nanodrug or pure drug nanoparticle) and a polymeric nanoparticle is that the drug nanocrystal is 100% pure drug whereas the polymeric nanoparticle comprises the drug with a carrier material. The advent of nanocrystals is credited to SkyePharma Canada Inc. (Verdun, Quebec, Canada) and Elan (Dublin, Ireland) who hold patents for nanocrystal technologies (Liversidge et al., 1992; Khan and Pace 2002.). The initial reluctance towards nanocrystal technology is slowly evolving. The change in perception came about due to the problems encountered with 70-90% of newly discovered therapeutic compounds such as the poor aqueous solubility. This can be overcome by formulating as a nanosystem. Further, a nanosuspension is a dispersion containing 100% pure drug nanocrystals (Junghanns and Müller, 2008). A small amount of surfactant may be added to the suspension to stabilise the formulation.

2.4.2.6 Nanogels

A nanogel is a nanosystem of polymers cross-linked by physical or chemical means which is capable of swelling in a compatible solvent. Nanogels are favoured as they show good stability, have relatively simple formulation procedures and possess a higher drug loading capacity compared to nanoparticles (Vinogradov et al., 2002; Vinogradov et al., 2004). Numerous advantages of nanoparticulate systems in drug delivery is adding to an increase in the number or types of these systems which is beyond the scope of discussion of this review but to name a few it includes magnetic nanoparticles, metal and inorganic

nanoparticles, quantum dots, polymeric micelles, phospholipid micelles and colloidal nano-liposomes. The development of simple, safe, effective and economical nanoparticulate drug delivery systems is the main goal of many pharmaceutical scientists. Figure 2.3 shows the different types of nanosystems discussed. The therapeutic effect of drugs is augmented by nanoparticles as they improve bioavailability, solubility and retention time of the active. This results in a decrease in toxicity as well as expense to the patient. Efficacy, tolerability, specificity and therapeutic index of a drug can be extended when they are encapsulated as nanoparticles (Kumari et al., 2010). Additional positive features of nanoparticles are: i) premature degradation is prevented, ii) there is minimal or no interaction with the biological environment, iii) absorption of the drug by a specific tissue is increased, iv) improved bioavailability, v) longer retention time thus sustained and controlled release and vi) better intracellular penetration (Alexis et al., 2008).

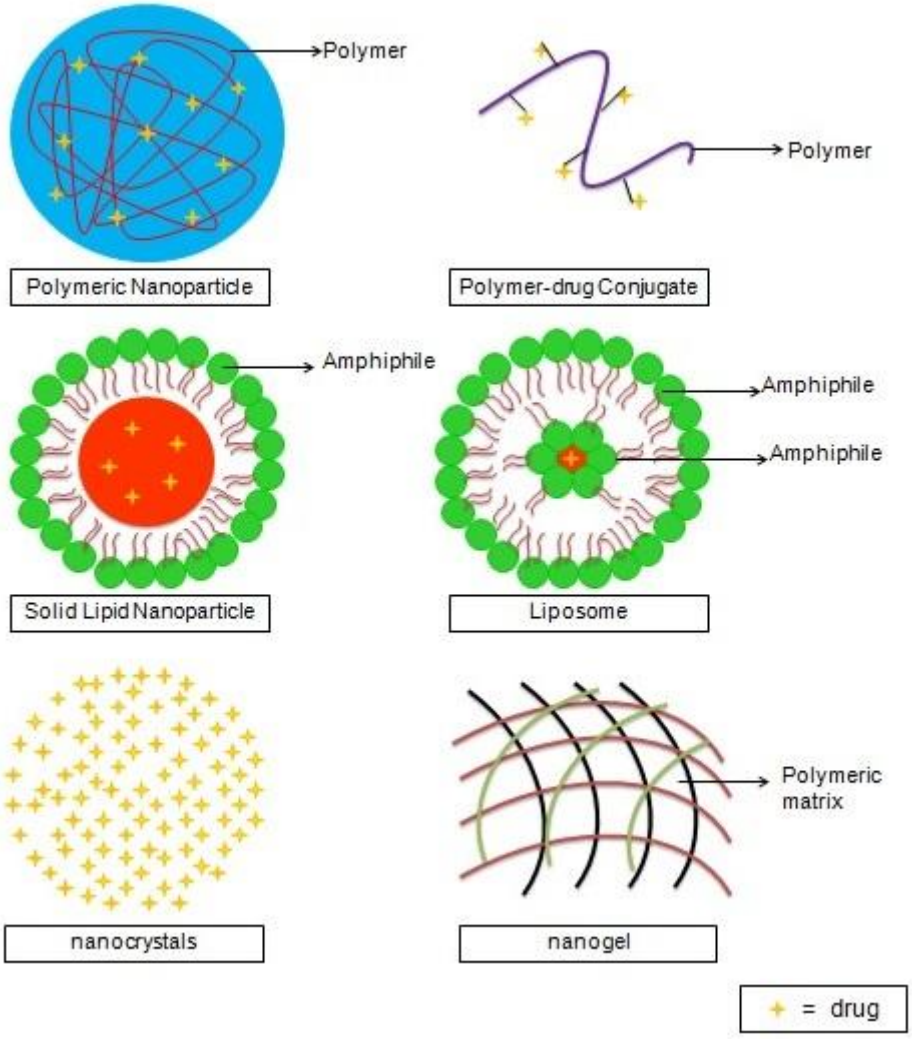

Figure 2.3: The different types of nanosystems.

Physicochemical characterization of the drug is essential in ascertaining if a formulation will progress from the research stage to the clinical stage. For this reason the size of the particle, the polydispersity index, the zeta potential, shape, impurities, drug payload, hydrophobic-hydrophilic balance and the molecular weights must be evaluated. The particle size, surface charge, surface modification and hydrophobicity of a nanosystem are the characteristics that can be modified in order to yield particles with the above mentioned advantages. The size will determine which barriers in the body the particle will be able to cross (Kumari et al., 2010). Surface charge determines the interaction of the particle with the cells of the body as well as its behaviour in the blood. Surface modification is needed to extend the time spent in circulation as hydrophobicity has an impact on the rate of clearance by the macrophages of the immune system. Furthermore, morphological characteristics, surface chemistry and molecular weight of the polymer impact on the *in vitro* and *in vivo* behaviour of the system. Modifying the surface to yield anti-adhesive particles reduces removal by macrophages which can allow for better permeation (Shenoy and Amiji, 2005). Molecular weight is related to the release of the drug as the higher the molecular weight of the polymer, the slower the release of drug occurs *in vitro*. The drug release from a nano- or microparticle is a measure of its success as a formulation. *In vitro* drug release can be measured in various ways such as juxtaposed diffusion cells with a separating membrane (a dialysis membrane), dialysis bag diffusion method, reverse dialysis sac technique, ultrafiltration and ultracentrifugation. In view of the above, major concerns with both microsystems and nanosystems are (Padalkar et al., 2011):

- The size range of the system should meet the desired requirement.
- Drug entrapment must be sufficiently high.
- The quality of the system and the release profile must have reproducibility.
- The preparation method must not affect the stability and activity of the drug/active compound.

Due to their defining characteristics they can be combined in such a manner as to overcome each systems limitation as well as amplify their advantages in order to yield an optimal drug delivery system.

2.5 Preparation of Multiparticulate Systems

There is an overlap in the preparation methods for nanoparticulate and microparticulate systems. Choosing the correct method is imperative as each method has advantages and disadvantages. Methods commonly used for microsystems include phase separation, coacervation (simple and complex), solvent evaporation and extraction, microemulsion

techniques, micro-fluidic technology, spray drying and spray congealing, polymerization, wet inversion and hot melt microencapsulation. The method of preparation for pure drug nanoparticles differs from those used to prepare nano-sized drug carriers such as polymeric nanoparticles. Pure drug nanoparticles can be formulated using high pressure homogenisation or high energy wet milling (top-down processes) or solvent evaporation methods (such spray drying, cryogenic solvent evaporation and rapid expansion of supercritical solutions) and antisolvent methods (such as liquid antisolvent and supercritical antisolvent). The latter are known as bottom-up processes. Nanosuspensions can also be produced using the top-down and bottom-up approaches. Polymeric nanoparticles can be formulated using emulsion polymerisation techniques and interfacial polymerisation (employed in the polymerisation of monomers) or dialysis, salting out, solvent evaporation, solvent displacement method (i.e. nanoprecipitation), and supercritical fluid technology (used for preformed polymers).

2.6 Comparison of Microsystems and Nanosystems

Nanosystems and microsystems are ideal for long term therapy as they allow a high drug loading into a small volume albeit to different degrees (with nanosystems showing a higher loading compared to microsystems). Nanoparticles are versatile as they can be delivered as a solid powder or a fluid by incorporation into a liquid vehicle. Microspheres are generally chosen for IM or subcutaneous (SC) depots while nanoparticles are favoured in short acting preparations. However, modification of constituents can render nanoparticles as long acting systems as well. Nanoparticle formulations are not governed by fed/fasted variation as microparticles are (Gao et al., 2012). In addition, a reduction in dosing frequency is brought about by these systems which augment patient compliance (Kumari et al., 2010). The size difference between microsystems and nanosystems is not negligible as this can have significant implications on the manner in which the system behaves and its effect on the desired outcome. Table 2.2 provides a summary of the major differences between microsystems and nanosystems with regards to their delivery of drugs and other bioactives (Kohane, 2006).

Table 2.2: Comparison of microsystems and nanosystems in drug delivery (Kohane, 2006).

Feature	Microparticles	Nanoparticles
Drug-loading	Low due to small surface area	High due to large surface area
Drug release	Slower therefore favoured for depot formulations	More rapid water penetration resulting in faster drug release
Degradation	Slower due to larger size	Faster due to smaller size

Aggregation	Less prone	More prone
Effect on circulatory system	Greater chance of embolism when given intravenously	Easy circulation through the vascular system. If particles are coated they can avoid clearance by the Reticulo-endothelial System (RES).
Ability to cross biological barriers	Unable to cross many biological barriers	Able to cross biological barriers depending on the size of the particles and the barrier in question
Type of endocytosis	Can only enter phagocytic cells	Can enter both phagocytic and pinocytic cells
Ability to illicit inflammatory response	Yes	Yes

2.7 Challenges of Multiparticulate Systems

As with any delivery system there exists certain attributes that may be of concern. This is true with multiparticulate systems as well. However it is imperative that researchers identify these concerns and work towards overcoming them so that the final system meets the standard safety requirements. A concern with microsystems is that they may have a short residence time at the absorption site; this can be overcome by giving the particles bioadhesive properties which will prolong the contact time between absorption membranes and the particles (Vasir et al., 2003). Particles may aggregate due to their small size and large surface area which can pose problems in handling of liquid or solid preparations. Additionally, regarding polymeric microspheres, the safety of these have not been studied extensively (Jaspart et al., 2007). Other problems encountered with microparticles include difficulty in controlling drug release rates (e.g. burst release), preparation methods may inactivate the drug and large-scale manufacturing may be laborious (Kim and Pack, 2007). A unique feature of nano-products is that they give novel characteristics to chemicals that do not have these properties when formulated as larger products. Due to their size they can access areas that microparticles cannot thus nanoparticles can be more cytotoxic than their larger counterparts. This is particularly important because FDA approval is largely dependent on the safety profile of a compound. Another toxic effect stems from using materials that are not biodegradable. The choice of surfactants used as well as its binding to the particles also influences toxicity (Müller et al., 1997). The physicochemical and physicomechanical properties of drug carriers greatly control their ability to exert a therapeutic effect; this includes their size, shape, surface chemistry, composition and mechanical flexibility. By optimising these traits it is possible to create advanced carriers. However there are still limitations of these carriers such as selectivity of target region,

clearance by the immune system and poor drug concentration at the target area (Farokhzad and Langer, 2009). These limitations arise from the fact that the carrier has to overcome many physiological impediments from the time of administration until they reach their destination. Hurdles that are faced include renal clearance and the RES which is responsible for clearing the body of foreign matter. These issues lead to the development of adaptive particles; these are able to change their characteristics by evolving in response to a stimulus (Yoo et al., 2011). Nanoparticles have shown great promise in this field and can aid in addiction treatment as a formulation is only truly successful if it can overcome the biological mechanisms that prevent it from reaching the target site. Although nanoparticles have been studied extensively for years, only a small number are used clinically (Zhang et al., 2008; Gaspar and Duncan, 2009; Sanchis et al., 2010). Of those that have, none of them are indicated for CNS disorders despite the widespread occurrence and severity of these illnesses (Costantino and Boraschi, 2012).

2.8 Selection of Polymers for Multiparticulate Systems

The choice of compatible polymers is influenced by the desired release profile. An important application of polymers that are biodegradable is for use in controlled drug delivery systems. It is imperative that all polymers used be biodegradable to avoid the risk of toxicity thus making them safe for parenteral administration. Polymers exhibit different traits and, depending on the formulation requirements, they can be selected accordingly. The drug loading capacity, drug release, physicochemical drug properties and the biological activity can be altered depending on the choice of polymer. This allows polymeric nanoparticles and microparticles to be applicable to many classes of drugs as well as various routes of administration. This is directly relevant to the treatment of addiction as manipulation of the polymers can result in a system that meets the requirements of a successful anti-addiction system. Polymers can be natural or synthetic. FDA approved synthetic polymers suitable for use in humans include *poly(lactic-co-glycolic acid*) (PLGA), polylactic acid (PLA) and polycaprolactone (PCL). These biodegradable and biocompatible polymers are important as they have shown positive outcomes as carriers for drugs used in CNS disorders. PLGA is favoured in the formulation of nano and microsystems as its versatile nature allows it to have a broad spectrum of application. It can be used with a variety of therapeutic agents. This is evident from the successful incorporation of naltrexone into PLGA microspheres (Vivitrol®) (see Table 2.1.) as well as methadone in PLGA microspheres (Negrın et al., 2001). PLA is also well-suited for nanosystems and microsystems. PLA has been studied as a microsphere carrier for methadone (Negrın et al., 2001) as well as a nanoparticle carrier for other CNS drugs (thus confirming its ability to be used in CNS disorders such as addiction) (Kumari et al., 2010). Additionally, studies on polymeric nanoparticles containing PLGA and

PLA showed sustained release as well as suitable sizes for parenteral administration (Musumeci et al., 2006). PCL is favoured in long-term preparations due to its slow rate of degradation. It has also been used for the controlled release of narcotic antagonists (Pitt et al., 1980). Microspheres of PCL have shown excellent tolerance and prolonged duration of action (9 months) when implanted into the rat brain (Menei et al., 1994). Figure 2.4 and Figure 2.5 clearly illustrate the compatibility of PLGA and PLA with microsystems. The internal matrix of a blank PLGA microsphere can be seen in Figure 2.4 (Checa-Casalengua et al., 2011). Figure 2.5a and 2.5b depict methadone-loaded PLA microspheres and methadone-loaded PLGA microspheres respectively (Negrın et al., 2001). Natural polymers which are compatible in nanoparticulate and microparticulate systems are alginate, polysaccharides (hyaluronic acid, chitosan and starch) and proteins (collagen, albumin, gelatin).

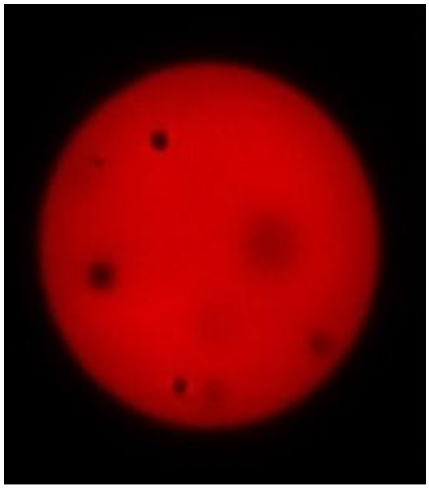

Figure 2.4: Confocal microscopy image of blank PLGA microspheres prepared with Nile red dye. Reproduced with permission from Checa-Casalengua and co-workers (2011).

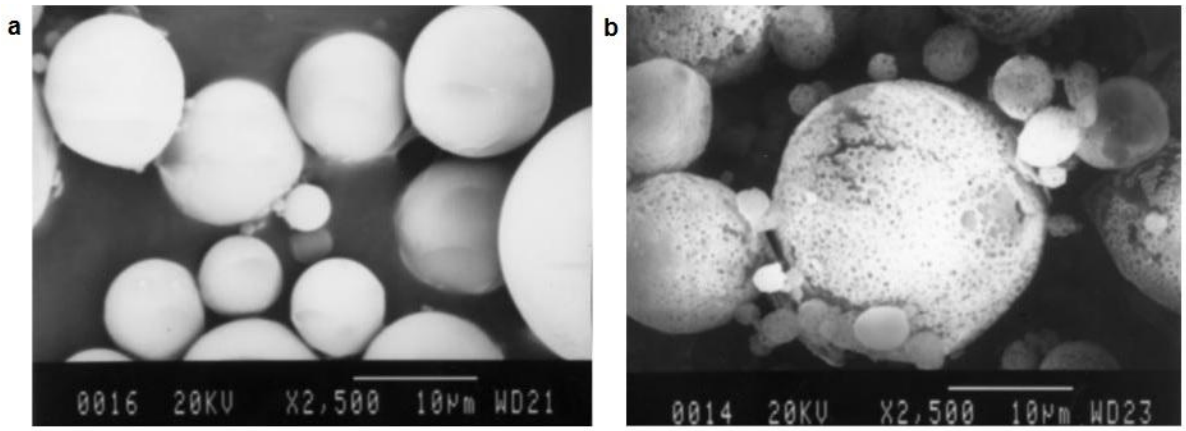

Figure 2.5: Photomicrographs of a) methadone-PLA and b) methadone-PLGA microspheres. Reproduced with permission from Negrin and co-workers (2001).

2.9 Drug Delivery to the Brain

The brain is well perfused but drug delivery to the CNS is poor due to the BBB and Blood-Cerebrospinal Fluid Barrier (BCSFB). The BBB, together with the BCSFB and meninges form a physical and biochemical barrier that work in conjunction with each other to maintain homeostasis of the CNS. The mechanism involved is a controlled, complex process that protects the neuronal tissue from foreign substances. The capillary endothelial wall of the brain, which makes up the BBB, prevents the transport of numerous drugs into the CNS. Due to this intricate anatomy and physiology approximately 98% of actives are unable to cross the barrier and reach the brain (Tosi et al., 2008).

Drug abuse has a detrimental effect on the brain. These substances cause damage to the BBB which in turn causes degeneration of the CNS (Sharma and Kiyatkin, 2009). An unfortunate fact of substance abuse and its treatment is that while the drug of abuse easily affects the CNS, those same drugs that can treat it are not easily transported to the CNS. Effective treatment of brain disorders requires that the drug cross over the BBB in order to exert its effect but the impermeable nature of the BBB results in suboptimal therapeutic outcomes. Despite these limitations, treatment of CNS disorders is rapidly progressing and some of the facets of pharmaceutical breakthroughs are infusion pumps which deliver drugs into the CSF, disruption of the BBB via osmotic mechanisms, drugs coupled to a specific carrier, tissue or cell implants as well as gene therapy (Benoit et al., 2000). Regarding the carrier mediated option, nanoparticulate and microparticulate systems are specific types which can be employed. While microparticles are unable to cross the BBB it is possible for them to be administered to the brain directly via injection (Kohane, 2006). The small size of microparticles allows them to be implanted using stereotaxy (Benoit et al., 2000).

Nanosystems that have been investigated for CNS disorders include those for neuronal regeneration (Cho and Borgens, 2012) as well nano-carriers for drugs (Kreuter, 2001). Nanosystems that are applicable for CNS delivery are nanoparticles, nanospheres, nanosuspensions, nanoemulsions, nanogels, nanomicelles, nanoliposomes, carbon nanotubes (CNT), nanofibres, nanorobots, SLN's, NLC's and lipid-drug conjugates. While the exact mechanism of transport across the BBB is not completely defined, it is nonetheless a successful method of overcoming many limitations (Kreuter, 2001). Brain retention of polymeric nanoparticles can be prolonged by coating or linking the nanoparticles to PEG, coating the particles with surfactants or conjugating the particles to specific ligands (Bhatt et al., 2013). Oligonucleotides have been used in neurodegenerative disorders as diagnostic and therapeutic tools. The incorporation of oligonucleotides into a modified cationic nanogel comprised of covalently cross-linked poly (ethylene glycol) (PEG) and polyethylenimine (PEI)

chains were successfully used in delivery to the brain (Vinogradov et al., 2004). The size, shape and physicochemical properties of particles (such as lipophilicity) have important implications in nanosystem drug delivery to the brain. Particles can cross the BBB by passive diffusion provided they are lipophillic and have the ideal molecular weight (Kreuter, 2001). For effective BBB delivery particles must be 50nm or smaller (Wong et al., 2011) and further coating of particles with polysorbate is a requirement for transport to the brain (Kreuter, 2001). Poly (butyl cyanoacrylate) (PBC) is a biodegradable polymer which has had success in *in vivo* brain drug delivery. In addition for successful penetration of the BBB, PBC nanoparticles coated with polysorbate 80 can also prolong the action of those CNS drugs that have a short duration of action (Cho and Borgens, 2012).

2.10 Reformulation of Anti-Addiction Drugs into Multiparticulates

A crucial aspect which establishes how successful a pharmaceutical product will be is the drug delivery system that is employed. The following drugs have been formulated into microparticulate and nanoparticulate systems with varying degrees of success.

2.10.1 Disulfiram

Various efforts have been undertaken to incorporate disulfiram into a nanosystem. One of the earlier studies involved disulfiram-loaded nanoparticles for drug delivery to the cochlea. The particles formulated were liposomes and polymersome nanoparticles; both of these were formed from amphiphilic molecules (Buckiova et al., 2012). The lipid used in the liposome formulation was phopsphatidyl choline from egg yolk and 1,2-distearoyl-*sn*-glycero-3-phosphoethanolamine-N-[methoxy(polyethylene glycol)-2000] (EggPC:DSPE-PEG-2000). The polymersome block copolymer employed was polyethylene glycol-/block/-poly (ε-caprolactone). Disulfiram was selected as a model neurotoxic agent. In another study disulfiram was complexed to group 12 metals; the resulting complexes were then used as precursors, together with surfactants, for the successful synthesis of metal sulphide nanoparticles (Shukla et al., 2014). Disulfiram nanoparticles were also formulated for use in treatment of glaucoma (Nagai et al., 2015). The nanoparticle system of disulfiram, benzalkonium chloride (BAC), D-mannitol, (2-Hydroxypropyl)-β-cyclodextrin (HPβCD) and methylcellulose (MC) were prepared by a bead mill method. Disulfiram has been frequently employed in chemotherapeutic studies utilising nanosystems. A research group developed pH-sensitive acid-cleavable polymeric micelles for the co-delivery of doxorubicin and disulfiram were developed (Duan et al., 2013). In this study poly(styrene-co-maleic anhydride) was derivatised with adipic dihydrazide. Doxorubicin was then conjugated to this through an acid-cleavable hydrazone bond. This conjugate had the ability to self assemble into micelles during which the encapsulation of disulfiram occurred. The system displayed

desirable properties which made it suitable for cancer therapy. The anticancer potential of disulfiram polymeric nanoparticles was also investigated. The nanoparticles were made up of PLGA and different surfactants and the outcome of the study stated that these particles had significant promise against hepatocellular carcinoma (Hoda et al., 2015). The diverse application of disulfiram nanoparticles is evident from the above; consequently it can be assumed that disulfiram nanoparticles can also be used for alcohol abuse by modifying the route of administration. Disulfiram has so far not been incorporated into any form of microsystem.

2.10.2 Naltrexone

Naltrexone is a potent yet safe opioid antagonist with application in opioid and alcohol addiction. Effectiveness is enhanced if given for long term in sufficient quantities but water solubility of naltrexone posed an issue relating to its release and various studies have been conducted to slow down its release. This includes the use of complexes of the drug in oil, polyglyceride pellets and polyleucine-polyglutamate tubes (National Institute on Drug Abuse Research Monographs Series, 1976). A naltrexone incorporated PLA-PEG-PLA nanogel polymer system showed drug release up to 35 days (Asadi et al., 2011). Another study detailed on the method of preparation of microspheres and used PLA as the polymer and naltrexone as the active being tested (Falk et al., 1997). The microspheres showed naltrexone release for up to 3 weeks. Other investigations of PLA-naltrexone involved formulating these microspheres using the solvent evaporation method (Dinarvand et al., 2003). An additional study on naltrexone involved microspheres with PLGA which were capable of release for 30-150 days (Akala et al., 2011). The FDA approved drug Vivitrol® that has shown efficacy in treating alcohol abuse has the opioid antagonist, naltrexone, in a PLGA microsphere system. The efficacy and safety was tested for six months using a randomised, double-blind, placebo controlled trial (Garbutt et al., 2005). The outcome of the trial showed that the IM injection is well tolerated and is affiliated with a marked decrease in heavy drinking. Nanoparticles loaded with naltrexone were prepared from grafted poly(ethylene glycol-co-methyl methacrylate) (PEO-MMA) (Yin et al., 2002). Two formulations were made- one with a 1:1 PEO-MMA composition and one with a 1:4 PEO-MMA composition and the aim of the study was to develop a long-acting injectable nano-sized drug delivery system. Both systems showed biphasic release where the initial release is a burst effect and the second phase was over a period of time. Both formulations released drug for at least 20 days. This is significant as the overall aim of sustained release formulations is to minimise the administration thereby enhancing compliance. In another study poly(N-isopropylacrylamide)-block-poly(D,L-lactide) (PNIPAAm-b-PLA) was used as the polymer carrier to prepare naltrexone-loaded micellar nanoparticles (Salehi et al., 2013).

Sustained release for 35 days was achieved with both copolymers. The PLA content was reported to affect the release and drug loading ability of the micelles. The drug release can be changed by altering the length of the PLA component. This provides further proof that the Vivitrol® injection is definitely capable of sustained release for the long term treatment of alcoholism and narcotic addiction. Pagar et al. (Pagar and Vavia, 2013) reported on naltrexone-loaded lactide-depsipeptide poly[LA-(Glc-Leu)] microspheres that were capable of sustained release. The results indicated 80% of naltrexone release after 30 days. A novel thermosensitive penta-block copolymer poly(N-isopropylacrylamide)-*b*-poly(ε-caprolactone)-*b*-poly ethylene glycol-*b*-poly(ε-caprolactone)-*b*-poly(N-isopropylacrylamide) (PNIPAAm-*b*-PCL-*b*-PEG-*b*-PCL-*b*-PNIPAAm), capable of self assembly into nanomicelles, was synthesised by Abandansari et al. (Abandansari et al., 2013). The copolymer was utilised as a hydrogel to study the release profile of naltrexone. The system showed good potential for use in injectable sustained release systems.

2.10.3 Nicotine Replacement Therapy

A microparticulate system comprising of nicotine encapsulated in Sephadex® microspheres was formulated for nasal administration (Cornaz et al., 1996). The system released 90% of nicotine within 15 minutes and this rapid delivery of nicotine is believed to assist smokers in overcoming the desire to smoke. Consequently this system is promising and further work can lead to an improved form of NRT. Nicotine and cotinine loaded lipid-based nanoparticles were also developed for use in nicotine addiction (Lautenschlager and Elias, 2010). The use of nano drug delivery for nicotine addiction was also investigated (Strasinger et al., 2009). Their formulation approach consisted of CNT membranes in a transdermal system. CNT have distinctive chemical, geometrical and electrical features that assist in overcoming the difficulties associated with variable rates of drug delivery. The investigators propose that the patch will have a unique set-up that will enable multiple and variable dosing depending on the need of the patient. Skin conductance variability due to withdrawal symptoms (increased sweating, varying circulation etc.) may be problematic with conventional transdermal preparations but the CNT will have increased dosing flexibility so that this will no longer be a problem. Researchers argue that the risk of abuse may be present due to the high dose of nicotine delivered and the patient-activated system, but this can be prevented by a ‘multi-use lock-out system’ which shuts off the patch when the correct amount has been administered as well as prevents administration from occurring too often. The outcome of the study was in favour of the CNT system for nicotine addiction and opioid withdrawal. The use of this system is not limited to clonidine and NRT and can be applied to any skin permeable drug and could even be used for multiple drug delivery. Other options for nicotine and its metabolites can also contain microspheres amongst other delivery systems (Hugerth et al.,

2010). The system aims to overcome the limitations of current therapies such as compliance and efficacy. The system will allow controlled as well as sustained release which will ultimately reduce nicotine cravings. Nicotine gum has long been a mainstay in the treatment of nicotine addiction. Current options recommend using 6-12 pieces of gum a day depending on the strength of the gum. Furthermore, one piece can only be chewed for a maximum of 30 minutes before the flavour is lost. Microencapsulation offers a solution to this problem as it can allow sustained release of the active, the sweetener used and/or the flavouring used in the gum. In addition, it inhibits damage to the dental enamel as small particles (≤ 100μm) prevent the disagreeable grainy sensation from chewing (Ghadavi et al., 2011). In 2013 researchers summarized the development of spray dried bioadhesive nicotine microparticles for compressed medicated chewing gum (Sander et al., 2013). It is believed that by encapsulating nicotine into a polymeric matrix, nicotine is retained in the oral cavity. This minimises GIT disturbances. The outcome of the study showed that spray drying microparticles maintained an encapsulation efficiency of close to 100% which is advantageous as the dose of nicotine being delivered is important in NRT. Additionally, spray drying did not adversely affect *in vitro* release.

2.10.4 Bupropion

Sustained release bupropion nanospheres for pulmonary delivery were formulated from agar (Varshosaz et al., 2014). These can be modified to deliver bupropion in a controlled and extended manner. To date bupropion has not been studied in microsystems.

2.10.5 Varenicline

Proposed delivery systems for varenicline encompass intranasal, buccal, pulmonary and sublingual preparations (Ziegler and Johnson, 2006). The invention states that the intranasal dosage form may be made up of microspheres which are composed of starch, gelatine, albumin or collagen. If formulated using bioadhesive polymers, such as cross-linked starches, the efficacy of this drug will be enhanced. Bioadhesive spheres can be used for intranasal delivery which has shown promise in the delivery of drugs to the Central Nervous System (Dhuria et al., 2010). Nanosystems of varenicline have not been investigated to date.

2.10.6 Methadone

Using a controlled release preparation for a longer duration eliminates the need for daily dosing which positively influences efficacy and compliance. Research on biodegradable microspheres using poly (D,L-lactide) showed 70-80% *in vitro* release of drug over 7 days (Delgado et al., 1996). Methadone-PLA microspheres and methadone-PLGA microspheres

showed drug release over 6-9 days (Negrın et al., 2001). Similarly PLGA and PLA implants showed release over a week and over a month (depending on the components of the formulation) (Negrın et al., 2004). Further studies conducted on methadone (as well as naltrexone and buprenorphine) incorporate these actives in microparticles for the treatment of substance abuse (Tice et al., 2009). The microparticles consisted of the active ingredient and poly (D,L-lactide). Depending upon the composition of the formulation effective release of the active continued for at least 28 days in some cases and in other cases it continued for greater than 28 days. The technology has been patented and the patent states that microparticles refers to nanospheres, nanocapsules and nanoparticles. Furthermore, a nanocarrier based long acting delivery system for methadone was patented in 2015 (Hamidi, 2015b). The system contains a lipid layer, a phospholipid bilayer with the methadone; and a polymer coating. According to the patent there are a variety of suitable excipients for each component. The lipid layer could consist of monostearyl glycerol, a distearyl glycerol, a palmitic acid, a stearic acid or a glyceryl stearate. The phospholipid bilayers could consist of a phosphatidylcholine, a phosphatidylethanolamine,or a phosphatidylinositol. The polymer coating could be made up of chitosan, a polyethylene glycol, or a polyvinyl alcohol.

2.10.7 Buprenorphine

Due to extensive intestinal and hepatic metabolism buprenorphine has only been available in a sublingual form and a parenteral form. These preparations do not have continuous release properties (Wang et al., 2009). Another limitation of buprenorphine is its potential for abuse but this can be overcome by a modified drug delivery system as patients will not be able to abuse it in this form. Yet another clinical concern with buprenorphine is the issue of adherence and compliance. Dealing with this an extended release preparations of buprenorphine were designed (26, 85). A study carried out in 2009 proved that slow and sustained release of buprenorphine from nanoparticles was possible (Wang et al., 2009). They investigated ester prodrugs of buprenorphine formulated as SLNs, NLCs and lipid emulsions (LE). The liquid lipid used was linseed oil while the solid lipid used was cetyl palmitate. All the formulations tested displayed slow and sustained delivery with SLNs having the highest release followed by NLCs and thereafter LE. A further study regarding an extended release formulation has also shown promising results (Koocheki et al., 2011). The release of buprenorphine hydrochloride was studied from a PLGA (capped PLGA and uncapped PLGA) system with and without Tween 80. The capped PLGA (RG752S) had a lower percentage release than the uncapped PLGA (RG752H) with and without Tween 80, due to the difference in polarity between the two forms of PLGA. Moreover, Tween 80 increased the release rate of both capped and uncapped PLGA. All formulations showed release for at least 48 hours. The delivery of buprenorphine-PLGA microspheres into the

skin to sustain release while simultaneously maintaining compliance was also assessed. However this proposal did not yield any positive results with regards to delivering microspheres using electroporation (Bose et al., 2001). In 2005 buprenorphine microparticle systems were explored as a credible option for substance abuse and analgesia (Mangena and Murty, 2005). Formulations comprised of buprenorphine and PLGA. In 2013 buprenorphine microparticles were studied for the treatment of opioid dependency (Fischer, 2013). The particles were formulated using weak acids and are claimed to be used for the rapid release of drug to allow fast onset of action. A recent invention provided a method of efficient encapsulation of buprenorphine and the release thereof in a controlled way (Mandal and Graves, 2014). The preferred polymer for this microencapsulation is PLGA, however it is not limited to this. The *in vitro* release profile displayed steady release over several months. Additionally, the patent mentioned under methadone (Hamidi, 2015b) is also applicable to buprenorphine (Hamidi, 2015a).

2.10.8 Naloxone

The weak acid microparticles mentioned under buprenorphine (Fischer, 2013) are appropriate for naloxone particle formation as well. Prior to this study naloxone-loaded poly-ε-caprolactone microspheres were produced which showed a release of 80% of naloxone within 8 days (Gil-Alegre et al., 2005). No further records of naloxone nanosystems have been found. However, in situ forming microparticle implants have been used for the administration of narcotic antagonists (Yapar et al., 2012). To date, the above mentioned drugs are the only FDA approved addiction treatments that have been researched as potential nano and/or microsystems. Table 2.3. provides a summary of this. Acamprosate has not been studied in nanosystems or microsystems.

Table 2.3: Summary of FDA approved treatments formulated as nanosystems and/or microsystems.

Drug Name	Nanosystem	Reference	Microsystem	Reference
Acamprosate	None	-	None	-
Disulfiram	Polymer nanoparticles	Buckiova et al., 2012	None	-
	Metal sulphide complex nanoparticles	Shukla et al., 2014		
	BAC/ HPβCD/MC nanoparticles	Nagai et al., 2015		
	Disulfiram-			

	Doxorubicin loaded derivatised poly(Styrene-co-Maleic Anhydride) micelles	Duan et al., 2013		
	PLGA nanoparticles	Hoda et al., 2015		
Naltrexone	PLA-PEG-PLA nanogel	Asadi et al., 2011	Poly(L-lactide) microspheres	Falk et al., 1997
	PEO-MMA nanoparticles	Yin et al., 2002	PLA microspheres	Dinarvand et al., 2003
	PNIPAAm-b-PLA nanomicelles	Salehi et al., 2013	PLGA microspheres (Vivitrol ®)	Garbutt et al., 2005; Akala et al., 2011
	Penta-block copolymer hydrogel	Abandansari et al., 2013		
			Lactide-depsipeptide poly[LA-(Glc-Leu)] microspheres	Pagar and Vavia, 2013
Nicotine (NRT)	Carbon nanotubes	Strasinger et al., 2009	Sephadex® microspheres	Cornaz et al., 1996
	Lipid nanoparticles	Lautenschlager and Elias, 2010	Cellulose/starch microspheres	Hugerth et al., 2010
			Polymer microencapsulation in chewing gum	Ghadavi et al., 2011
			Spray-dried bioadhesive hypromellose/alginate microparticles in chewing gum	Sander et al., 2013
Bupropion	Agar nanospheres	Varshosaz et al., 2014	None	-
Varenicline	None		Natural (starch, albumin, gelatine, collagen) polymer microspheres	Ziegler and Johnson BA, 2006
Methadone	Lipid, phospholipid polymer coated nanocarrier	Hamidi, 2015	Poly(D,L-lactide) microspheres	Delgado et al., 1996
			PLA and PLGA microspheres	Negrın et al., 2001

			Poly(D,L-lactide) microparticles	Tice et al., 2009
Buprenorphine	Lipid nanoparticles	Wang et al., 2009	PLGA microspheres	Bose et al., 2001
	Lipid, phospholipid polymer coated nanocarrier	Hamidi, 2015	PLGA microparticles	Mangena and Murty, 2005
			Cellulosic microparticles admixed with a weak acid (citric/acetic/fumaric acids)	Fischer, 2013
			PLGA microparticles	Mandal and Graves , 2014
Naloxone	None		Cellulosic microparticles admixed with a weak acid (citric/acetic/fumaric acid)	Fischer, 2013
			poly-ε-caprolactone microspheres	Gil-Alegre et al., 2005

2.11 Other Potential Treatment Options for Drug Addiction

In the quest to cure addiction research has progressed beyond the traditional pharmaceutical actives. Studies have extended to encompass viable options ranging from different active pharmaceutical ingredients to proteins and immunopharmacology. While these have not been FDA approved they have shown potential in addiction disorders in the hope that they may fill in the gaps in current treatment options. Below is a summary of these findings.

2.11.1 Glial Cell Line-Derived Neurotrophic Factor

Glial cell line-derived neurotrophic factor (GDNF) has been studied in the treatment of cocaine addiction as it enhances dopaminergic neuron survival, provides protection from ill effects of neurotoxic lesions and reduces cocaine-seeking behaviour in experimental rats. The effect of conjugating GDNF to maghemite nanoparticles in order to determine the feasibility in the treatment of cocaine dependence was investigated (Green-Sadan et al., 2005). Sprague-Dawley rats underwent stereotaxic surgery or intra-brain injections of varying combinations of nanoparticle-GDNF as well as solely nanoparticle formulations. The rats were then monitored to observe the effect of the formulation on the self administration of

cocaine. The nanoparticle formulation led to the inhibition of self administration of cocaine especially when compared to free GDNF or free nanoparticles.

2.11.2 Topiramate Microparticles and Nanoparticles

Pre-clinical and early stage clinical trials have shown that the use of topiramate and amphetamine (both independently and together) have a positive effect on cocaine addiction (Mariani et al., 2012). In 2011 a patent was filed relating to taste masked microparticles of topiramate in an orally disintegrating tablet (Venkatesh and Harmon, 2011). The formulation is applicable to various medical conditions as well as alcoholism and drug addiction. The microparticle aspect of the formulation aims to be 400µm maximum in order to allow for a smooth feeling in the mouth as well as minimal after taste. This microsystem will thus enhance compliance as patients will be more willing to take the medication as it is pleasant tasting. Furthermore the drug release could be altered by employing different polymers and excipients. Another invention reported topiramate nanoparticles of size less than 2000nm (Gustow et al., 2008). The patent quotes of using topiramate for a variety of illnesses and disorders including alcoholism, nicotine and drug addiction. Moreover, other research shows its potential in the treatment of cocaine addiction. The invention aims to improve the pharmacokinetic profile of topiramate, decrease side effects, reach the same therapeutic effect with fewer/lower doses, decrease cost and increase compliance. The nanoparticles were tested in male Beagle dogs; one group received a tablet form while the other received a liquid dispersion. The time to reach the maximum concentration in the blood in all dogs studied was 2 hours. However this can be modified by changes in the formulation.

2.11.3 Risperidone Microspheres

The atypical antipsychotic risperidone is available as a microsphere product for the treatment of schizophrenia (Kohane, 2006). Microspheres have showed promise in the treatment of Parkinson's, Alzheimer's, neural degeneration, neuro-oncology as well as for anaesthesia (Benoit et al., 2000) and Huntington's Disease (Nicholas et al., 2002). This further strengthens the argument that microsystems can be used to enhance delivery of CNS drugs and thus improve treatment of CNS disorders including addiction.

2.11.4 Immunopharmacology

Immunopharmacology is a viable option for substance abuse treatment. It encompasses the production of an antibody which binds the drug of abuse (Heidbreder, 2005). By binding to the drug it will alter the pharmacokinetic in such a way that it produces a therapeutic effect (Heidbreder, 2005). Adjuvants which are an integral component of vaccines allows them to set off an immune response (Wieber et al., 2011). PLGA is the polymer that has shown

potential of having adjuvant action (Wieber et al., 2011). Nanoparticles with PLGA incorporated as an adjuvant have had successful results in vaccination (Wieber et al., 2011). Additionally, the use of microspheres in vaccines has been researched as well (Alagusandaram et al., 2009) which is important as vaccines are being considered a suitable method for treating addiction (Orson et al., 2008). An *in vivo* and *in vitro* study carried out in 2003 investigated the viability of an anti-cocaine catalytic antibody in a PLGA microsphere system (Homayoun et al., 2003). The outcome of the study showed that the microsphere preparation administered subcutaneously allowed for controlled release of the antibody. Further manipulation of the formulation can allow for greater therapeutic effect. An alternative that is being studied for smoking cessation is the use of vaccines. The vaccine contains antibodies which prevent nicotine from entering the CNS (Bevins et al., 2008). Several different forms of the vaccine have shown therapeutic benefit. Selecta Biosciences Inc. (Watertown, Massachusetts, USA) has developed an SEL-068 vaccine composed of four major elements: an artificial TLR agonist, a novel universal T-cell helper peptide, a polymeric matrix which is biodegradable and biocompatible, and nicotine. In this system, nicotine is covalently conjugated to the surface of the nanoparticle (Fahim et al., 2013). It is believed that the vaccine has duration of action that can extend over years. A physical constraint modulation system containing PLGA microparticles was developed in 1998 (Kitchell et al., 1995). The active ingredient employed is lobeline- a natural alkaloid with pharmacological similarity to nicotine. The objective is to allow sustained and controlled release so that long-term therapeutic levels can be obtained. The formulation is administered as subcutaneous or intramuscular injections and the minimum *in vitro* release observed is 1 week establishing its capability of sustained release. Formulating abuse-prone drugs as an abuse deterrent formulation can greatly lessen the impact of drug abuse. It is uncertain if nano and microsystems can assist in this regard but based on its broad spectrum there is no reason why it cannot be useful in the preparation of abuse deterrent formulations. A novel nicotine vaccine which could overcome the shortcomings of previous nicotine vaccines was looked at by Hu et al. (Hu et al., 2014). In this study a nano-lipoplex was created by conjugation of bovine serum albumin to the surface of cationic liposomes made of 1,2-dioleoyl-3-trimethylammonium-propane (chloride salt) (DOTAP) and 1,2-distearoyl-sn-glycero-3-phosphoethanolamine-N-(maleimide[polyethylene glycol]-2000) (ammonium salt) (DSPE-PEG[2000]-maleimide). The outcome stated that this nano-lipoplex could be useful in improving the immunogenic ability of existing nicotine vaccines.

2.11.5 Gene Silencing Nanotechnology

Gene silencing nanotechnology has also been explored as a viable option for addiction treatment (Bonoiu et al., 2009). The neuronal phosphoprotein DARPP-32 is a key

component in the activation of the dopaminergic signalling pathway. Activation of this pathway results in addiction to substances of abuse (e.g. opiates). The rationale behind this research stems from the knowledge that suppression of the DARRP-32 gene can inhibit addiction by blocking the reward pathway. DARPP-32 can be silenced by its siRNA antagonist. Complexation of siRNA with gold nanorods yielded promising *in vitro* results. This nanoplex not only silenced the DARPP-32 gene but other effector genes as well. Furthermore the gold nanorods provided an efficient carrier for siRNA, and in doing so, enabled targeted delivery to the brain as well as protected the siRNA molecules from rapid degradation.

2.12 Concluding Remarks

There is a dire need for effective pharmacological intervention in the treatment of substance abuse as it has a synergistic effect when used in conjunction with psychosocial interventions. It has been proven that there are definite advantages of medication-assisted treatment in addiction. Regardless of the modest number of commercial products available that use biodegradable polymers, the therapeutic benefit is firmly cemented in research. This provides the best stepping stone towards clinical use. There appears to be an overlap in the treatment for alcohol and opioid abuse. This is significant as successful micro-forms and nano-forms of one drug can be used to treat both conditions. Formulating available actives into multiparticulate novel drug delivery systems strengthens numerous aspects of these formulations such as performance, efficacy, safety and compliance. The following quote succinctly captures the beneficial outcomes of novel and innovative drug delivery systems: "In the form of a NDDS, an existing drug molecule can get new life, thereby increasing its market value and competitiveness and even extending patent life" (Dey et al., 2008).

CHAPTER 3

DESIGN FABRICATION, OPTIMIZATION AND *IN VITRO* CHARACTERIZATION OF DISULFIRAM-LOADED d-α-TOCOPHERYL POLYETHYLENE GLYCOL 1000 SUCCINATE NANOMICELLES

3.1 Introduction

The inherent instability of disulfiram in gastric fluids and blood demotes the oral form of disulfiram to a status of limited clinical application. Furthermore, the fashioning of an injectable formulation of disulfiram is onerous due to the immensely hydrophobic nature of disulfiram (Chen et al., 2015) (Figure 3.1). This drawback can be overcome with a suitable carrier system such as an intramuscular injectable gel based nanosystem.

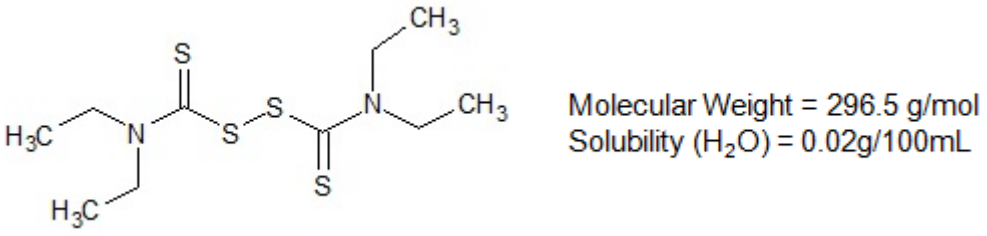

Figure 3.1: Chemical structure of disulfiram.

In recent years the drug delivery domain has been inordinately diffused with nano delivery systems and justifiably so. Of particular interest is that of nanomicelles. These carriers possess a wide array of beneficial elements (Table 3.1). The exclusive structure of a micelle comprises two components- a hydrophilic outer layer and a hydrophobic inner core (Nishiyama and Kataoka, 2006). This core-shell formation affords this carrier a multitude of advantages (Table 3.1).

Table 3.1: Advantages of nanomicelles.

Advantages	Reference
The inner core allows containment of the drug.	Nishiyama and Kataoka, 2006
The outer layer has been known to increase bloodstream retention time.	Nishiyama and Kataoka, 2006
Nanomicelles promote controlled drug release and efficient drug loading.	Nishiyama and Kataoka, 2006
The parent compound does not need chemical modification enhancing ease of preparation.	Nishiyama and Kataoka, 2006
Drug incorporation into the core boosts bioavailability as well as safeguards against inactivation by biological media.	Sezgin, 2006
Nanomicelles are also favoured due to the	Sezgin, 2006

small size of the particles formed (<100nm).	
Capable of targeted delivery.	Sezgin, 2006
They have prolonged circulation time.	Sezgin, 2006
Display enhanced tissue perfusion.	Trivedi and Kompella, 2010
They have decreased toxicity.	Trivedi and Kompella, 2010
The in vivo feasibility of nanomedicines is confirmed.	Zhang et al., 2012
Certain nanomicelle carrier systems have advanced to the level of clinical trials.	Trivedi and Kompella, 2010

There exists many polymers that possess the ability to be synthesized into nanomicelles. Of special interest is a derivative of vitamin E. Esterification of the acid group of d-α-tocopheryl succinate and polyethylene glycol 1000 results in the creation of d-α-tocopheryl polyethylene glycol 1000 succinate or vitamin E TPGS (abbreviated here onwards as TPGS) (Figure 3.2) (Fan et al., 2015). TPGS has polyethylene glycol 1000 as its polar hydrophilic head portion and the phytyl chain of d-α-tocopherol as its lipophilic tail portion.

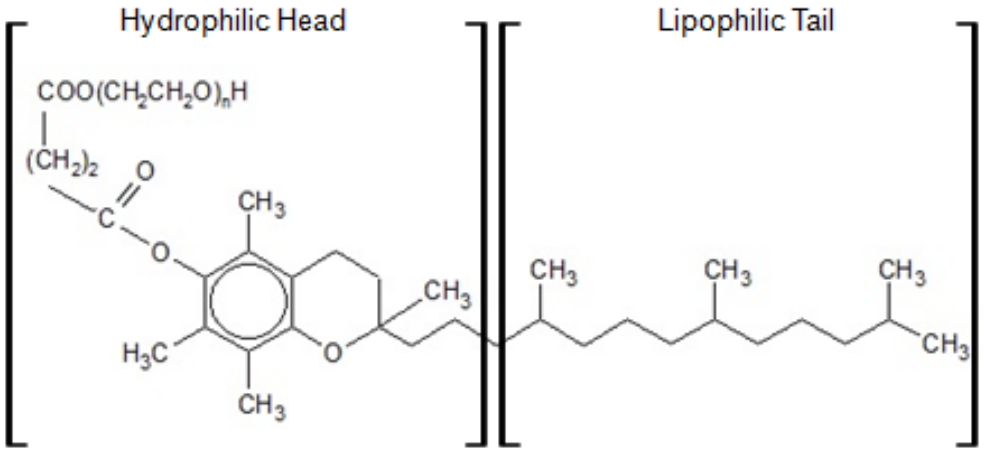

Figure 3.2: Chemical structure of TPGS.

The water soluble amphiphilic molecular structure and large surface area are promising features of TPGS. TPGS has great value as a solubiliser, emulsifier and most importantly, a bioavailability enhancer (Duhem et al., 2014). TPGS has the ability to solubilise both water-soluble and -insoluble compounds (Duhem et al., 2014). Being a non-ionic surfactant TPGS is more hydrophobic therefore it has an improved ability to dissolve drugs with poor solubility. High drug solubilisation is potentially encouraged by the bulky hydrophobic core (Suksiriworapong et al., 2014). TPGS has widespread success in improving the solubility and bioavailability of many poorly water soluble drugs (Collnot, 2007). Additionally it is advantageous as it has a low Critical Micelle Concentration (CMC) value (Zhang et al., 2012). Micelles formed from agents with high CMC's mean that they are more prone to dissociation as exposure to biological fluids (such as blood) results in dilution (Trivedi and

Kompella, 2010). Non-ionic surfactants are also less toxic than other surfactants. (Collnot, 2007). In fact, the safety profile of TPGS is of a high standard as it is approved by the USFDA for use as a drug delivery vehicle. TPGS nanomedicines can be utilised for sustained, controlled or targeted delivery (Duhem et al., 2014). They also improve the stability of the drug (Duhem et al., 2014). Nanomicelles made of TPGS are also safe from removal via the RES (Zhang et al., 2012). Mu and Seow (2006) reported that TPGS nano-particulate systems have promise in controlled release of poorly soluble drugs. Furthermore, TPGS has been used intramuscularly with success (EFSA, 2007). All of these aspects are advantageous as they are key requirements for a successful depot formulation.

TPGS was selected as the polymer to synthesize the nano-carrier in this study due to its ability to overcome shortcomings posed by immensely hydrophobic drugs. One such example is paclitaxel. TPGS has shown success in markedly enhancing the encapsulation efficiency of paclitaxel (Mu and Feng, 2006). Over and above that, TPGS is capable of extending the circulation half life of a drug. This feat was observed in mixed-TPGS nanosystems which demonstrated pronounced sustained release (Zhang et al., 2012).

In order to yield an optimal delivery system it is imperative that the influence of all formulation and process variables is considered. The traditional approach of optimization involved changing one aspect at a time whilst keeping the others constant i.e. One Variable At a Time (OVAT) approach. This trial and error method can result in wasting of time, energy and resources and the optimization outcome is heavily reliant on prior knowledge, experience and instinctive fortune (Singh et al., 2005). Complete understanding of product/process response variation as a function of input variables can be created through the implementation of experimental designs, generation of mathematical equations and graphical outcomes. This technique is an optimization one referred to as Design of Experiments (DoE) (Singh et al., 2005). A DoE allows for accurate and efficient achievement of experimental objectives taking into account the critical quality attributes of the delivery system (Patil et al., 2014). The DoE is especially advantageous as it enables understanding of the system by providing information on variable interactions as well as the significance of factors. Accuracy and quality are maintained through the implementation of mathematical correlations. The DoE also allows a large number of variables to be studied independently and in combination but with fewer experiments thus saving time and decreasing costs (Patil et al., 2014).

In this chapter disulfiram was encapsulated into TPGS nanomicelles utilising a design of experiments approach with selected variables and desired responses. Thereafter a series of characterization tests were conducted on the optimized formulation.

3.2 Materials and Methods

3.2.1 Materials

Kolliphor® TPGS was obtained from BASF (Ludwigshafen, Germany). Tetraethylthiuram disulfide (disulfiram) was purchased from Sigma Aldrich (Steinheim, Germany). Deionised water was obtained from a Milli-Q water purification system (Milli-Q, Millipore, Billerica, MA, USA). Simulated Body Fluid (SBF) (pH 7.4) was prepared from analytical grade reagents according to the method reported by Marques et al., (2011). All other reagents were of analytical grade and were used as purchased.

3.2.2 Design criteria and considerations for the disulfiram-loaded nanomicelles

Prior to the construction of the design, two independent variables were identified and tested in order to determine their relevance as design responses. The variables selected were: 1) the amount of TPGS used (mg) and 2) the stirring time (hours) of the nanomicelle formulation. The decision to maximise entrapment efficiency and drug loading and minimise drug release, obtained from preformulation studies, stemmed from the requirement to ensure maximum loading and entrapment due to the hydrophobicity of disulfiram while ensuring adequate release over a minimum period of 28 days in order to fulfil the sustained release requirement of depot formulations.

3.2.3 Construction of a randomized Central Composite Design for the optimization of the TPGS nanomicelles

There is no guarantee of achieving an optimized formulation and, furthermore, if one is obtained it may be incorrect due to inaccurate result interpretation. For this to be avoided the implementation of response surface methodology is fundamental.

Response Surface Methodology (RSM) is a constructive statistical design strategy as it has affirmative application in optimising a response, or many responses, which are influenced by many variables (Bezerra et al., 2008). In RSM, experimental data is fitted to a polynomial equation which explains the behaviour of the data set. The objective of RSM is to obtain the optimal responses in relation to these variables (Bezerra et al., 2008). A central composite design (CCD) was selected as the ideal response surface design for optimization. The CCD contains an imbedded factorial design or fractional factorial design that is supplemented with a central point as well as a group of axial points which permit curvature estimation. A Face

Centred Central Composite Design (FCCCD) contains the axial points at the centre of each face of the factorial space. A two factor, three level FCCCD was generated by Minitab® statistical software (V15, Minitab Inc., PA, USA) for statistical optimization. The input factors generated 13 experimental runs (formulations).

The expected form of the polynomial equation generated was:

$$y_0 = b_0 + b_1 TPGS + b_2 StirringTime + b_{11} TPGS^2 + b_{22} StirringTime^2 + b_{12} TPGS*StirringTime$$

Equation 3.1

In the design the stirring time (magnetic stirring in hours) and the amount of polymer used (in mg) were taken as the independent variables whilst drug loading %, entrapment efficiency % and drug release % were taken as the dependent parameters, or responses.

Upper and lower limits of the two variables were selected due to their considerable influence in the nanomicelle preparation (Table 3.2). Preliminary response investigation revealed that alteration of the TPGS amount and stirring time had significant effect on the performance of the nanomicelles. The upper and lower limit for TPGS amount and stirring time were determined by varying one parameter whilst keeping the other constant. The effect on drug loading %, entrapment efficiency, drug release and particle size was investigated in order to ascertain the upper and lower limits.

Table 3.2: Variables to be employed for incorporation into the Face Centred Central Composite statistical design.

Independent Variables	**Limits**	
	Upper	**Lower**
TPGS amount (mg)	500	1000
Stirring time (hours)	1	5

3.2.4 Fabrication of disulfiram-loaded self-assembled TPGS nanomicelles utilising the solvent casting method

Due to the hydrophobic nature of disulfiram, solvent casting was selected as the most suitable method for the fabrication of disulfiram-loaded self-assembled TPGS nanomicelles (Rao et al., 2015). Appropriate amounts of disulfiram and TPGS (as per the design template shown in Table 3.3) were solubilised in chloroform. Chloroform was the organic solvent of choice due to its ability to completely dissolve both the drug and the polymer. Once mixed well, the disulfiram-TPGS-chloroform mixture (10mL) was poured into petri dishes and left overnight at room temperature to allow complete evaporation of the chloroform. The remaining solid polymer-drug matrix was then hydrated with deionised water (5mL) and stirred using a magnetic stirrer for a certain amount of time (as per the design template

shown in Table 3.3) resulting in the formation nanomicelles in solution. The micellar solution was then frozen at -80°C for 12 hours and lyophilized for further characterization. The drug-loaded nanomicelles are formed upon hydration through association of the hydrophobic drug molecules with the hydrophobic micelle core.

Thirteen formulations were generated from the FCCCD (Table 3.3). The formulations were prepared and tested in triplicate (n=3). Experiments were completely randomised to reduce systematic errors. The results were input into the Minitab® statistical software (V15, Minitab Inc., PA, USA) which computed the optimized formulations' independent parameters and expected response values.

Table 3.3: Formulations generated using a Face Centred Central Composite statistical design for the optimization of disulfiram-loaded nanomicelles.

Formulation Number (F)	TPGS amount (mg)	Stirring Time (hours)
1	750	3
2	500	1
3	500	5
4	750	1
5	1000	3
6	750	3
7	500	3
8	1000	1
9	750	3
10	750	3
11	1000	5
12	750	3
13	750	5

3.2.5 Particle size determination by Dynamic Light Scattering

The average particle size, size distribution and zeta potential of the nanomicelles was measured by the Dynamic Light Scattering (DLS) method using Zetasizer NanoZS (Malvern Instruments Ltd., Malvern, Worcestershire, UK). Samples were diluted and filtered using a 0.22μm filter (Millipore Co., Massachusetts, USA) and filled into disposal cuvettes (size) or capillary cells (zeta potential) (Malvern Instruments Ltd., Malvern, Worcestershire, UK). Tests were performed in triplicate and the mean ±SD reported.

3.2.6 Preparation of simulated body fluid

Artificial Simulated Body Fluid (SBF) was prepared to adequately simulate intramuscular conditions according to the method outlined by Marques et al., (2011). By making use of simulated biological fluids as dissolution media clarity and understanding of release mechanisms is achieved. This improves the predictability of *in vivo* behaviour as the

contents of the media closely match the physiological contents. SBF was prepared by using the reagents listed in Table 3.4.

Table 3.4: Reagents used for preparation of 1L of SBF (Marques et al., 2011).

Reagent	Amount for 1 L of SBF
Sodium chloride	8.035g
Sodium bicarbonate	0.355g
Potassium chloride	0.225 g
Potassium phosphate dibasic trihydrate	0.231 g
Magnesium chloride hexahydrate	0.311 g
1 M Hydrochloric acid	39 mL
Calcium chloride	0.292 g
Sodium sulfate	0.072 g
Tris(hydroxymethyl) aminomethane	6.118 g

Each reagent was added, in the order listed, to 700mL of deionised water. The pH was adjusted to 7.4 with 1M HCl. The final volume was adjusted to 1L with deionised water.

3.2.7 Acetone-buffer solution preparation

A ratio of SBF to acetone was utilised as both, a disulfiram extraction medium and a disulfiram-absorbance detector for all subsequent UV analysis. The acetone-buffer solution (ABS) was made of acetone to SBF buffer in a ratio of 1:18.

3.2.8 Drug entrapment efficiency and drug loading capacity of the nanomicelles

Disulfiram-loaded nanomicelles were added to 10mL of SBF and stirred for 48 hours at 37°C using a magnetic stirrer. Chloroform (10mL) was added to this and the formulation was vigorously shaken to completely extract the disulfiram. The emulsion was allowed to separate and the chloroform layer was syringed out and left to dry to allow evaporation of the chloroform. The remaining solid, containing the drug, was reconstituted with 40mL of the extraction medium (i.e. ABS). The absorbance was tested at λ_{262} using UV spectroscopy (Implen Nanophotometer™, Implen GmbH, München, Germany). The entrapment efficiency (EE%) and drug loading (DL%) of the formulations was determined according to Equation 3.2 and Equation 3.3, respectively:

$$\mathrm{EE\%} = \frac{\text{actual amount of disulfiram (mg)}}{\text{theoretical amount of disulfiram (mg)}} \times 100 \qquad \textbf{Equation 3.2}$$

$$\mathrm{DL\%} = \frac{\text{disulfiram mass in sample (mg)}}{\text{total mass of sample (mg)}} \times 100 \qquad \textbf{Equation 3.3}$$

(Sadat et al., 2012)

Determination of the entrapment efficiency and drug loading was done in triplicate and results presented as the mean ±SD.

3.2.9 Calibration curve construction for the quantification of disulfiram

A calibration curve was constructed for disulfiram. Due to the hydrophobic nature of disulfiram a known amount was first dissolved in 5mL of acetone and thereafter made up to 100mL with buffer. The final concentration of this stock solution was 0.01%. Dilutions were made from this stock solution in the range of 0.002-0.01%. The UV absorbance value for each concentration was determined using a nanophotometer (Implen Nanophotometer™, Implen GmbH, München, Germany) at a wavelength of 262nm. The observed absorbance (dependent variable) was plotted against the corresponding concentration (independent variable) in order to obtain a linear curve.

3.2.10 *In vitro* dissolution studies of disulfiram-loaded nanomicelles

In vitro drug release studies were conducted by means of the dialysis method (Kulhari et al., 2015). Disulfiram-loaded nanomicelles were placed in dialysis tubing (MWCO 1000Da) with 5mL of SBF and both ends were sealed and the closed tube was placed into a jar with 50mL of release medium (SBF). The airtight system was placed in an orbital shaker bath (Labex, Stuart SBS40®, Gauteng, South Africa) set at 37°C and 25rpm. At predetermined time intervals, over a 28 day period, 1mL of sample was removed from the release media and replaced with 1mL of fresh SBF to maintain sink conditions. The sample was diluted with ABS and the disulfiram content determined using UV spectroscopy. Drug release was quantified using the predefined calibration curve. The study was conducted in triplicate and results presented as the mean ±SD.

3.2.11 Statistical analysis of the Face-Centred Central Composite Design

A Face-Centred Central Composite Design (FCCCD) was employed to analyse the effect of TPGS amount (in mg) and stirring time (in hours) in response to drug loading, entrapment efficiency and drug release. The FCCCD was statistically analysed using the MiniTab® V15 software with Analysis of Variance (ANOVA) protocols.

3.2.12 Constraint optimization of formulation responses

Statistical optimization was carried out utilising Minitab® V15 software configured to maximize drug loading and entrapment efficiency and minimize drug release at both 2 hours and 7 days. Maximization of drug loading and entrapment efficiency will allow delivery of adequate drug to facilitate sustained release of disulfiram. Minimization of drug release at 2

hours prevents burst release and minimization of drug release at 7 days enables controlled release over 28 days.

3.2.13 Preparation of the optimized nanomicelles

The FCCCD optimization output indicated utilisation of 500mg TPGS with a stirring time of 1 hour in order to generate optimized nanomicelles. The disulfiram-loaded and drug free nanomicelles were formulated as per the method previously described in *Section 3.2.4.*

3.2.14 Experimental responses of the optimized nanomicelles

The particle and zeta potential analysis, drug entrapment and drug loading as well as *in vitro* release of the optimized TPGS nanomicelles were measured as described in Sections 3.2.5., *3.2.8 and 3.2.10* respectively.

3.2.15 Characterization of the optimal TPGS-nanomicelle system

3.2.15.1 Morphological characterization of nanomicelles using Transmission Electron Microscopy

The size and shape of the nanomicelles were visually investigated utilising a Transmission Electron Microscope (TEM) (JEOL 1200 Ex, Tokyo, Japan, 120keV). A dispersion of nanomicelles was placed onto a carbon-coated copper grid. Samples were then negatively stained with 1% uranyl acetate (Lu et al., 2013). The grid was allowed to dry before viewing.

3.2.15.2 Determination of the Critical Micelle Concentration of the TPGS-nanomicelles

The Critical Micelle Concentration (CMC) of the TPGS-nanomicelles was determined by UV spectroscopy using iodine (Fan et al., 2015). An aqueous solution of TPGS was formulated and was diluted to concentrations varying from $1x10^{-1}$mg/mL to $1x10^{-5}$mg/mL. the iodine solution comprised iodine (0.5g) and potassium iodide (KI) (1g) in 50mL deionised water. KI/I_2 (25μL) was added to each polymer solution. Formulations were incubated in a dark room for 12 hours. Thereafter the UV absorbance value was measured for each solution at λ_{366} using a nanophotometer (Implen Nanophotometer™, Implen GmbH, München, Germany). The absorbance intensity was plotted against the log of polymer concentration. The CMC value is calculated from the concentration of polymer at which a sharp rise in absorbance is noted. It is calculated Equation 3.4. The test was performed in triplicate (SD≤0.0017).

CMC = AntiLog [TPGS] %w/v **Equation 3.4**

3.2.15.3 Redispersability studies to determine the effect of lyophilization on the nanomicelles

The ability of the nanomicelles to redisperse after lyophilization was evaluated according to the method outlined by Suksiriworapong et al. (2014). Particle size was measured before and after lyophilization as outlined in Section *3.2.5*. Redispersability is measured from the ratio of particle size after reconstitution to particle size before lyophilization (Equation 3.5).

$$\frac{S_2}{S_1}\ \text{ratio} = \frac{\text{particle size after reconstitution } (S_2)}{\text{particle size before lyophilization } (S_1)} \qquad \textbf{Equation 3.5}$$

3.2.15.4 Characterization of the molecular vibrational transitions using Fourier Transform Infrared Spectroscopy

Investigation of the structural properties was carried out on the native disulfiram and TPGS as well as lyophilized drug-free nanomicelles and lyophilized disulfiram-loaded nanomicelles using a Perkin Elmer Spectrum 2000 FTIR spectrometer with a MIRTGS detector (PerkinElmer Spectrum 100, Llantrisant, Wales, UK). Samples were processed at a resolution of 4cm^{-1} and were analyzed at wavenumbers ranging from 650-4000cm^{-1}. The infrared spectra is useful in deduction of the vibrational molecular characteristics and correspondingly providing a structural profile of a compound. FTIR is useful in identification of compounds , amounts of constituents, and sample quality and consistency.

3.2.15.5 Characterization of thermal transitions using Differential Scanning Calorimetry

Differential Scanning Calorimetry was used to assess thermo-degradation and thermal transitions. The DSC curves were generated with a Differential Scanning Calorimeter (Mettler Toledo) fitted with Stare software (Mettler Toledo, Switzerland). The thermal transitions of native TPGS and disulfiram were compared to the TPGS-disulfiram nanomicelle mixture. Accurately weighed samples (±10mg) were placed into standard 40µL aluminum crucibles. The crucibles were perforated and hermetically sealed. Samples were then heated at a heating rate of 10°C/minute between a temperature range of 0-300°C under a constant purge of inert nitrogen (Afrox, Germiston, Gauteng, South Africa) in order to diminish oxidation. The reference standard used was an empty aluminium crucible.

3.2.15.6 Determination of the degree of crystallinity employing X-Ray Diffraction analysis

The crystalline or amorphous disposition of the individual components as well as nanomicelles were determined using X-Ray diffraction patterns. The diffractograms were obtained using a Benchtop X-Ray Diffractometer (Rigaku Miniflex 600, Rigaku Corporation, Matsubara-cho, Akishima-shi, Tokyo, Japan). The measurement parameters were a 10mm Incident Height Slit (IHS), 1.25° Divergence Slit (DS), 13mm Solar Slit (SS) and 13mm Receiving Slit (RS). The diffractometer was operated using the Rigaku MiniFlex Guidance software, version 1.2.0.0. All experimental procedures were conducted over a diffraction angle range of 0º-90º 2θ. Integrated X-ray powder diffraction software (PDXL 2.1, Rigaku Corporation, Matsubara-cho, Akishima-shi, Tokyo, Japan) was used for data acquisition and analysis. The diffractometer was fitted with; a 600W (40Kv-15mA) X-ray generator, a counter monochromator and a high intensity D/tex ultra high speed 1D detector. Experimental temperature was maintained at 19ºC.

3.3 Results and Discussion

3.3.1 Assessment of particle size using DLS

Particle size analysis was measured on the 13 design formulations in order to confirm that the micelles were in the nano-size range of 10-100nm (Mohamed et al., 2014). The micelle sizes and Poly Dispersity Index (PDI) are recorded in Table 3.5. Analysis of the results showed that sizes ranged from 15.26nm-31.20nm (SD ≤ 1.89, n=3). Thus all formulations are within the acceptable range for polymeric nanomicelles. There was no noticeable trend in particle size change due to change in polymer amount or stirring time. This was also observed by Muthu et al., (2012). The PDI's ranged from 0.19-0.42 (SD ≤ 0.094, n=3) which indicates narrow size distribution. Sizes obtained were in accordance with those previously reported (Sonali et al., 2015; Butt et al., 2012).

Table 3.5: Particle sizes and PDI values for F1-F13.

Design Formulation Number	Particle Size (nm)	PDI
1	23.36	0.26
2	25.09	0.25
3	31.20	0.42
4	18.09	0.21
5	19.96	0.35
6	17.05	0.26
7	22.95	0.35
8	24.14	0.36
9	15.26	0.25
10	17.55	0.26
11	17.25	0.22

12	15.56	0.19
13	16.44	0.24

3.3.2 Morphological characterization of the TPGS nanomicelles

TEM affirmed the formation of nanomicelles. Figure 3.3 is a representative TEM image of the design nanomicelles and both display spherical shaped particles in the size range of approximately 20nm-40nm (as obtained from image scale). Thus the TEM images confirm the size results obtained through DLS. One or two larger particles are also present (±50nm). Differences in sizes can be attributed to agglomeration of particles during TEM preparation as the solution used for the grid is highly concentrated. Moisture evaporation during sample preparation can also lead to agglomeration (Guo et al., 2013). In some cases the size of the particle in the TEM image may seem slightly larger than the size obtained in DLS. This is attributable to the low melting point of TPGS which is about 38°C. The high energy electron beam of the TEM generates heat. This heat can cause the micelles to undergo a certain degree of melting and expansion. This event can make the micelles appear marginally bigger in the TEM image than in the DLS test (Mi et al., 2012). As can be seen in Figure 3.3, despite changing the stirring time (stirring time a) = 1 hour; b) = 3 hours) or polymer amount (mg of TPGS a) = 1000mg; b = 500mg), there is no difference in the shape and surface morphology amongst the design samples. This was also observed in DLS particle size. This uniformity is an additional benefit.

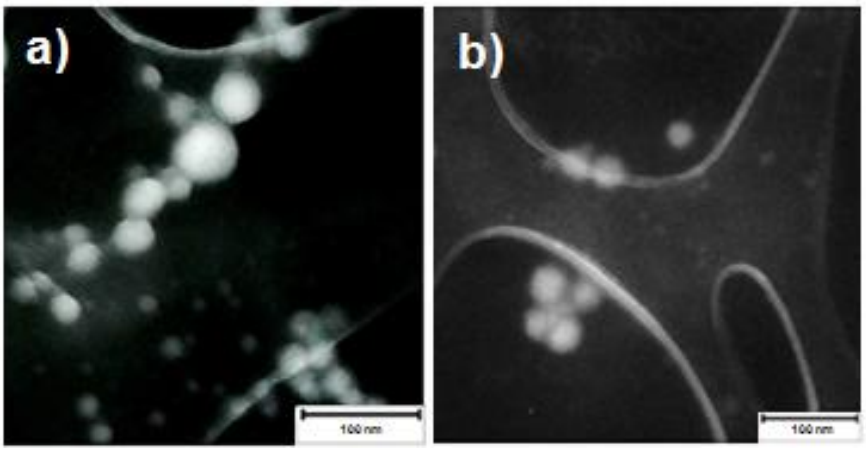

Figure 3.3: Transmission electron micrograph of disulfiram-loaded nanomicelles at 50000x magnification (a = F8, b = F7).

3.3.3 A calibration curve for the quantification of disulfiram

Using UV spectroscopy the maximum wavelength for disulfiram was found to be at $\lambda_{262.}$ This is in accordance with the literature reporting an absorbance peak of 250-275nm (Zembko et al., 2015; Saracino et al., 2010). Serial dilutions were tested and the curve plotted to

generate a calibration curve (Figure 3.4). The calibration curve had an R^2 value of 0.99 indicating perfect correlation.

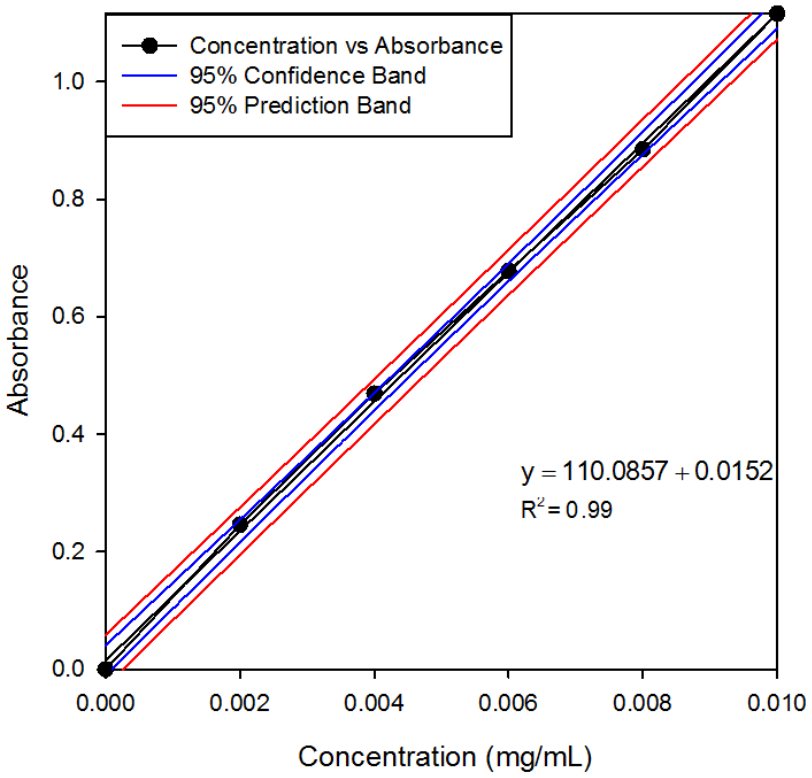

Figure 3.4: Calibration curve of disulfiram at $\lambda_{262.}$

3.3.4 Assessment of the drug loading and drug entrapment of the design formulations

The DL% of the formulations ranged from 14% - 34% (SD ≤ 2.32, n=3 in all cases). F2 had the highest drug loading whilst F3 had the lowest drug loading. The percentage drug loading for each formulation of the FCCD is displayed in Figure 3.5.

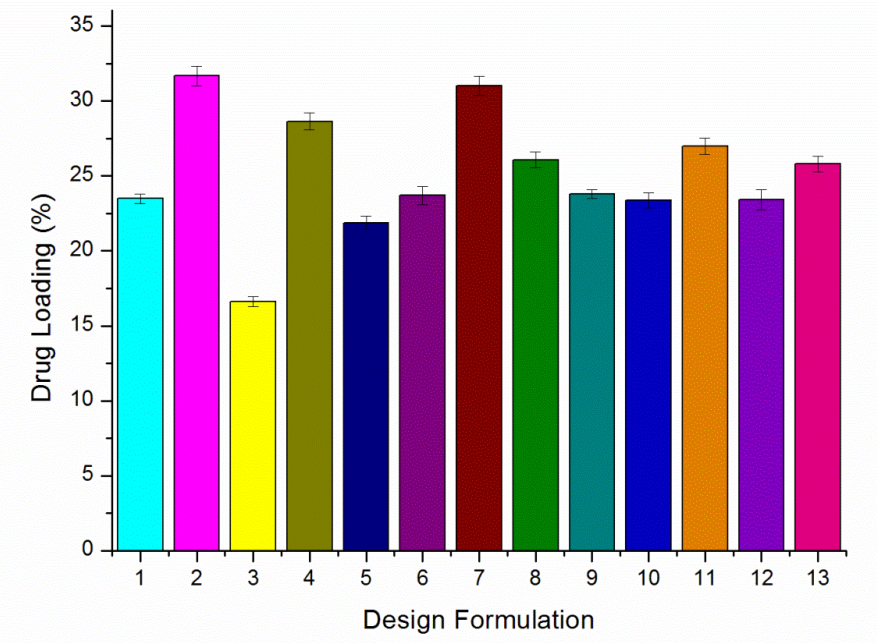

Figure 3.5: Drug loading % for each formulation of the FCCD.

The entrapment percentage of disulfiram into nanomicelles ranged from 24% - 59% (SD ≤ 1.42, n=3 in all cases). The highest entrapment efficiency was seen in F11 whereas the lowest was F3. The entrapment efficiency for each formulation is displayed in Figure 3.6.

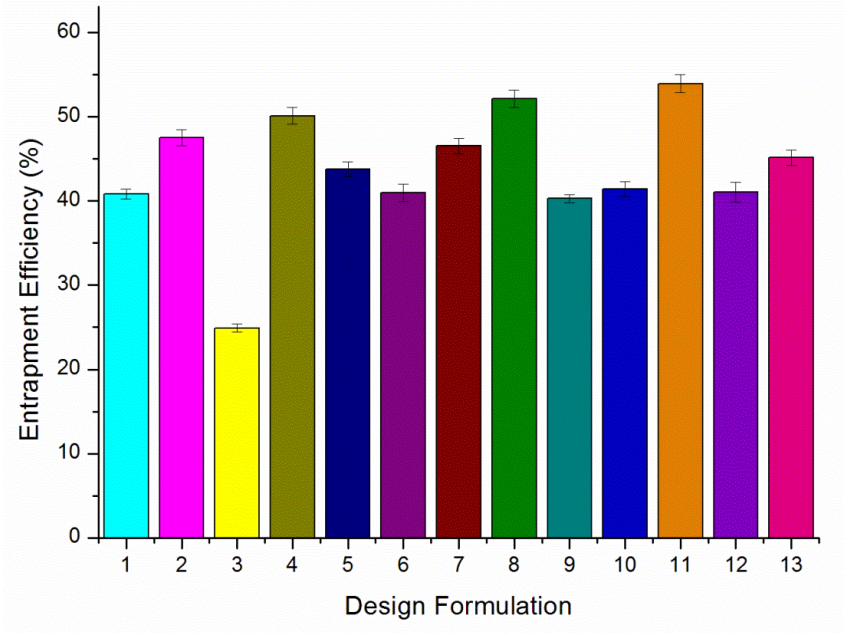

Figure 3.6: Entrapment efficiency % for each formulation of the FCCD.

3.3.5 *In vitro* drug release profiles of design formulations

The percentage cumulative release over 28 days for the 13 design formulations is displayed in Figure 3.7 (SD ≤ 2.28 in all cases, n=3). The fastest release was from F3 followed by F2. The slowest release was seen in F7. An initial burst release on the first day (>15% but ≤

20%) was seen in all formulations. This may be due to the poorly entrapped drug that is adsorbed to the surface of the micelles (Zeng et al., 2013). A general trend that was present was that at low drug loading and entrapment efficiency percentages, the faster the release and the higher the entrapment efficiency and drug loading the slower the release. This can be attributed to the fact that in those formulations with higher entrapment efficiency and drug loading a greater amount of drug was well encapsulated in the micelle core thus requiring a longer time to be released from the micelle and into the dissolution medium. Those with less drug need less time to release the drug that is contained in the micelle thus the faster release rate.

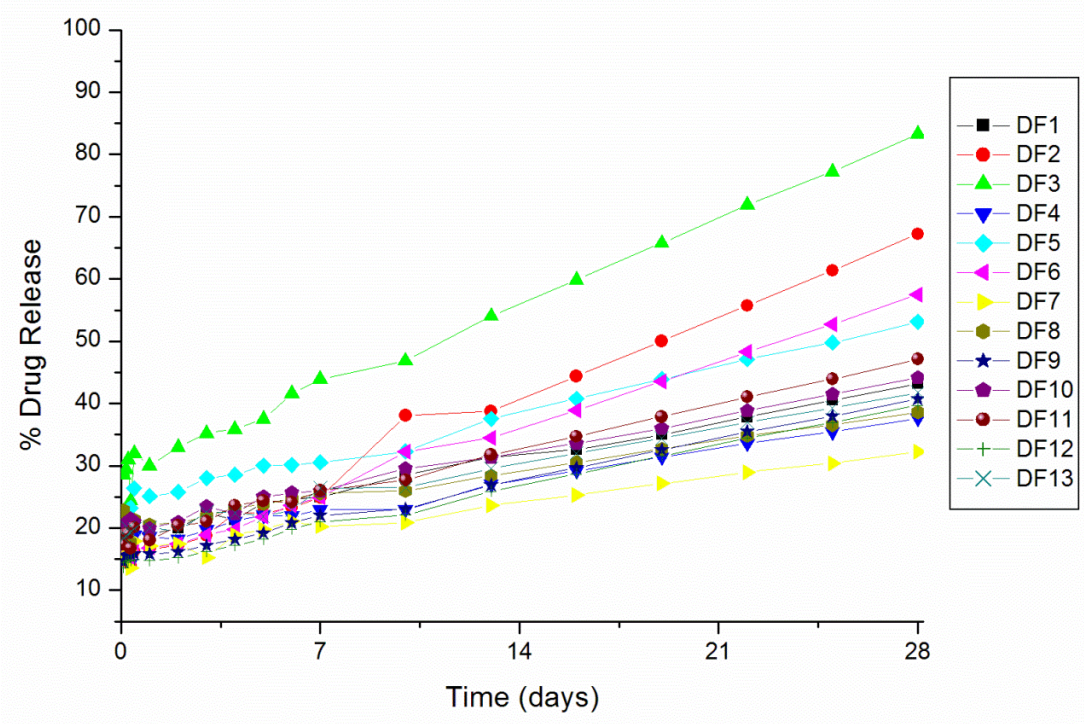

Figure 3.7: Cumulative disulfiram release from F1-F13 over 28 days.

A detailed discussion of drug loading, drug entrapment and *in vitro* drug release of the design formulations can be found in *Chapter 3, Section 3.3.6.2 (Response surface and contour plot analysis).*

3.3.6 Statistical analysis of the FCCCD

3.3.6.1 Residual error plot analysis

The complete regression equations generated for entrapment efficiency, drug loading, drug release (2hour) and drug release (day 7) are indicated below in Equations 3.6 to 3.9 respectively:

Entrapment efficiency (%) = 70.0227 - 0.0231 (TPGS) - 15.4594 (stirring time) + 0.6945 (stirring time)^2 + 0.0122 (TPGS)(stirring time) **Equation 3.6**

Drug loading (%) = 55.3941 - 0.0371 (TPGS) - 9.1889 (stirring time) + 0.2976 (stirring time)^2 + 0.0080 (TPGS)(stirring time) **Equation 3.7**

Drug release (%, 2 hours) = 12.2071 - 0.0183 (TPGS) + 6.5784 (stirring time) + 0.2524 (stirring time)^2 - 0.0096 (TPGS)(stirring time) **Equation 3.8**

Drug release (%, 7 days) = 21.9775 - 0.0211 (TPGS) + 7.1549 (stirring time) + 0.2849 (stirring time)^2 - 0.0093 (TPGS)(stirring time) **Equation 3.9**

Residual analysis was utilised to determine the suitability of the regression model (Figure 3.8a - Figure 3.8d).

Residual vs. fitted values showed random scattering around zero with slight visible trends thus indicating that the error variance of the residuals is constant (Figure 3.8).

Normal plot of residuals fall predominantly straight thus indicating normal uniform distribution. One or two points deviate from the straight line which can be attributed to external influence. Overall the data followed a normal distribution reasonably closely. Histograms were fairly symmetrical except for drug release % (day 7). Symmetrical bell-shaped histograms indicate normal distribution of variance. Histograms displaying abnormal distribution of random error suggests the presence of outliers (Figure 3.8).

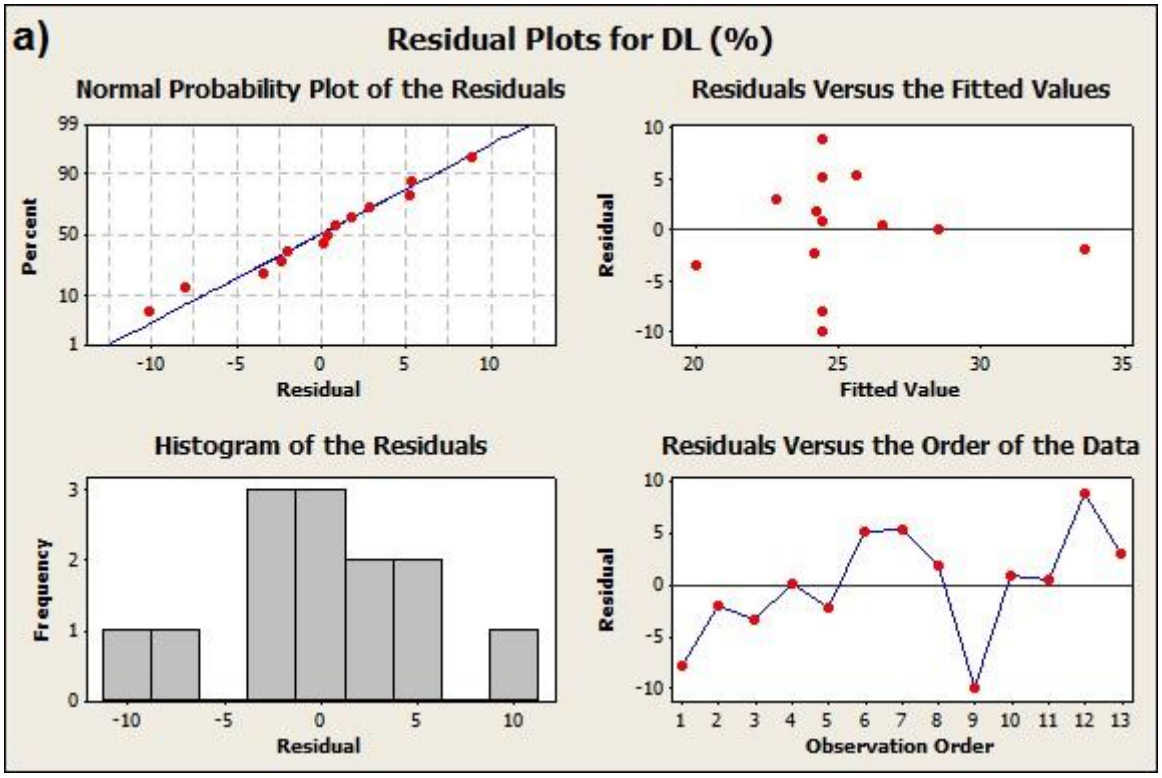
a)
Residual Plots for DL (%)
Normal Probability Plot of the Residuals
Percent
Residual
Residuals Versus the Fitted Values
Residual
Fitted Value
Histogram of the Residuals
Frequency
Residual
Residuals Versus the Order of the Data
Residual
Observation Order

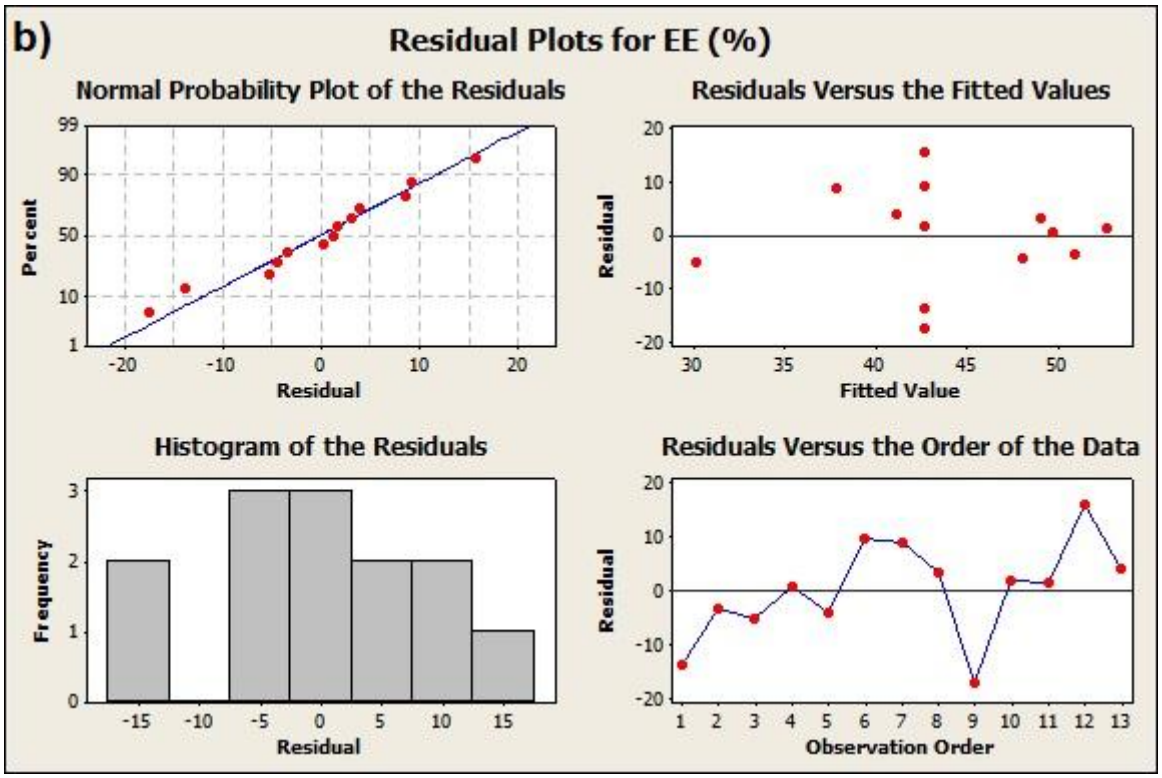
b)
Residual Plots for EE (%)
Normal Probability Plot of the Residuals
Percent
Residual
Residuals Versus the Fitted Values
Residual
Fitted Value
Histogram of the Residuals
Frequency
Residual
Residuals Versus the Order of the Data
Residual
Observation Order

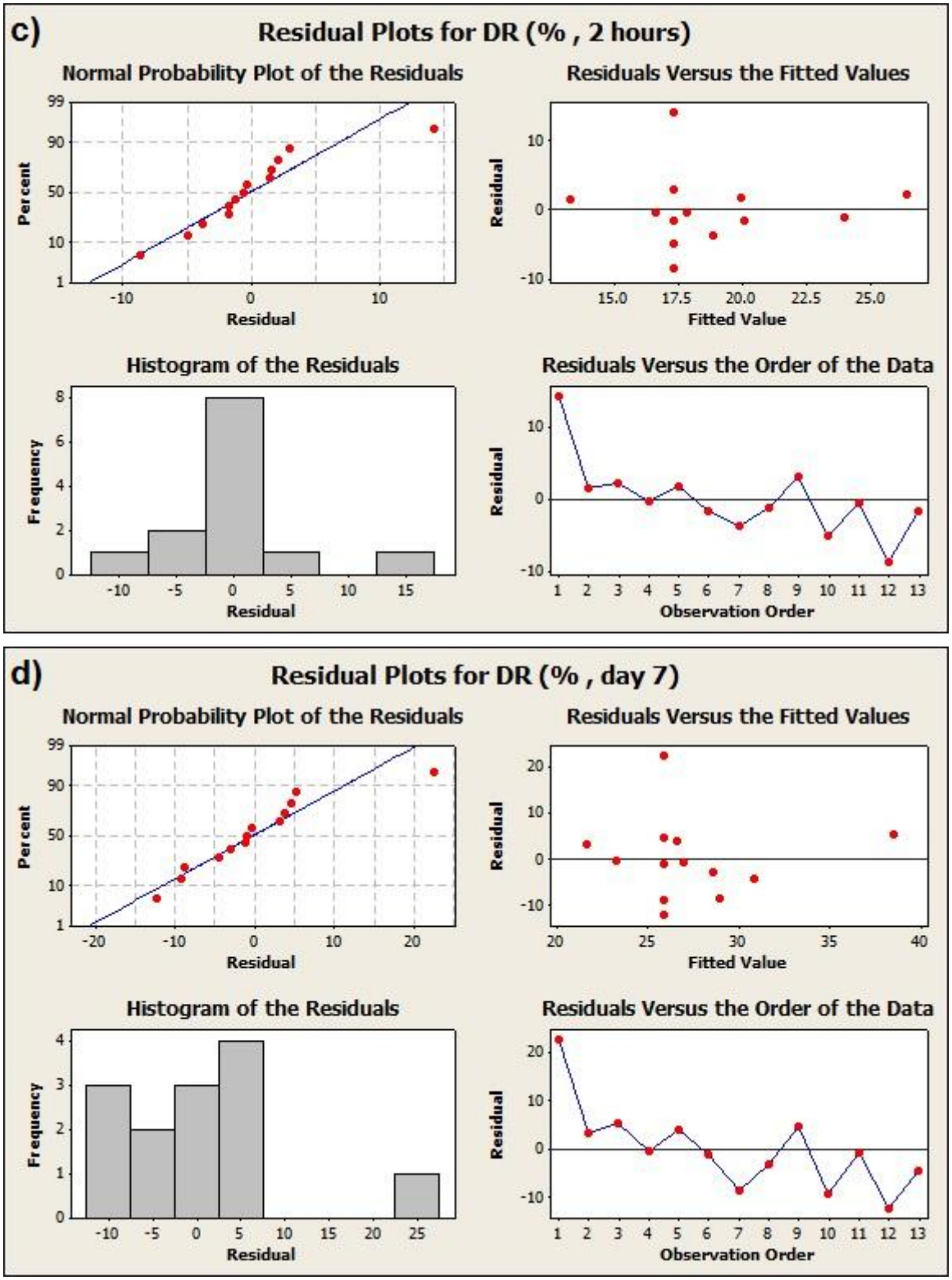

Figure 3.8: Residual plots for the responses a) drug loading %, b) drug entrapment %, c) drug release % at 2 hours and d) drug release % at 7 days.

3.3.6.2 Response surface and contour plot analysis

Response surface plots and contour plots provide graphical visualisation of the influence of the independent variables on the design responses. Figure 3.9 portrays the effect of TPGS

amount and stirring time on drug loading percentage. Lower levels of TPGS result in a higher drug loading of >30%. A shorter stirring time results in the highest drug loading whilst the longer the stirring time the lower the drug loading becomes. An increase in stirring time causes breakdown of the particles as dissolution begins resulting in drug leaching out of the micelles. This leads to a lower loading. The higher loading at lower levels of TPGS is logical as less polymer results in a greater drug loading. This is based on the fact that drug loading is calculated utilising the entire mass of the system and so an increase in polymer causes an increase in the ratio of the drug to the entire system thereby decreasing the percentage.

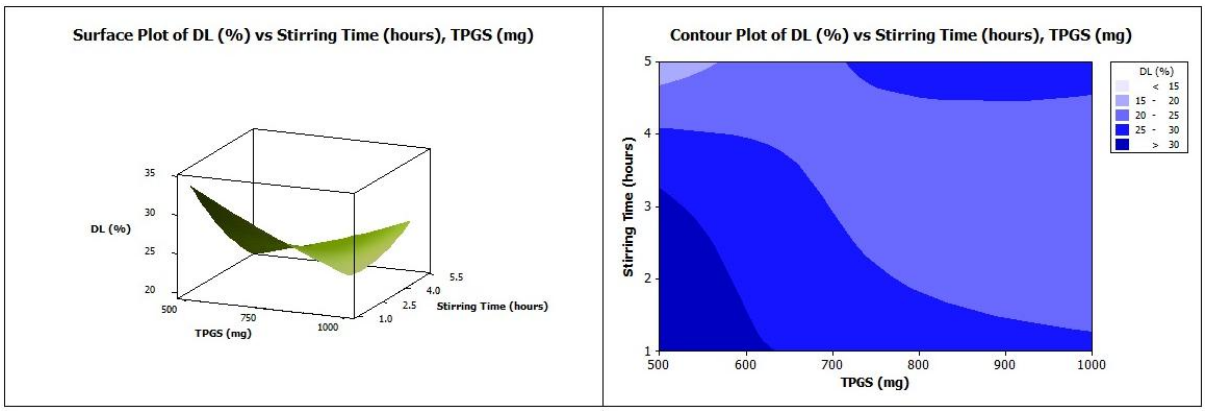

Figure 3.9: Response surface and contour plots illustrating the effects of stirring time (hours) and TPGS amount (mg) on drug loading %.

The effect of TPGS and stirring time on entrapment efficiency is displayed in Figure 3.10. At low TPGS amounts the entrapment efficiency is low while an increase in TPGS shows an increase in entrapment efficiency. This is because at low levels of TPGS there is less polymer available to encapsulate the drug. However at higher levels there is more polymer available which, consequently, can encapsulate more drug. An increase in stirring time leads to a decrease in entrapment efficiency. Stirring for too long results in micellar breakdown, thus less drug is entrapped. An increase in polymer can lead to an increase in the core size of the micelle and in doing so allows an increase in entrapment efficiency (Butt et al., 2012).

The combined effect of both on entrapment efficiency shows that an increase in stirring time and an increase in TPGS results in high entrapment. This is due to the excess polymer in the solution that leads to a greater adherence of the drug to the polymer thus rising above the effect of particle breakdown.

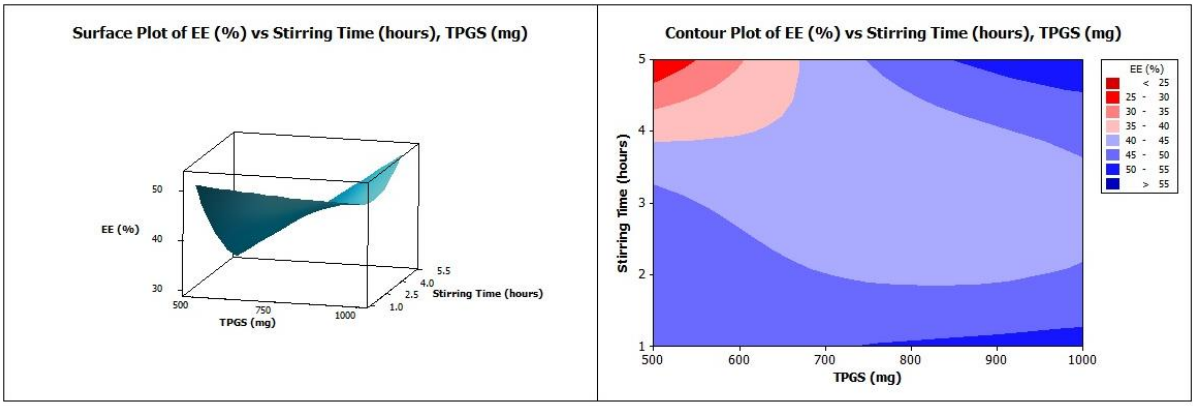

Figure 3.10: Response surface and contour plots illustrating the effects of stirring time (hours) and TPGS amount (mg) on entrapment efficiency %.

The contour and surface plots for percentage drug release (at 2 hours and 7 days) is shown in Figure 3.11 and Figure 3.12. The effects of TPGS and stirring time on drug release is similar for both the drug release points. For both of them the trends are the same but the percentage of drug release differs where drug release percentage of 7 days is higher than that at 2 hours as would be expected. Low levels of TPGS and short stirring result in a slow release. This is correct as at low levels of both the entrapment efficiency and drug loading was high. More time is needed to release larger amounts of entrapped drug. At low TPGS and a long stirring time the drug release is fast. This is also correct as this combination yielded low entrapment efficiency and drug loading. Drug is released much faster when there is less drug entrapped. Additionally the drug could be adsorbing to the surface (thus the low entrapment efficiency) which would result in a faster release. A high TPGS levels and a long stirring time the drug release is slow. This concurs with the finding of a high entrapment % in response to increased stirring time and increased TPGS. The more TPGS present, the greater the hydrophobic interaction between disulfiram and TPGS thus causing a delay in the release. This means that more time is needed for drug that is bound to the nanomicelle core to leave the core and pass through the outer shell and into the dissolution medium. As the aim is to minimise drug release at these points (i.e. 2 hours and 7 days) in order to prevent burst release and to allow sustained and controlled release but also to maintain high entrapment efficiency and high drug loading (to ensure a maximum therapeutic outcome as disulfiram therapy is dose dependent) the optimal combination is a short stirring time and low amount of TPGS as is illustrated by the contour plots and surface plots.

This ideal situation was observed in F2 of the design. F2 showed interesting findings in terms of drug loading and entrapment efficiency. An expected result for this formulation would be a low drug loading and a low entrapment efficiency due to the small amount of TPGS present which would indicate less polymer to entrap the drug and low stirring to

indicate less time to entrap all the drug. A rapid release rate with a high burst release would also be supposed for this formulation. Astoundingly, this formulation is the only one in the entire design to display all three desired attributes: a high drug loading and entrapment efficiency percentage and moderately fast release. Other formulations with high drug loading had a too slow release rate with only ±30% releasing in 28 days. Conversely, if the release was desirable then either the drug loading or entrapment efficiency was undesirable. Thus the interaction of TPGS with disulfiram has great influence on the drug loading, entrapment efficiency and drug release endorsing the employment of TPGS as the most fitting carrier for the enigmatic disulfiram.

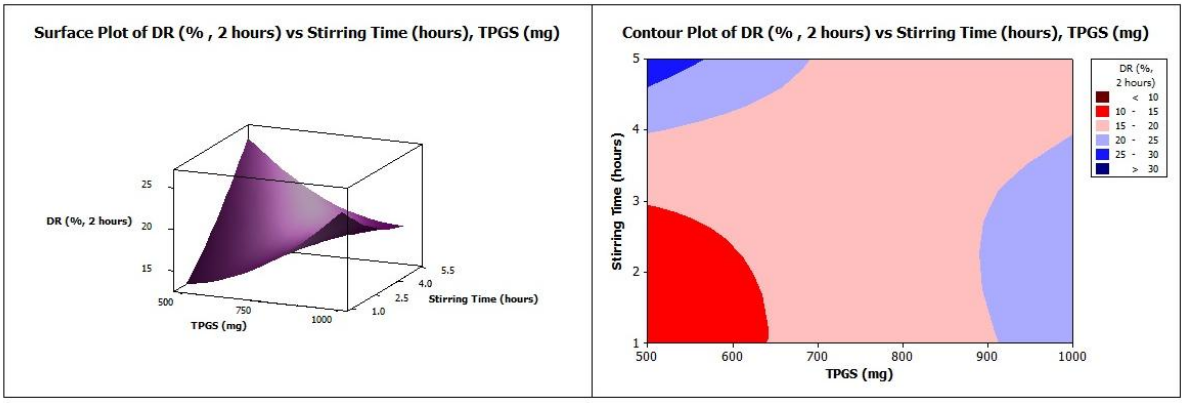

Figure 3.11: Response surface and contour plots illustrating the effects of stirring time (hours) and TPGS amount (mg) on % drug release at 2 hours.

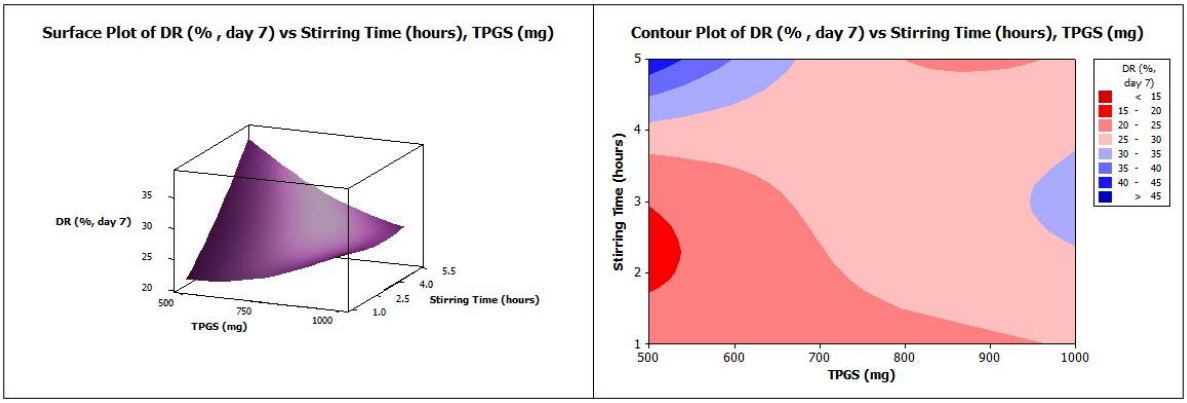

Figure 3.12: Response surface and contour plots illustrating the effects of stirring time (hours) and TPGS amount (mg) on % drug release at 7 days.

3.3.7 Constraint optimization of formulation responses

Following constraint optimization of drug loading, entrapment efficiency and drug release, a single optimized formulation was generated. Table 3.6 shows the constraint settings utilized.

Table 3.6: Formulation constraints utilised for response optimization.

Responses	Objectives
Entrapment Efficiency (%)	Maximize
Drug Loading (%)	Maximize
Drug Release (%)	Minimize

Figure 3.13 summarises the obtained values for the responses with the optimized formulation as well as the predicted values and the individual and composite desirability scores. The overall composite desirability (D) for the responses in the design was 1. The optimal formulation was fitted to consist of 500mg TPGS with a stirring time of 1 hour. The statistical desirability index (D) of the optimized formulation was equal to 1 which is ideal.

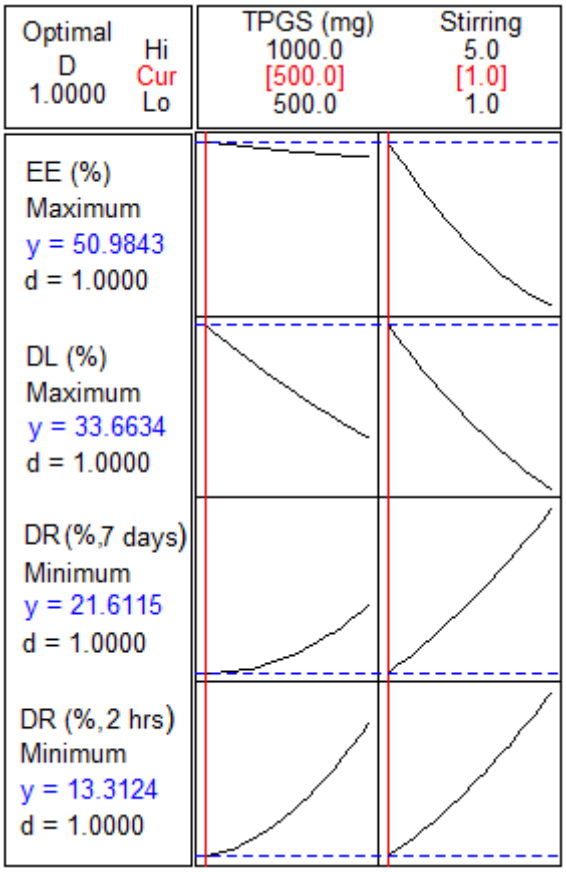

Figure 3.13: Desirability plots representing the level of TPGS and the stirring time required to synthesize the optimized formulation.

3.3.8 Experimental responses of the optimized system

Upon attainment of the model conditions required in order to fabricate an optimal system it is imperative that the accuracy of this system is then evaluated. The optimized methodology was executed and the drug loading, entrapment efficiency and drug release studies conducted with the purpose of comparing the desirability of the experimental responses to

the predicted values. Table 3.7 displays the predicted, experimental and desirability values of the disulfiram- loaded TPGS based nanomicelle formulation.

Table 3.7: Predicted, experimental and desirability values of the disulfiram- loaded TPGS based nanomicelle formulation.

Measured Response	Predicted Value	Experimental Value	Desirability
Entrapment Efficiency (%)	50.98	53.89	1.00
Drug Loading (%)	33.66	35.90	1.00
Drug Release (%, 2hours)	13.31	12.55	0.94
Drug Release (%, 7 days)	21.61	19.10	0.88

The experimentally derived value for drug loading (35.90%) was in agreement with the predicted value (33.66%). The results obtained for drug loading are favourable as it exceeds the values reported in previous studies for nano-sized formulations created from TPGS alone or in combination with other polymers (Table 3.8).

Table 3.8: Drug loading values for various TPGS-containing nano-sized formulations.

Drug Delivery System	Polymers	Drug Loading %	Reference
Doxorubicin mixed micelles	PF127:TPGS 7:3 5:5 3:7	2.1 ± 0.22 2.8 ± 0.14 4.1 ± 0.13	Butt et al., 2012
Camptothecin mixed micelles	PF105:TPGS 7:3 5:5 3:7	0.0278 ± 0.001 0.0260 ± 0.002 0.0363 ± 0.0011	Gao et al., 2008
Gambogic Acid mixed micelles	P407:TPGS 68mg:23mg	9.38 ± 0.29	Saxena and Hussain, 2012
Quercetin loaded micelles	PF123:TPGS 7:3	10.59	Zhang et al.,2012
Docetaxel nanoparticles	PLGA-b-TPGS Cholic Acid-PLGA-b-TPGS	8.75 10.08	Zeng et al., 2013
TPGS-cisplatin prodrug micelles	TPGS	4.95 ± 0.27	Mi et al., 2012
Docetaxel nanoparticles	PLGA-TPGS PLGA-TPGS-Polaxamer 235	9.96 10.04	Tang et al., 2015
Camptothecin nanoparticles	PLC-TPGS	0.073-0.092	Sirithananchai et al., 2015

DMAB modified docetaxel nanoparticles	PLGA-TPGS	8.93-9.83	Chan et al., 2011
Doxorubicin nanoparticles	Chitosan-g-TPGS		Guo et al., 2013
	TPGS:chitosan 1:5 1:10	 43.5 ± 5.0 31.2 ± 0.9	
tpgs micelles	TPGS	2.81 ± 0.06	Wang et al., 2015
Docetaxel micelles	TPGS	22.81 ± 0.203	Sonali et al., 2015
Paclitaxel nanomicelles	PEG_{2000} - DSPE TPGS Dequalinium	1.57 ± 0.15 2.55 2.58 ± 0.18	Yao et al., 2011
Crizotinib-palbociclib-sildenafil micelles	TPGS-PLA	11.43 ± 1.80	de Melo-Diogo et al., 2014
Diazepam polymeric micelles	1% - 20% TPGS	3-7	Suksiriworapong et al., 2014

This shows that TPGS is ideal for encapsulation of disulfiram as it has a high ability to entrap the drug. The mechanism by which this occurs is the affinity of the hydrophobic core with the hydrophobic drug molecule which results in encapsulation of the drug within the core.

The entrapment efficiency value obtained (53.89%) is in line with the predicted value of 50.98%. This value is in agreement with other TPGS micelles showing an entrapment efficiency of 33% - 84% depending on drug used and polymer concentration. This result was obtained through the solvent casting method. The micelles formed through the direct dissolution method had an entrapment efficiency of 27% - 41% (Muthu et al., 2012) . This is further evidence that the method used in the current study (i.e. solvent casting) brings forth optimal results (Muthu et al., 2012).

The favourable drug loading and entrapment efficiency values obtained are a result of the strong hydrophobic interactions between the drug and polymer in the micelle core (Gao et al., 2008). TPGS is known to have a high encapsulation efficiency (Pan and Feng, 2008).

The solvent casting method is preferred as it allows for a higher entrapment efficiency compared to the direct dissolution method. This positive aspect is attributed to the creation of a solid dispersion of disulfiram with TPGS when dissolved in the organic solvent (Muthu et al., 2012).

The drug release experimental values at 2 hours and 7 days are in close agreement with the predicted values as can be seen from the acceptable desirability values of 0.94 and 0.88 respectively. Controlling of this response facilitated an advantageous release pattern that released 65% of disulfiram in 28 days (Figure 3.14). The initial burst release within the first 2-4 hours is still present however it has reduced considerably (by 40%) compared to the design formulations. The percentage of the burst release from the optimized is 12% compared to a burst release of 15-40% in 4 hours from TPGS micelles as reported by Sonali et al., (2015). Thus the disulfiram-loaded TPGS-nanomicelles have a lower burst release which is favourable. The burst release can be assigned to the relatively high concentration of disulfiram in the micelles (Mi et al., 2012) or to a small quantity of drug that is adhering to the interface of the nanomicelles' outer shell and inner core or perhaps even within the shell itself. As a result passive diffusion and hydration of the interfacial drug molecules can commence resulting in a slight burst effect (Mu et al., 2005). The majority of the drug is incorporated firmly in the inner core of the nanomicelle resulting in a slow release. Retention of the drug inside the micelle core is ascribed to the bulky inner core fashioned by TPGS resulting in a high loading capacity (Suksiriworapong et al., 2014). The hydrophobic nature of disulfiram and the aromatic ring of TPGS cause a strong hydrophobic interaction thus promoting entrapment within the micelle. This aspect of TPGS also enhances the stability of disulfiram's entrapment thereby supporting slow release (Gao et al., 2008). Slow diffusion due to disulfiram being well encapsulated in the core results in subsequent sustained release, whilst small burst release is due to a miniscule amount of disulfiram that was inadequately entrapped (Zeng et al., 2013). To recapitulate, the structure of TPGS and that of the micelle formed as well as the intense hydrophobicity of disulfiram all combine to promote high drug loading, high entrapment efficiency and slow release.

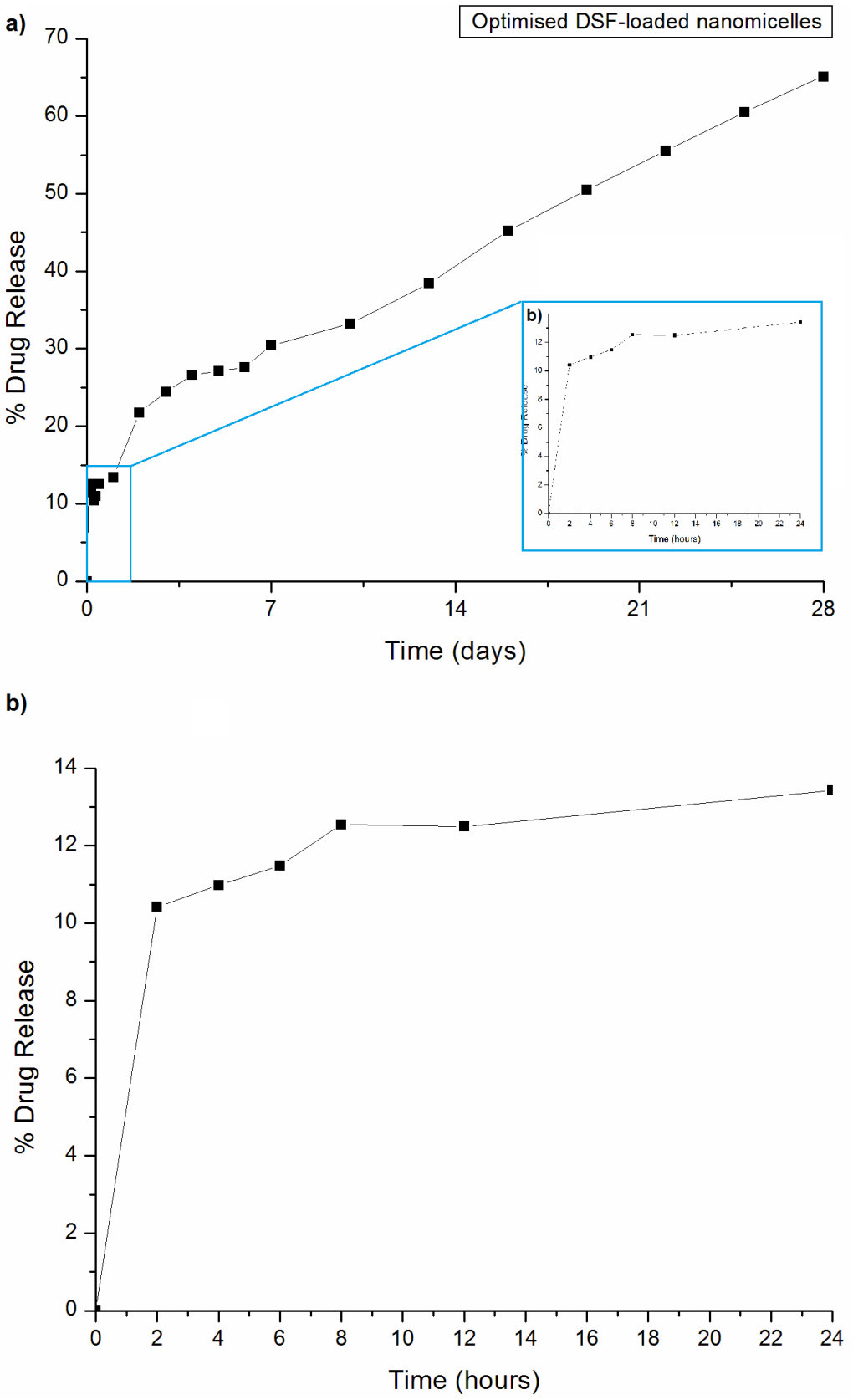

Figure 3.14: a) *In vitro* drug release from the optimized disulfiram-loaded TPGS nanomicelles over 28 days and b) enlarged inset depicting *in vitro* drug release from the optimized disulfiram-loaded TPGS nanomicelles over the first 24 hours.

The congruity of the actual and fitted response values emphasizes the significance of the optimization process and validates the success of the optimization methodology employed.

3.3.9 Analysis of particle size and zeta potential of TPGS nanomicelles

Blank and disulfiram-loaded nanomicelles were analysed according to particle size, PDI and zeta potential (Table 3.9). Sizes for both nanomicelle formulations were 21.61nm (SD ≤ 6.86, n=3) for disulfiram-loaded nanomicelles and 23.16nm (SD ≤ 10.95, n=3) for drug free nanomicelles which were in agreement with the values obtained in the design. The small size of the particles may be as a consequence of strong interaction between the hydrophobic chains of the polymer thus creating a more compact architecture (Butt et al., 2012). These sizes are preferred as particles in the size range of 10nm-70nm are able to penetrate small capillaries thus increasing the extent of circulation (Goldberg et al., 2007). The small size conceals them from detection by the RES and Mononuclear Phagocyte System (MPS) thus protecting them from destruction. In this manner they attain longevity during systemic circulation. Additionally, they are not too small thereby saving them from rapid removal due to renal clearance and extravasation as is common with particles ≤ 10nm (Goldberg et al., 2007).

Table 3.9: Particle size, PDI and zeta potential for disulfiram-loaded and drug free nanomicelles.

Formulation	Size (nm)	PDI	Zeta Potential (mV)
Drug free nanomicelles	23.16	0.37	-26.4
Disulfiram-loaded nanomicelles	21.61	0.31	-52.0

The disulfiram-loaded nanomicelles exhibited a slightly smaller particle size compared to the drug free nanomicelles. This is due to the effect of the entrapment mechanism occurring during micelle formation. Hydrophobic drugs can be encapsulated through physical entrapment or chemical conjugation (Dou et al., 2014). In the case of disulfiram nanomicelles physical entrapment occurs due to the hydrophobic moieties of the polymer and drug. By virtue of this, the cohesive force present in the core of the micelle is amplified causing a decrease in the size of the micelles (Dou et al., 2014). The size distribution profiles for disulfiram-loaded nanomicelles and drug free nanomicelles are depicted in Figure 3.15 and Figure 3.16 respectively.

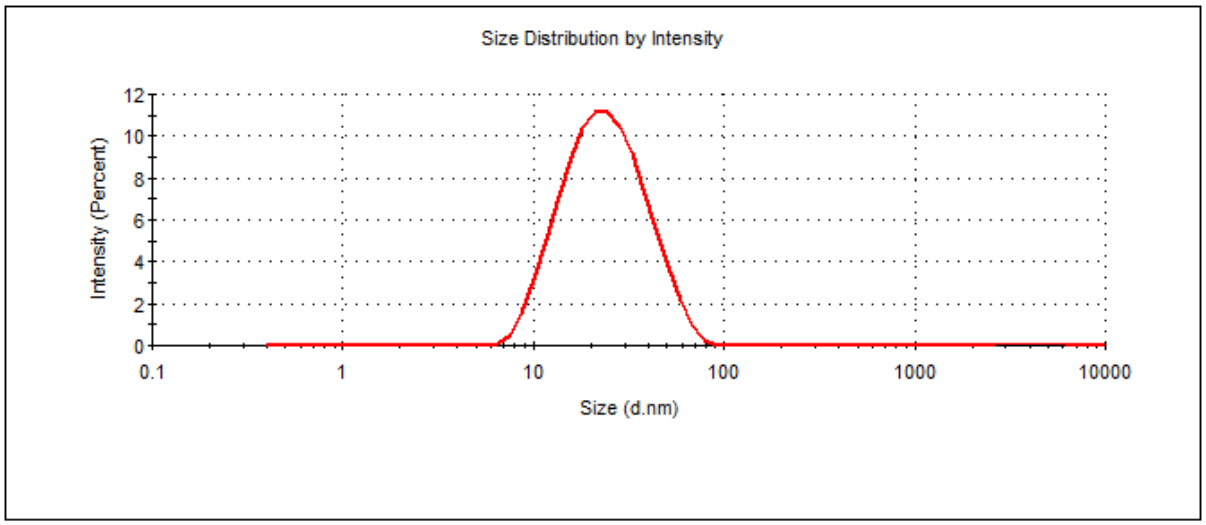

Figure 3.15: Size distribution profile for optimized disulfiram-loaded TPGS nanomicelles.

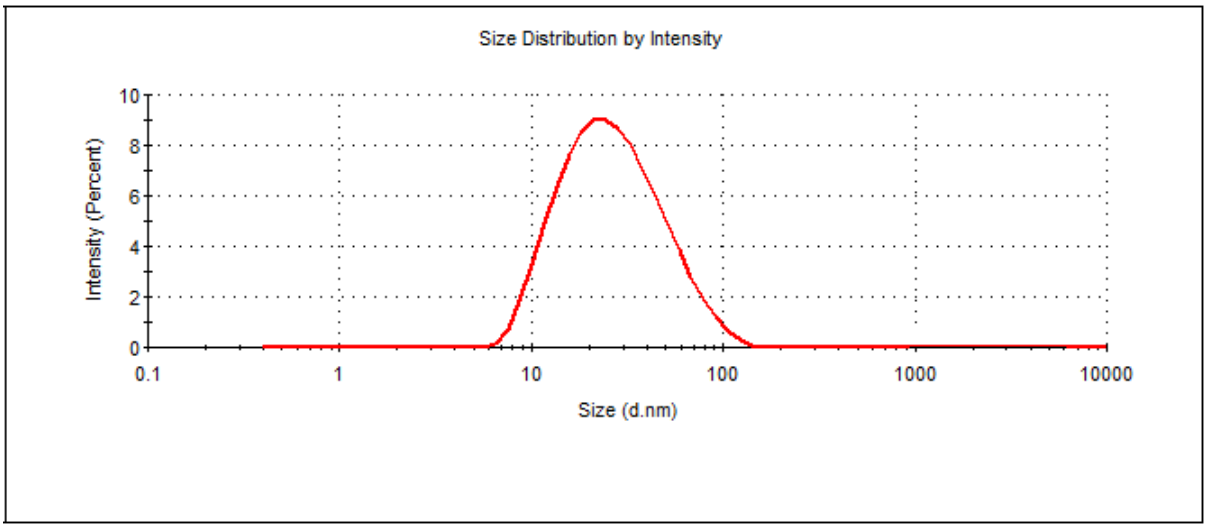

Figure 3.16: Size distribution profile for optimized drug free TPGS nanomicelles.

PDI is a measure of the broadness of the particle size distribution. PDI values of <0.5 are acceptable as they indicate narrow distribution of particles (Gibis et al., 2013). PDI values for disulfiram-loaded nanomicelles and drug free nanomicelles were 0.31 (SD ≤ 0.1, n=3) and 0.37 (SD ≤ 0.12, n=3) respectively. These values of approximately 0.3-0.4 are indicative of narrow distribution and are within the acceptable range. PDI values provide an indication of the particle size dispersion. A high DPI denotes a polydisperse system whilst values closer to zero reflect monodisperse systems. Accordingly, the nanomicelles are relatively monodisperse with the particle sizes being mostly the same.

The zeta potential of a system allows predictability of the long term stability of the nanomicelles. Values below ±30mV signify systems that are prone to aggregation of the

particles owing to limited stability (Duffy et al., 2011). Values ±30mV indicate systems with good physical stability. The zeta potential for drug free nanomicelles was recorded at 26.4mV (SD ≤ 4.20, n=3). These particles are on the threshold of light dispersion and may be prone to aggregation but very minimally. The disulfiram-loaded nanomicelles value for zeta potential is -52.0mV. The high negative charge means that the particles will repel each other and therefore will not possess the tendency to agglomerate. This enhanced stability can be assigned to the strong disulfiram-TPGS interactions that form a firm, steady micellar arrangement. The zeta potential distribution profiles for disulfiram-loaded nanomicelles and drug free nanomicelles are depicted in Figure 3.17 and Figure 3.18 respectively.

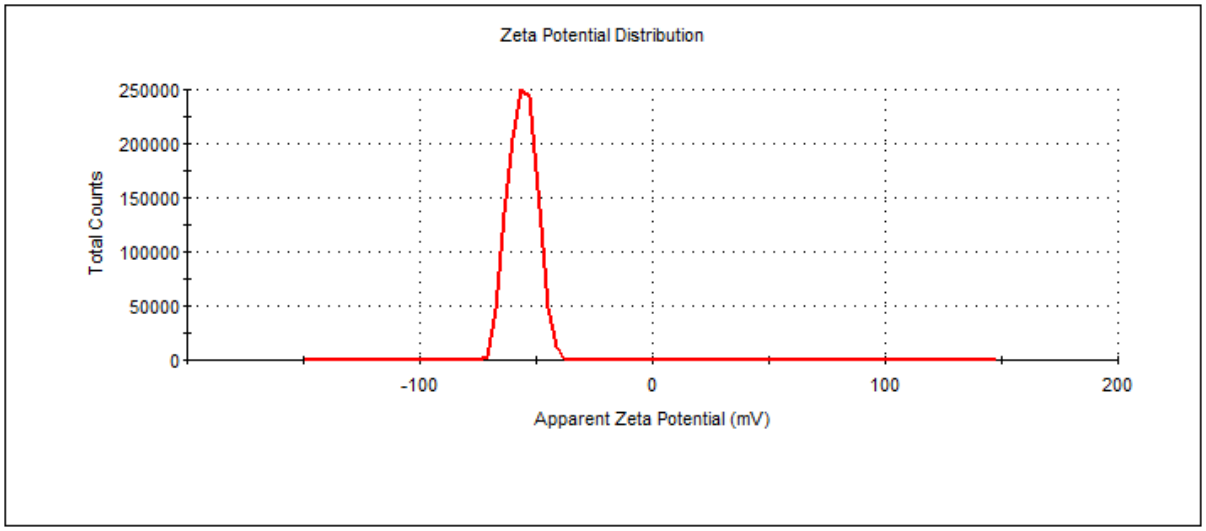

Figure 3.17: Zeta potential distribution profile for optimized disulfiram-loaded TPGS nanomicelles.

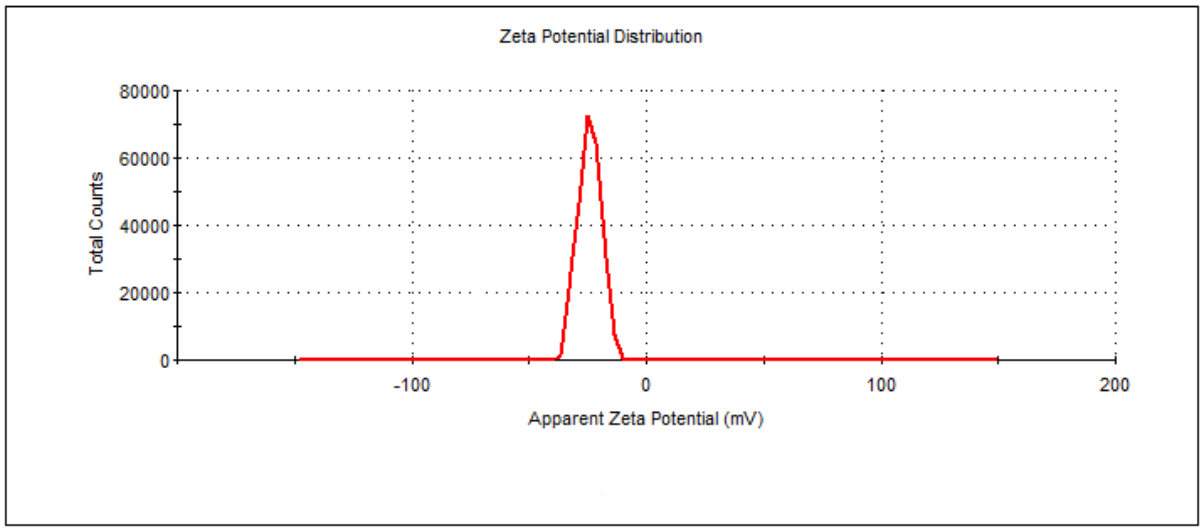

Figure 3.18: Zeta potential distribution profile for optimized drug free TPGS nanomicelles.

3.3.10 Morphological analysis of the TPGS nanomicelles using Transmission Electron Microscopy

Figure 3.19 portrays a) disulfiram-loaded nanomicelles and b) drug free nanomicelles. The nanomicelles are spherical in shape, and homogenous as is evident from the size uniformity present in the image. Sizes are very similar to those obtained through DLS thus a positive correlation exists between DLS and TEM results. Of significance as well is the observation that the incorporation of drug did not alter the morphology of the particle. Disulfiram nanomicelles are well dispersed due to their large zeta potential which prevents agglomeration. Slight agglomeration is seen with the drug free nanomicelles as expected due to the lower zeta potential. Therefore the disulfiram nanomicelles possess inherent stability, greater than the drug free nanomicelles, due to the incorporation of disulfiram which magnifies the hydrophobic interactions forming a stable micellar network.

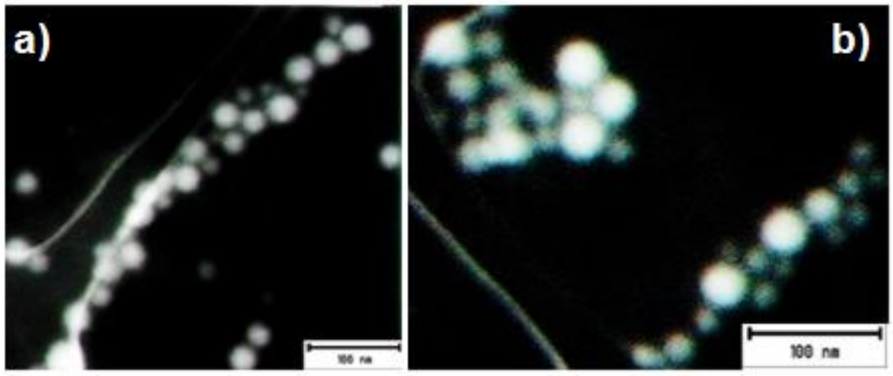

Figure 3.19: Electron micrographs of a) disulfiram-loaded nanomicelles and b) drug free nanomicelles at 50 000x magnification.

3.3.11 Confirmation of the Critical Micelle Concentration of TPGS nanomicelles

The Critical Micelle Concentration (CMC) value is a crucial parameter for *in vitro* and *in vivo* stability of the nanomicelle system. In this experiment iodine was utilised as the hydrophobic probe to detect the formation of nanomicelles. Solubilised I_2 is more partial to the hydrophobic microenvironment of TPGS (thus it has the ability to be enclosed into the core of the micelle). Excess KI in solution results in a conversion of I_3^- to I_2 thereby maintaining the saturated concentration of I_2 in solution (Fan et al., 2015). The absorbance intensity of I_2 is plotted as a function of polymer concentration in Figure 3.20. The value which is used to calculate the CMC is the intersection point of the two tangent lines drawn (Lin et al., 2013). At lower concentrations of TPGS the change in absorbance is small. As the concentration increases there is a sudden rise in absorbance values. It is at this point that a micelle is formed and the I_2 entrapped within the micelle core. The CMC was calculated to be 0.02% w/v. This low CMC value is in accordance with the literature which states that TPGS has a

CMC of 0.02% w/v (Eastman Chemical Company, 2005). A low CMC is favourable as it is indicative of high stability as well as the ability to preserve integrity even upon dilution in body fluids (e.g. blood) (Dou et al., 2014, Mi et al., 2012).

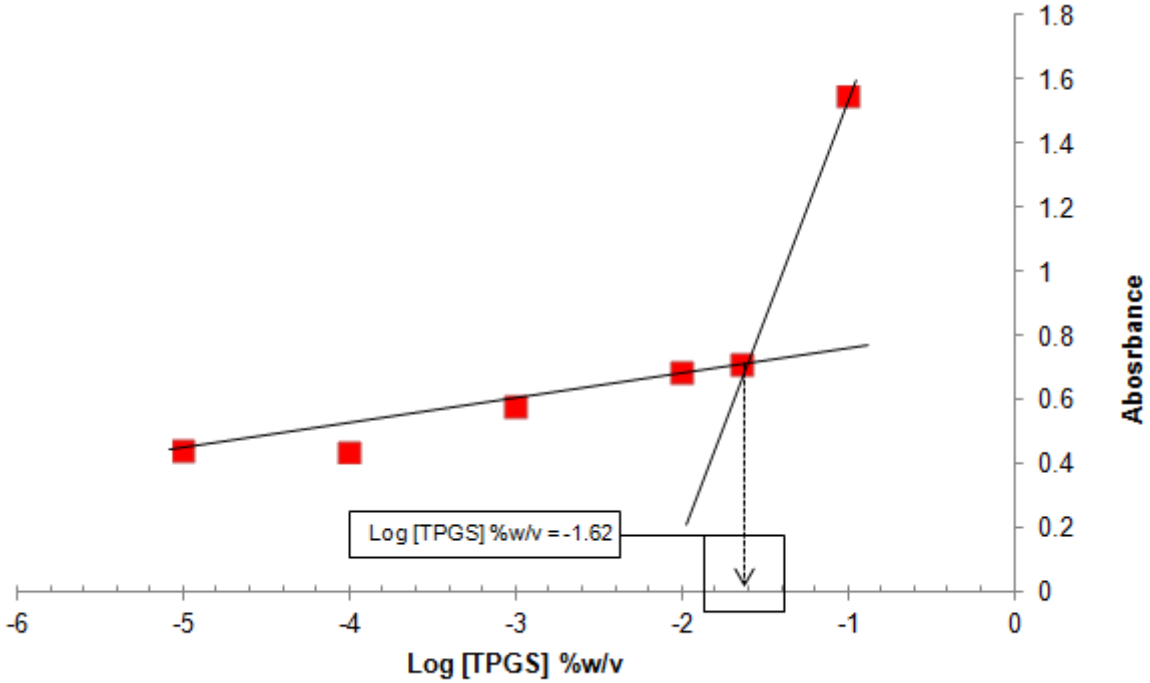

Figure 3.20: The determination of the CMC value for TPGS nanomicelles.

3.3.12 Redispersability of the optimized TPGS nanomicelles

The redispersability study was conducted in order to ascertain the effect of lyophilization on in terms of physical stability (Figure 3.21). Physical instability is a major limitation of polymeric nanomicelles. Nanomicelles are more susceptible than nanoparticles to aggregation as a result of kinetic motion. This is because of their smaller size and more dynamic nature compared to nanoparticles. It is possible that drug may diffuse out of the micelle resulting in drug leakage. This could occur as a consequence of temperature fluctuations during transportation and storage (Suksiriworapong et al., 2014). In order to prevent this from occurring, conversion of nanomicelles into a dried powder through complete water elimination can be beneficial. Lyophilization inhibits aggregation and drug leakage and in doing so prolongs shelf-life (Suksiriworapong et al., 2014). However, lyophilization itself can be a disadvantage. Due to the small sizes of the particles formulated redispersability studies are necessary as smaller particles have a greater tendency to aggregate during lyophilization (Mu and Feng, 2006). This negative effect of lyophilization can have a detrimental outcome on the efficacy of the final product. Redispersability provides an effective test to determine if lyophilization is suitable for maintaining the physical stability of the product. If the particle size increases after lyophilization this represents

aggregation (characterized by a large redispersability ratio). In this case additional stabilisers will be needed which can complicate the fabrication process as well as increase the costing and lengthen the production time.

The redispersability ratio for disulfiram-loaded nanomicelles and drug free nanomicelles is 0.69 and 0.75 respectively. These values are low which is suggestive of good stability and redispersion ability. Particles inclination to shrink and collapse in the dry state is accountable for the decrease in size after lyophilization (Zeng et al., 2013). As a result lyophilization is a suitable process to enhance the physical stability of the nanomicelles.

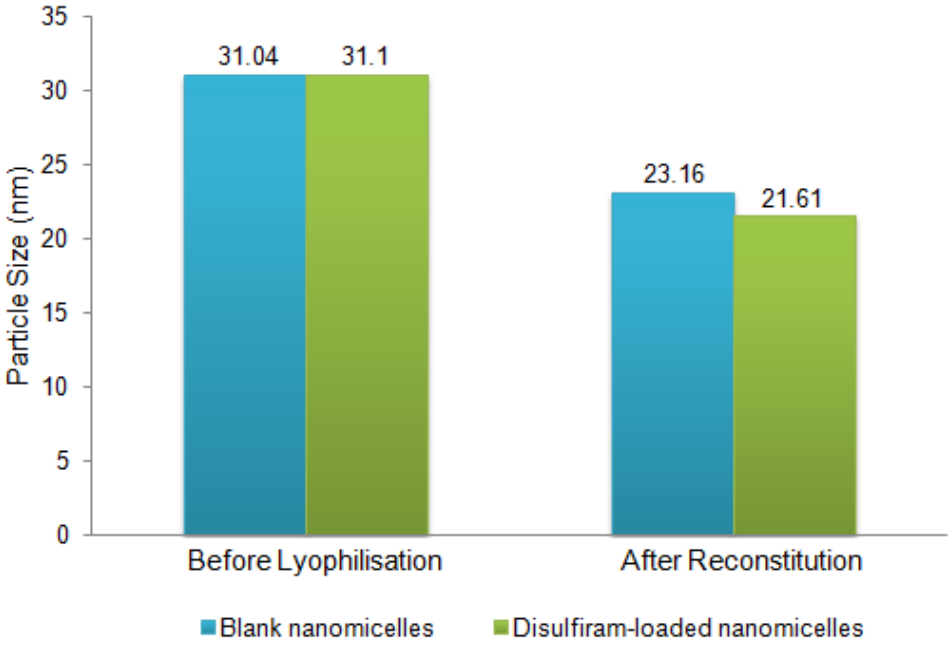

Figure 3.21: Comparison of particle size before and after lyophilization for disulfiram-loaded nanomicelles and drug free nanomicelles (SD ≤ 1.09 in all cases, n=3).

3.3.13 Investigation of structural variation via Fourier Transform Infrared spectroscopy analysis

FTIR was used to determined the structural integrity of the nanomicelles and the native constituents. Figure 3.22 displays the individual components of the nanomicelles as well as drug free nanomicelles and disulfiram-loaded nanomicelles.

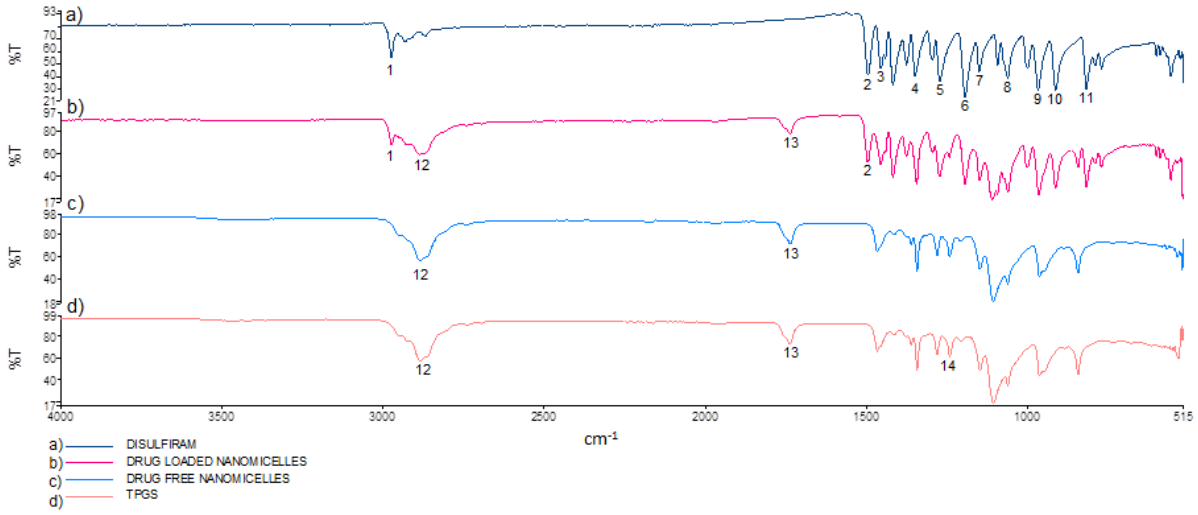

Figure 3.22: FTIR spectra of a) disulfiram, b) disulfiram-loaded nanomicelles, c) drug-free nanomicelles and d) TPGS.

Disulfiram exhibited two characteristic peaks at 2975cm^{-1} (peak 1) and 1493cm^{-1} (peak 2) signifying C-H (CH_3) stretching and C-H symmetrical deformation vibrations respectively. The bands at 1345-1455cm^{-1} (peak 4 - peak 3) can be attributed to CH_2-CH_3 vibrations. C=S stretching is represented by 1272cm^{-1} (peak 5). At 1193cm^{-1} (peak 6) C-H skeletal vibrations can be observed and at 1150cm^{-1} (peak 7) C-C skeletal vibrations can be observed. C-N stretching can be assigned to the bands at 965-1060cm^{-1} (peak 9 - peak 8). Bands at 816-912cm^{-1} (peak 11 - peak 10) represent C-S stretching. A comparison of the native disulfiram spectra to that of disulfiram-loaded nanomicelles spectra shows that the characteristic peaks at 2975cm^{-1} (peak 1) and 1493cm^{-1} (peak 2) are still present in the nanomicelle formulation. This indicates the presence of drug in the nanomicelle system as well as the stability of the drug. At 2884cm^{-1} (peak 12) the TPGS spectra displays characteristic C-H stretching of CH_3. The carbonyl band at 1736cm^{-1} (peak 13) indicates C=O stretching vibration. The bands in the region of 1250cm^{-1} (peak 14) are due to C-O stretching. Comparison of the native TPGS spectra to that of the drug free nanomicelles illustrates extremely similar spectra with negligible shifts or changes in bands. This signifies that the nanomicelle fabrication and lyophilization processes did not alter or destroy the structure of TPGS. The characteristic bands of TPGS in its native form are also present in the disulfiram-loaded nanomicelles spectra albeit with some displaying a minimal shift. These slight differences are indicative of intermolecular interactions between the drug and polymer (Liao et al, 2015). A small peak at 1979cm^{-1} (not visible here due to compression of the graph), indicating C=C asymmetric stretching, is also present in native TPGS, drug-free nanomicelles and disulfiram-loaded nanomicelles. Comparison of all four spectra indicates that majority of the distinctive peaks from each native constituent is present in the nanomicelle spectra and that peaks from TPGS that are not present are due to overlapping of disulfiram peaks on those. Thus it can

be established that amalgamation of disulfiram and TPGS has occurred and the appearance of peaks from both native compounds shows that no chemical interaction has occurred between the polymer and drug. Furthermore it can be confirmed that lyophilization as well as the utilisation of an organic solvent during preparation did not adversely affect the formulation as no chemical structural changes have occurred. The absence of foreign peaks indicates that all organic solvent was adequately removed prior to lyophilization.

3.3.14 Thermal profile analysis of the nanomicelles

DSC was utilised to determine the thermal characteristics of native TPGS, native disulfiram, drug-free nanomicelles and disulfiram-loaded nanomicelles. The thermograms are displayed in Figure 3.23. The native TPGS thermogram displays two phenomena. The first is an endothermic peak at 38°C. this peak is representative of the melting point (T_m) of TPGS. This T_m value indicates the crystalline nature of TPGS (Lee et al., 2015). The second thermal event has an onset at 215.6°C. this denotes the thermal non-oxidative degradation temperature of TPGS. These findings are in agreement with reported thermal behaviour for TPGS (Eastman Chemical Company, 2005; Ahn et al., 2011). The high degradation temperature of TPGS implies that it is a fitting choice of polymer as it is thermally stable under standard processing temperatures utilised in pharmaceutical application (Shin and Kim, 2003). The blank nanomicelle thermogram shares similarity to the native TPGS curve. The one major difference is the absence of the degradation peak. The T_m peak of the blank nanomicelles is present at the same temperature (38°C) as that of pure TPGS. There is no change in the peaks nor are there any new peaks. This emergence of the TPGS peak without any change in the peak or new peaks indicates that the TPGS structure is maintained and is present intact in the drug-free nanomicelles (Vuddanda et al., 2014). The disulfiram thermogram displays one endothermic peak at 209.6°C. This peak indicates the decomposition of disulfiram (Carreño and Gajardo, 2011). The disulfiram-loaded nanomicelles also display the exact same event indicating that disulfiram is present in the nanomicelle.

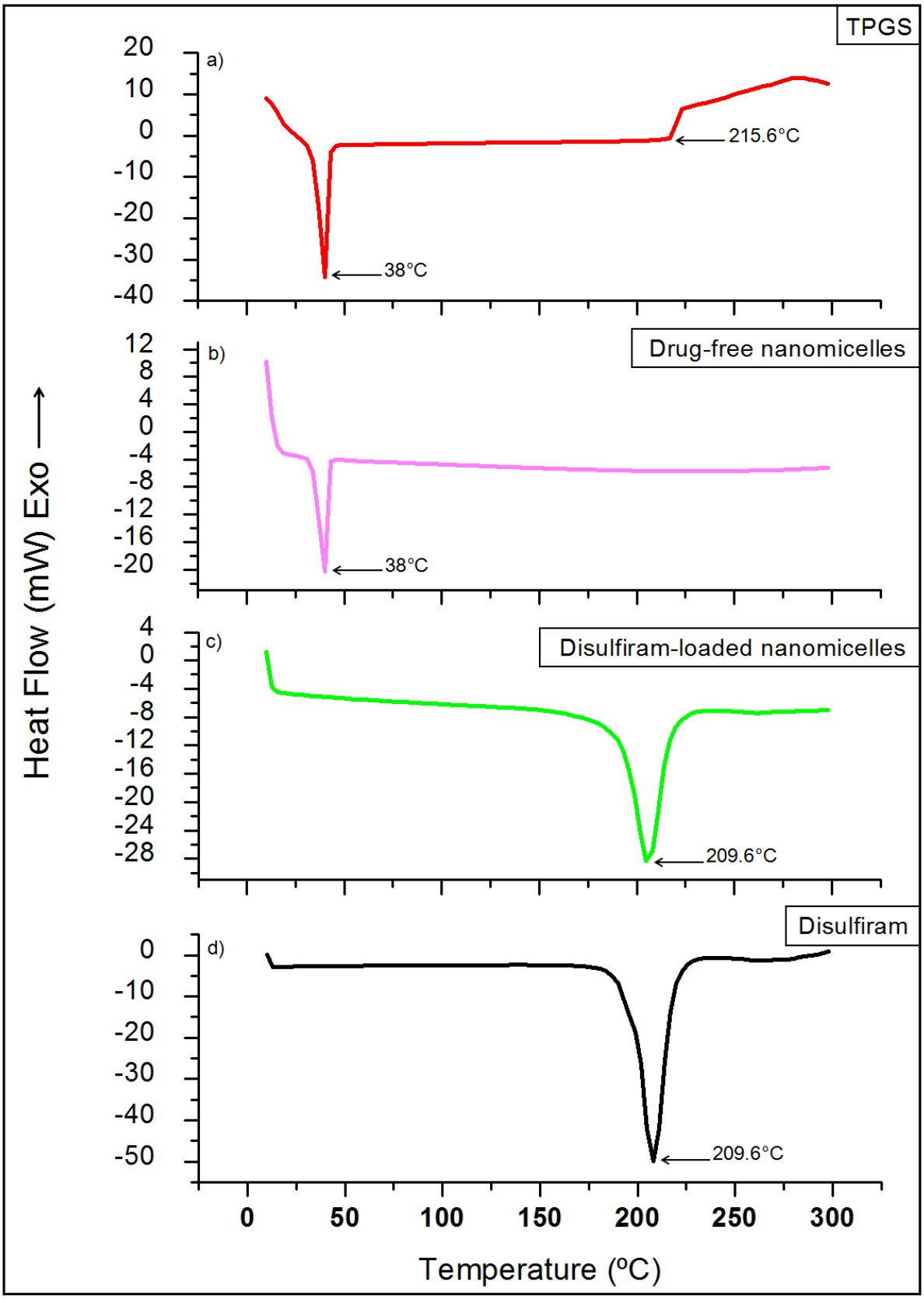

Figure 3.23: Thermograms of a) TPGS, b) drug-free nanomicelles, c) disulfiram-loaded nanomicelles and d) pure disulfiram.

3.3.15 Analysis of the degree of crystallinity of nanomicelles

XRD is a useful chemical analysis tool in which the interaction of x-rays with atoms causes scattering of the x-rays which leads to the formation of the diffraction pattern. This can aid in compound identification and degree of polymer crystallinity. The crystal structure provides a description of the atomic arrangement of the material. The crystalline state of TPGS, disulfiram, drug-free nanomicelles and disulfiram-loaded nanomicelles was investigated using XRD (Figure 3.24).

TPGS has two sharp peaks at 2θ of 19° and 23°. This is indicative of the crystal nature of TPGS (Srivalli and Mishra, 2015). These peaks correspond to the semicrystalline polyethylene glycol chains of TPGS (Janssens et al., 2007). These peaks are in accordance with previously reported values (Goddeeris et al., 2008; Shin et al., 2016). Drug-free nanomicelles displayed the defining peaks of pure TPGS. The decrease in intensity is representative of a slight decrease in crystallinity. The overall profile is not significantly different to that of native TPGS. The disulfiram diffractogram displays a large number of sharp, high intensity diffraction peaks symbolising the highly crystalline nature of disulfiram. The diffractogram for disulfiram-loaded nanomicelles shows the peaks of both disulfiram and TPGS. Both components have retained their crystallinity with the very sharp peaks being attributed to disulfiram and those that are slightly broader being attributed to TPGS.

It is evident from the diffractograms that nanomicelles prepared using the solvent casting method has had no effect on the physical state of the active as well as the polymer. Whilst both still maintain a predominantly crystal state the decrease in intensity is synonymous with a decrease in crystallinity. This could be due to the method of preparation by which both components were dissolved in chloroform and in doing so both were maintained in the dissolved state upon chloroform extraction (Zembko et al., 2014).

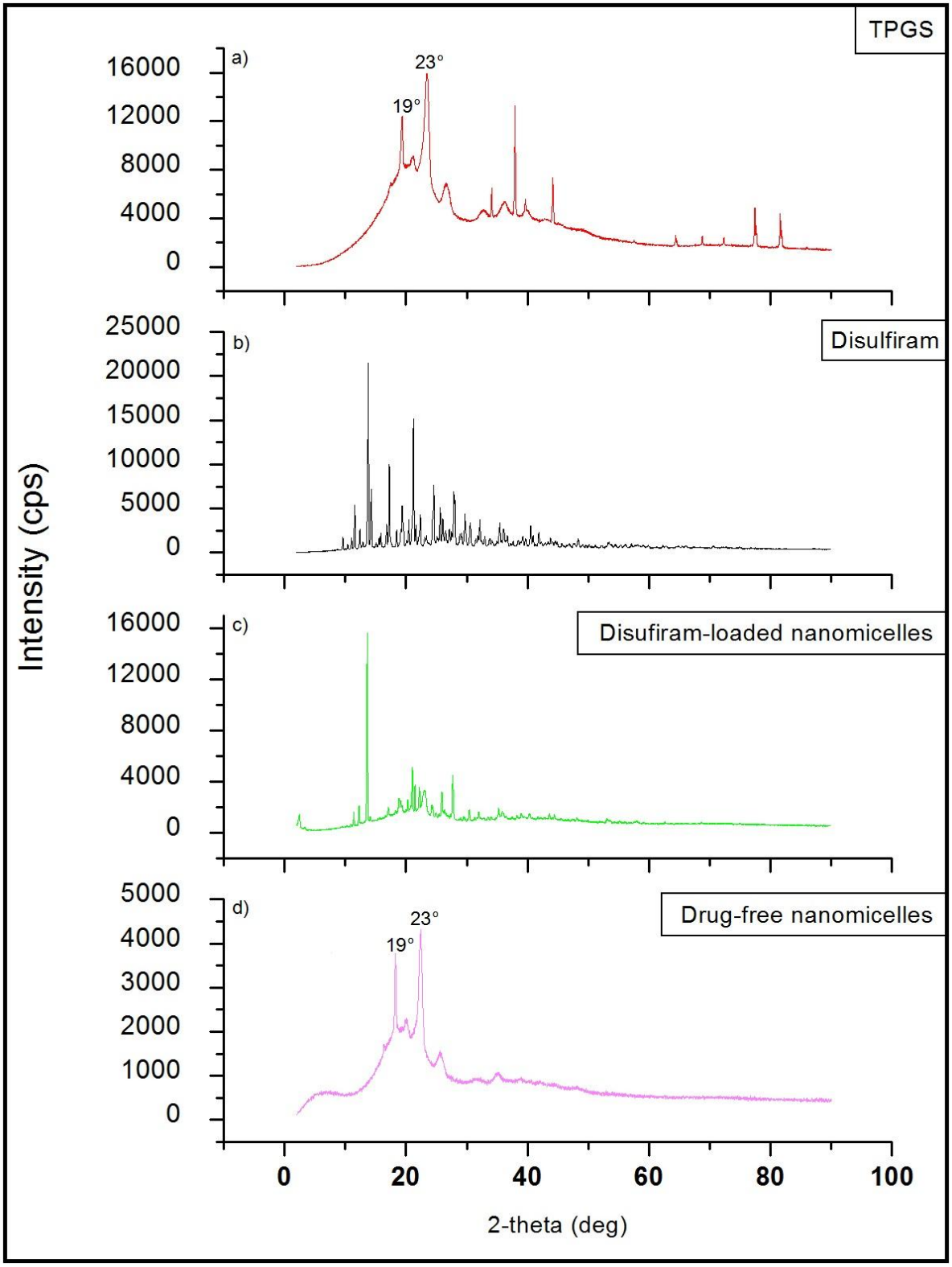

Figure 3.24: Diffractograms of a) TPGS, b) disulfiram, c) disulfiram-loaded nanomicelles and d) drug free nanomicelles.

3.4 Concluding Remarks

Nanomicelles were successfully designed, developed and optimised utilising the DoE approach. A Face Centred Central Composite Design was used to generate 13 formulations. The solvent casting method was employed which possesses a simplicity that is favourable. The effect of two independent variables (stirring time in hours and polymer amount in milligrams) on specific responses (entrapment efficiency %, drug loading % and drug release %) was investigated and statistically analyzed. The constraint optimization of the formulation responses generated a single, optimized formulation. The experimental responses of this optimized formulation were evaluated and the results were determined to correlate highly with the predicted responses thereby validating the optimization methodology employed. Extensive studies were conducted on the optimized nanomicelles in order to obtain the physicochemical and physicomechanical profile of the nanomicelles. Results from the characterization tests were positive with the optimized nanomicelles displaying uniformity in size, as well as a small size which endorses extended circulation and evasion of the RES. The nanomicelles demonstrated good stability and favourable drug loading and drug entrapment. Additionally the nanomicelles were capable of sustained release and a low CMC which makes them stable to dilution.

A second component is needed as a delivery vehicle for the nanomicelles. Ideally this component should augment the advantages of the nanomicelles that are already present. A prospective solution is an *in situ* gel which will serve the dual purpose of a vehicle as well as promote stable, sustained release of disulfiram and disulfiram-loaded nanomicelles. The formulation, rheological characterisation and selection of the model gel is extensively described in the following chapter.

CHAPTER 4

THE INFLUENCE OF THE DEGREE OF GELLAN GUM ACETYLATION ON THE RHEOLOGICAL PROPERTIES OF PLURONIC F127-GELLAN GUM GELS

4.1 Introduction

The disulfiram-loaded TPGS nanomicelles have been confirmed to possess a desired profile as determined by statistical optimisation in Chapter 3. Consequently, the next step is to obtain a suitable vehicle to utilise in the parenteral administration of the nanomicelles. Many of the vehicles employed for parenteral delivery have no further benefit to the delivery system except that they provide a suitable means of transferring the system into the body. This necessity for a vehicle can be positively exploited to confer added advantages to the already beneficial nanomicelles and, in doing so, create a dual delivery system with heightened therapeutic benefit that surpasses the use of a single delivery system. An situ gel is a prime example of such a beneficial vehicle. A primary advantage of loading the nanomicelles into a gel is that this allows the nanomicelles to be retained for a longer period of time (Gupta et al., 2013). As a result, this extends the release of drug at a therapeutic rate (Jung et al., 2013). It also provides additional stabilisation of the nanomicelles (Juby et al., 2012). Administration of in situ gels occurs in the liquid state and a change transpires on exposure to the related stimuli thus making them easy to formulate and handle. They can be effortlessly administered via injection, thus eliminating the need for invasive surgical procedures (Packhaeuser et al., 2004). They can be modified to impart desirable release properties to the active thus maximising efficacy and compliance and minimising harm through toxicity (Madan et al., 2009). A myriad of polymers exist which can be employed in these delivery systems. For the purpose of a long term depot preparation a thermally influenced system has most benefit.

Pluronic F127 (PF127) is an amphiphilic triblock copolymer comprising polyethylene oxide (PEO) and polypropylene oxide (PPO). The repeating units comprise a core of PPO surrounded by PEO on either side (Figure 4.1). It has great potential in drug delivery due to its advantageous properties. Of particular value are its biocompatibility with cells and body fluids, low toxicity and weak immunogenicity, bioadhesivity, syringability, sustained release and thermoreversible characteristics (Akash et al., 2014; Ricci et al., 2005). Additionally PF127 does not require any crosslinking agents, it has excellent compatibility with a wide range of pharmaceutical actives and excipients with quick and effortless preparation (Koffi et al., 2006; Kim et al., 2014). The intricate molecular architecture of PF127 gives rise to its amphiphilic and thermoreversible elements, making it ideal for *in situ* gelling systems (van Hemelrijck and Müller-Goymann, 2012) . The sol-gel conversion facet allows PF127 to be

easily administered as a liquid at low temperatures and morph into a solid configuration once heated up to body temperature (37,5°C). The temperature at which the transition occurs is dependent on the concentration of PF127 (Cunha-Filho et al., 2012). Furthermore, PF127 can be administered intra-muscularly (Dumortier et al., 2006).

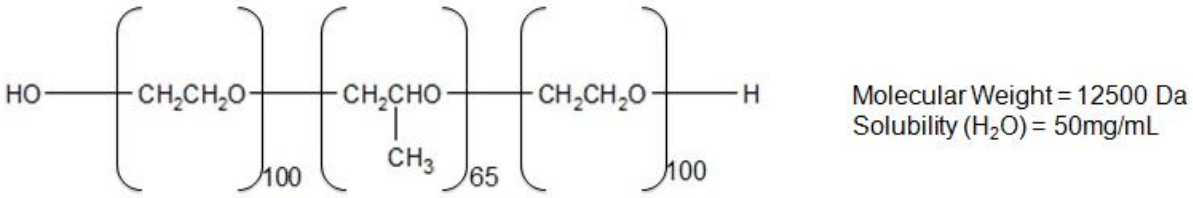

Figure 4.1: Chemical structure of PF127.

A major challenge of PF127 is the unfavourable properties of weak mechanical strength and poor stability (Gradinaru e al, 2012). Furthermore, high concentrations are required for a firmer gel to form (Varshosaz et al., 2008). Additionally the packed micelles may dissociate due to the presence of excess water. This can compromise gel integrity by initiating degradation that shortens the usage duration (Jeong et al., 2002). It is possible to add other polymers in order to modify the gel properties of PF127 such that the benefits of PF127 are maintained while the weaknesses are overcome (Akash et al., 2014). A previous attempt to rise above the shortcomings of PF127 involved modifying the chemical structure resulting in the formation of a toxic residue that posed complicated safety concerns (Liu et al., 2009). A less explored but potentially viable option that can counteract the inadequacies of PF127 are through the use of biological macromolecules (Liu et al., 2009). Of particular interest is the anionic extracellular heteropolysaccharide gellan gum (GG). Obtained through inoculation of *Sphingomonas elodea* (formerly *Pseudomonas elodea*) in fermentation broth, this macromolecule has received widespread acclaim across diverse research fields due to its natural properties, gelation effects, textural aspects and its suitability to a plethora of applications (for example, GG has application in the sustained release of drugs (Banik et al., 2000). Two strains of GG are commercially available: the native high acyl (HAGG) strain, which is directly recovered from the fermentation broth and a low acyl (LAGG) strain that is produced via alkali deacetylation. The distinct chemical compositions of HAGG and LAGG confer uniquely desirable traits to each strain. The chemical structure comprises repeating tetrasaccharide units of glucose, glucuronic acid and rhamnose residues in a 2:1:1 ratio (Figure 4.1.). HA has O-5-acetyl and O-2-glyceryl groups attached to this unit (Figure 4.2.). Selection of the appropriate strain is predetermined by the ultimate outcome required. LAGG is favoured when firm brittle gels are needed; conversely HAGG is the strain of choice when elastic gels are sought.

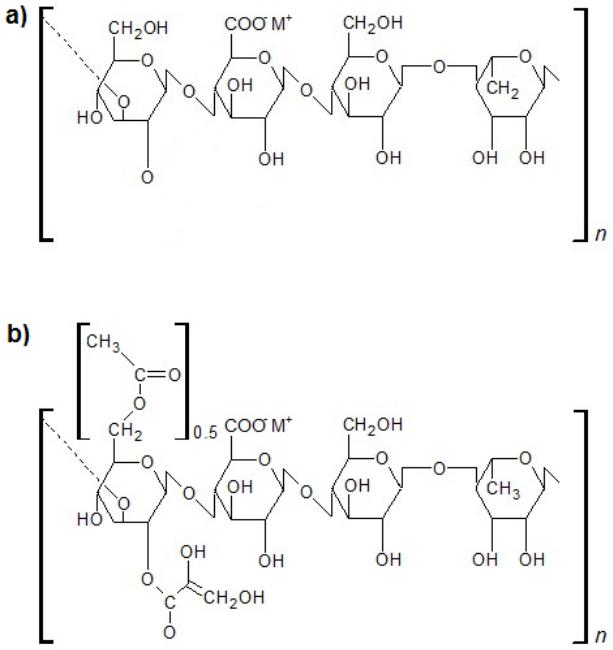

Figure 4.2: Chemical structure of a) LAGG and b) HAGG.

The rheological data of a sample has immeasurable worth in advanced drug delivery system development. The following can all be obtained from thorough rheological characterization of a sample: rheological properties (such as stability, flow, deformation), molecular composition, intrinsic traits, therapeutic utility, mechanical attributes and response to real-life conditions (such as storage and temperature). Two types of rheological testing are beneficial: steady state rheology and dynamic rheology. Steady state rheology is ideal for determination of flow behaviour. Dynamic rheology provides the viscoelastic profile of a sample; this is an excellent tool as it prevents structure breakdown while allowing the sample to be analysed (Arici et al., 2014).

The aim of this chapter is to investigate the effect of acyl content on the rheological properties of PF127 and GG gels as well as determine which form of GG is best suited for the desired application of an intramuscular depot system as well as incorporation of the nanomicelles.. For the purpose of this study an ideal gel would be one that exhibits gel-like properties between 25°C-32°C in order to ensure that a solid gel is formed upon injection into muscle tissue that is between 36.5°C-37.5°C.

4.2 Materials and Methods

4.2.1 Materials

Pluronic F127 (poloxamer 407) was purchased from Sigma-Aldrich Co. (Steinheim, Germany). High Acyl Gellan Gum (Kelcogel LT100) and Low Acyl Gellan Gum (Kelcogel F)

were obtained from CP Kelco Germany GmbH (Grossenbrode, Germany). All other chemicals and solvents were reagent grade.

4.2.2 Preparation of the gel systems

Two sets of gels were formulated. One set comprised of gels made from the combination of PF127 with HAGG (hereon referred to as PF127-HAGG gels) whilst the second set comprised of gel made from the combination of PF127 with LAGG (hereon referred to as PF127-LAGG gels). To formulate the gels varying concentrations of each polymer powder were dispersed in deionised water and stirred for approximately 3 hours using a magnetic stirrer. Once fully dissolved the formulations were refrigerated at 10°C for 12 hours (Ricci et al., 2005). Concentration ranges were selected based on a concentration range where the lower limit was determined as the lowest concentration needed for gelation to occur and the upper limit was determined as the highest concentration that can be used without forming a solid, hard mass of gel. This approach yielded 48 different gels (24 utilising HAGG and 24 utilising LAGG). These formulations are illustrated in Table 4.1 and Table 4.2.

Table 4.1: Combination of PF127 with HAGG to yield 24 different gels.

Formulation (H = HAGG)	**% F127 (w/v)**	**% HAGG (w/v)**
H1	15	0.1
H2	15	0.2
H3	15	0.3
H4	15	0.4
H5	16	0.1
H6	16	0.2
H7	16	0.3
H8	16	0.4
H9	17	0.1
H10	17	0.2
H11	17	0.3
H12	17	0.4
H13	18	0.1
H14	18	0.2
H15	18	0.3
H16	18	0.4
H17	19	0.1
H18	19	0.2
H19	19	0.3
H20	19	0.4
H21	20	0.1
H22	20	0.2
H23	20	0.3
H24	20	0.4

Table 4.2: Combination of PF127 with LAGG to yield 24 different gels.

Formulation (L = LAGG)	% F127 (w/v)	% LAGG (w/v)
L1	15	0.1
L2	15	0.2
L3	15	0.3
L4	15	0.4
L5	16	0.1
L6	16	0.2
L7	16	0.3
L8	16	0.4
L9	17	0.1
L10	17	0.2
L11	17	0.3
L12	17	0.4
L13	18	0.1
L14	18	0.2
L15	18	0.3
L16	18	0.4
L17	19	0.1
L18	19	0.2
L19	19	0.3
L20	19	0.4
L21	20	0.1
L22	20	0.2
L23	20	0.3
L24	20	0.4

4.2.3 Rheological analysis of the gel systems

All rheological experiments were performed using a Haake Modular Advanced Rheometer System (ThermoFischer Scientific, Karlsruhe, Germany) equipped with parallel plate geometry. The rheometer was operated using Haake Software, Rheowin Job Manager V 3.30. The gel sample being tested (0.5mL) was placed onto the lower plate of the rheometer. It was confirmed that there were no air bubbles present in the test sample. An anti-evaporation device was used to prevent sample evaporation. This protocol was maintained for all sample evaluation.

Oscillatory and flow curve experiments were performed on gels to evaluate their rheological properties. Commonly used rheological indicators utilised in this chapter include:

G' (Pa): represents storage modulus which typifies the samples mechanical rigidity. It is the stored deformation energy that is available to the sample. It is also referred to as the elastic modulus. It is calculated using:

G' = stress/strain x cos (δ) **Equation 4.1**

G"(Pa): represents loss modulus which is representative of the dissipated mechanical energy. It is the used deformation energy that is lost from the sample. It is also referred to as the viscous modulus. It is calculated using:

G"= stress/strain x sin (δ) **Equation 4.2**

η (Pa.s): represents viscosity which is the ratio of shear stress (τ) to shear rate ($\dot{\gamma}$). It is calculated using:

$$\eta = \frac{\tau}{\dot{\gamma}}$$ **Equation 4.3**

η^* (m.Pas): represents the complex viscosity which comprises both the elastic and viscous components.

$$\eta^* = \sqrt{(\mathrm{G'^2} + \mathrm{G''^2})} \div \omega$$ **Equation 4.4**

Where ω is the angular frequency in rad/s.

The following rheological tests were undertaken:

- Amplitude sweep
- Temperature sweep
- Frequency sweep
- Time sweep
- Flow analysis

4.2.3.1 Amplitude sweep

Prior to any oscillatory tests, it is imperative that the Linear Visco-Elastic Region (LVER) be determined for each sample. The necessity of LVER determination stems from the rule that the moduli is only significant if it is independent of the applied stress. Thus an amplitude sweep is conducted whereby G' is measured as a function of varying stresses at a constant temperature and frequency. This area, where G' and G", and correspondingly the viscoelastic properties of the gel, are independent of the imposed stresses, is known as the LVER. Conducting the experiment within the LVER ensures that no structural breakage occurs throughout the test procedure. The LVER was determined for all 48 gels from the plot log G' against shear stress. A typical amplitude sweep graph depicting the LVER is displayed in Figure 4.3.

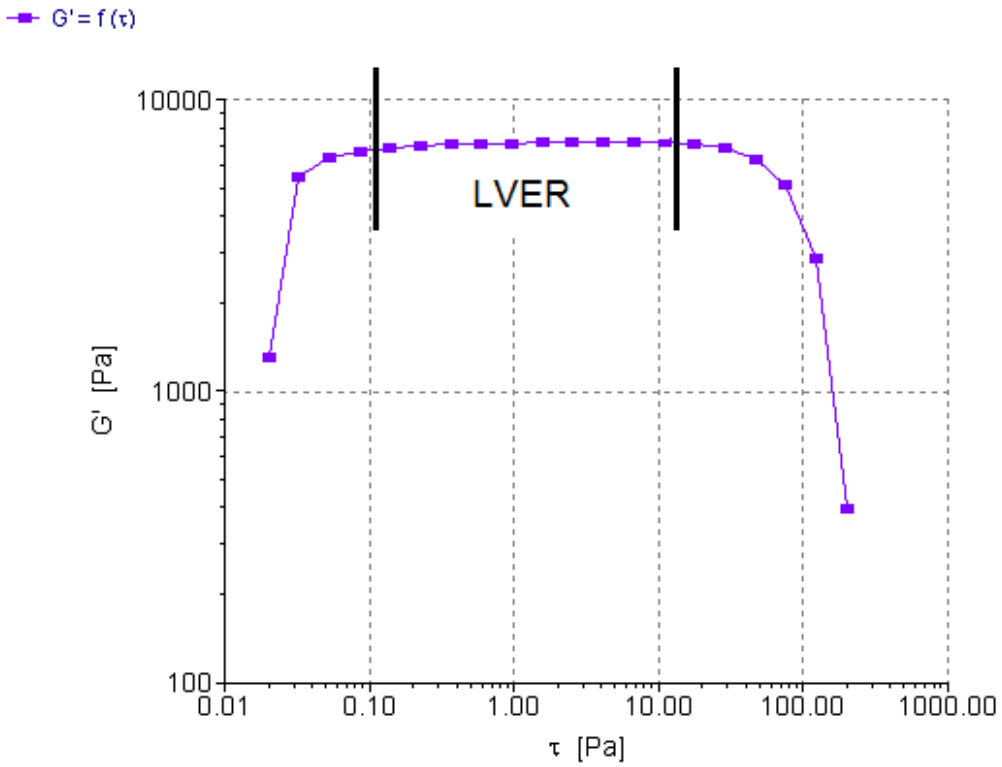

Figure 4.3: Typical amplitude sweep curve showing the LVER.

4.2.3.2 Temperature sweep

The effect of temperature was established for all 48 gels using a temperature sweep test. G', G" and η* were determined as a function of temperature. The temperature range is based upon the preparation, storage and administration conditions as well as physiological temperature. The gel will be stored at 10°C and administered immediately into the muscle tissue.

4.2.3.3 Frequency sweep, time sweep and flow analysis

Frequency sweeps, time sweeps and flow curve analysis tests were performed on selected samples. Frequency sweep tests provide information on the mechanical spectra of the gel. Oscillatory time sweeps determine the gelation time of each gel formulation. In a time sweep test the cross-over between G' and G" is measured in relation to time. The test is conducted at a set temperature of 36.5 °C and thus the gelation time (Gt) is calculated as:

$Gt = t_1 - t_2$ **Equation 4.5**

Where t_1 is the time taken for G' and G" to cross-over and t_2 is the time at which the rheometer plate reached 36.5 °C after placing the sample. Flow curves are used to observe the effect of temperature on flow behaviour of the gels. The experimental setup for each test is displayed in Table 4.3. All tests were conducted at stresses within the LVER. All the data was processed with the aid of Rheowin Data Manager V 3.30.

Table 4.3: Experimental setup for rheological tests.

Experiment	Parameters Measured	Test Temperature (°C)	Stress (Pa)	Shear Rate (s^{-1})	Frequency (Hz)
Amplitude Sweep	G',G", LVER	25	0.02 - 200	-	0.1
Temperature Sweep	G', G", η^*	10 - 40	As per LVER	-	1.0
Frequency Sweep	G', G", η^*	10 and 36.5	As per LVER	-	0.02 - 5
Time Sweep		36.5	As per LVER	-	1.0
Flow Curve	$\tau, \dot{\gamma}$	10 and 36.5	-	0 - 450	-

4.3 Results and Discussion

4.3.1 Temperature sweep

Temperature sweeps were conducted on each of the 48 gels in order to determine the effect of concentration of PF127 and GG on the gelation temperature as well as to determine the difference between LAGG and HAGG on the gelation process.

Before discussing the temperature curves in depth, it is essential to clarify the terms used to describe the gelation processes of HAGG and LAGG gels. As a result of differences in structure, and consequently mechanism of gelation, the temperature sweep curves of HAGG and LAGG illustrated distinctive patterns:

- LAGG samples (with a minority of exceptions) and a small portion of HAGG samples displayed a clear cross-over of G' and G" where prior to cross-over G" was dominant and post cross-over G' was dominant. These samples undergo a sol-gel transition and are termed 'thermoreversible'. All samples displayed an increase in G' and G".
- Majority of the HAGG samples presented a continuously dominating G' with a lower G". In these samples gelling has occurred but the structure was still weak. These samples are termed 'thermosensitive'. All samples displayed an increase in G' and G".

Due to this distinction the use of the term gel point or gel temperature (as is commonly employed) is incorrect, as the latter are already in a gel state from the outset and thus no gelation point can be observed for a gel that is preformed. To avoid further confusion the term Kairotic Point (from the Greek word *kairos*, meaning a defining moment, very crucial moment, critical moment, turning point; abbreviated from here on as KP) will be used as an all encompassing term and will refer to: 1) G'-G" cross-over (for thermoreversible samples) or 2) the point at which G' and G" dramatically rise signifying an increase in structure

strength (for thermosensitive samples). Analysis of the temperature sweep data is divided into the following sections:

4.3.1.1 Effect of PF127 concentration on different concentrations of GG

4.3.1.1.1 Effect of PF127 concentration on different concentrations of HAGG

i. At 0.1% HAGG (H1, H5, H9, H13, H17, H21):
An increase in the concentration of PF127 with 0.1% GG was inversely proportional to KP. As PF127 concentration increases from 15% to 20% the KP decreases from 39.7 °C to 21.5 °C (Figure 4.4a). This effect is illustrated in Figure 4.5.

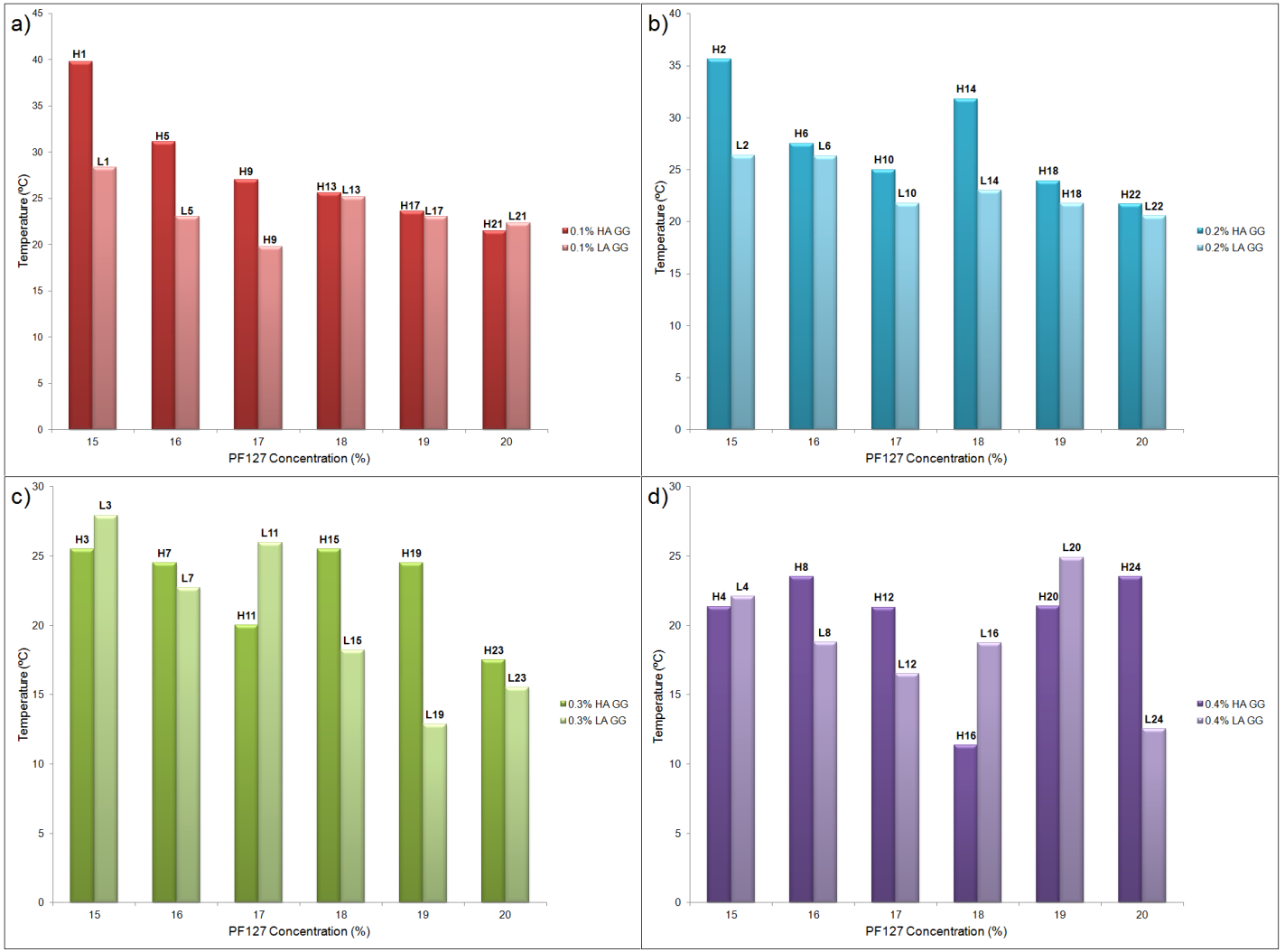

Figure 4.4: KP values for varying concentrations of PF127 at: a) 0.1% GG, b) 0.2% GG, c) 0.3% GG and d) 0.4% GG.

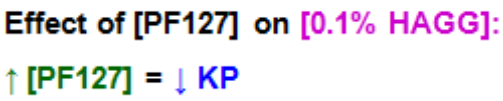

Figure 4.5: Schematic illustrating the effect of PF127 concentration with 0.1% HAGG.

ii. At 0.2% HAGG (H2, H6, H10, H14, H18, H22):

The effect of PF127 with 0.2% was similar to that of 0.1% GG with one exception, H14. Instead of the KP of this sample being lower than that of 16% and 17% PF127 as predicted, the KP was greater than both. The KP's for H18 AND H22 are equal to the KPs of H17 and H21 respectively (Figure 4.4b). This effect is illustrated in Figure 4.6.

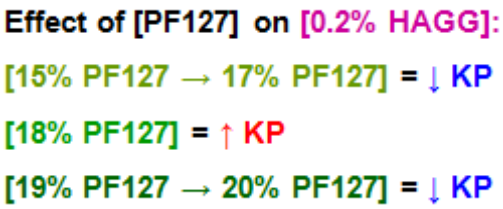

Figure 4.6: Schematic illustrating the effect of PF127 concentration with 0.2% HAGG.

iii. At 0.3% HAGG (H3, H7, H11, H15, H19, H23):

At this concentration a deviation from the established trend occurs. An increase in PF127 concentration up to 17% shows the correlating decrease in KP. However at 18% PF127 (H15) an increase occurred to such an extent that the KP is then identical to that of H3. Thereafter a drop in KP occurs with the increase from 19% to 20%. At this GG concentration the KP of H7 is equal to the KP of H19 (Figure 4.4c). This effect is illustrated in Figure 4.7.

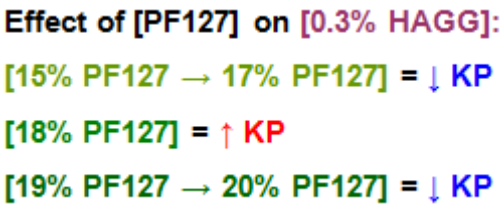

Figure 4.7: Schematic illustrating the effect of PF127 concentration with 0.3% HAGG.

iv. At 0.4% HAGG (H4, H8, H12, H16, H20, H24):

At this concentration no observable trend was present in relation to PF127 concentration. KP values of H4, H12 and H20 were the same and KPs of H8 and H24 were equal, although lower than the former group. The lowest KP was that of H16 (Figure 4.4d). This effect is illustrated in Figure 4.8.



Figure 4.8: Schematic illustrating the effect of PF127 concentration with 0.4% HAGG.

It is well accepted that F127 concentration and gelation temperature are inversely proportional whereas GG concentration and gelation temperature are directly proportional (Lee et al., 2011). It is evident that at lower concentrations of GG (0.1% and 0.2%) PF127 is the dominating polymer controlling the KP as both these concentration sets follow the known trend of PF127. As GG concentration increases to 0.3% there is a disruption in this process whereby GG begins to limit the decrease in KP with increasing PF127 concentration. This disruption is particularly apparent at 18% PF127. At 0.4% HA GG total digression occurs and at this stage no PF127 trend is discernible. This proves that the concentration of GG is the limiting factor in KP. This point is further augmented by the common KPs despite the considerable difference in concentrations of PF127. These common KPs initially occur inter-set (i.e. 0.1% HA GG and 0.2% HA GG had the same KP for 19% and 20% PF127 respectively). As progression is made to higher GG concentrations the incidence of common KPs advances to intra-set occurrence (2 occurrences at 0.3%: H3 = H15 and H17 = H19; 2 occurrences at 0.4%: H4 = H12 = H20 and H8 = H24). The effect of concentration of PF127 and HAGG on the KP is illustrated in Figure 4.9.

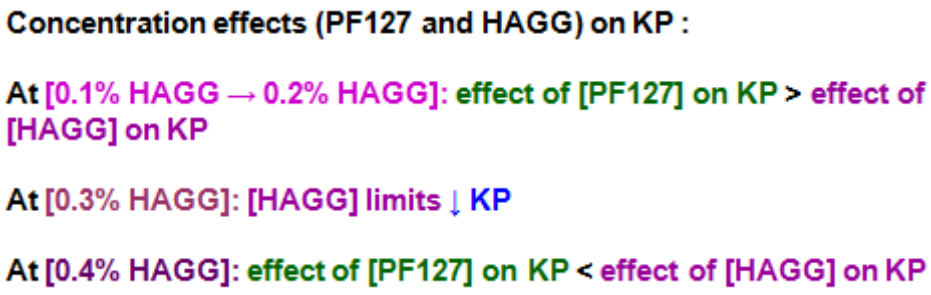

Figure 4.9: The effect of concentration of PF127 and HAGG on the KP.

4.3.1.1.2 Effect of PF127 concentration on different concentrations of LAGG

i. At 0.1% LAGG (L1, L5, L9, L13, L17, L21):

An increase in PF127 concentration corresponds to a decrease in KP up to 17% PF127. At L13 (18% PF127) the KP is greater than that of L5 (16%) but lower than L1 (15% PF127). Thereafter with rising PF127 concentration (19% - 20%) the KP decreases. The KP for L5 is the same as that of L17 (Figure 4.4a). This effect is illustrated in Figure 4.10.

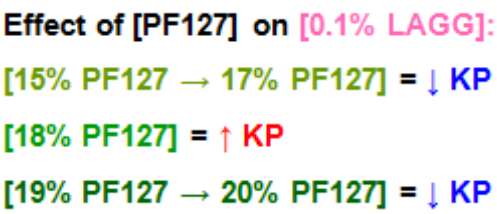

Figure 4.10: Schematic illustrating the effect of PF127 concentration with 0.1% LAGG.

ii. At 0.2% LAGG (L2, L6, L10, L14, L18, L22):

A rise in PF127 concentration is linked to a drop in KP until 17% PF127 (L10). At L14 (18%) there is a rise again which is followed by a subsequent decrease in KP with increasing PF127 concentration. Thus the trend is the same as that of 0.1% LA GG. The only difference is that the number of common KPs increases. L2 and L6 are duplicates as well as L10 and L18 (Figure 4.4b). This effect is illustrated in Figure 4.11.

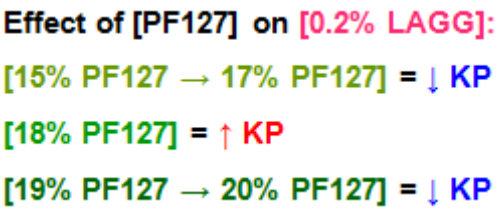

Figure 4.11: Schematic illustrating the effect of PF127 concentration with 0.2% LAGG.

iii. At 0.3% LAGG (L3, L7, L11, L15, L19, L23):

Increasing PF127 from 15% to 16% shows a decrease in KP. At L11 (17%) a dramatic increase occurs. L3 (18%) and L19 (19%) both show decline in KP whereas at L23 (20% PF127) there is a rise and the KP at this is greater than L19. At this stage the effect of concentration is erratic (Figure 4.4c). This effect is illustrated in Figure 4.12.

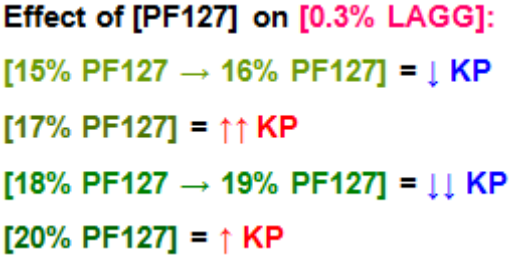

Figure 4.12: Schematic illustrating the effect of PF127 concentration with 0.3% LAGG.

iv. At 0.4% LAGG (L4, L8, L12, L16, L20, L24):

No obvious significant effect occurs at this concentration. The highest KP recorded for this set is at F44 (19% PF127) (Figure 4.4d). This effect is illustrated in Figure 4.13.

Effect of [PF127] on [0.4% LAGG]:

No observable trend in ΔKP

Figure 4.13: Schematic illustrating the effect of PF127 concentration with 0.4% LAGG.

The events with LAGG also demonstrate a dependence of KP on PF127 concentration at lower GG concentrations but as GG concentration increases the effect of PF127 lessens. This trend is less structured compared to HAGG. HAGG flaunted an ordered change in KP in relation to concentration. The alteration to KP by LAGG concentration is sporadic. In the LAGG gels 18%, as well as 17%, displayed atypical properties. The effect of concentration of PF127 and LAGG on the KP is illustrated in Figure 4.14.

Concentration effects (PF127 and LAGG) on KP:

[Low LAGG]: KP dependent on [PF127]

[↑ LAGG]: effect of [PF127] on KP ↓

Figure 4.14: The effect of concentration of PF127 and LAGG on the KP.

4.3.1.2 Comparison of temperature sweep data for HAGG and LAGG

Inspection of the temperature sweep curves revealed that majority of the HAGG gels were thermosensitive with only 9 of the samples being thermoreversible. For the LAGG samples, the greater portions were thermoreversible with only 3 displaying thermosensitive behaviour. A comparison of the KP for HAGG and LAGG showed that for the most part HAGG samples had a higher KP when judged against its LAGG counterpart. This finding strengthens the argument that GG and acetylation degree does contribute to the overall thermal gelation properties despite the presence of PF127. This outcome was also reported by Mao et al (2000). Six of the LAGG gels had a higher KP than the corresponding HAGG sample. It is important to note that of these six, four of them were thermosensitive thus the KP is merely an indication of growing gel strength rather than phase transition point. The results of the remaining two can be attributed to experimental error.

All samples displayed temperature sweep graphs with a characteristic 3 phased curve (sigmoid shape) The three phases are tabulated below (Table 4.4). The temperature sweep curves of all formulations are depicted in Figure 4.15 to Figure 4.20.

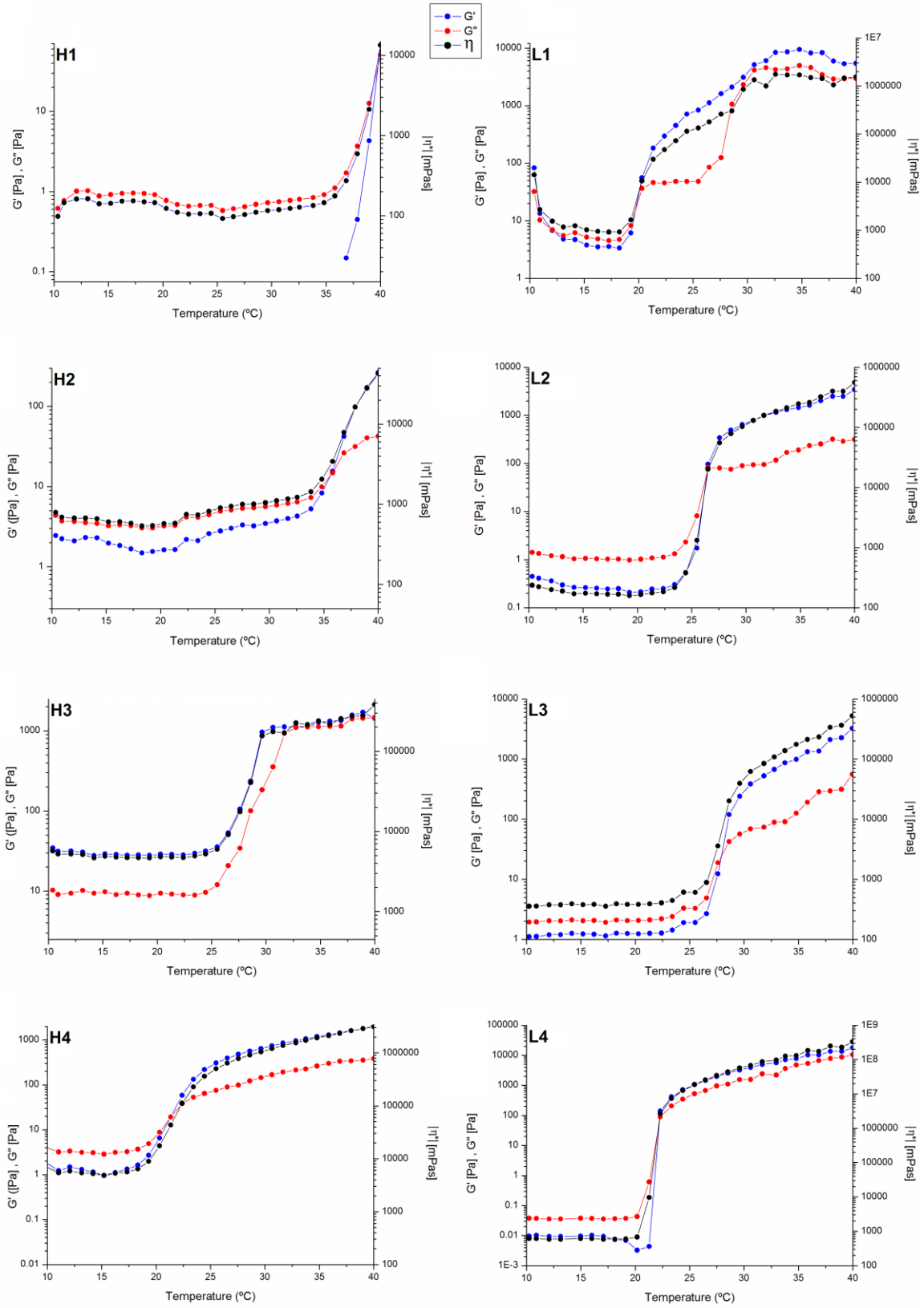

Figure 4.15: Temperature sweeps of H1 - H4 (left) and L1 - L4 (right).

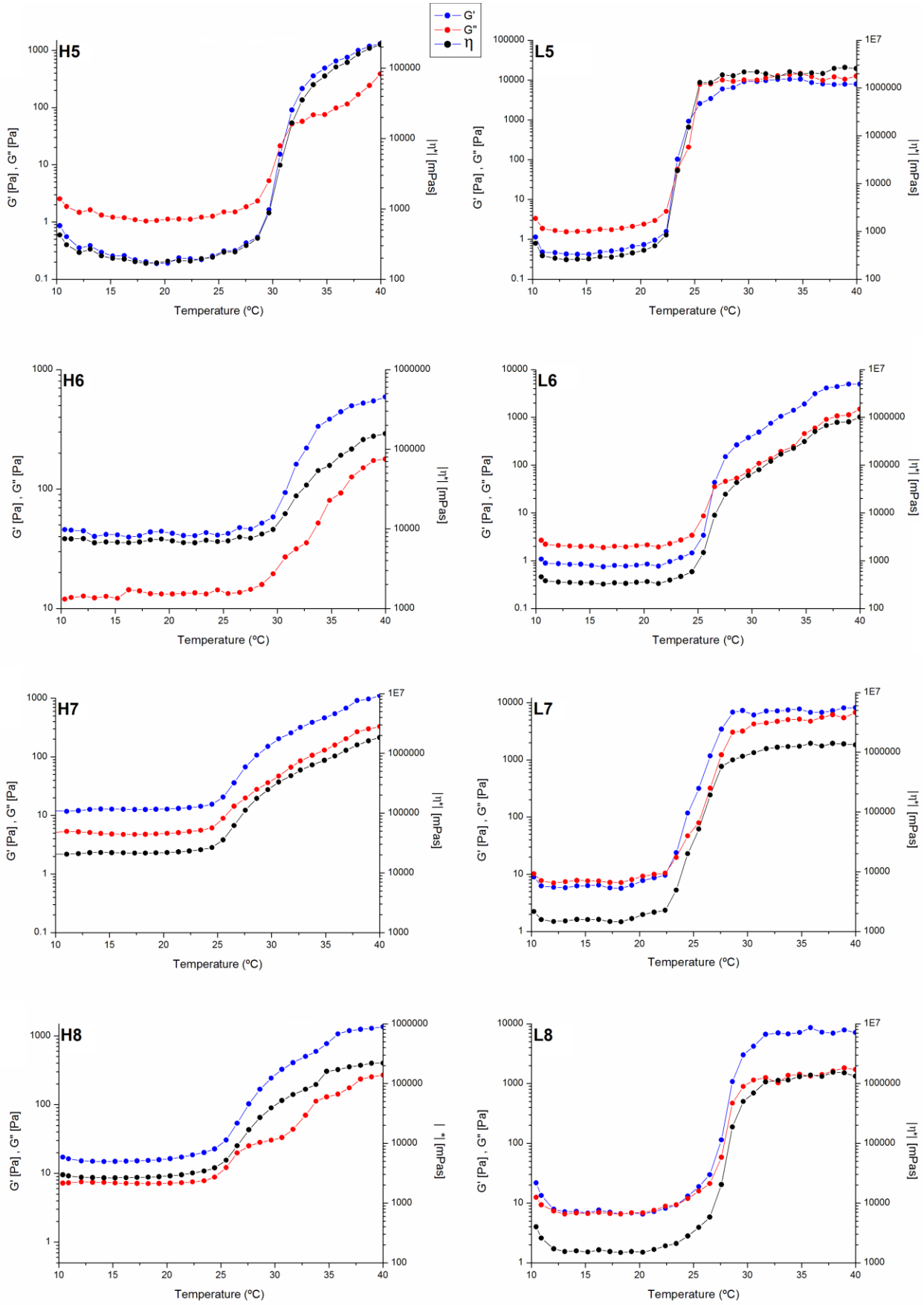

Figure 4.16: Temperature sweeps of H5 - H8 (left) and L5 - L8 (right).

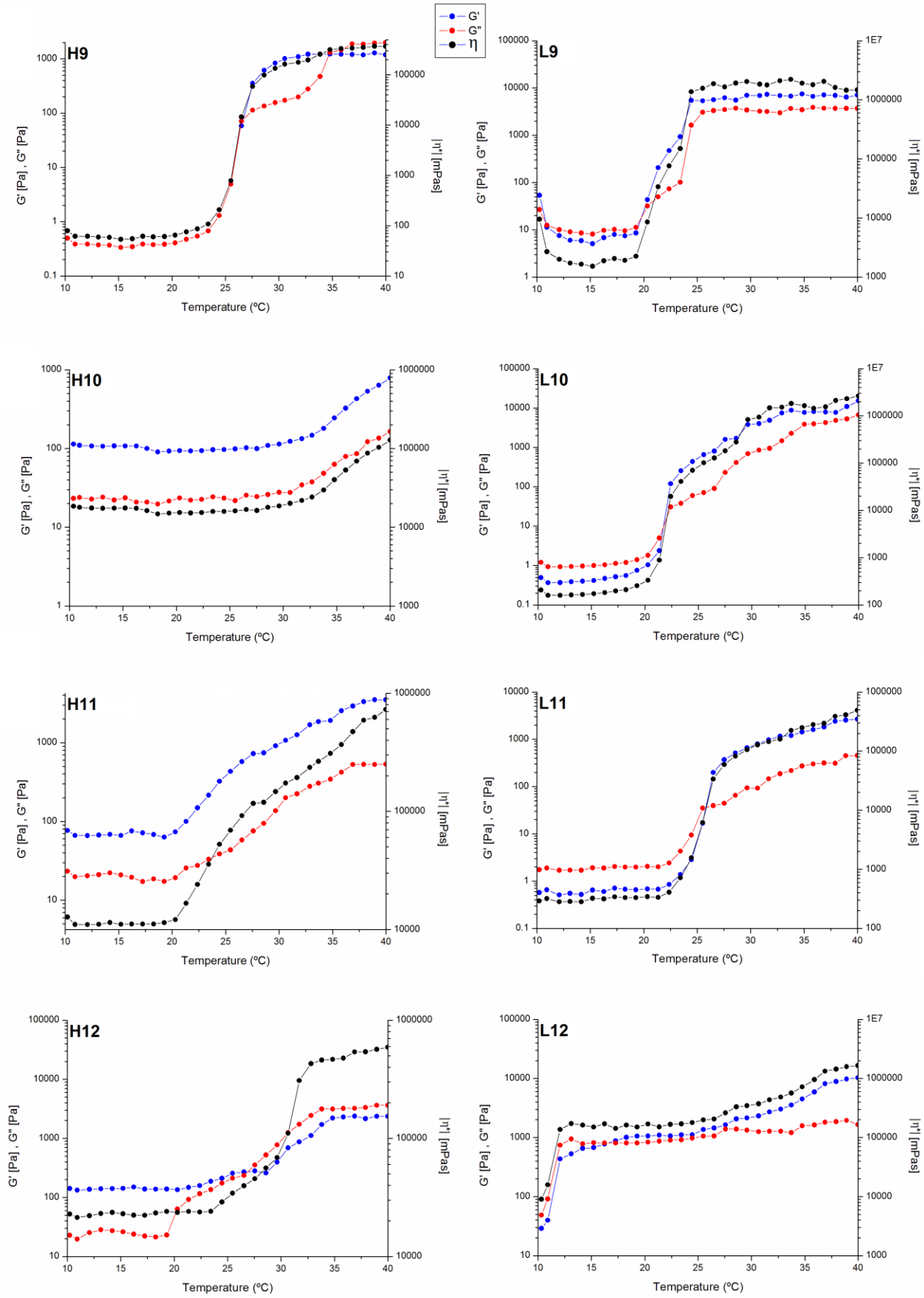

Figure 4.17: Temperature sweeps of H9 - H12 (left) and L9 - L12 (right).

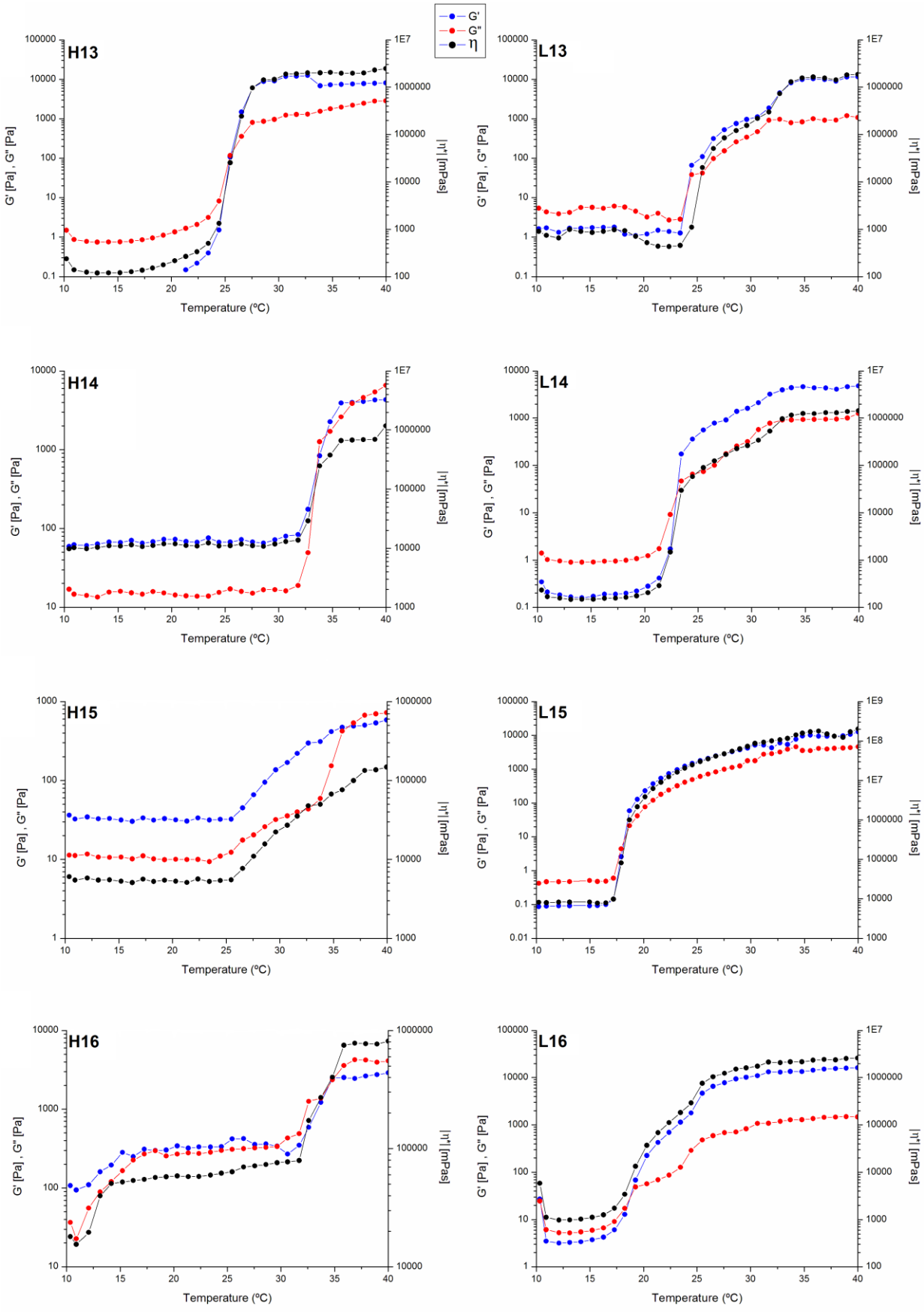

Figure 4.18: Temperature sweeps of H13 - H16 (left) and L13 - L16 (right).

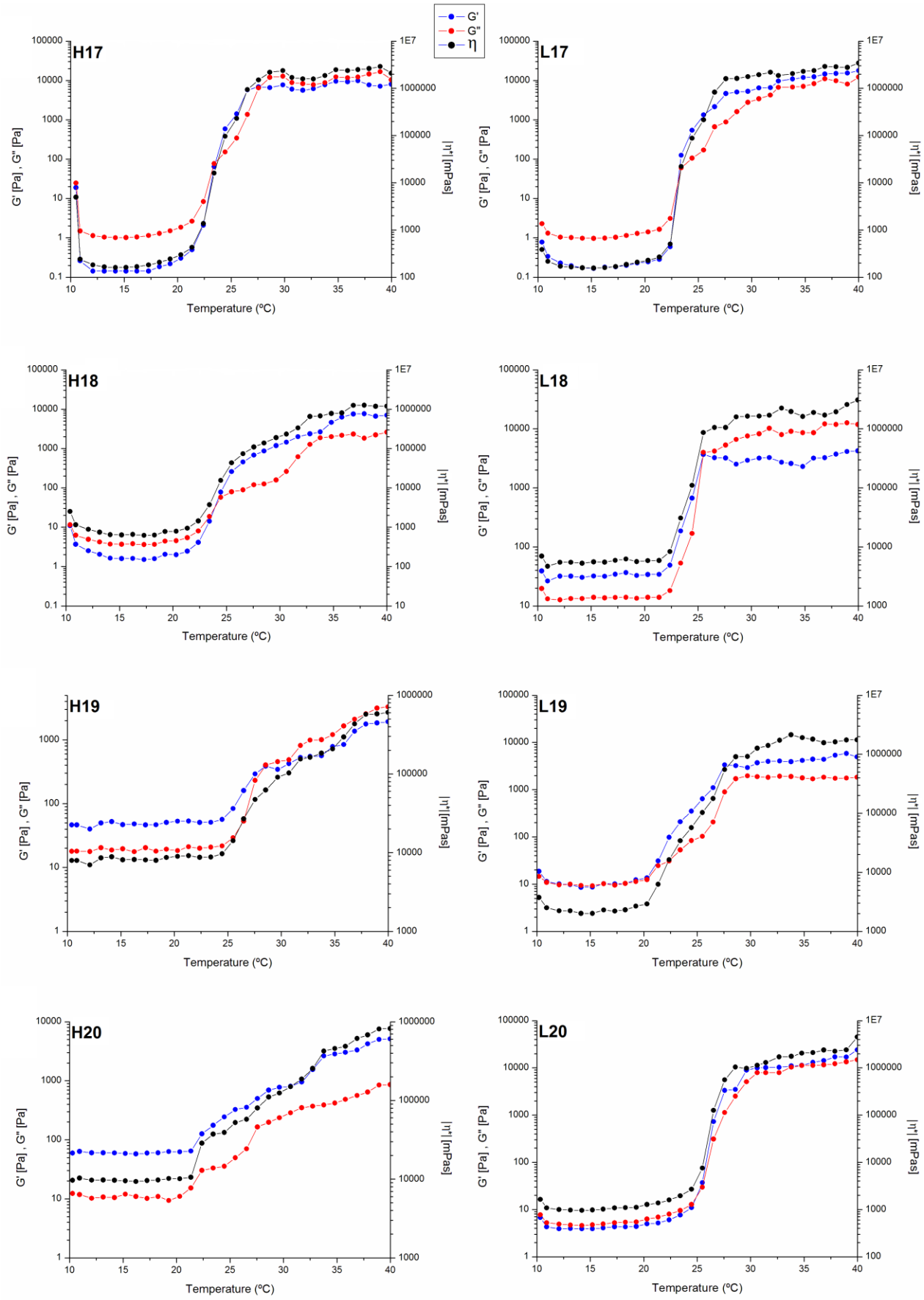

Figure 4.19: Temperature sweeps of H17 - H20 (left) and L17 - L20 (right).

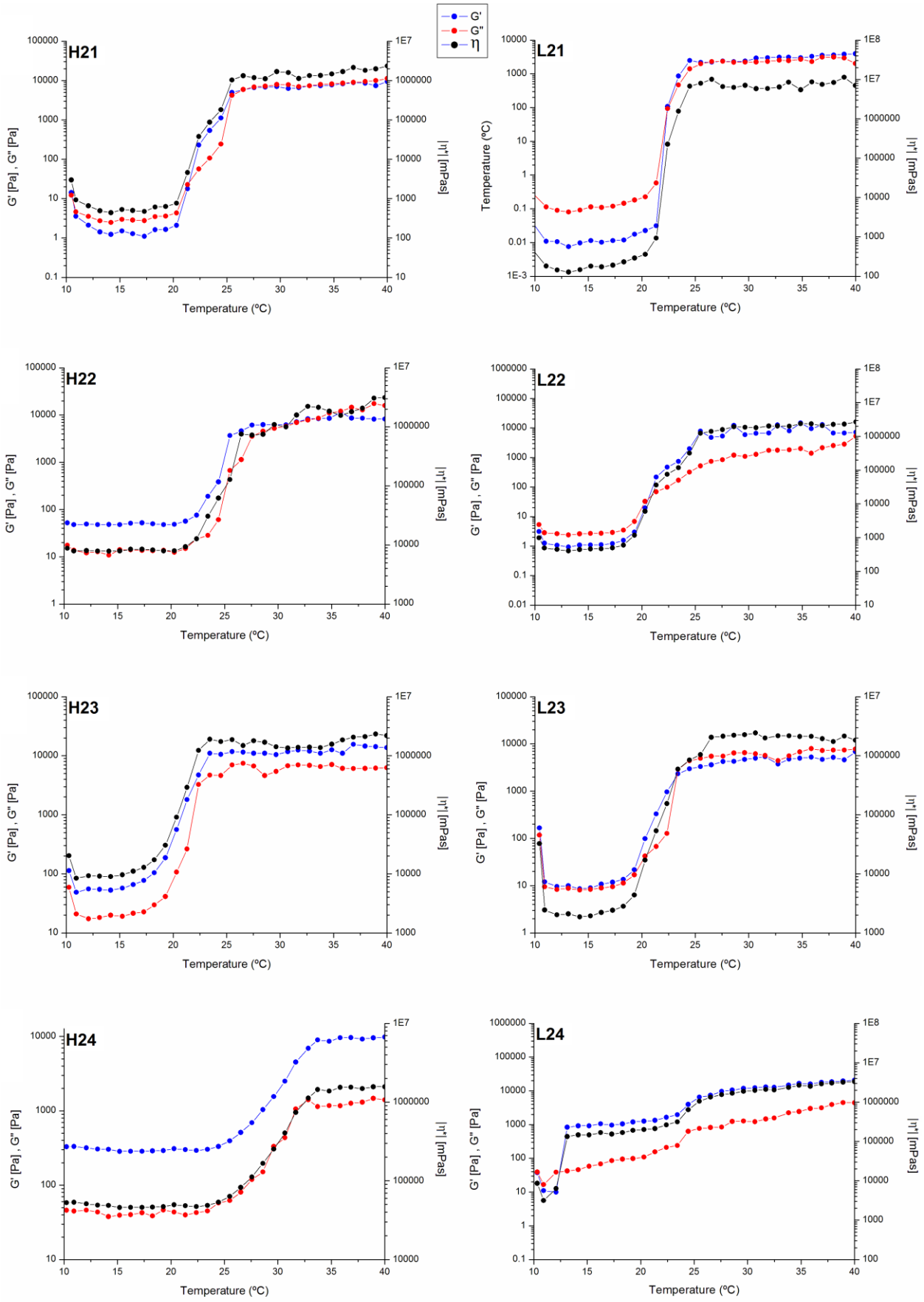

Figure 4.20: Temperature sweeps of H21 - H24 (left) and L21 - L24 (right).

Table 4.4: Breakdown of temperature sweep graphs.

Phase	Thermoreversible Sample	Thermosensitive Sample
1 - Initial plateau	G" dominant	G' dominant
2 - increase	G'-G" cross-over	Increase in G' and G" . G' dominant.
3 - final plateau	G' dominant	G' still dominant

As would be expected, the gradient of phase two and the plateau phases vary from sample to sample. The flatter and longer the plateau the greater the stability of the sample at that phase. In addition when the final plateau is flat it also indicates that the gelation process is complete. A slight gradual increase in the final plateau shows that the gel reaction is still progressing.

4.3.1.3 Effect of GG concentration and PF127 concentration on storage modulus (G'), loss modulus (G") and complex viscosity (η)*

A few samples were chosen, based on the above-mentioned results, in order to conduct further in depth temperature sweep analysis, frequency sweep testing, time sweep testing and flow curve analysis. The samples that were selected were those that had the correct gelation temperature (as stated in section 1) based on their KP values. For comparative purpose only HAGG and LAGG gel pairs from each GG concentration set that showed gelation within the required range were selected. The rest of the gels were excluded due to limited practical application with regards to the scope of the study (i.e. thermoreversible depot). The selected samples are H3 and L3 (15% PF127 + 0.3% GG), F6 and L6 (16% PF127 + 0.2% GG) and F15 and L15 (18% PF127 + 0.3% GG).

For HAGG: An increase in the PF127 concentration showed an increase in G', G" and η* at each concentration of GG. An increase in GG concentration at each concentration of PF127 did not show significant changes.

For LAGG: An increase in PF127 showed slight increase in G' and G" although the effect was not as pronounced as that of HA. Viscosity was not affected by increase in GG of PF127.

Comparison of HAGG G', G" and η* to that of LAGG revealed that for 15% - 17% PF127 LAGG had higher moduli and viscosity overall. This outcome differs from that reported by Morris et al. (2012) who stated that an increase in acetylation caused an increase in G' and viscosity. This difference can be credited to the presence of PF127. Furthermore at 18% - 20% PF127 the three moduli for LAGG and HAGG are roughly equal.

Bradbeer et al (2014) reported that an increase in the acyl content resulted in an increase in viscosity. As discussed the opposite occurs in the presence of PF127 where LAGG actually showed a higher viscosity than HAGG. This could be due to the ability of PF127 to limit the viscosity of HAGG gels as well as the intrinsic nature of LAGG to form hard gels. Furthermore LAGG is susceptible to syneresis as stated by Gohel et al (2009).

4.3.2 Frequency Sweep

Frequency sweep tests provide information on the strength, stability and visco-elastic properties of the gel. It allows us to determine the mechanical spectra of the gel. The spectrum is obtained from the plot of either G' and G", tan delta and viscosity as a function of shifting frequency. Frequency sweep provides the properties of the sample in different states (i.e. in the sol state or gel state).

At 10°C all gels displays frequency dependent behaviour whereas at 36.5°C all samples tested are less dependent with some of them being completely independent. Frequency dependence is indicative of a viscoelastic structure while independence or very low dependence signifies gel-like behaviour (Yasar et al., 2009). A difference between G' and G" is also conventional gel behaviour (Matricardi et al., 2009). Furthermore at sol-state (10°C) a few of the gels had a greater G" than G' at low frequencies which is a known feature of liquid-like formulations (Zhang and Ding, 2010). These facts hold true for all samples as at low temperature the formulations are slightly viscous liquids whilst at body temperature they have solidified into a gel.

At 36.5°C the frequency sweep curves correlate with the frequency sweep curve of a typical gel as described by Morris et al (2012). They stated that a sample in a gel condition presents the following characteristics: 1) G'>G" by a approximately one order of magnitude or more, 2) G' and G" are independent, or very slightly dependent, on frequency and 3) log η* decreases linearly as log ω rises. Frequency sweeps for selected samples at 10°C and 36.5°C are shown in Figures 4.21 - 4.23.

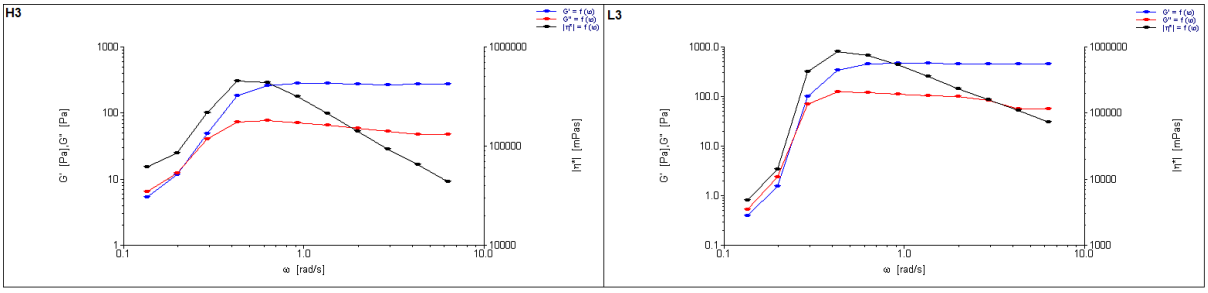

Figure 4.21.1: Frequency Sweep of H3 and L3 at 10°C (right HAGG, left LAGG).

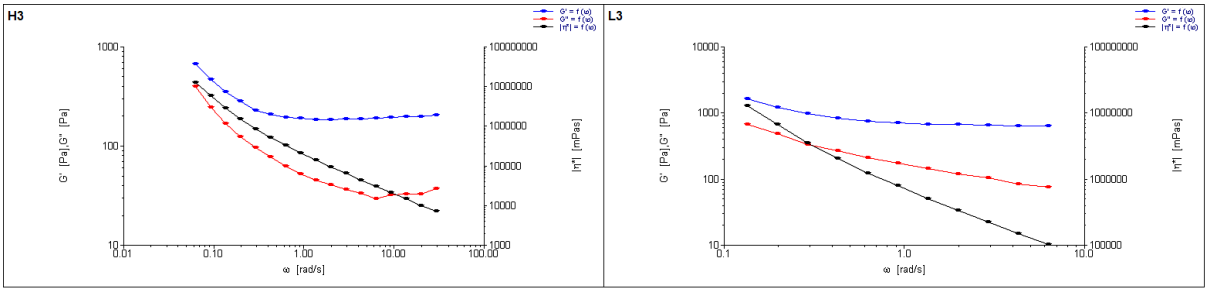

Figure 4.21.2: Frequency Sweep of H3 and L3 at 36.5°C (right HAGG, left LAGG).

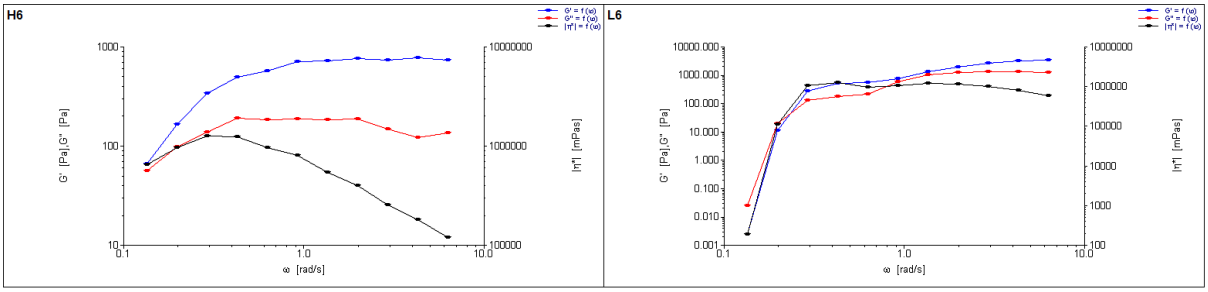

Figure 4.22.1: Frequency Sweep of H6 and L6 at 10°C (right HAGG, left LAGG).

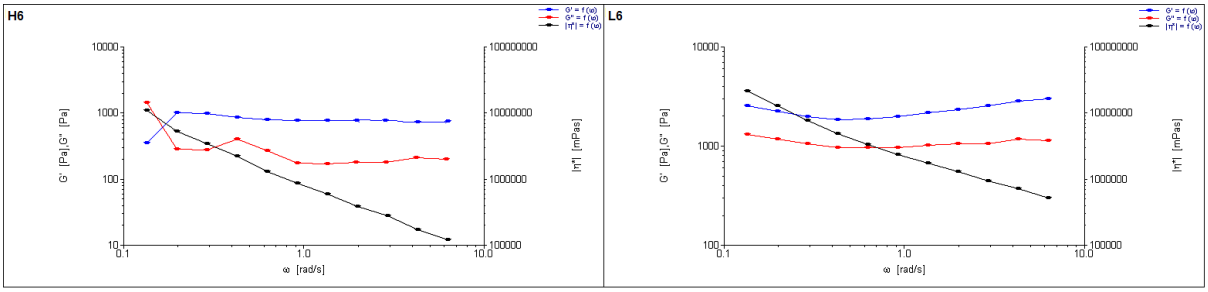

Figure 4.22.2: Frequency Sweep of H6 and L6 at 36.5°C (right HAGG, left LAGG).

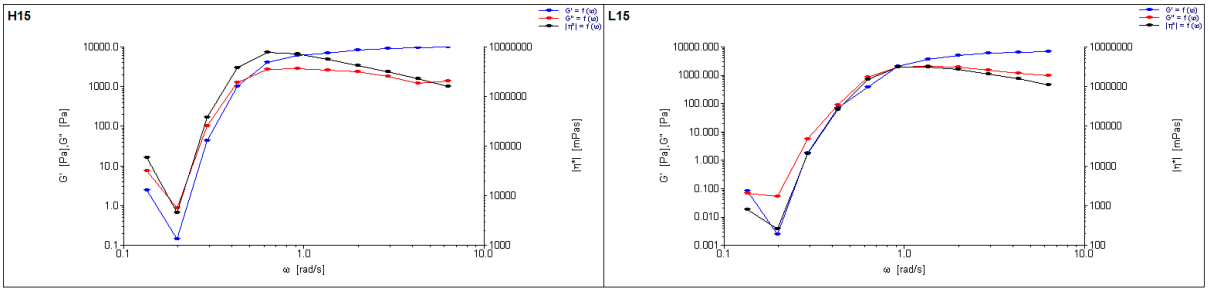

Figure 4.23.1: Frequency Sweep of H15 and L15 at 10°C (right HAGG, left LAGG).

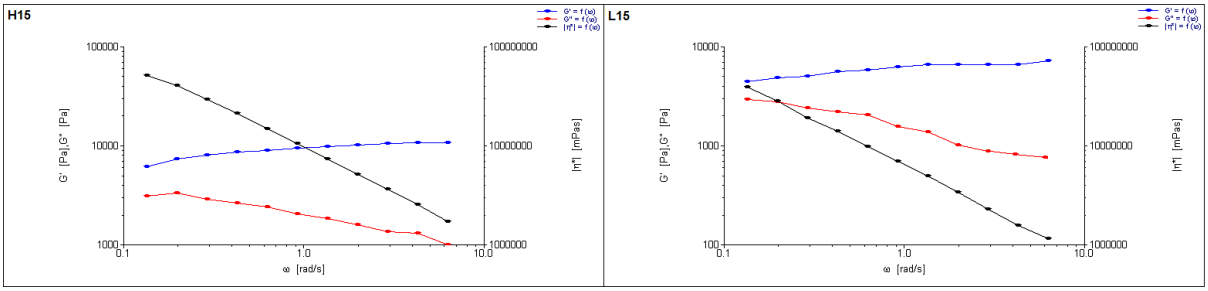

Figure 4.23.2: Frequency Sweep of H15 and L15 at 36.5°C (right HAGG, left LAGG).

Samples are in accordance with the storage moduli rule described by Engledar et al (2014) which states that at very low frequencies (0.01 rad/s) a G' > 10Pa is representative of stability of the formulation as well as preservation of the gel structure. It can be construed, according to this decree, that the gels in this study should thus exhibit a G' < 10Pa at 10°C as the samples structures are weak and unstable at this state. This is based on the notion that at such low temperatures all samples are primarily sol-like or exceptionally weak gel (depending on concentration and acetylation degree). Correspondingly at higher temperatures such as body temperature (36.5°C) the structure changes to a solidified state with enhanced strength thus enabling structural stabilisation and preservation. Analysis of the data supported this rule.

The magnitude of G' and G'' as well as the difference between G' and G'' provide data on the strength of the gel. Large values for G' and G'' (several kPa) and a large difference between the two signifies a strong gel (Chenite et al., 2001). Typically LAGG demonstrates higher moduli due to the stronger gel structure formed. In contrast HAGG has lower modulus due to the weak structure of these gels as a result of the acetyl groups. Thus it is expected that the difference in moduli between LAGG and HAGG would be significant. Frequency sweeps revealed that, while LAGG does have higher moduli than the HAGG gels on average, the difference in moduli between HAGG and LAGG is less than one order of magnitude. This increased strength of HAGG is attributed to the addition of PF127.

The unique trend of the curves at sol state can be attributed to the influence of random coil systems such as GG. At low temperatures all the samples showed formation of entanglement networks via topological interaction of the chains. This type of interaction is classical behaviour of random coils. The frequency sweep of an entangled network possesses four defining traits:

1) at low frequencies $G' \approx \omega^2$

2) at low frequencies $G'' \approx \omega^1$

3) G'-G'' cross-over transpires at decreasing frequencies

4) at extremely low frequencies (in the terminal zone) flow mimics that of a high viscous fluid (Picout et al., 2003). Furthermore at high temperatures no entanglement occurs since the sample is a gel as confirmed by G' parallel to G", G' > G" and both are independent of frequency at this stage (see Figure 4.24 from Picout et al., 2003).

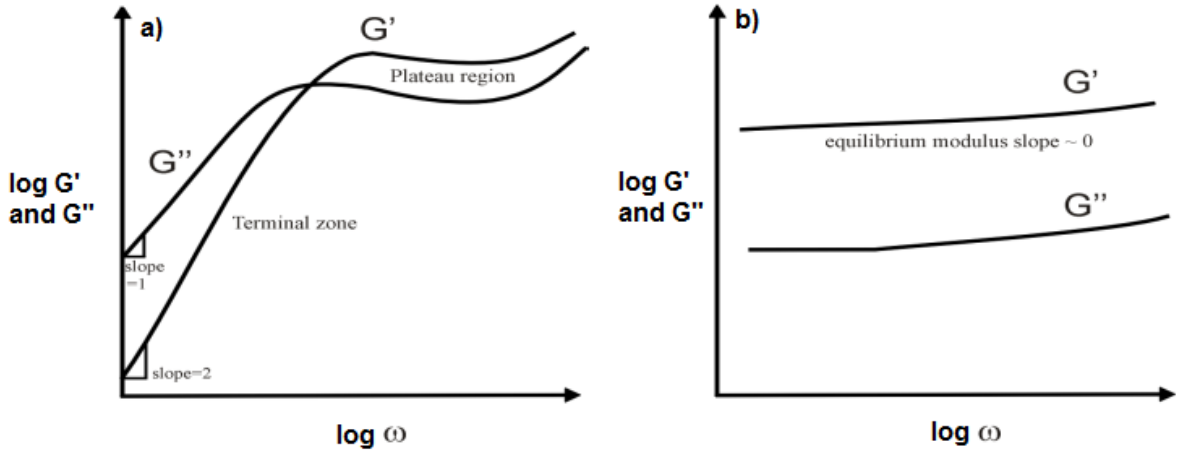

Figure 4.24: Mechanical spectra for a) an entanglement network and b) a gel system (Source: adapted from Picout et al., 2003).

Despite the variations in each sample it is evident that the samples all formed true gels as proven by the frequency sweep data. The difference only arises in terms of the physical aspects of the gel such as weak or strong, soft or brittle etc.

4.3.3 Time Sweep

Oscillatory time sweeps are essential in order to determine the gelation time of each gel formulation. The Gt for each gel is listed in Table 4.5.

Table 4.5: Gelation times for PF127 + HAGG gels and PF127 + LAGG gels

% PF127 + % GG	Gelation Time (Gt) (seconds) High Acyl	Low Acyl
15 + 0.3	9.27	61,9
16 + 0.2	39	70,5
18 + 0.3	17,36	60

The difference in Gt between the HAGG and LAGG gels is substantial. In both sets the formulation with less GG and the same amount of PF127 took the longest to transform from liquid to gel whereas those with more GG had a quicker Gt thus promoting the premise that GG has a significant role in the gelation process despite the small concentration being used.

Additionally, the Gt of the HA gels was considerably quicker than that of the LAGG gels. This is a favourable feature as depots require a quick in situ gelation time in order to minimise leaching of active and/or particles. If the Gt is too long then the formulation remains in a liquid state for a longer period despite already being in the body. The consequence of this is that there is a great risk of active ingredient or other excipients escaping into the surrounding tissues. This can impact on drug release profiles as well as safety/toxicology profiles of the drug if the concentration is too high. Based on this the LAGG Gt are much too long for these to be a viable option especially when compare to the HAGG gels. Of the HAGG gels 15 + 0.3 has superiority in this regard.

4.3.4 Flow Analysis using Rheological Models

In order to gain better understanding of the flow properties of the formulations each one was subjected to a flow curve test. Tests were run at 10°C and 36.5°C in order to observe the effect of temperature on flow behaviour. Quantitative analysis of the data was conducted by employing widely used rheological models. Five flow curve models were applied using the Rheowin 3 (Haake) software. The model with best fit was selected to accurately describe the flow properties of the gels. The models applied were the Bingham model (Equation 4.6), Casson model (Equation 4.7), Cross model (Equation 4.8), *Herschel-Bulkley* (Equation 4.9) and *Ostwald–de Waele* (Equation 4.10).

$$\tau = \tau_0 + K'.\dot{\gamma} \qquad \textbf{Equation 4.6}$$

$$\tau^{0.5} = k_0^{0.5} + k_1.\dot{\gamma}^{0.5} \qquad \textbf{Equation 4.7}$$

$$\tau = \dot{\gamma}(\eta_\infty + (\eta_0 - \eta_\infty) \div 1 + \left(\frac{\dot{\gamma}}{\dot{\gamma}_0}\right)^m) \qquad \textbf{Equation 4.8}$$

$$\tau = \tau_0 + K.\dot{\gamma}^n \qquad \textbf{Equation 4.9}$$

$$\tau = K.\dot{\gamma}^n \qquad \textbf{Equation 4.10}$$

The model with the best fit is one that demonstrated a coefficient of determination (R^2) value closest to 1 and a low Chi^2 value (Table 4.6.1. - 4.6.3.).

Table 4.6.1: R^2 and Chi^2 values for 15% PF127 with 0.3% HAGG and 15% PF127 with 0.3% LAGG.

Rheological Model	**15% + 0.3% at 10 °C**				**15% + 0.3% at 36,5 °C**			
	HAGG		**LAGG**		**HAGG**		**LAGG**	
	R^2	**Chi^2**	R^2	**Chi^2**	R^2	**Chi^2**	R^2	**Chi^2**
Bingham	0.9945	187.7	0.9947	17.50	0.9907	1686.0	0.9951	76.31
Casson	0.9995	17.92	0.9995	1.620	0.9951	882.0	-	-
Cross	0.9999	3.928	1.000	0.1613	0.9959	738.0	-0.7663	1.240E + 04
Herschel-Bulkley	0.9995	17.74	0.9996	1.377	0.9962	693.5	0.9951	76.28
Ostwald–de Waele	0.9986	48.24	0.9990	3.485	0.9960	730.8	0.9951	77.03

Table 4.6.2: R^2 and Chi^2 values for 16% PF127 with 0.2% HAGG and 16% PF127 with 0.2% LAGG.

Rheological Model	**16% + 0.2% at 10 °C**				**16% + 0.2% at 36,5 °C**			
	HAGG		**LAGG**		**HAGG**		**LAGG**	
	R^2	**Chi^2**	R^2	**Chi^2**	R^2	**Chi^2**	R^2	**Chi^2**
Bingham	0.9961	28.83	0.9959	13.19	0.9943	469.7	0.9922	179.8
Casson	0.9966	25.66	0.9996	1.223	0.9938	504.7	-	-
Cross	0.9994	4.831	1.000	0.0981	-	-	0.9994	13.81
Herschel-Bulkley	0.9966	25.74	0.9997	0.8153	0.9991	71.81	0.9980	45.90
Ostwald–de Waele	0.9908	68.99	0.9994	1.838	0.9942	478.1	0.9964	82.08

Table 4.6.3: R^2 and Chi^2 values for 18% PF127 with 0.3% HAGG and 18% PF127 with 0.3% LAGG.

Rheological Model	**18% + 0.3% at 10 °C**				**18% + 0.3% at 36,5 °C**			
	HA GG		**LA GG**		**HA GG**		**LA GG**	
	R^2	**Chi^2**	R^2	**Chi^2**	R^2	**Chi^2**	R^2	**Chi^2**
Bingham	0.9915	442.1	0.9967	13.67	0.678	1.473E + 04	0.9671	2707
Casson	0.9988	64.65	0.9930	3.057	0.7838	1.049E + 04	0.9825	1451
Cross	0.9998	8.755	0.9932	27.64	-0.635	3.818E + 04	0.9963	309.1
Herschel-Bulkley	0.9997	15.24	0.9988	4.962	0.9899	1029	0.9832	1393
Ostwald–de Waele	0.9993	34.66	0.9967	13.58	0.9863	1799	0.9803	1634

As can be seen from the R^2 and Chi^2 values the two most suitable models are the Cross and Herschel-Bulkley models. The Herschel Bulkley model comprises three adjustable parameters: yield stress (τ_o), consistency index (K) and flow behaviour index (n). The Cross model is a four parameter model for fluids that do not have a yield stress. Asymptotic values of viscosity at low and high shear rates are represented by η_0 and η_∞ respectively. The parameter K is constant and has the dimension of time. m is a dimensionless constant.

For the HAGG formulations all three gels followed the Cross model at low temperatures and changed to the Herschel-Bulkley at higher temperatures. This is fitting as at low temperatures all three flow easily without any need for additional force thus no yield stress is present. At higher temperatures they begin to solidify and would need force to be applied in order for motion to occur. This physical alteration is represented by the Herschel-Bulkley model which accounts for a yield stress that is present.

The LAGG gels displayed an unusual trend. At low concentrations of PF127 (i.e. 15% PF127) they fitted the cross model at low temperatures and the Herschel-Bulkley model at high temperatures. For 16% PF127 and 0.2% GG the formulation showed Cross model fitting of both temperatures. Intriguingly at 18% PF127 and 0.3% GG the model fit was the inverse of the 15% and 0.3%, where it was Herschel-Bulkley at low temperatures and Cross at higher temperatures. This atypical behaviour is in line with the rest of the LA data further cementing the fact that HA follows a well-ordered and structured pattern whereas LA continues to reveal erratic and unpredictable characteristics.

The Cross model is indicative of shear thinning behaviour (Rao, 2014). This is ideal as shear thinning is favourable in parenteral formulations. The Herschel-Bulkley formulations can be classified as shear thinning behaviour ($n < 1$), Bingham behaviour ($n = 1$) or shear thickening behaviour ($n > 1$) (Rudolph et al., 2014). According to the values for those fitting the Herschel-Bulkley model the majority of them displayed shear thinning and the remainder shear thickening (Table 4.7). A shear thinning response was also reported for other PF127 combination gels (Balakrishnan et al., 2015).

Table 4.7: Flow behaviour index (n) values for gels fitting the Herschel-Bulkley model.

Formulation	**Flow behaviour index (n)**
HA 15% + 0.3% (36.5 °C)	0.7344
HA 16% + 0.2% (36.5 °C)	1.331
HA 18% + 0.3% (36.5 °C)	0.0521
LA 15% + 0.3% (36.5 °C)	1.006
LA 18% + 0.3% (10 °C)	0.8135

The degree of acetylation can clearly be seen to impact the rheological properties of GG-PF127 gels. A distinctive trend was seen in PF127 with HAGG where the union of the two polymers overcame the individual weakness possessed by each. Furthermore HAGG was able to control the KP and PF127 controlled the moduli. LAGG also displayed different nonconforming behaviour when combined with PF127. Rheological analysis is vital as the formulation quality can be prognosticated by its rheological performance.

4.3.5 Mechanism of gelation and analysis of trends

Gels are formed through chemical or physical processes. Chemical gelation involves covalent bonding and is irreversible. Physical gelation utilises physical bonds such as hydrogen bonds and Van der Waals forces. These bonds are weak and as a result the crosslinks formed are usually reversible. PF127 and GG are both capable of physical gelation (Li et al., 2006; Matricardi et al., 2009).

The mechanism of PF127 gelation has been a source of debate for years. A general consensus derived through reviewing the literature disclosed that gelation is a tripartite procedure involving micelle packing, chain entanglements and copolymer dehydration (Akash et al., 2014; Escobar-Chávez et al., 2006; Moore et al., 2000, Ruel-Gariépy and Leroux, 2004).

As the temperature of the solution rises the PEO chains remain hydrophilic while the PPO block becomes increasingly hydrophobic. This hydrophobicity takes place through hydrogen bond rupture resulting in PPO core dehydration. This leads to increased friction and entanglement of the chains which facilitates micellisation. This formation of spherical micelles is concentration dependent and occurs at the Critical Micellar Concentration (CMC). As temperature continues to increase further packing and entanglement of the micelles takes place until such a point where aggregation occurs and movement stops. The moment at which the micelles form a tightly packed 3D cubic lattice is considered to be the moment of gel formation (Trong et al., 2008; Parekh et al., 2014).

The gelation of GG is attributed to the disorder-order transition that takes place due to a coil-helix transition (Coutinho et al., 2010). This transition is a two step procedure that happens when a heated solution of GG is cooled. At high temperatures the GG solution comprises of a disordered single-chained coil. The first step begins when the temperature is decreased; at this stage an ordered double-helix with distinct junction zones is created. The bonds between the helices are weak hydrogen and Van der Waal forces. The second step involves molecular associations which lead to the aggregation of the helical segments. These 'knot-like' physical junctions generate a 3D network which is thermoreversible.

The chemical structure of HAGG and LAGG as well as the individual properties of all the polymers involved converge to craft a gel with unique traits and gelation mechanisms. In order to appreciate the trends that have been discovered, background knowledge on the chemistry of HAGG and LAGG is crucial.

HAGG and LAGG share a common backbone however the HAGG backbone is esterified with two acyl groups (glycerate and acetate) whereas LAGG is void of these. The acetyl content is a key component influencing GG gels and their properties (Bajaj et al., 2007).

At lower concentrations of HAGG and LAGG the effect of PF127 is superior. This is due to the incomplete aggregation of the double helices that results from low concentration of GG. Small concentrations of GG yield an ordered helical structure with partial aggregations. Thus the resultant structure is weaker and prone to manipulation by other polymers. On the other hand, at high GG concentrations PF127 influence becomes negligible as GG dominates the KP. The reason for this is that at higher concentrations of GG the number of helical aggregates grows allowing the gelation process to continue. The sol-gel transition takes place and the reaction reaches completion yielding a proper fully formed structure (Miyoshi et al., 1996).

The higher KP of HAGG compared to LAGG is a consequence of the inherent greater thermal stability of HAGG. This effect is produced by the glycerate substituent located inside the double helix which provides a higher helical stability even at elevated temperatures (Mao et al., 2000; Noda et al., 2008).

As discussed, the HAGG gels displayed a more structured trend compared to LAGG. This can be accredited to the greater elastic nature of HAGG. The acetyl group located on the periphery of the double helix plays a crucial role in the prevention of helix-helix aggregation (Morris et al., 2012). This barrier inhibits polymer chain association causing the structure to be soft and elastic (Flores et al., 2013; Lorenzo et al.; 2013). This elastic ('soft') aspect allows HAGG to be moulded by PF127 with the degree of moulding dependant on the GG concentration. Degree of moulding decreases with increasing GG concentration until eventually GG overpowers the PF127. This calculated occurrence is responsible for the controlled change in gelation. LAGG does not possess this pliable nature therefore the trend changes are harsh and somewhat erratic.

The unusual activity at 17% and 18% PF127 can be simply explained as opposing behaviour taking place between PF127 and GG. GG gels on cooling whereas PF127 gels on heating. Additionally PF127 is dominant at lower concentrations of GG while GG is superior at higher concentrations of PF127. Consequently it is only logical to infer that at the midpoint some extraordinary reaction will arise as a result of this complex situation.

The general viewpoint, as deduced from literature, favours LAGG to HAGG as LAGG gels are firmer than HAGG. The bulky acetyl and glycerate inhibit compact packing of the helices thereby decreasing the strength of the resultant gel (Mao et al., 2000). Furthermore PF127 is also notorious for forming weak gels. Nonetheless the combination of these two polymers that share a mutual shortcoming interact in a remarkably unexpected manner fashioning a gel with improved strength. The creation of a positive outcome from two negative traits is a noteworthy inverse reaction that is verified by the types of thermally influenced gels formed by LAGG and HAGG. As stated previously, LAGG gels are thermoreversible where the gelation process only begins at the rise in G' and the change from sol-state to gel-state occurs at G'-G'' cross-over. HAGG gels are thermosensitive wherein the gel is already formed, albeit weak. However at KP the strength of the gel increases enormously. The improved strength of GG-PF127 gels is known as a "Thermorigidity Phenomena" (TRP) and is exclusive to HAGG. These occurrences are illustrated in the temperature sweep graphs. TRP is governed by the synergistic reaction between PF127 and HAGG at specific concentrations. It only occurs at concentrations >0.1% and >15% for GG and PF127 respectively. The glycerate group of HAGG is the primary factor controlling KP and PF127 is the controlling factor of G', G'' and η* (as stated earlier that HA GG had minimal effect on the moduli however alteration of these was through increasing PF127 concentration).

4.4 Concluding Remarks

It can be concluded that the degree of acetylation has a pronounced impact on the rheological properties of PF127 gels in combination with LAGG or HAGG. The concentration of polymers was also significant as displayed in the study. Concentration was particularly important in the PF127 with HAGG gels resulting in a unique phenomenon (TRP). The sol-gel transition and formation of true gels was also confirmed through frequency sweeps. PF127 gels with HAGG displayed favourable gelation times and flow behaviour. LAGG displayed unusual and erratic trends when joined with PF127. Utilisation of PF127 with HAGG provides an overall advantageous rheological profile making it ideal for an intramuscular depot. The conjunction of two ordinary polymers revealed interesting findings (attesting to the age old notion that simplicity is the key to success). This system is ideal as it can be used in conjunction with the formulated nanomicelles and the pharmaceutical aspects of the entire composite can be determined.

CHAPTER 5

ASSEMBLY, PHYSICOCHEMICAL AND PHYSICOMECHANICAL CHARACTERIZATION OF THE NANOMICELLE-ENCLATHERATED-GEL-COMPOSITE

5.1 Introduction

An optimally therapeutic delivery system can be developed through consolidation of two delivery systems composed in *Chapter 3 and Chapter 4*. The successful amalgamation of disulfiram-loaded TPGS nanomicelles and PF127-HAGG gel combines the advantages of both systems into a single *in situ* depot composite termed a nano-enclatherated gel composite (NEGC). *In situ* depots present a number of appealing attributes. These are summarised in Figure 5.1 (Shandbagh and Pandhare, 2013; Avachat and Kapure, 2014).

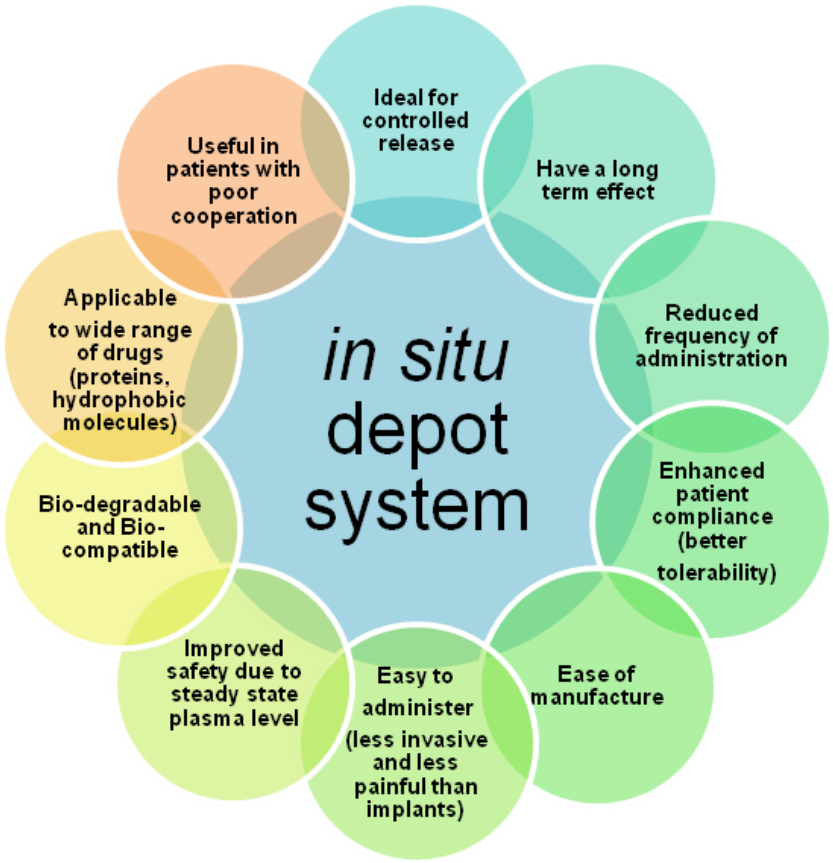

Figure 5.1: Advantages of *in situ* depot systems.

Prediction of the therapeutic effect of a system can be carried out through *in vitro* and *in vivo* experimental procedures (Brayden, 2007). *In vitro* studies are vital as they allow the detection of any formulation short-comings or concerns prior to advancing to *in vivo* testing. In this manner unnecessary animal studies can be avoided therefore *in vitro* assessments can be considered as ethically considerate (Polli, 2008). *In vitro* analysis also makes it possible to differentiate between inherent effects of the delivery system and effects due to physiological processes as the laboratory environment eliminates the possibility of

interactions due to biological processes (such as metabolism and enterohepatic recycling) (Polli, 2008). *In vitro* characterization ensures that the delivery systems qualities are elucidated so that once the *in vivo* phase is initiated no unknowns remain with regards to the systems' physicochemical, physicomechanical and drug release aspects.

Incorporation of the nanomicelles into the gel will overcome the negative aspects of using the nanomicelles in isolation. Encapsulation in the gel will also protect against premature micelle dissociation. The physicochemical, physicomechanical and *in vitro* release studies of the composite and derivatives thereof were studied in-depth in this chapter. Particle size determination was conducted using Dynamic Light Scattering (DLS). Fourier Transform Electron Microscopy (FTIR) and X-Ray Diffraction (XRD) provided the structural profile of the composite and its parts. The thermal properties of the system were investigated through Differential Scanning Calorimetry (DSC). Morphological analysis was completed using Scanning Electron Microscopy (SEM). The characterization tests impart a thorough pharmaceutical vignette of the NEGC so that complete understanding of the individual components and their combined physicochemical and physicomechanical facets is achieved.

5.2 Materials and Methods

5.2.1 Materials

Tetraethylthiuram disulfide (disulfiram) and Pluronic F127 were procured from Sigma Aldrich (Steinheim, Germany). Kolliphor® TPGS was supplied by BASF (Ludwigshafen, Germany). High Acyl Gellan Gum (Kelcogel LT100) was received from CP Kelco Germany GmbH (Grossenbrode, Germany). Deionised water was obtained from a Milli-Q water purification system (Milli-Q, Millipore, Billerica, MA, USA). All other chemicals and solvents were of analytic grade and were used as received.

5.2.2 Amalgamation of the various gel composites

The gel was formulated as outlined in chapter 4, Section 4.2.2. Once the gel was prepared, 10mg of either disulfiram-loaded nanomicelles, pure disulfiram, drug-free nanomicelles or disulfiram-loaded nanomicelles together with additional un-encapsulated disulfiram were added to the gel and stirred until a uniform dispersion was obtained. The following combinations (illustrated in Figure 5.2) were formulated for further characterization:

1) Drug free nanomicelles + PF127-HAGG gel (hereon referred to as Composite 1).
2) Disulfiram-loaded nanomicelles + PF127-HAGG gel (hereon referred to as Composite 2).
3) Free disulfiram + PF127-HAGG gel (hereon referred to as Composite 3).
4) Free disulfiram + disulfiram-loaded nanomicelles + PF127-HAGG gel (hereon referred to as Composite 4).

5) Plain PF127-HAGG gel (i.e. without any disulfiram or nanomicelles) (hereon referred to as composite 5).

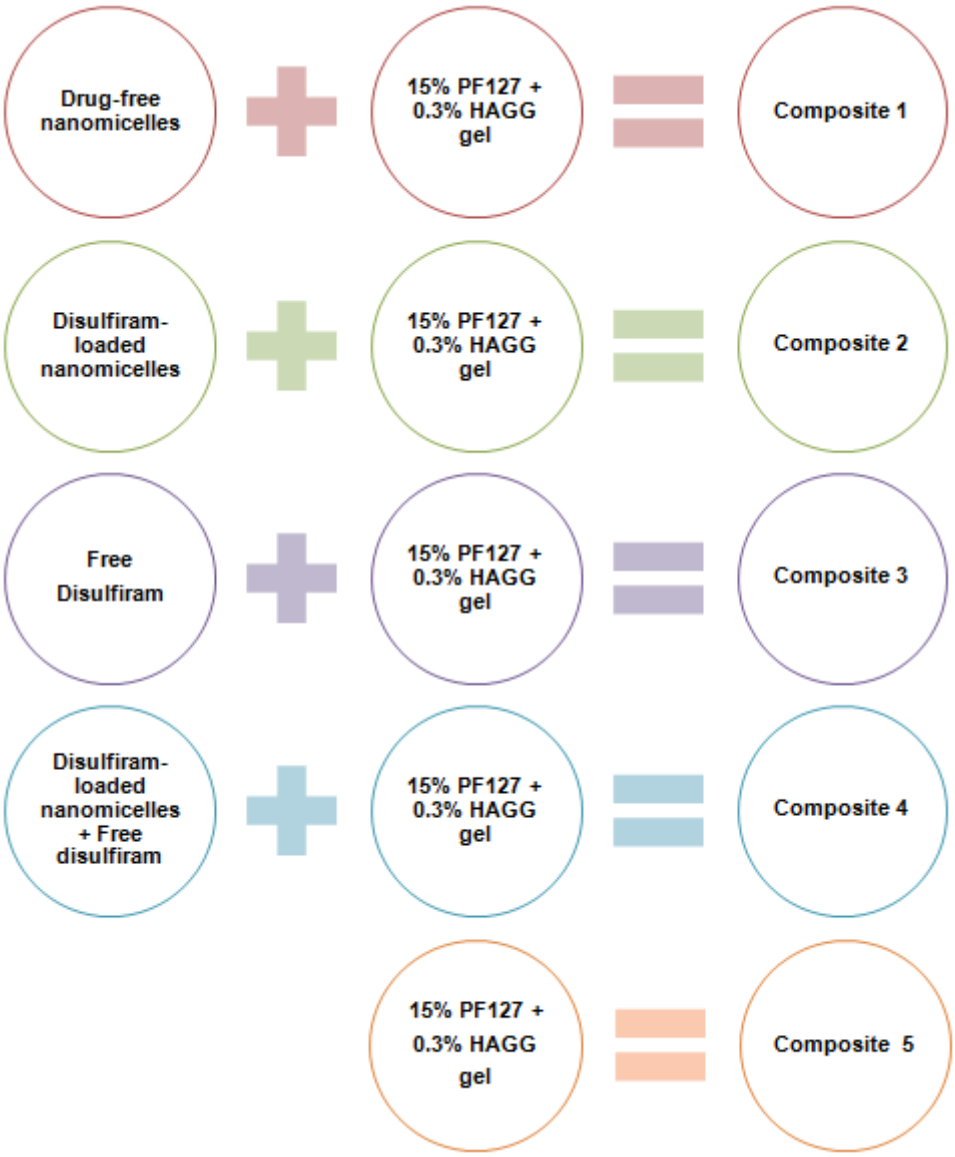

Figure 5.2: Various gel composites formed for further characterization and *in vitro* testing.

5.2.3 Flash freezing of the various composites

Flash freezing was conducted in order to allow preservation of the sample structure at different temperatures. Samples of each of the composites formulated were cooled to 10°C to allow the formulation to be in its liquid state. Alternatively, additional samples of each of the combinations formulated were heated to 37°C to allow the formulation to be in its solid state. Once the desired state was obtained the sample was immediately flash frozen by rapid immersion into liquid nitrogen and this state was maintained by storage in a freezer at -80°C for 12 hours and thereafter lyophilized. In doing so the formulation structure is

preserved as it would be at the flash-frozen state. The samples could then be characterized and dissimilarities compared due to differing phases of matter.

5.2.4 Macroscopic evaluation of the gel

Macroscopic evaluation involves visual examination of the gels. Gels were inspected for homogeneity, physical appearance at different temperatures and clarity.

5.2.5 *In vitro* drug release of the various gel composites

In vitro drug release studies were conducted by means of the dialysis method (Kulhari et al., 2015). The various disulfiram-containing gel composites (1mL) were placed in dialysis tubing (MWCO 12000) with 5mL of SBF and both ends were sealed and the closed tube was placed into a jar with 50mL of dissolution medium (SBF). The method followed was the same as that followed in *Chapter 3, Section 3.2.10.*

5.2.6 Rheological analysis of the various gel composites

Rheological analysis was executed on the 5 composites formulated. Tests conducted include Temperature Sweep tests, Time Curve tests and Flow Curve analysis. All methods have been outlined in *Chapter 4, Section 4.2.3.*

5.2.7 Characterization of the molecular vibrational transitions of the various gel composites using Fourier Transform Infrared Spectroscopy

FTIR Spectroscopy was utilised to detect the vibration characteristics of chemical functional groups in the various gel composite samples as well as native gel polymers and was carried out as detailed in *Chapter 3, Section 3.2.18.*

5.2.8 Characterization of thermal transitions of the various gel composites using Differential Scanning Calorimetry

Thermo-degradation and thermal transitions of the various gel composites as well as native gel polymers was assessed as outlined in *Chapter 3, Section 3.2.19.*

5.2.9 Determination of the degree of crystallinity of the various gel composites employing X-Ray Diffraction analysis

The crystalline or amorphous disposition of the various gel composites as well as native gel polymers was determined using X-Ray diffraction patterns as described in *Chapter 3, 3.2.20.*

5.2.10 Evaluation of the surface morphology of the gel composites using Scanning Electron Microscopy

The surface morphology of the various gel formulations was analysed using a scanning electron microscope (FEI Phenom^{TM}, Hillsboro, Oregon, USA). Carbon tape was used to attach samples to the aluminium stubs. Samples were then coated with gold in the presence of argon gas under a vacuum (0.5 Torr) for 60 seconds using an SPI-MODULE^{TM} Sputter Coater and SPI-MODULE^{TM} Control (SPI Supplies, Division of Structure Probe Inc., West Chester, PA, USA).

5.3 Results and Discussion

5.3.1 Macroscopic examination of the gel

Figure 5.3 displays the PF127-HAGG formulation at 10°C (A), 25°C (B) and 37.5°C (C).



Figure 5.3: PF127-HAGG formulation at 10°C (A), 25°C (B) and 37.5°C (C).

As can be seen, at low temperatures (A) the formulation is more liquid-like and at room temperature (B) the formulation is less liquid-like. At body temperature (C) the formulation has solidified into a gel (no movement upon tilting of the vial). The gel is opaque as is expected due to the inclusion of HAGG (Garcia et al., 2011). Gels are homogenous in appearance without the presence of any lumps or air bubbles which is an important aspect to consider in parenteral delivery systems.

5.3.2 *In vitro* drug release from the various drug-loaded gel composites

Figure 5.4 depicts the *in vitro* drug release curves of four different formulations viz. the optimized nanomicelle in isolation (i.e. without the PF127-HAGG gel) (A), the optimized nanomicelle in the PF127-HAGG gel (B), free disulfiram in the PF127-HAGG gel (C) and free disulfiram together with the optimized nanomicelle in the PF127-HAGG gel (D).

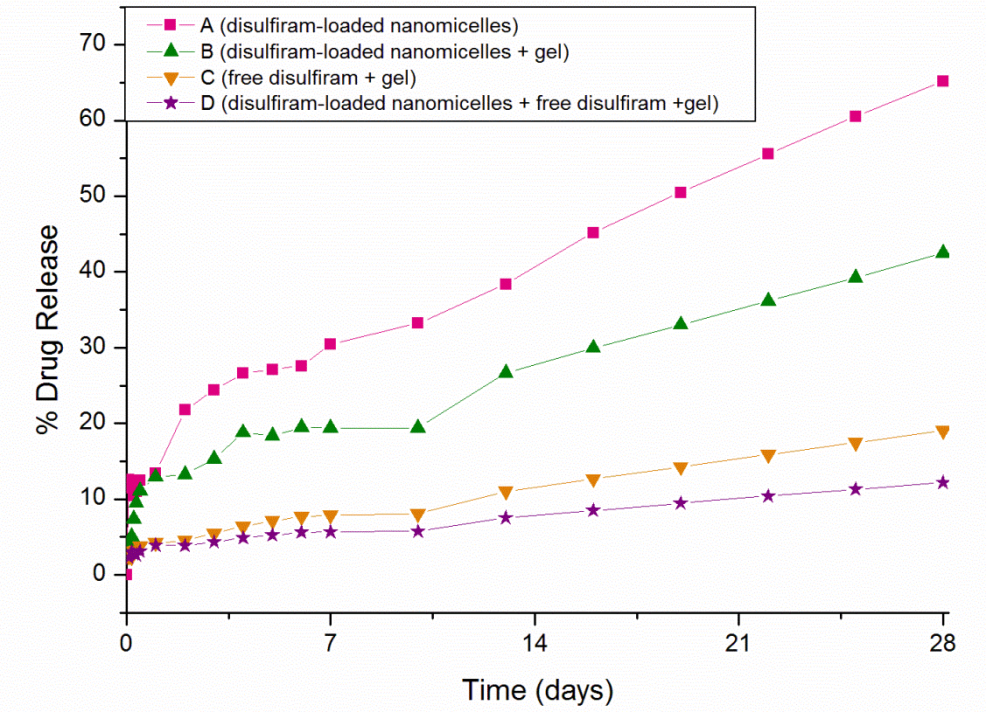

Figure 5.4: Drug release from various gel composites (SD ≤ 0.7 in all cases, n=3).

The nanomicelle formulation (curve A) shows the fastest release compared to the gels. This is expected as the gel system is intended to reduce the release of disulfiram further in order to sustain release over a longer period of time.

Release of disulfiram from the gel containing disulfiram-loaded nanomicelles (curve B) verifies that the gel system does indeed decrease the release of drug due to the strong stable system formed by the union of PF127 and HAGG as well as the inherent properties of long chain polymers to sustain release of actives. The release rate is decreased by approximately 25% by addition of the gel system.

The integration of free drug into the nanomicelle-gel system fosters an intriguing and important event. Instead of accelerating the release of disulfiram, the free drug actually stabilises the release of disulfiram. This occurrence is evidenced by drug release curve D which displays a further decrease in disulfiram release upon incorporation of free disulfiram into the system. This occurs as a result of an exchange of drug occurring between the free drug and the drug in the nanomicelles. This exchange forms an equilibrium which stabilises the release of disulfiram. In this manner, rapid and erratic release is prevented and the components of the entire organization integrate to produce a system with an improved sustained release profile. Projection calculations computed revealed that 100% release for A, B, C, and D would take approximately 46 days, 79 days, 176 days and 303 days

respectively. Based on these calculations it is apparent that the system most capable of meeting the objectives of this study is D due to its significantly slower release rate as well as a greater drug loading. This statement is augmented by the poor loading obtained when formulating disulfiram into micelles using a different polymer. Duan et al., (2014) formulated disulfiram-loaded redox sensitive shell crosslinked micelles. The polymer used was poly(styrene-co-maleic) anhydride micelles crosslinked with cystamine. Despite the larger size of these particles (±80nm) the drug loading was only 7.5%.

5.3.3 Rheological analysis of the gel composites

The gels were analysed rheologically in order to establish the effect of nanomicelle and disulfiram inclusion on the KP, gelation time and flow properties of the gels.

Temperature sweep curves for the various composites are presented in Figures 5.5a-5.5d and values are listed in Table 5.1. Incorporation of drug free nanomicelles, free disulfiram and disulfiram-loaded nanomicelles with free disulfiram in gel all led to a decrease in KP whereas the gel with disulfiram-loaded nanomicelles showed an increase in KP. The KP of 21.5°C for the final formulation is acceptable as it will ensure rapid solidification of the solution once the system enters the muscle thereby reducing the risk of drug leakage. The low viscosity at lower temperatures makes the formulation easily injectable.

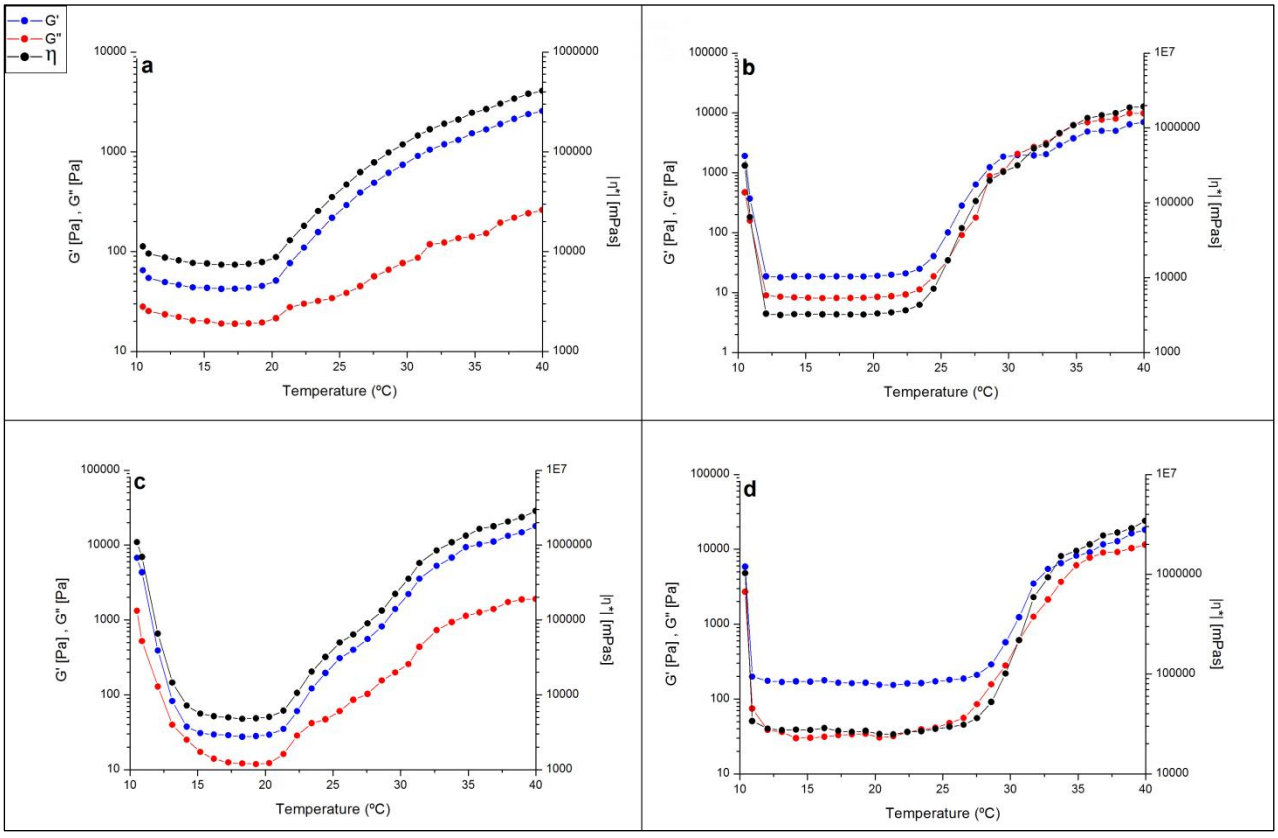

Figure 5.5: Temperature Sweep of a) drug free nanomicelles in gel, b) free disulfiram in gel, c) free disulfiram with disulfiram-loaded nanomicelles in gel and d) disulfiram-loaded nanomicelles in gel.

Gelation time also increased with an increase in constituents (Table 5.1). The gel time for the final formulation is recorded at <30 seconds. A fast *in situ* sol-gel transition time is essential for the formation of a sustained release depot system (Kojarunchitt et al., 2011). The transition time of 28.9 seconds is excellent and is much faster than that recorded for 15% PF127 alone which took approximately 2 minutes to complete as reported by Kojarunchitt et al. (2011). This gelation time is ideal as it minimises a lag time between injection and gel formation which, if too long, can result in burst release (Avachat and Kapure, 2014). Furthermore, the complex viscosity at 37°C was in the region of $1x10^6$ - $1x10^7$ mPa.s. A complex viscosity >10000 Pa.s is indicative of a solid gel (Kojarunchitt et al., 2011). Furthermore the development of a strong gel is dependent on a short gelation time (Cohen et al., 1997). Thus the NEGC is indeed a true solid gel system with a fast gelation time.

The general flow curve trend is synonymous with that reported in Chapter 4 where the gels of HAGG exhibit cross behaviour at low temperatures and Herschel-Bulkley flow behaviour at high temperatures (Table 5.1.).

Table 5.1: Summary of gelation temperature, gelation time and flow curve behaviour of the various composites.

Formulation	**Gelation Temperature (°C)**	**Gelation Time (seconds)**	**Flow Curve Model (10°C)**	**Flow Curve Model (37.5°C)**
PF127-HAGG gel	25.5	17.00	Cross	Herschel-Bulkley
PF127-HAGG + drug free nanomicelles	20.5	14.37	Cross	Herschel-Bulkley
PF127-HAGG +free disulfiram + disulfiram-loaded nanomicelles	21.5	28.90	N/A	Herschel-Bulkley
PF127-HAGG + free disulfiram	23.5	68.40	Cross	Herschel-Bulkley
PF127-HAGG gel + disulfiram-loaded nanomicelles	27.0	25.00	Cross	Herschel-Bulkley

The flow behaviour index for the Herschel-Bulkley equation are all <1 signifying shear-thinning behaviour (Table 5.2).

Table 5.2: Flow behaviour index for composites displaying Herschel-Bulkley flow behaviour.

Formulation	Flow Behaviour Index
PF127-HAGG gel	0.6383
PF127-HAGG + drug free nanomicelles	0.5287
PF127-HAGG + free disulfiram + disulfiram-loaded nanomicelles	0.5366
PF127-HAGG + free disulfiram	0.5318
PF127-HAGG gel + disulfiram-loaded nanomicelles	0.4988

Shear thinning is favourable for IM preparations as it promotes injectability of the gel (Kapoor et al., 2012). Shear-thinning behaviour has been reported previously for PF127 (El-Kamel, 2002).

Thus the incorporation of free disulfiram and disulfiram-loaded nanomicelles did not have unfavourable influence on the structural strength, gelation aspects and flow properties of the PF127-HAGG gel. The gel, encompassing the free disulfiram and disulfiram-loaded nanomicelles, still preserves its favourable traits of notable structural strength, considerably fast gelation time and adequate flow behaviour. The 3 facets combine advantageously to produce a refined delivery system that meets the acceptable rheological criteria necessary for the development of a functional depot-like delivery system.

5.3.4 Investigation of structural variation via Fourier Transform Infrared spectroscopy analysis

FTIR was conducted to ascertain that the structural properties of the optimized system were preserved during the formulation of the NEGC. FTIR analysis of the nanomicelles and disulfiram have already been discussed in *Chapter 3, Section 3.3.13.*

The spectra for native LAGG has fewer bands than that of HAGG which is in line with the chemical structures of the two whereby HA has added functional groups in its chemical composition. Although the two spectra differ in chemical structure there does exist common spectral bands between the two. In LA and HA GG the band at 3295cm^{-1} (peak 1) signifies H-bonded O-H stretch vibrations of hydroxyl groups. At 2888cm^{-1} (peak 2) for LA and 2930cm^{-1} (peak 6) for HA there are C-H stretching bands of CH and CH_2 present. Bands of 1600cm^{-1} (peak 3) for LAGG and HAGG can be attributed to asymmetric carboxylate anion stretching. The 1017cm^{-1} band (peak 5) in LAGG and the 1019cm^{-1} band (peak 10) in HAGG denote C-O stretching vibrations. LAGG displays a band at 1403cm^{-1} (peak 4) which represents symmetric carboxylate stretching vibrations. A prominent HAGG additional peak not present in LAGG is 1724cm^{-1} (peak 7), which can be attributed to a carbonyl group indicating C=O. HAGG displays a band at 1380cm^{-1} (peak 8) which signifies methyl C-H bonding and 1280cm^{-1} (peak 9) which signifies C-O-C vibrations (Figure 5.6).

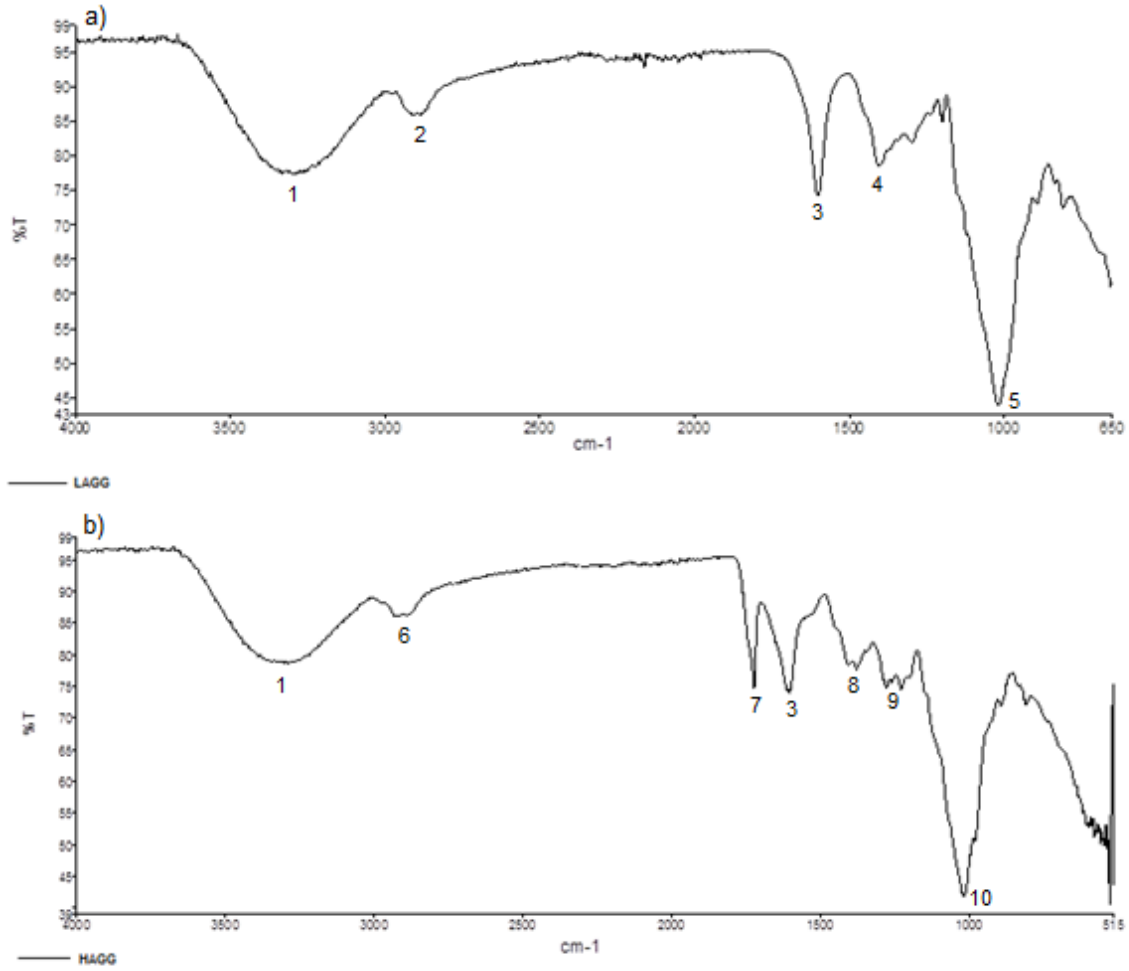

Figure 5.6: FTIR spectra of a) LAGG and b) HAGG.

Figure 5.7 displays the FTIR spectra of all the components as well as the various combinations. PF127 displays a band at 2878cm^{-1} (peak 1) which can be attributed to C-H stretching vibrations. 1466cm^{-1} (peak 2) signifies CH_2 and CH_3 bending. O-H in plane bending is represented by 1341cm^{-1} (peak 3). The peak at 1095cm^{-1} (peak 4) can be ascribed to R-O stretching. Minimal changes are present confirming that structural integrity was not compromised during the formation of the NEGC and the other composites. The spectra at 10°C were not included as they were identical to those at 36.5°C.

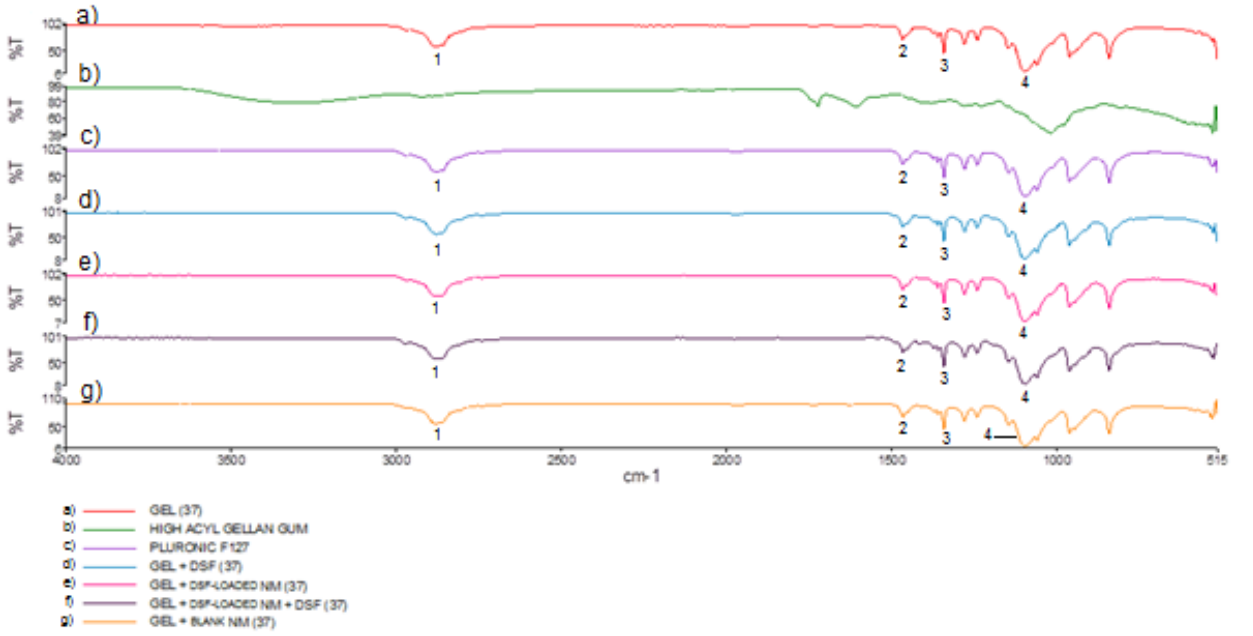

Figure 5.7: FTIR spectra of the native components of the NEGC as well as the combined NEGC and its variations.

5.3.5 Thermal profile analysis of the gel polymers and gel composites

A thermal description of LAGG, HAGG, PF127-GG gel and combinations of the gel with pure disulfiram and nanomicelles (drug-free nanomicelles and disulfiram-loaded nanomicelles) was obtained through DSC. Both forms of GG display an endothermic peak and a pronounced exothermic peak. The endothermic peak is present at 106.3°C and 113°C for HAGG and LAGG respectively and the exothermic peak is at 250°C for both. The endothermic event signifies a dehydration process whereby loss of absorbed moisture occurs (Vijan et al., 2012; Yang et al., 2013). The exothermic occurrence represents degradation whereby decomposition without melting occurs (Mahajan and Galtani, 2009; Dixit et al., 2011). This is confirmed by the amorphous structure of GG and amorphous materials lack a distinct melting point. This thermal degradation occurs as a result of disintegration of molecular chains (Xu et al., 2007). A third small peak is also present in both LAGG and HAGG at 265.5°C and 268.8°C respectively. HAGG has an additional endothermic peak at 182.2°C (Figure 5.8).

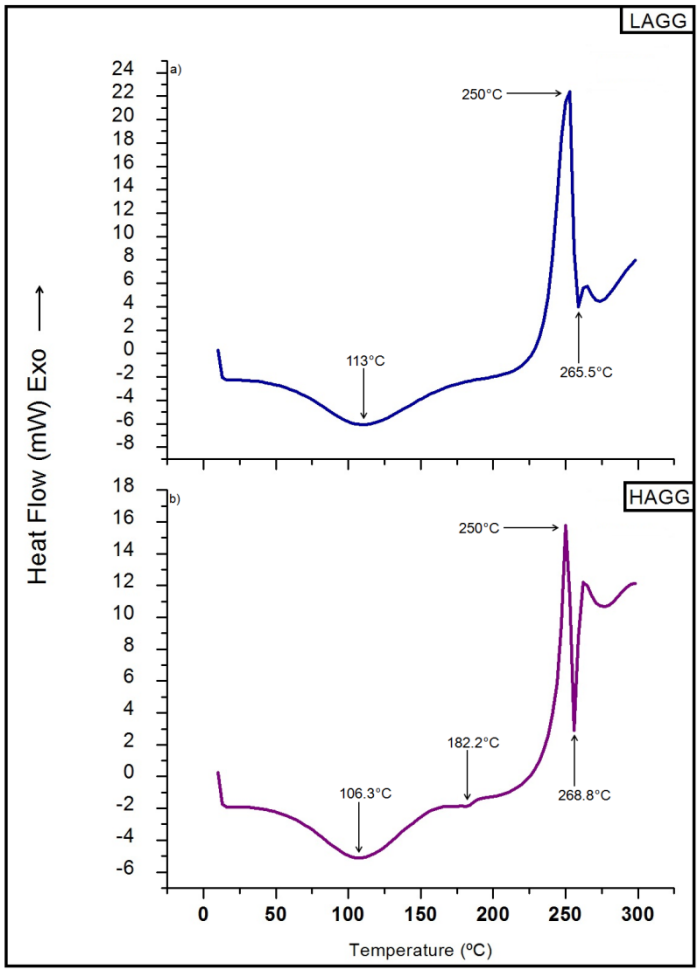

Figure 5.8: Thermograms of a) LAGG and b) HAGG.

PF127 has a characteristic endothermic peak at 56.3°C. Fathy and El-Badry (2003) and Albertini et al (2010) also reported such an endothermic peak in the range of ±50-60 °C. this peak is the T_m of PF127 proving that PF127 has a crystalline structure (Figure 5.9).

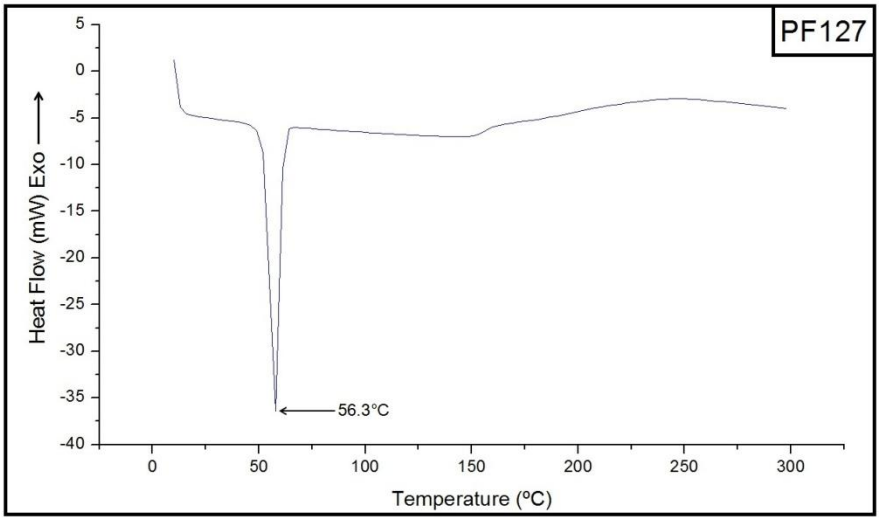

Figure 5.9: Thermogram of PF127.

Similarities in DSC indicate the absence of chemical interaction (Fathy and El-Badry, 2003). Combination formulations maintained chemical integrity as is evident by the similar DSC profile of each compared to the native constituents. Furthermore change from the liquid state to solid state did not a have a profound effect as thermograms for both temperatures (i.e. 10°C and 36.5°C are identical (Figure 5.10).

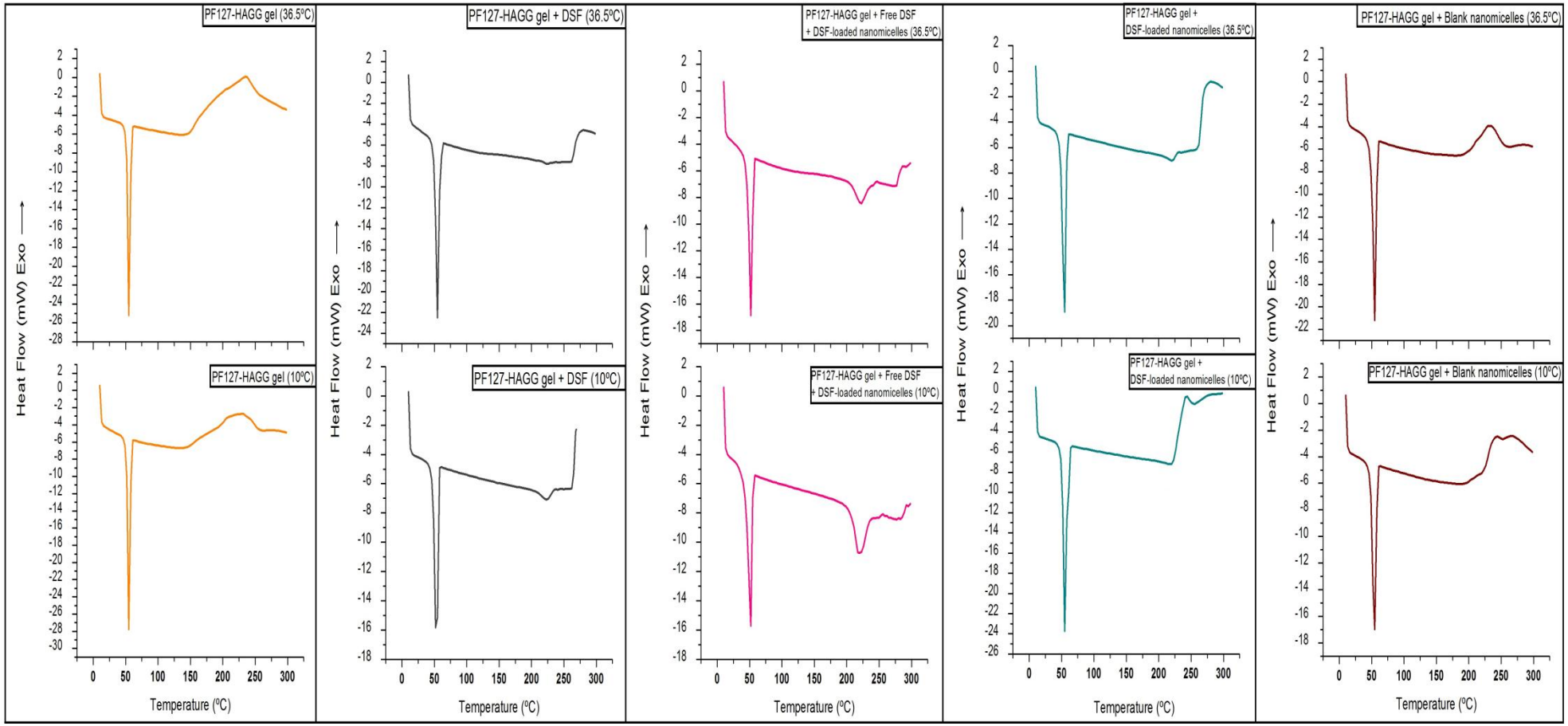

Figure 5.10: Thermograms of various combinations of gel, nanomicelles and disulfiram at 36.5°C (top row) and 10°C (bottom row).

5.3.6 Analysis of the degree of crystallinity of the gel polymers and gel composites

XRD provides information on the crystal structure of a compound which is helpful in determining the extent of crystallinity of that particular compound as well as identification of the substance. The crystal nature of LAGG, HAGG, PF127-GG gel and combinations of the gel with pure disulfiram and nanomicelles (drug-free nanomicelles and disulfiram-loaded nanomicelles) was obtained through XRD.

Both HAGG and LAGG diffractograms display crystalline peaks at 9° and 20° (Figure 5.11). This was also reported by Yang et al., (2013). The intensity of the HAGG peaks are lower than those of LAGG indicating that HAGG is less crystalline in structure. Side-by-side association and crystallisation is sterically inhibited by acylation. This reduces the extent of the gels crystallinity leading to decreased brittleness and increased elasticity of the gels. It is not the acetate substituent that restricts crystallisation of the helices; packing of the helices is prevented by the bulky L-glycerate ester groups in the unit cell (Stephen and Phillips, 2006).

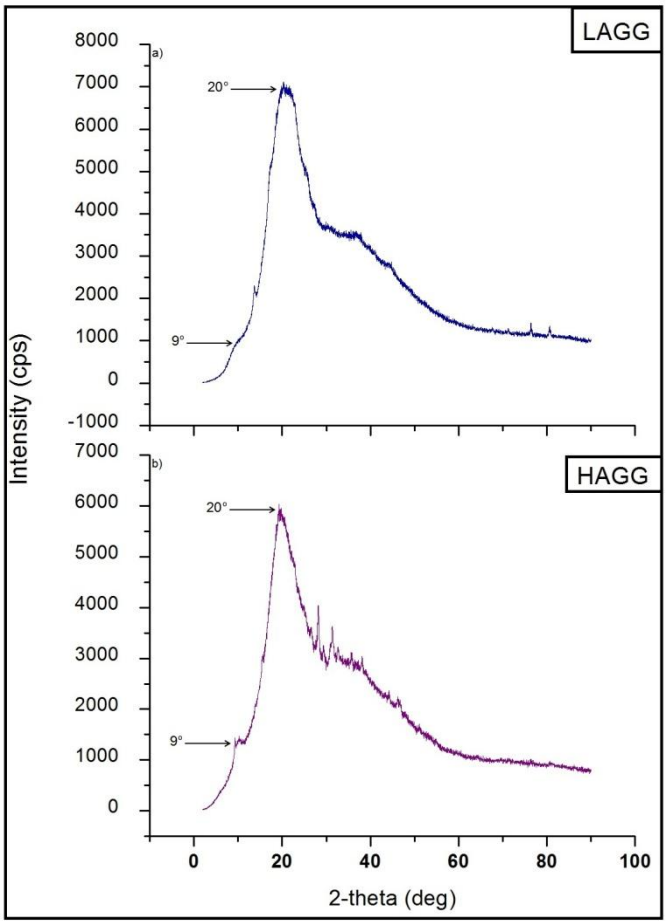

Figure 5.11: Diffractograms of LAGG (a) and HAGG (b).

PF127 also possesses two distinct diffraction peaks at 19° and 23° (Figure 5.12). These are due to the presence of PEO groups in the polymer (Albertini et al., 2010). These peaks illustrate the crystal structure of PF127 (Sahu et al., 2011).

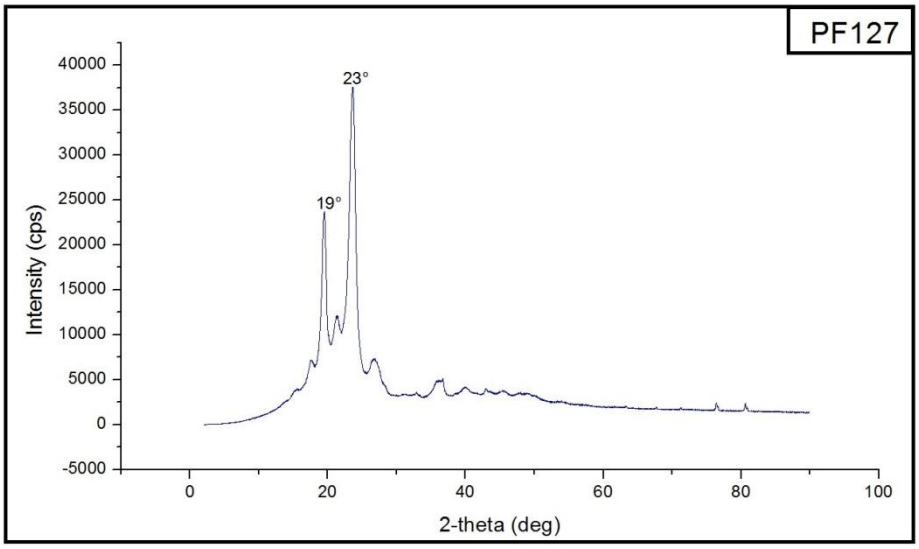

Figure 5.12: Diffractogram of PF127.

As can be seen from the various combined formulations at different temperatures similarities exist across all (Figure 5.13). Peaks that are identically positioned in the mixture indicate that there was no interference of the drug with lattice spacing of the polymer (Goddeeris et al., 2008). Differences in crystallinity are due to different ratios of constituents compared to individual components (Vaas et al., 2009). If peaks of a compound are not showing it means that the formulation is amorphous with regards to that compound (Sethia and Squillante, 2004). XRD analysis is important as the extent of crystallinity influences dissolution. If the intensity is reduced, the crystallinity is reduced; this enhances drug dissolution (Rao et al., 2014).

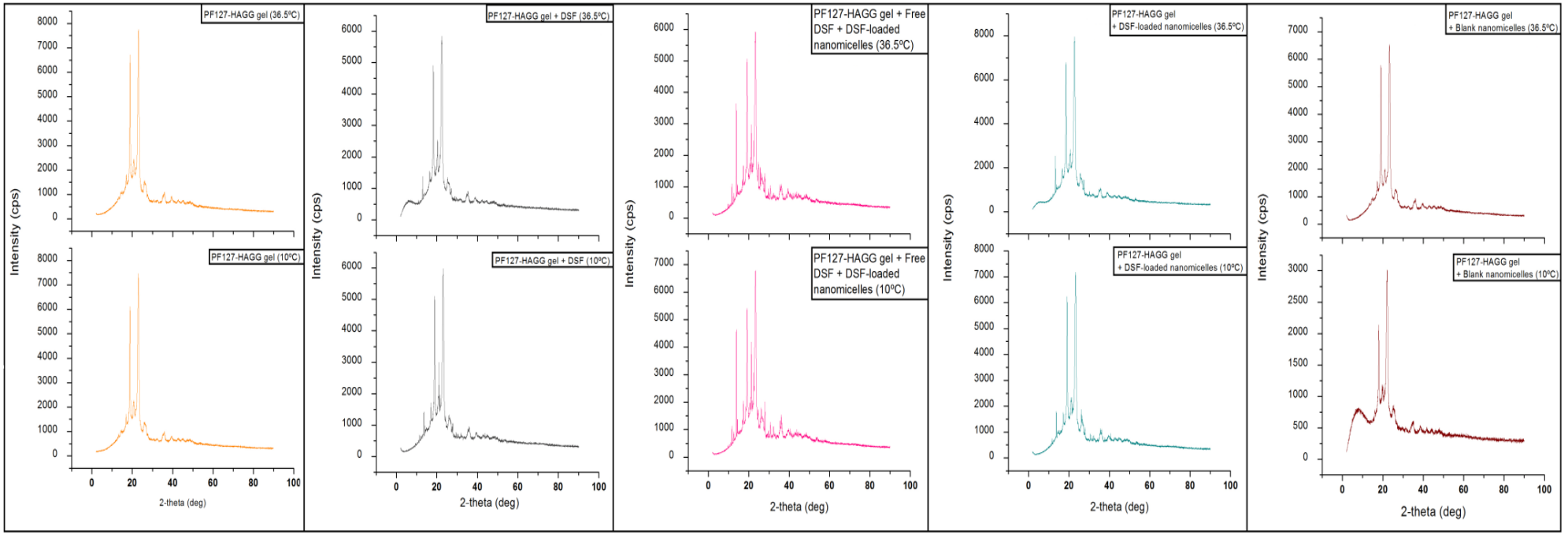

Figure 5.13: Diffractograms of various combinations of gel, nanomicelles and disulfiram at 36.5°C (top row) and 10°C (bottom row).

5.3.7 Surface morphology exploration of the various gel composites using Scanning Electron Microscopy (SEM)

SEM was utilised in order to characterize the structure and morphology of the various disulfiram-nm-gel combinations (Figure 5.14). SEM images showed a network of aggregated sheets densely covered with flaky appendages and sparse large pores interspersed with smaller pores. Homogeneity spans across the samples indicating that the fundamental gel structure was not influenced by the incorporation of disulfiram and nanomicelles. The dense, thick network and porous facets have been reported previously for gellan gum and PF127 (Sosnik et al., 2007; Vilela et al., 2011; Liu et al., 2014; Sabadani et al., 2015). Lyophilization can also impact the surface morphology but this was not notable in this instance.

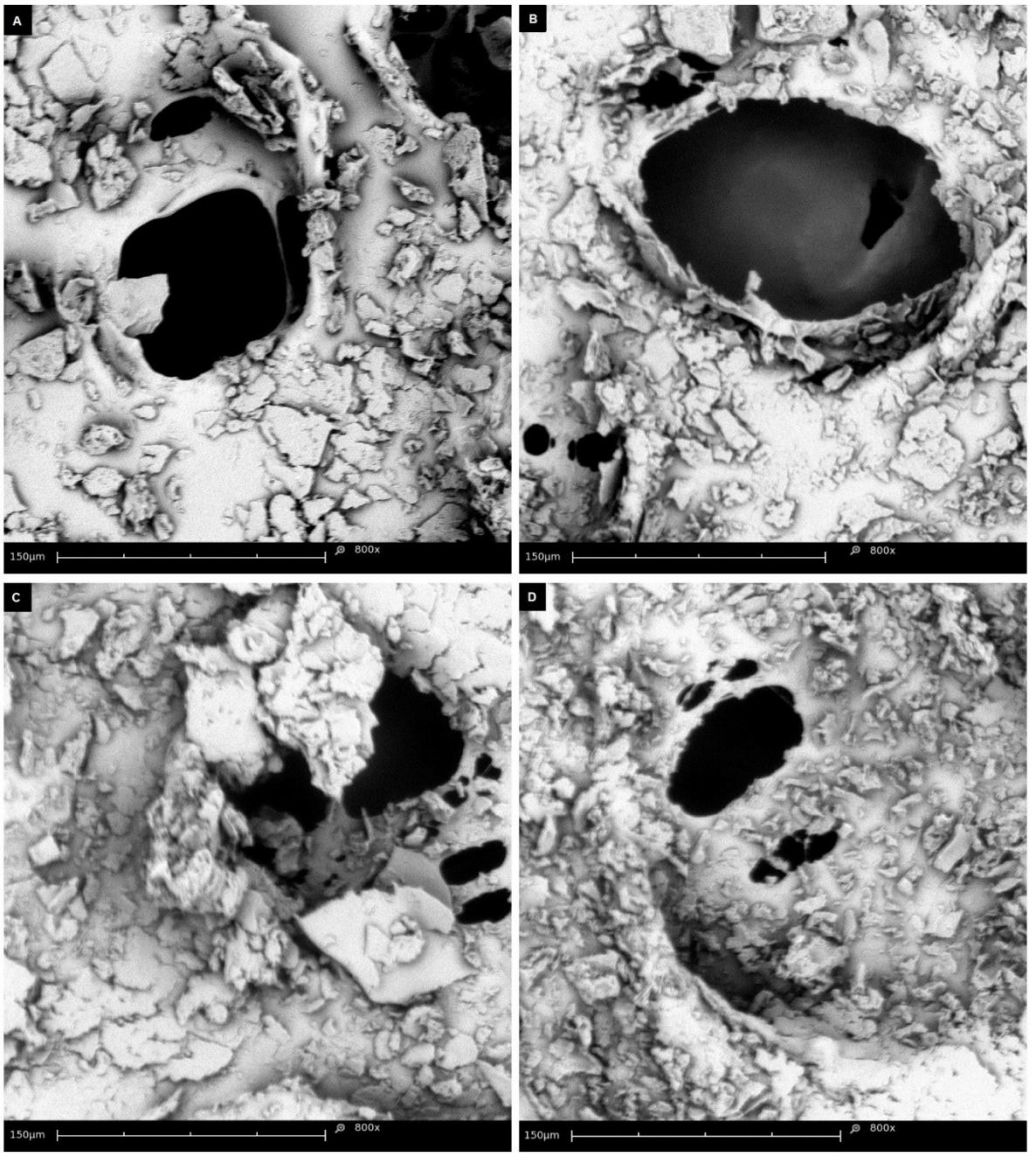

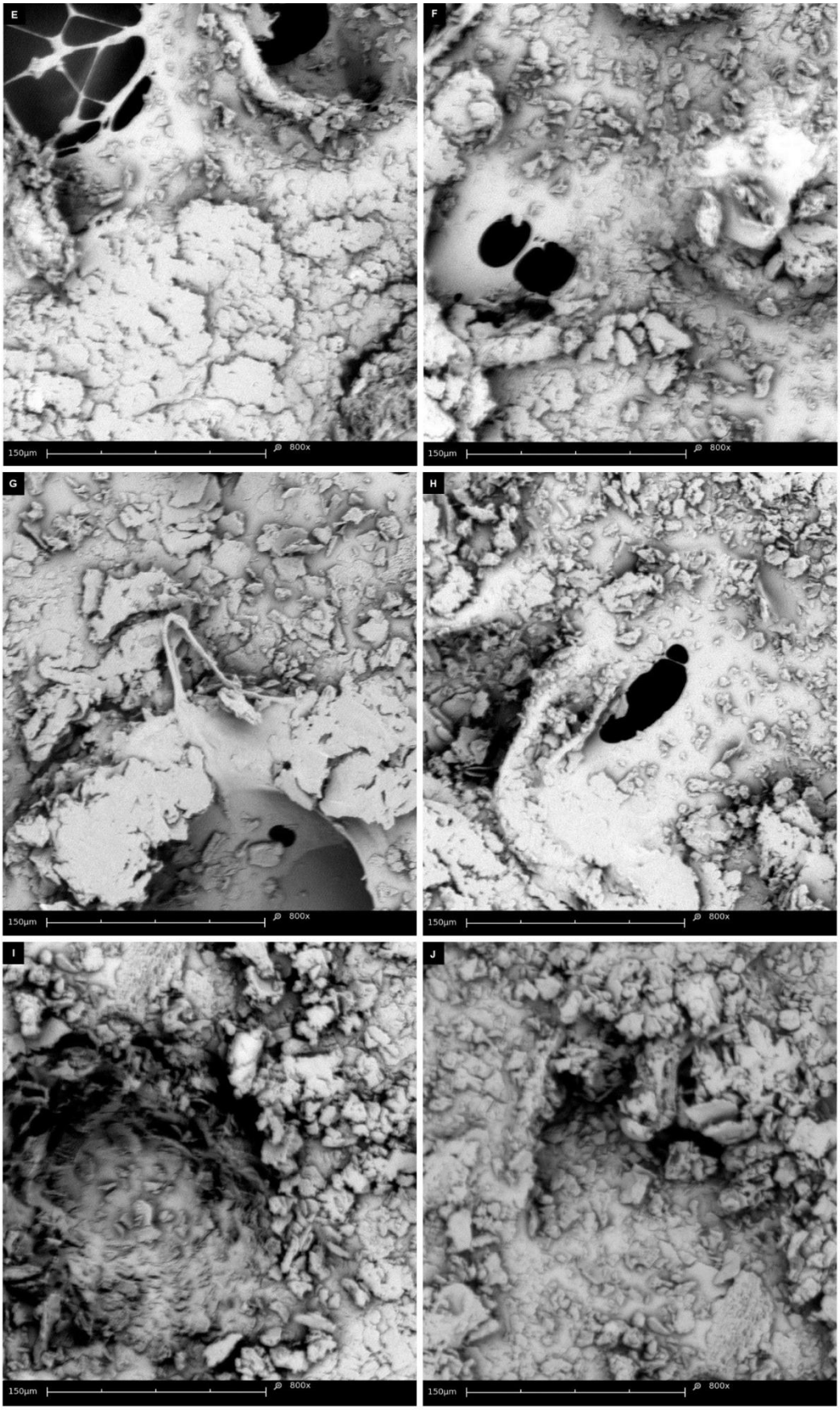

Figure 5.14: Photomicrographs of a) Composite 5 at 10°C, b) Composite 5 at 37.5 °C, c) Composite 1 at 10°C, d) Composite 1 at 37.5°C, e) Composite 2 at 10°C, f) Composite 2 at

37.5°C, g) Composite 3 at 10°C, h) Composite 3 at 37.5°C, i) Composite 4 at 10°C and j) Composite 4 at 37.5°C.

5.4 Concluding Remarks

In this chapter the optimized nanomicelles and the rheologically appropriate PF127-HAGG gel were successfully integrated to yield a nano-enclatherated-gel-composite. Thorough physicochemical, physicomechanical and *in vitro* release was conducted on the NEGC as well as derivatives of it. The NEGC displayed a slower release rate compared to the other variations of the composite making it the ideal system which meets the requirements of a sustained release depot. The rheological analysis of the composite proved that the incorporation of disulfiram and nanomicelles into the gel did not adversely affect the gelation, flow and structural strength of the gel component. Structural and thermal analysis confirmed that chemical changes did not occur and that the chemical structural integrity was maintained during formation of the NEGC and composites. Thus the combination of polymers utilized and the merging of the two systems generates a successful delivery system with great potential at an *in vitro* level. This positive outcome qualifies the NEGC to advance to the next research phase which is *in vivo* testing. In the following chapter the performance of the NEGC *ex vivo* and *in vivo* is assessed to determine the feasibility of the NEGC at a physiological level.

CHAPTER 6

EX VIVO AND *IN VIVO* EVALUATION OF THE NANOMICELLE-ENCLATHERATED-GEL-COMPOSITE

6.1 Introduction

Ethical approval for this in vivo investigation was obtained from the Animal Ethics Screening Committee of the University of the Witwatersrand. Clearance Number: AESC 2014/43/C (Appendix E).

Once a delivery system has been proven to be tenable in a controlled laboratory environment, the next crucial step is the assessment of its performance *ex vivo* and *in vivo*. An appraisal of the formulation must be implemented in terms of safety and efficacy screening as well as the mechanism of action of the system. *Ex vivo* and *in vivo* studies are vital tools that can be utilised to achieve these aims (Godin and Touitou, 2007). Additionally, discordance between *in vitro* and *in vivo* studies may arise (Polli, 2008). Due to the fact that results may differ, it is important to complete *ex vivo* and *in vivo* analysis. *Ex vivo* analysis fills in the knowledge gap between *in vitro* and *in vivo* whilst a true perception of the pharmacokinetic and pharmacodynamic attributes of the system can only be gained from *in vivo* research. Barriers which can inhibit systemic drug absorption or target tissue penetration, establishing safety of compounds and investigating pharmacokinetic and pharmacodynamic relationships are just a few of the justifiable reasons for using animal models (Brayden, 2007). Another consideration is that of ethical affairs. Methods of testing that raise ethical issues if studied in human subjects can be tested in animal models without the risks and consequences that could occur in human subjects.

Animal model studies are all-important in alcoholism research which can only be conducted superficially in human subjects due to ethical limitations and immanent risks (Tabakoff and Hoffman, 2006). The rat model has been selected as the ideal model as it has many useful advantages:

i. Rats are considered model subjects to study alcohol consumption and its associated effects. This is due to the voluntary consumption of alcohol in a laboratory setting by these animals as well as the consumption of rotten fruits in their natural environment which produces an intoxicating effect in them after consumption (Spanagle, 2000).

ii. This statement coupled with the fact that rats share physiological and anatomical similarity to humans makes them the ideal model for conduction of *in vivo* testing (Spanagle, 2000).

iii. Previous studies of disulfiram and its effects have mostly been carried out in rat models (Phillips and Cragg, 1983; Jensen and Faiman, 1984; Lipsky et al., 2001).

Testing of disulfiram in animals, particularly in rats, has been carried out before for various purposes. Below is a summary of these studies.

1. Hellstrom and Tottmar (1980) studied the effect of implantation of disulfiram in rats. Sprague- Dawley rats were implanted with two 100mg disulfiram tablets subcutaneously and the rats' heart rate, blood pressure and respiratory rate were measured for a period of 2-3 months.

2. Another study by Faiman et al. (1980) investigated the distribution and elimination of disulfiram in Sprague- Dawley rats after oral and intraperitoneal administration. Rats were given 7mg/kg of disulfiram either orally or intraperitoneally.

3. In 1982, Tottmar and Hellstrom focused their study on the effect of ethanol and acetaldehyde on the blood pressure and heart rate of disulfiram-treated Sprague- Dawley rats. In this study the dose of disulfiram was 100mg/kg administered intraperitoneally as a 5% gum arabicum suspension.

4. A study conducted determining the plasma concentration of disulfiram in Wistar rats after being injected by disulfiram micro-pellets was conducted by Cid et al. in 1991. Rats received a subcutaneous injection of a 5mg suspension. The study was conducted for longer a month.

5. Wistar rats given a dose of 12.5mg/kg and 25mg/kg were studied to establish if tolerance to disulfiram can occur from chronic alcohol intake (Tampier et al., 2008).

6. In all of the abovementioned studies, changes took place in the physiological aspects that were being monitored (blood pressure, heart rate, respiratory rate, body temperature, enzyme levels). However, no adverse or fatal incidents occurred due to disulfiram administration in any of the studies.

The therapeutic potentiality and toxicity profile of the delivery system was investigated in this chapter. This was carried out at an *ex vivo* and *in vivo* level. *Ex vivo* drug release, disulfiram plasma concentration, myotoxicity, histopathology and high frequency ultra sound imaging were the primary criteria that were evaluated. In vivo visualisation is worthwhile as it allows researchers to study the physiological and pathophysiological occurrences in relation to the delivery system in real-time without causing any discomfort to the patient (Swartz, 2005). Studying the effect of the drug or system *in vivo* (e.g. distribution) provides insight into the behaviour and fate of the drug directly in the body (Swartz, 2005).

Part I - *Ex Vivo* Studies

6.2 Materials and Methods

6.2.1 Materials

Tetraethylthiuram disulfide (disulfiram) and Pluronic F127 were purchased from Sigma Aldrich (Steinheim, Germany). High Acyl Gellan Gum (Kelcogel LT100) was obtained from CP Kelco Germany GmbH (Grossenbrode, Germany). Kolliphor® TPGS was provided by BASF (Ludwigshafen, Germany). Deionised water was obtained from a Milli-Q water purification system (Milli-Q, Millipore, Billerica, MA, USA). All other chemicals and solvents were of analytic grade and were used as received.

6.2.2 Preparation of the NEGC

The NEGC was prepared as per the method detailed in *Chapter 5, Section 5.2.2.*

6.2.3 Preparation of the rat muscle tissue samples

Healthy biceps femoris muscle tissue (800mg-1000mg) was cut from the Sprague Dawley rat. The tissue was rinsed in saline and stored at -80°C for future use. The maximum storage time was 2-3 weeks. Prior to use, the frozen tissue was thawed to room temperature.

6.2.4 Simulated organ bath

In order to simulate the muscle environment for *ex vivo* studies a modified organ bath system was constructed (Figure 6.1) (Brazeau and Fung, 1989). A cylindrical plastic tube was utilised as a holder for the tissue sample. The tube was perforated to allow SBF and air to flow through. This tube was then placed into a larger, graduated cylindrical tube which served as the incubation vessel. The incubation vessel contained 9mL of incubation medium. A heating mantle and thermometer were used to maintain a temperature of 37°C. An air supply was introduced by attaching an air pump and pipe system to one end of the

incubation vessel (Brazeau and Fung, 1989). Air was bubbled at a constant rate for the provision of aeration and agitation. The purpose of the organ bath was to create a controlled, physiologically-fitting environment in order to conduct *ex vivo* research over a short period of time (Radnoti, n.d.).

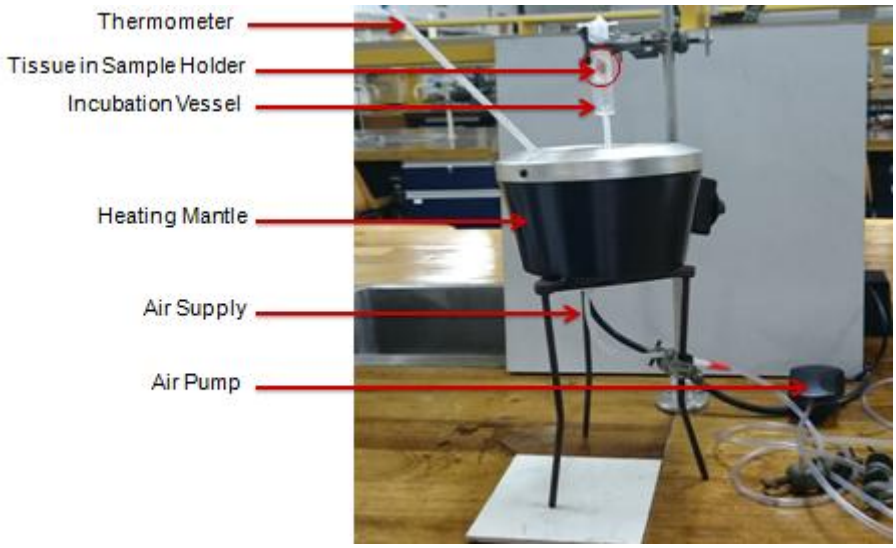

Figure 6.1: Setup of the modified simulated organ bath.

6.2.5 *Ex vivo* drug release study

A sample of NEGC (0.3mL) was injected into the muscle tissue using a 21G needle. The injected muscle was placed into the sample holder of the organ bath. At specified time points the release media was withdrawn for testing and replaced with fresh media. Samples were analysed using UV spectroscopy as described in *Chapter 3, Section 3.2.10.* The drug release was determined over 24 hours.

6.2.6 *Ex vivo* myotoxicity study

Samples were analysed for creatine kinase (CK) using a commercially available spectrophotometric kit (Sigma Aldrich, St Louis, MO, USA) at 340nm. Samples were analysed using UV spectroscopy as described in *Chapter 3, Section 3.2.10.* CK activity was computed according to the equation as instructed by the Sigma Aldrich CK Activity Assay Kit Technical Bulletin:

$$\text{CK Activity (units/L)} = \frac{A_{340(\text{final})} - A_{340(\text{initial})}}{A_{340(\text{calibrator})} - A_{340(\text{blank})}} \times 150 \qquad \textbf{Equation 6.1}$$

6.3 Results and Discussion

6.3.1 *Ex vivo* drug release

The mean *ex vivo* % drug release is depicted in Figure 6.2 (SD≤1.24, n=3). The study was conducted over a maximum period of 24 hours due to the degradative nature of harvested tissue. *Ex vivo* studies displayed a burst release of 24% of drug within the first hour. Thereafter the release rate decreased. At 24 hours 44% of all the drug entrapped had been released. The sample utilised for the study was significantly smaller than the size of the actual muscle. Thus the excised tissue sample was highly saturated with the NEGC resulting in a fast release rate. The important and focal outcome of the *ex vivo* study was not the release rate. Instead, it was to ascertain that the formulation is suitable for IM injection and furthermore, that it is capable of releasing the drug, in order to bridge the gap between *in vitro* and *in vivo* studies. These outcomes have been achieved thus the NEGC is approved to progress to the next phase i.e. *in vivo* studies.

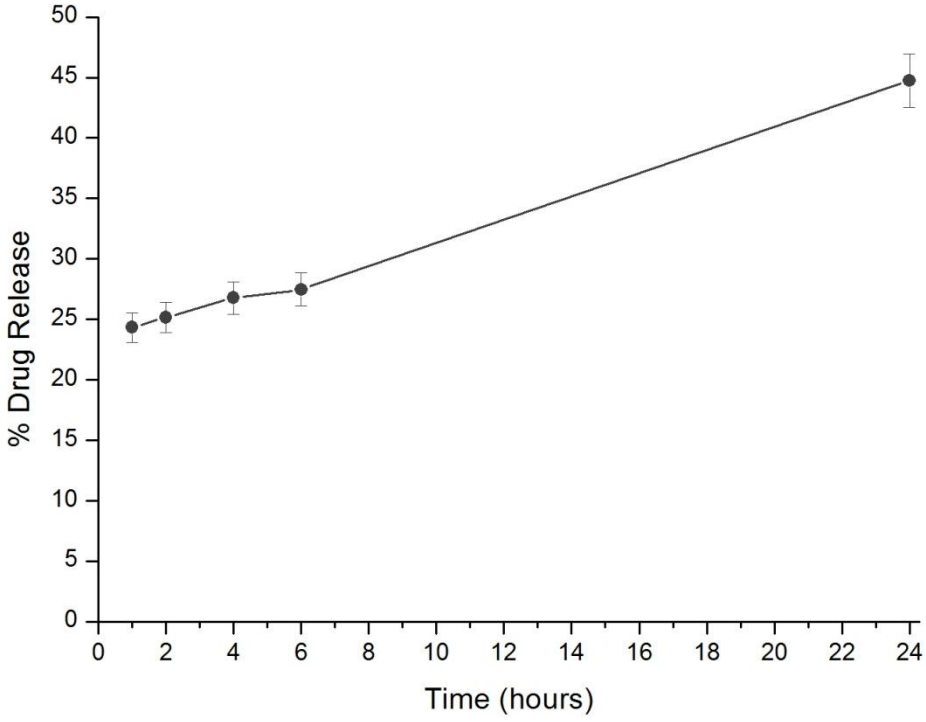

Figure 6.2: *Ex vivo* % drug release.

6.3.2 *Ex vivo* myotoxicity

Assessment of myotoxicity is imperative as compelling complications of the IM route are patient discomfort and skeletal muscle damage (Brazeau and Fung, 1989). CK is a commonly employed intracellular enzyme for the quantitative evaluation of muscle damage

arising from IM injections. Mechanical harm, trauma-induced muscle fibre destruction, toxic injury and enzymatic/structural protein alteration lead to a rise in CK activity (Goicoechea et al., 2008). The isolated rodent model is a widely used and accepted screening method for determining myotoxic capacity (Brazeau and Fung, 1989; Kranz et al., 2001; Rungseevijitprapa et al., 2008). In all these studies CK levels are determined following direct injection of the test substance into the isolated muscle tissue. The acute damage potential of compounds can be ascertained with this rapid screening system (Brazeau et al., 1998).

All results obtained were negligible. This can be attributed to decreased muscle viability which negatively affected the outcome. Rat muscle tissue has limited viability post-extraction (Brazeau et al., 1998). Despite the poor success rate of the *ex vivo* myotoxicity study previous reports have confirmed favourable outcomes from utilisation of this approach (Brazeau and Fung, 1989, Kranz et al., 2001). Brazeau and Fung (1989) authenticated the usefulness of this *ex vivo* technique for reducing the skeletal muscle damage following injections thus enabling rational development of IM formulations. Fortunately an *in vivo* study was also conducted as the *in vivo* model is assumed to be the optimal method to detect the toxic effects of long-term injectables as the *ex vivo* method cannot be used in this case.

Part II - *In Vivo* Studies

6.4 Materials and Methods

6.4.1 Materials

Sprague Dawley rats were utilised in this study and were obtained as per the Central Animal Services (CAS) protocol at the University of the Witwatersrand. Tetraethylthiuram disulfide (disulfiram) and Pluronic F127 were purchased from Sigma Aldrich (Steinheim, Germany). Disulfiram tablets (Antabuse® dispergettes) were obtained from PharmaCare Ltd (Port Elizabeth, South Africa) High Acyl Gellan Gum (Kelcogel LT100) was obtained from CP Kelco Germany GmbH (Grossenbrode, Germany). Kolliphor® TPGS was provided by BASF (Ludwigshafen, Germany). Double deionised water was obtained from a Milli-Q water purification system (Milli-Q, Millipore, Billerica, MA, USA). All solvents employed in UPLC-UV detection were of UPLC grade. All other chemicals and solvents were of analytic grade and were used as received.

6.4.2 Preparation of *in vivo* formulations

6.4.2.1 Preparation of oral disulfiram formulation for comparison group

The comparison group had to receive the conventional oral form of disulfiram daily. In order to minimise distress to the animals, oral gavage was not considered. The most practical solution was to employ voluntary ingestion (Diogo et al., 2015). Adherence of the rats to this technique was facilitated through the incorporation of the oral disulfiram in a safe yet palatable vehicle. Flavoured jelly cubes with the drug dispersed within failed as a suitable vehicle. Peanut butter was then tried due to its success in promoting voluntary administration in rodents (Diogo et al., 2015). Disulfiram tablets were crushed and blended into a peanut butter dough ball. Each rat was fed one disulfiram peanut butter dough ball daily for 28 days.

6.4.2.2 Preparation of the test group NEGC and placebo group NEGC for IM injection into the rat

The same method of preparation was followed as described in *Chapter 5, section 5.2.2.* All solid powders (disulfiram, disulfiram-loaded nanomicelles, drug-free nanomicelles, gel polymers) utilised were sterilised by ultraviolet radiation for 24 hours prior to use (Gu et al., 2012). Gel formulations were prepared using UV-sterilised polymers and sterile distilled water. Gels were prepared in a completely sterile laboratory under strict aseptic conditions with utilisation of a laminar flow unit. All glassware and equipment necessary was sterilised using dry heat sterilisation prior to usage. Disulfiram-loaded NEGC and the drug-free NEGC were formulated in the same manner. Cold chain was maintained during formulation, transportation and prior to administration in order to ensure that the NEGC was in liquid form ahead of injection. The intramuscular injection consisted of 0,3ml of NEGC through a needle size of 21G.

6.4.3 Animal ethics clearance

All the experimental procedures and protocols were reviewed and approved by the AESC (AESC No. 2014/43/C) (Appendix E). Ethical guidelines were strictly adhered to at all times.

6.4.4 Animal Husbandry

Sprague Dawley rats weighing approximately 250-300g were housed in single cages with a 12 hour light/dark cycle at a controlled temperature (±25°C). Rats were acclimatised for 7 days prior to *in vivo* examination during which they were monitored to ensure a general state of wellbeing. Rats were provided with nutritionally adequate rat feed and clean water *ad libitum*. This also allowed them to become familiar with the surroundings and the researcher. Housing conditions were maintained according to the CAS Standard Operating Procedures

which are in accordance with the South African Standard for the care and use of animals for scientific purposes. Rats were individually housed for ease of oral administration as well as monitoring of animals post IM administration. Rats were weighed on a weekly basis in order to observe their state of wellbeing.

6.4.5 *In vivo* experimental design and procedure

The study comprised 75 Sprague Dawley rats with an initial mass of 250-300g. The rats were randomly assigned to 3 groups.

Group 1: comparison group (n=25). This group received the conventional oral form of disulfiram in a peanut butter dough ball daily for 28 days.

Group 2: placebo group (n=25). The blank NEGC was injected once-off into the biceps femoris muscle of these healthy rats. This form of the NEGC contained drug-free nanomicelles and did not contain any free disulfiram.

Group 3: test group (n=25). The disulfiram-NEGC was injected once-off into the biceps femoris muscle of these healthy rats. This form of the NEGC contained drug-loaded nanomicelles and also contained free disulfiram.

Prior to the intramuscular injections for the test group and the placebo group the rats will be anesthetized with xylazine (5mg/kg) and ketamine (100mg/kg). Biodistribution imaging was conducted on the test group and placebo group post IM-administration and prior to termination.

The *in vivo* experimental design procedure is summarised in Figure 6.3.

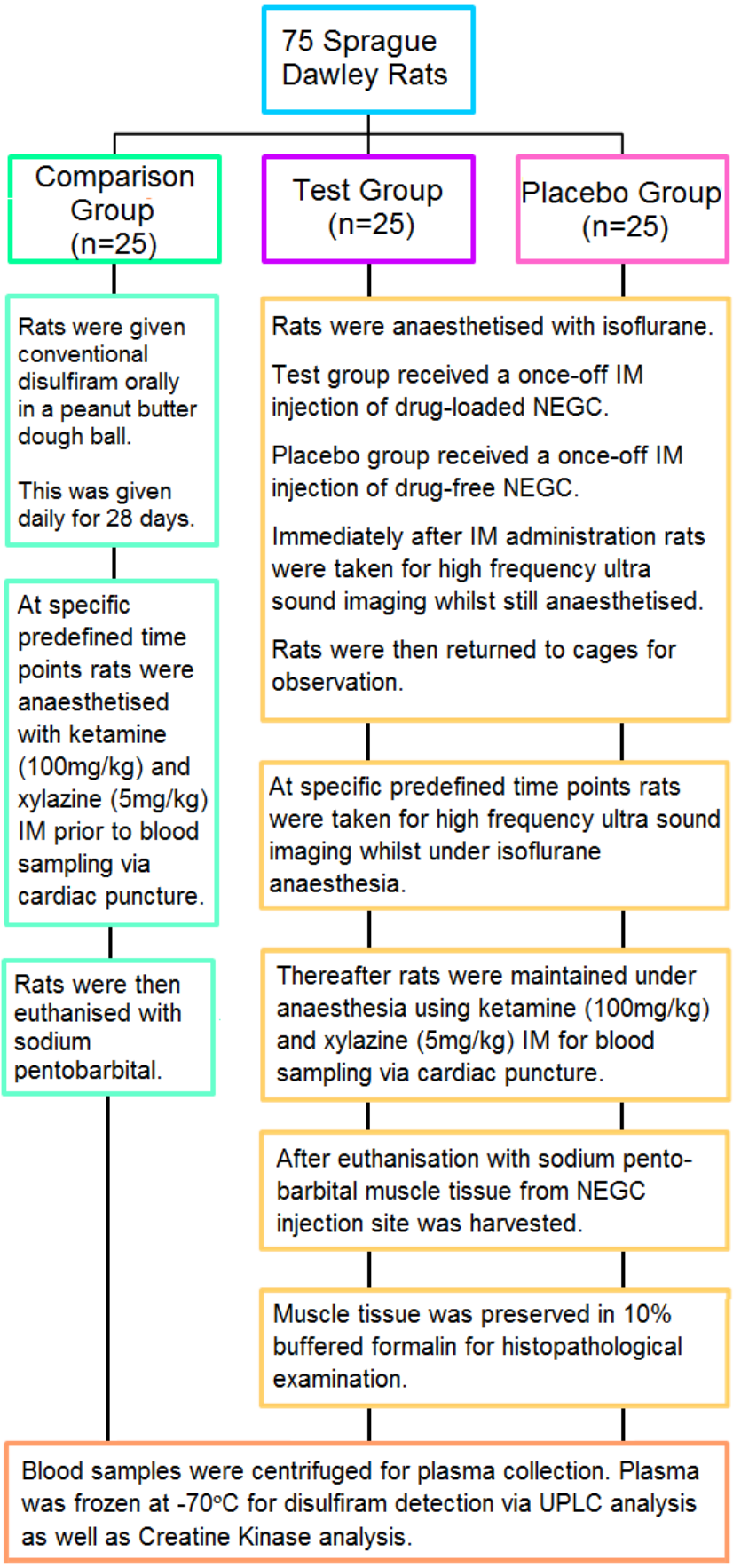

Figure 6.3: Flow- chart summary of the *in vivo* experimental design procedure.

6.4.6 Animal welfare and humane endpoints

Post IM administration all rats were monitored daily in order to examine their state of health and determine the effect of the NEGC on their behaviour and physiological state. Behavioural observations will take place to determine the condition of the rats. The following changes and behaviours are indicative of distress: excessive grooming such that the fur falls out, weight loss and aggression. Strict health and safety measures were implemented should any rat display signs of pain, discomfort or ill health. Rats were monitored for signs of pain. If pain was present pharmacological interventions would have been implemented.

Animals would be removed from the study if they displayed any of the following changes or abnormalities in relation to appearance (pallor, anaemia, jaundice, cyanosis, weight loss, unkempt appearance, loss of fur/hair), bodily function (self induced trauma, decreased ambulation), activity (lethargy, hyperactivity), behaviour (loss of appetite, easily scared, aggressiveness) and physiological change (difficulty breathing, oedema, dehydration, bleeding from any orifice, diarrhoea). Additionally they would also be monitored for the following signs of morbidity or moribundity which would require euthanasia (The John Hopkins University Animal Care and Use Committee) (Animal Welfare Branch).

The above will be looked out for via a daily period of observation. In addition to that the animals will be weighed weekly. All records will be kept on score sheets. Fortunately the rats did not display any of the above signs and symptoms.

6.4.7 High frequency ultra sound imaging

In order to observe the transformation of the liquid NEGC to a solid gel form upon IM injection as well as to confirm the long-term presence of the gel (i.e. its potential for sustained release), ultra sound imaging was employed. Imaging was conducted using the Vevo 2100® Micro Imaging Platform enhanced with the Cellvizio® Lab Module (Visual Sonics (Pty) Ltd, Toronto, Ontario, Canada) on the rats post-IM administration as well as prior to termination. Rats were anesthetised with ketamine and transported to the imaging lab (Drug Delivery Lab 6, WADDP, Department of Pharmacy and Pharmacology, University of the Witwatersrand) under the supervision of the CAS staff for the ultra sound imaging. The rat was placed on to the observation stage equipped with a heating pad. The nose was positioned in front of the tube opening which provided a supply of oxygen and 2% isoflurane gas to maintain sedation. Warm ultrasound gel was applied on the area of interest (the IM injection site). The ultrasound probe was placed on the area and imaging was conducted. Figure 6.4. displays a rat undergoing the ultrasound procedure.

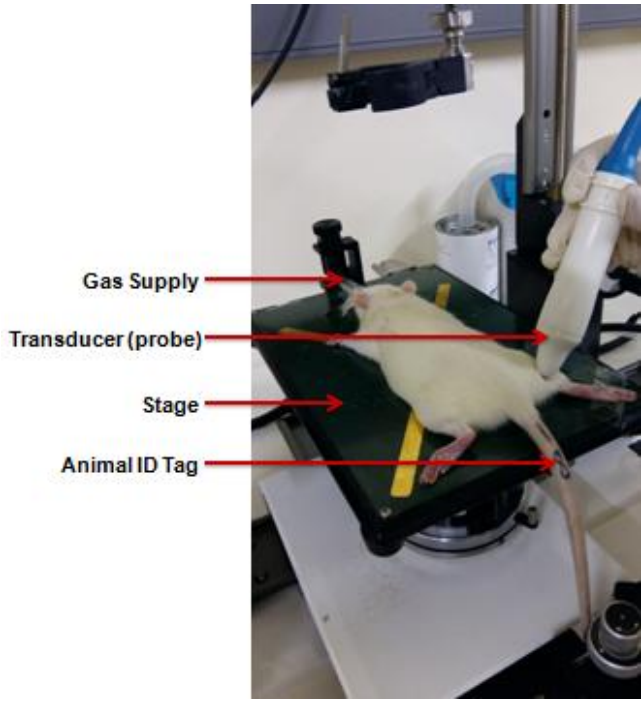

Figure 6.4: Rat undergoing High Frequency Ultra-Sound Imaging.

6.4.8 Blood sampling

Blood was collected from all groups on the specified termination days. A terminal procedure was necessary as a large volume of blood (5-10mL) and muscle tissue were both required. In order to properly detect the drug in the blood, a large volume of blood is needed (Parasuraman et al., 2010). Due to the small size of the animal, the only way in which to obtain a suitable volume is through cardiac puncture. Sodium pentobarbital (200 mg/kg) will be used to euthanize the rats after which cardiac puncture will occur. After withdrawal, blood was collected into 5mL heparinised vacutainers. The samples were then centrifuged at 3000rpm for 20 minutes and plasma was removed, placed into eppendorf tubes and frozen at -80°C until UPLC analysis.

6.4.9 Muscle tissue sampling

Muscle tissue was collected from the test group and placebo group on the specified termination days. Muscle tissue was harvested after blood collection and termination. Muscle tissue was stored in 10% buffered formalin for histopathological analysis.

6.4.10 Quantitative chromatographic determination of drug in plasma and tissue

UPLC was selected as the chromatographic method of choice due to its faster speed, higher resolution and greater sensitivity when compared to HPLC. In addition, UPLC utilises less solvents thereby reducing the cost of analyzation. It is a fitting technique for intricate analysis of pharmaceuticals (Novakova et al., 2006).

6.4.11 UPLC conditions analysis: solvents, mobile phases and parameter conditions for chromatographic separation

UPLC analysis of the blood was accomplished by using a Waters Acquity® UPLC system (Waters, Milford, MA, USA) coupled with a photoiodide array detector (PDA) and Empower® Pro Software (Waters, Milford, MA, USA). The UPLC was fitted with an Acquity® UPLC BEH C18 column, with a particle size of 1.7μm and a pore size of 130Å. The chromatographic conditions implemented were derived from methods outlined by Zhang et al., (2013) and Spivak et al., (2013). The mobile phase consisted of 0.1% formic acid in double deionised water and 0.1% formic acid in methanol (50:50). Drug detection was carried out at a temperature of 40°C. the instrument was primed with 100% methanol, 100% acetonitrile (ACN), a strong wash of 90:10 (ACN:H_2O) and a weak wash of 10:90 (ACN:H_2O). An isocratic method was employed for the separation, identification and quantification of drug with a flow rate of 0.5mL/min, an injection volume of 10μL and a run time of 6 minutes. The PDA detector was set at a wavelength of 262nm for the detection of disulfiram. Diclofenac was selected as the internal standard (IS). All solvents and solutions were filtered prior to use. Experimental procedures were conducted at room temperature (±25°C).

6.4.11.1. *Preparation of diluent and calibration standards*

A solution of 0.1% v/v formic acid in water and 0.1% v/v formic acid in methanol in a ratio of 50:50 v/v was prepared for use as the diluent. Disulfiram and diclofenac primary stock solutions were prepared in ultra-pure double-deionised water (Milli-Q, Millipore, Billerica, MA, USA). The disulfiram stock solution (10μg/mL) was prepared by dissolving 1mg of disulfiram into 100mL of diluent. This was then serially diluted to prepare the working calibration standard solutions at concentrations ranging from 2μg/mL to 10μg/mL.

6.4.11.2 *Sample preparation utilising liquid-liquid extraction*

Liquid-liquid extraction was selected for the extraction of disulfiram. This step is vital due to the high protein binding of exhibited by disulfiram (Johannson, 1990). Frozen blood plasma samples were allowed to thaw. A volume of 500μL of sample was added to a clean eppendorf in combination with 500μL of ACN. This solution was vortexed for 1 minute to facilitate precipitation of the proteins. This mixture was then centrifuged for 10 minutes at 12000RCF (Nison Instrument Ltd, Shanghai, China). The supernatant was withdrawn (500μL) and was filtered through a 0.22μm Millipore® filter into Waters® certified UPLC vials. The filtrate was then spiked with a filtered constant volume of a known concentration of the IS. The vial was vortexed for 1 minute and thereafter placed into the sample holder compartment. This procedure was completed on all samples.

6.4.11.3 *Validation of the liquid-liquid extraction procedure*

Validation of the liquid-phase extraction procedure was completed by calculating the percentage yield of disulfiram (equation 6.2).

$$\%\ \text{yield} = \frac{\text{disulfiram}_{\text{blood}}}{\text{disulfiram}_{\text{mobile phase}}} \times 100 \qquad \textbf{Equation 6.2}$$

To ascertain the percentage yield, 450μL of blank plasma was spike with 50μL of disulfiram-diluent solution (1mg/100mL). this solution was vortexed for 30 seconds and the disulfiram was extracted utilising the extraction method stated in Section 6.2.10.3. For comparison, 450μL of mobile phase (diluent) was spiked with 50μL of disulfiram-diluent solution and the yield was calculated from the values for the two mixtures.

Intra-day and inter-day variability of the extraction procedure was also established. These reproducibility tests elucidate the accuracy and precision of the extraction process. The procedure outlined in Section 6.2.10.3 is repeated on 3 consecutive days to allow for inter-day validation as well as 3 samples spread out during a 24 hour period to allow for intra-day variability. The precision variability was calculated with the percentage Relative Standard Deviation (RSD) according to the following equation:

$$\%\ \text{RSD} = \frac{\text{Standard Deviation}}{\text{Mean}} \times 100 \qquad \textbf{Equation 6.3}$$

6.4.11.4 *Construction of a calibration curve for the quantification of disulfiram in blood plasma*

Blank, thawed plasma samples (450μL) were spiked with differing concentrations of disulfiram-diluent solution (50μL). Samples were vortexed and the extraction protocol mentioned in Section 6.2.10.3 was carried out on the samples. A standard volume of IS (500μL) was also added and UPLC was run on the samples. The disulfiram/IS peak area ratios were plotted against the corresponding disulfiram concentration (μg/mL) in order to generate a calibration curve.

6.4.12 Histomorphological analysis of muscle tissue post-IM injection

Histopathological tests were conducted in order to ascertain any abnormal or toxic effects that may have occurred as a result of the NEGC. Excised rat muscle tissue was fixed with 10% normal buffered formalin. Samples were submitted to Idexx Laboratories for

histomorphological analysis. Samples from each time point (test group and placebo group) were submitted as well as a healthy, normal muscle sample to serve as a control. Sections from the central area of the biopsy were subjected to routine histological tissue processing in an automated tissue processor (in accordance with Idexx SOP's). Thereafter slides were prepared from cut sections (5-6μm) and stained with Haematoxylin and Eosin tissue stainer. Thereafter, histological evaluation was carried out.

The sections were graded according to the following criteria:
1. the presence of haemorrhage, fibrin and oedema
2. hyaline degeneration of the muscle fibres
3. fragmentation of the muscle fibres
4. the presence of inflammation
5. the presence and degree of fibrosis
6. the presence and quantity of amorphous substance

6.4.13 *In vivo* myotoxicity study

Blood samples from the placebo and test group from the first 24 hours were centrifuged and the plasma frozen for quantitative determination of CK. CK is a useful biochemical marker of muscle injury or damage (Brancacchio et al., 2010). This is significant as it can provide information on the toxicity of the NEGC *in vivo*. CK must be tested within the first 6 hours after administration as beyond this time frame the CK levels return to baseline after which CK cannot be used as a marker for myotoxicity (Rungseevijitprapa et al., 2008).

6.5 Results and Discussion

6.5.1 High frequency ultra sound imaging

High Frequency Ultra Sound Imaging was carried out immediately after IM administration as well as at 1 hour, 2 hours, 4 hours, 6 hours, 24 hours, 2 days, 3 days, 7 days, 14 days, 21 days and 28 days post administration. Imaging was conducted in order to visualise the gel in the muscle tissue in order to confirm its presence and to determine if it is able to remain in the muscle for a long duration of time.

Efficacy of drugs and delivery systems can be evaluated using small animal high frequency ultra sound imaging (Shung, 2009). Small pulses of ultrasound echo are transmitted from the transducer into the body. Body tissue and the NEGC have different acoustic impedances. As the ultrasound waves penetrate the area, some waves travel deeper in whilst others reflect back to the transducer. These echo signals are transformed to develop an Image. A

mismatch in acoustic impedance between two mediums results in the generation of a reflected echo which in turn allows image generation (Chan and Perlas, 2011).

As can be seen in Figures 6.5a - 6.5j the NEGC is visible throughout the study right up to day 28 in both, the test group and placebo group. Thus the gel has the ability to be retained at the site of administration for a long period of time. This observation is in accordance with the previous reports of these polymers to maintain long-term treatment. The ultrasound images at the various time points are displayed in Figures 6.10a to 6.10j. The echogenicity of the NEGC differs to that of normal muscle fibres and this is evident in Figure 6.11. Healthy muscle fibres can be seen in the rat and they are differentiated from the gel by their appearance. Healthy muscle displays pronounced striations whereas the gel displays a blurry, continuous mass as can be seen in Figure 6.6. The healthy portion is circled in green and the gel is circled in red. The former images all display the echogenic pattern of the NEGC.

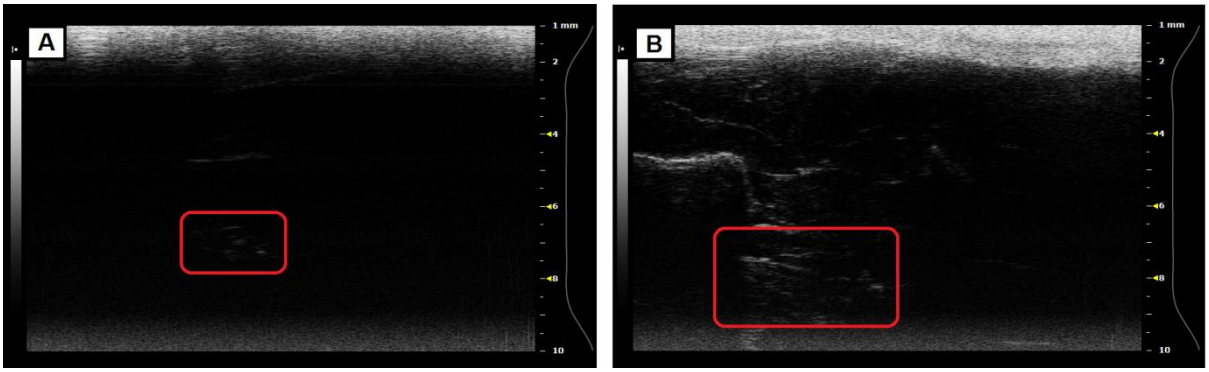

Figure 6.5a: NEGC in placebo (left) and test group (right) at 1 hour after administration.

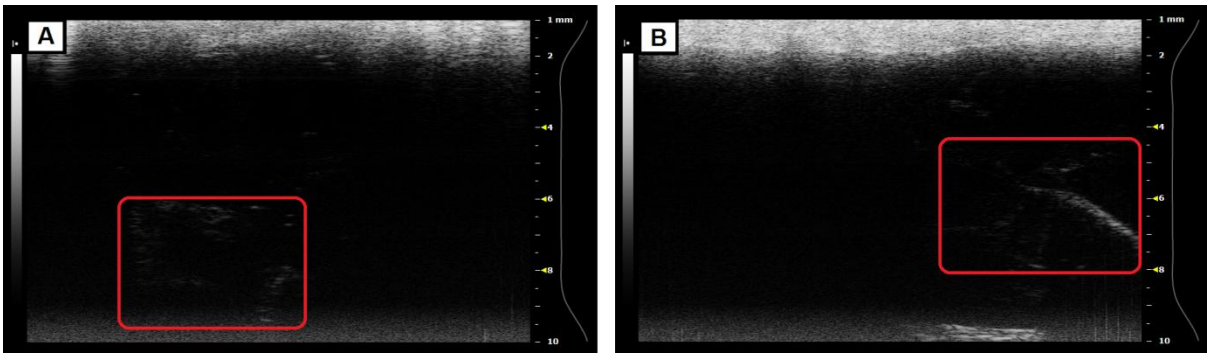

Figure 6.5b: NEGC in placebo (left) and test group (right) at 2 hour after administration.

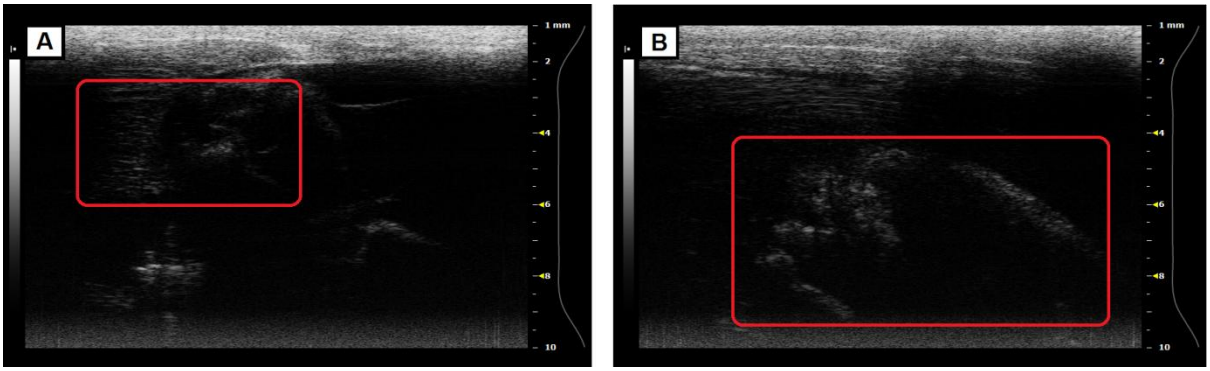

Figure 6.5c: NEGC in placebo (left) and test group (right) at 6 hour after administration.

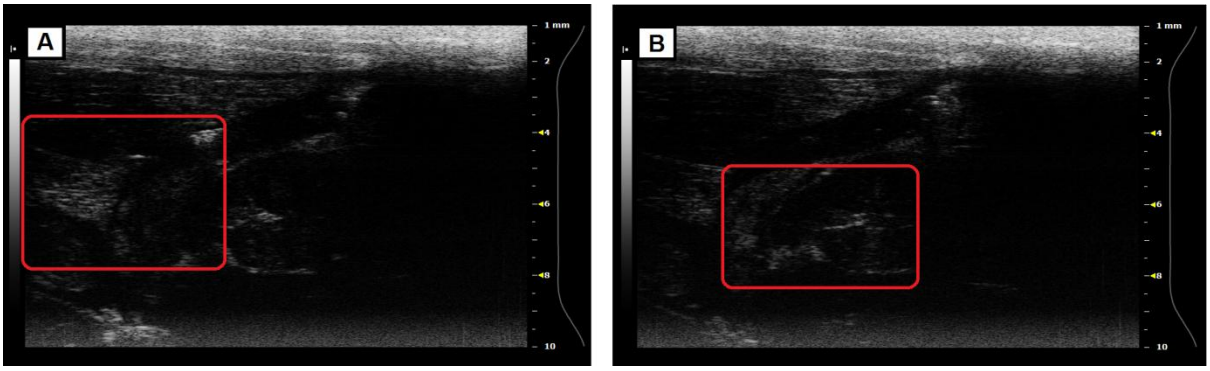

Figure 6.5d: NEGC in placebo (left) and test group (right) at 24 hour after administration.

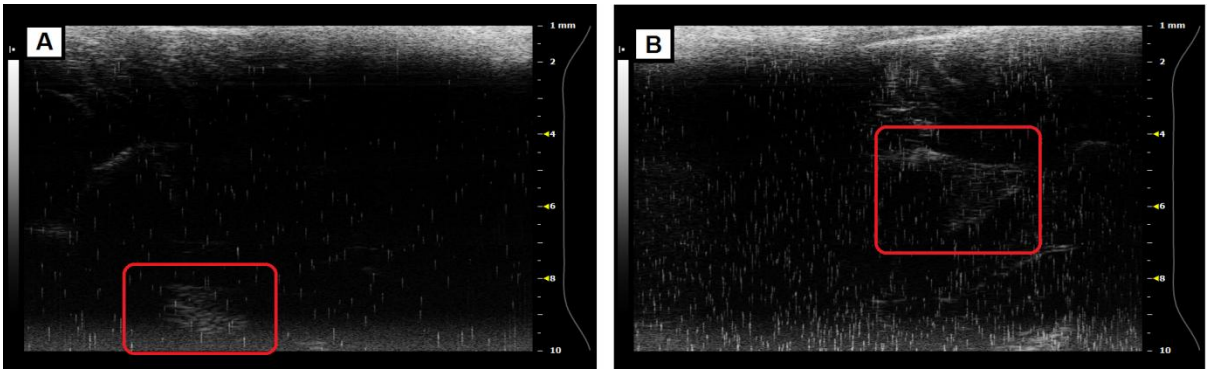

Figure 6.5e: NEGC in placebo (left) and test group (right) at 2 days after administration.

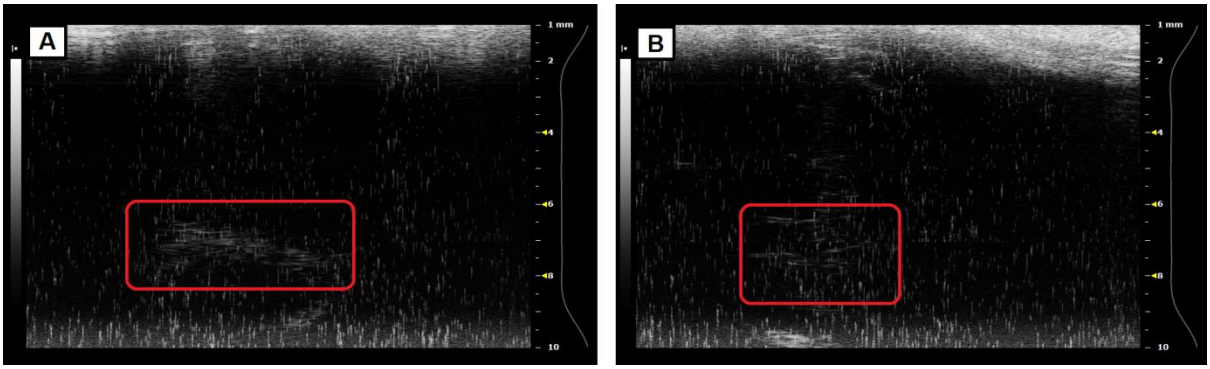

Figure 6.5f: NEGC in placebo (left) and test group (right) at 3 days after administration.

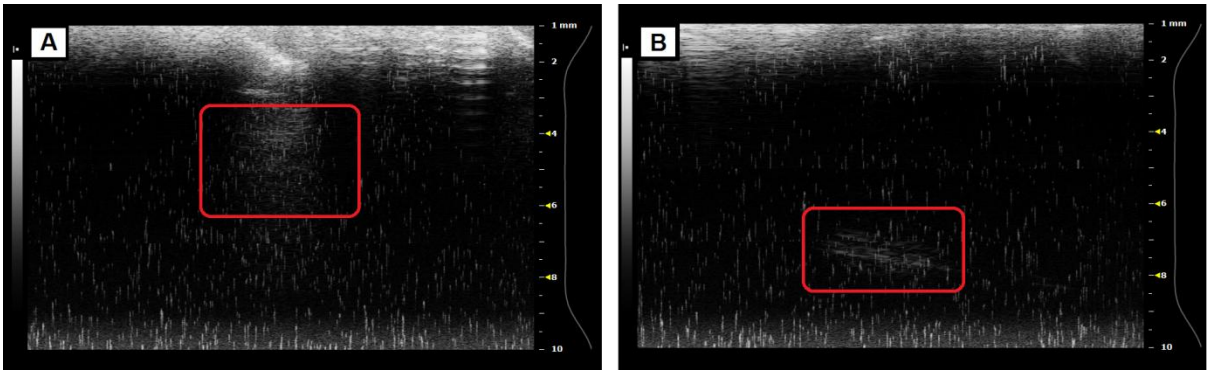

Figure 6.5g: NEGC in placebo (left) and test group (right) at 7 days after administration.

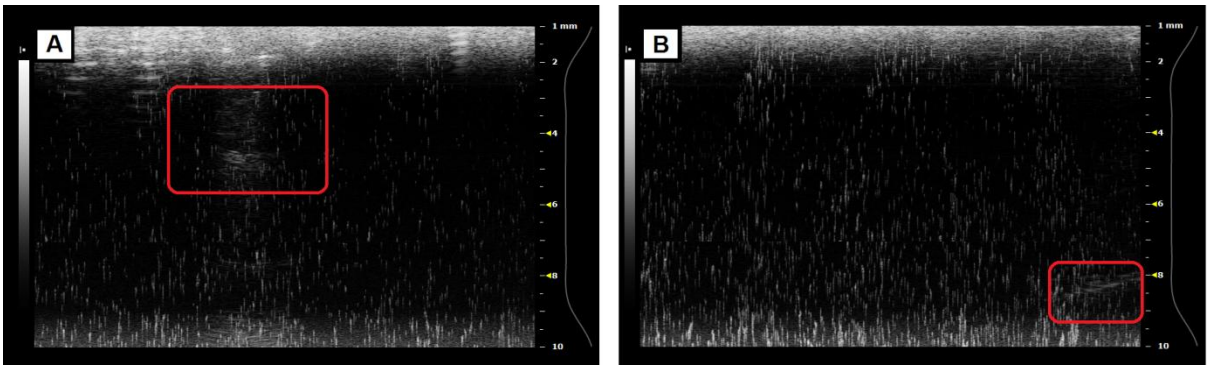

Figure 6.5h: NEGC in placebo (left) and test group (right) at 14 days after administration.

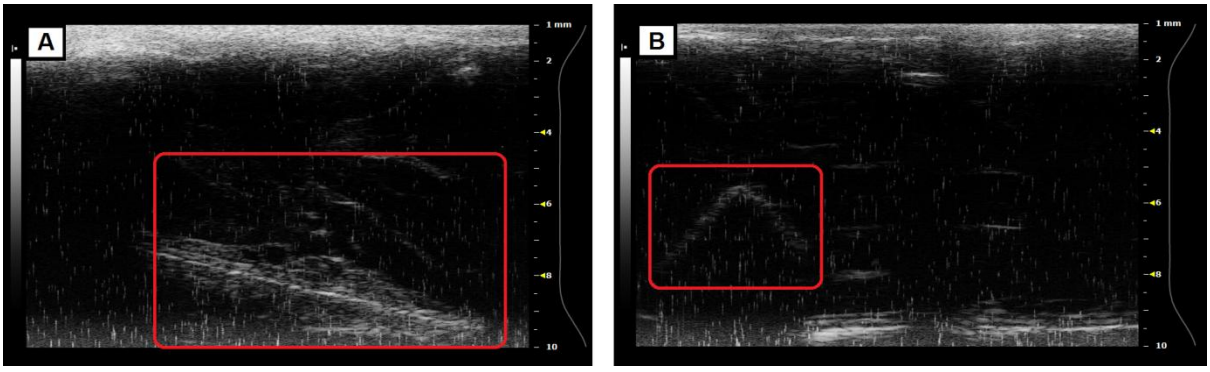

Figure 6.5i: NEGC in placebo (left) and test group (right) at 21 days after administration.

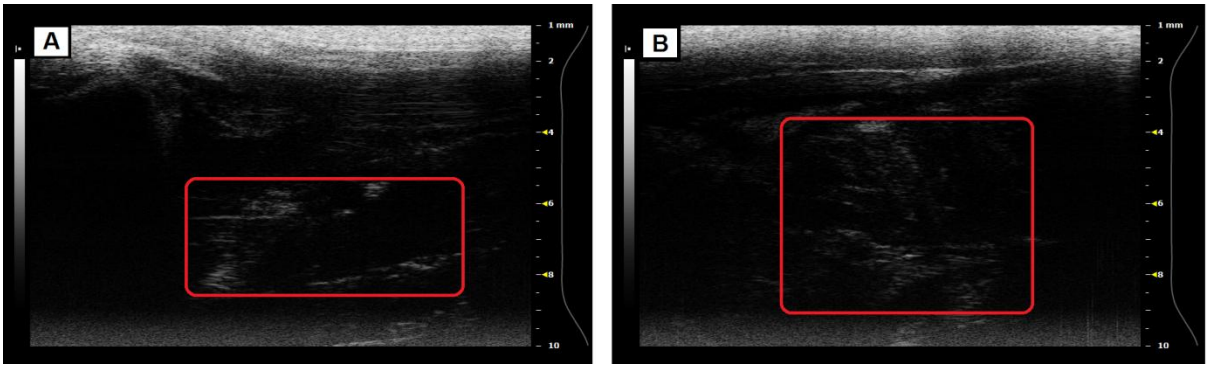

Figure 6.5j: NEGC in placebo (left) and test group (right) at 28 days after administration.

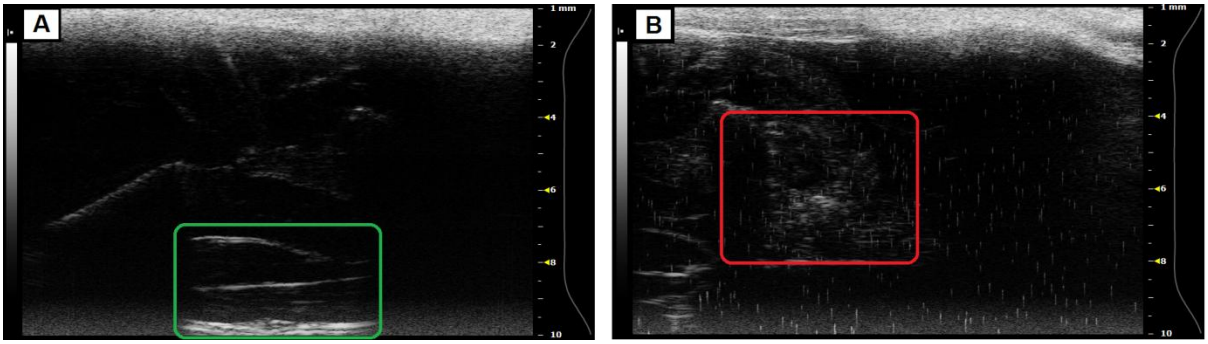

Figure 6.6: Ultrasound images displaying healthy muscle fibres (left) and the *in situ* gel system (right).

Confirmation of the results of Vevo imaging can be seen in Figure 6.7 which was taken after euthanisation and prior to muscle harvesting on day 28. The image depicts the *in situ* gel visible in the rat muscle.



Figure 6.7: Digital photograph displaying the presence of the *in situ* gel in the rat muscle (circled in red).

6.5.2 Validation of the liquid-liquid extraction procedure

In order to validate the extraction procedure and establish intra-day and inter-day variability the percentage yield of disulfiram and the co-efficient of variation was calculated respectively. The percentage yield of disulfiram in plasma was computed to be 92.55% when compared to the spiked mobile phase. The high percentage yield is indicative of the effectiveness of the applied liquid-liquid extraction protocol. The RSD% for intra-day and inter-day variability were 4.69% and 2.10% respectively. Low variability percentages typically represent high reproducibility of the extraction procedure. These findings are suggestive of a valid method for liquid-phase extraction.

6.5.3 Elution times of disulfiram and internal standard

Inspection of the chromatograms displayed elution time peaks at 0.67 minutes for disulfiram and 1.37 minutes for the IS. In order to authenticate the elution times blank plasma was spiked with disulfiram and IS separately and in combination. These were all subjected to the same extraction procedure outlined in Section 6.3.12.2 and analysed. The elution times of the individual chromatograms were mutually related to the chromatogram of the combined elution times. The IS had a reasonably short retention time. The IS drug itself did not interact with disulfiram neither did its retention peak interact with that of disulfiram. The drug had good recovery through extraction and was stable. These factors made it a practically suitable IS (Zhang et al., 2013). The 2D plot and related 3D PDA plot for disulfiram and IS combined in plasma is reflected in Figure 6.8a-6.8b.

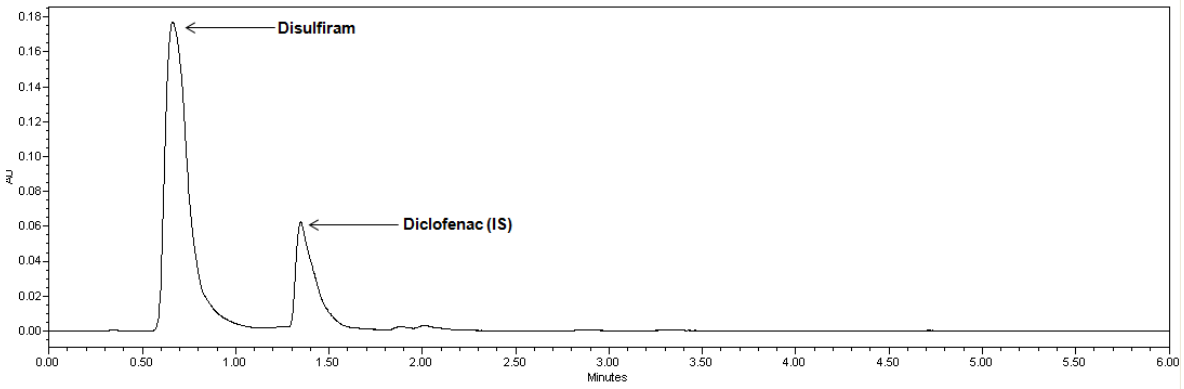

Figure 6.8a: 2D chromatogram plot of disulfiram (left peak) and diclofenac (right peak).

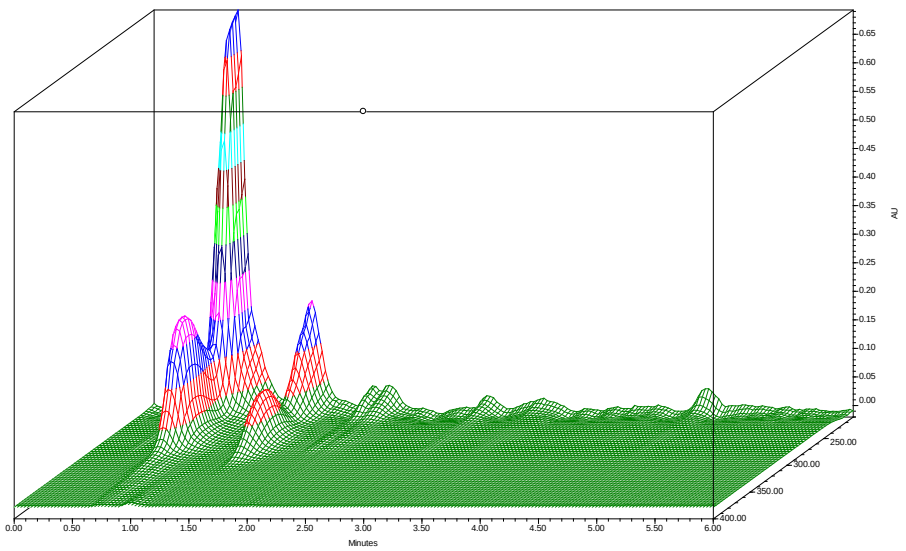

Figure 6.8b: 3D PDA plot of disulfiram (left peak) and diclofenac (right peak).

Assessment of the above facets provided affirmation of the success of the chromatographic method employed.

6.5.4 A calibration curve for the quantification of disulfiram concentration in plasma

A calibration curve was plotted for use in the quantification of disulfiram in plasma samples. The curve is shown in Figure 6.9. The ratio of the area under the curve of disulfiram to that of diclofenac was calculated and plotted against concentration (µg/mL). The good linearity of the curve (R^2 of 0.986) corroborates the use of the calibration curve for the determination of disulfiram plasma levels.

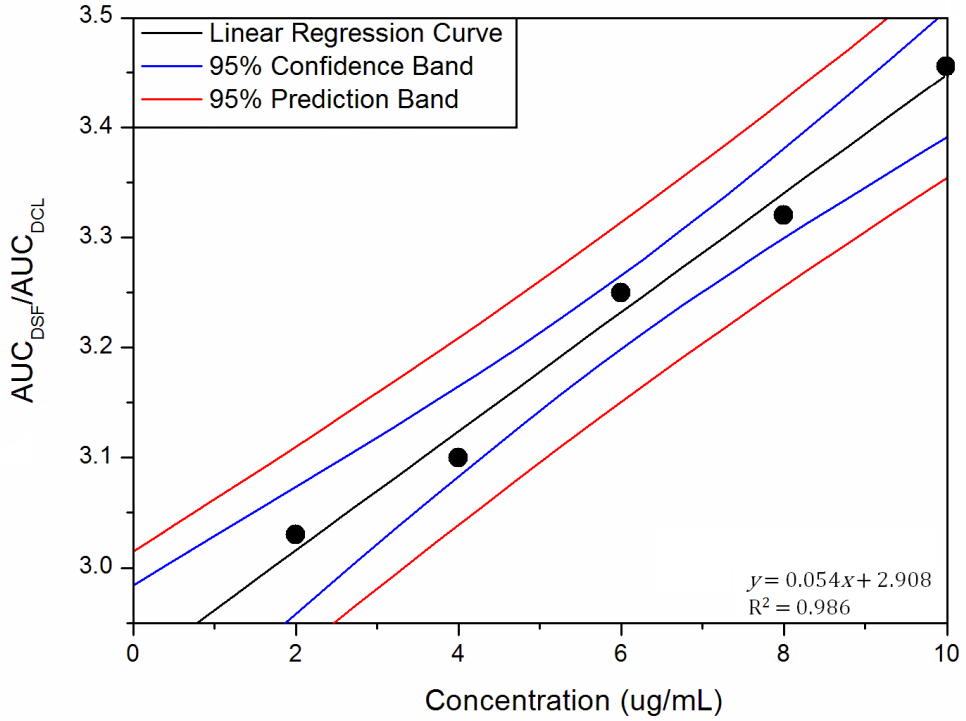

Figure 6.9: UPLC calibration curve of known plasma disulfiram concentrations.

6.5.5 *In vivo* profiles of the comparison group, test group and placebo group

The mean plasma concentrations for the comparison group, test group and placebo group are displayed in Figure 6.10.

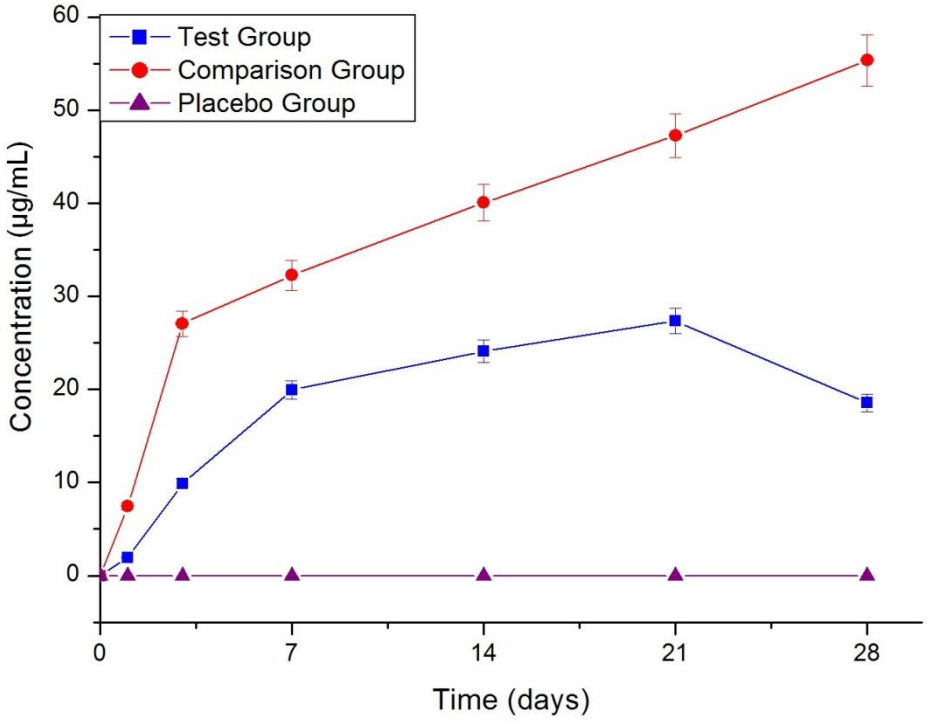

Figure 6.10: *In vivo* disulfiram profiles of the various groups tested.

The placebo group does not contain any disulfiram thus no disulfiram was present in the plasma. This is evident from the placebo group chromatogram (Figure 6.11). The comparison group which received the disulfiram-loaded peanut butter ball daily displayed an increase in plasma concentration. This can be explained by the $t_{½}$ of disulfiram which is 60-120 hours. It is evident that the rate of release into plasma is greater than the excretion rate thereby resulting in increased plasma levels. The release from the NEGC (test group) displays a typical sustained release profile with peak levels of disulfiram (27.33µg/mL) being reached in 21 days. The SD for the test group and comparison group were ≤0.95 and 1.86 respectively. The levels of disulfiram in blood from the NEGC were lower than the oral dose. No fluctuations in disulfiram release were observed.

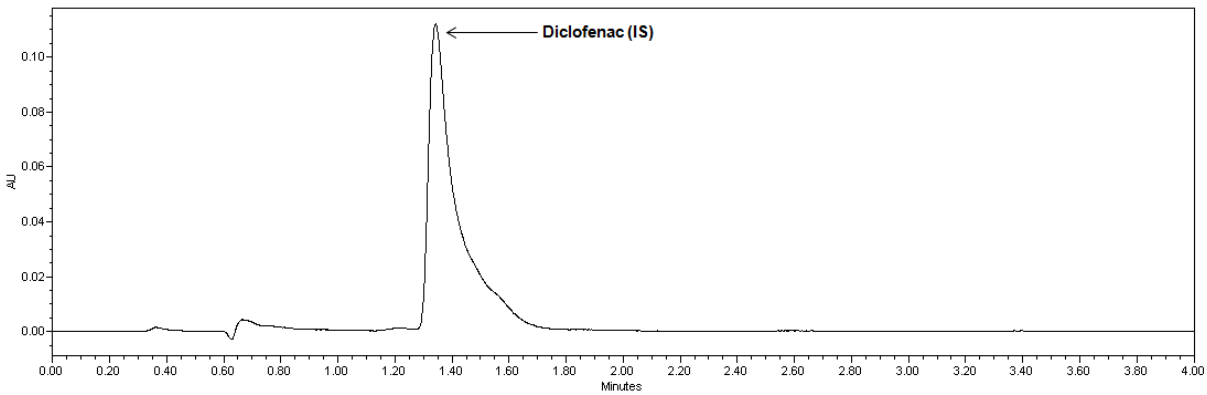

Figure 6.11: Chromatogram of placebo group showing peak for IS only.

Taking into consideration the many challenges that researchers have faced over the years with this peculiar drug; the ability to detect disulfiram in plasma with minimal variation is an astonishing conclusion. In order to put this into perspective, below is an account of the various tests conducted and the outcomes of each.

One of the initial attempts to overcome the poor compliance associated with oral disulfiram was a subcutaneous implant of sterile tablets. The effect of these was referred to as a 'potent placebo' as the release was inadequate to trigger a pharmacological outcome (Phillips et al., 1992).

In 1992, Phillips and co-workers explored the effect of two disulfiram depots: 1) disulfiram in saline with 5% methylcellulose and 2) disulfiram in saline with 0.1% polysorbate as well as oral disulfiram. The effect of these formulations in response to ethanol challenges was investigated. Formulation 1 displayed irregular responses to alcohol challenges. The DER elicited had low subjective intensity. Additionally, the formulation was difficult to inject as it was too viscous resulting in local irritation. Disulfiram and its metabolites could not be detected in the serum by HPLC assay. Thus only carbon disulfide and clinical effects of the DER were measured. The second formulation was more favourable due to the combination of the oral dose as well as the depot. The oral loading dose caused high rapid induction of enzyme (ALDH) inhibition and thereafter the depot disulfiram maintained the enzyme inhibition. Hellstrom and colleagues (1983) examined the ability of 1g of disulfiram to inhibit ALDH activity *in vitro* as well as if disulfiram is able to inhibit blood ALDH in humans. The results from the study indicated that the disulfiram released was too little to affect the ALDH activity.

Early studies concluded that the best method for detecting disulfiram *in vivo* is the carbon disulfide breath test and possibly blood levels depending on the development of improved methods of detecting plasma levels in order to establish compliance (Rogers et al., 1978). However, it was then stated that carbon disulfide excretion has limited reliability for accurate investigation of disulfiram metabolism due to the metabolic alteration it undergoes *in vivo* (Neiderhiser and Fuller, 1980).

A vast number of the studies conducted have focused on the determination of acetaldehyde in the blood or inhibition of ALDH (Tottmar et al., 1978; Helstrom and Tottmar, 1982; Helander and Tottmar, 1987; Lipsky et al., 2001) or on the clinical manifestations of the DER (Jensen and Faiman, 1984). Whilst some have concentrated on the metabolites of disulfiram and not on the parent compound itself (Madan and Faiman, 1994; Hoichreiter et al., 2012).

The reason for this is the claim that disulfiram is rapidly metabolised thus detection of disulfiram in plasma yields varying results. In spite of this allegation, recent studies have successfully proven otherwise (Saracino et al., 2010; Spivak et al., 2013; Zhang et al., 2013).

Saracino and partners (2010) evaluated the level of disulfiram and bupropion in plasma. Disulfiram was detected in plasma at a low concentration of 13.4ng/mL. the study proved to be successful for the determination of both drugs (even at low concentrations) in the plasma of alcohol and nicotine abusers.

Spivak and co-workers (2013) developed a UPLC-MS method for the quantification of disulfiram in plasma. Subjects were given 500mg of disulfiram orally for 14 days and plasma concentration was detectable in a number of the subjects. A sensitive, reliable and quick UPLC-MS method of measuring plasma levels of disulfiram in rats was devised by Zhang and researchers (2013). They were successful in determination of orally administered disulfiram in plasma despite variability in the results. The reason behind this is not known but may be alluded to the high lipid solubility of disulfiram. However intravenous injection of disulfiram-lipid microspheres produced higher average plasma levels as well as a reduction in individual variability. As is evident from the plasma profiles of the NEGC variability in the data is minimal. Further advantages of employing a parenteral formulation is that it removes the powerful effect of first pass metabolism as well as the hydrolysis of disulfiram in gastric fluid (Zhang et al., 2013). This favourable outcome of Zhang and co-workers (2013) reiterates the hypothesis that the delivery system employed can foster enhanced properties. Jensen and Faiman (1980) were also successful in detecting disulfiram in the blood and other biological fluids utilising HPLC.

Individual variability in disulfiram pharmacokinetics was also reported in other studies as well. The mechanism of this is not known but it was suggested that higher doses of disulfiram could be more effective (Spivak et al., 2013). Johnsen and Morland (1992) conducted a study on depot preparations of 1g disulfiram subcutaneously. Acetaldehyde concentration after IV and oral ethanol administration, inhibition of blood ALDH activity and blood acetone were measured. They hypothesised that an immediate, intense and reliable aversive acetaldehyde accumulation is necessary to deter drinking. The implant failed to exhibit any pharmacological effect. Pulse rate, blood pressure, ECG and flushing did not show any noteworthy changes when compared to baseline values. Acetaldehyde levels were not higher than levels pre-implantation. Subjective complaints were also not significant. The concentration of acetaldehyde in the blood and breath were similar in alcoholics and healthy

volunteers with disulfiram or placebo implants. However, consumption of alcohol did decrease in test and placebo groups thereby indicating that the mere threat of a DER can deter drinking even if the dose of disulfiram is too low to elicit an actual response.

The potential of disulfiram as a sustained release system has been analysed by Phillips and Gresser (1984). Solid rods of 80% poly (glycolic-co-L-lactic-acid) and 20% ^{14}C-labelled disulfiram were implanted subcutaneously into Wistar rats. The control group received 100mg of ^{14}C-labelled disulfiram subcutaneously. The system did not exhibit any local or systemic toxicity thus supporting the data obtained in the present study. The system had clinical promise as the performance mimicked a true sustained release system.

Wound complications due to subcutaneous implantation have negatively influenced the efficacy of these implants (Sezgin et al., 2014). Additionally, in some cases, implant extrusion occurred. A further limiting factor of subcutaneous implant of disulfiram tablets is the incomplete absorption of these despite implantation occurring one year before. Implants given in the sub-scapular IM plane did not reveal any implant exposure as the location is out of reach. Additionally, healing was uneventful. As a result, implants may still be a highly chosen treatment alternative for alcohol abuse.

The effectiveness of implants is uncertain. Wilson and co-workers (1976, 1978, 1980, 1984) conducted various studies which supported both the psychological deterring effect of disulfiram as well as the pharmacological effects of it. However, shortcomings in the study designs render these findings of the efficacy of disulfiram implants inconclusive. Other studies (Hughes and Cook, 1997) also reported that the effect of disulfiram is primarily psychological and that poor pharmacological action is due to insignificant disulfiram absorption or insufficient disulfiram being released.

The minimum level of DF from the NEGC in the plasma is 1.94ng/mL and the maximum is 27.33μg/mL. These values are above-par according to the reported minimum therapeutic range of 0.05μg/mL-0.4μg/mL (Saracino et al., 2010). Withal, disulfiram irreversibly binds to ALDH (Lipsky et al., 2001). It takes 2 weeks to synthesize unbound enzyme which is capable of metabolising alcohol (Suh et al., 2006). Thus the effect of disulfiram can extend beyond its disappearance from plasma. From the above it is evident that the detection of disulfiram in plasma is a significant achievement.

It is evident from the above that the results from the *in vivo* study have provided beneficial and conclusive data. The detection of disulfiram in plasma with minimal variability is a promising outcome.

6.5.6 *In vivo* myotoxicity

The functional status of muscle tissue can be determined through serum levels of skeletal muscle enzymes. This is based on the fact that these levels fluctuate broadly in physiological versus pathological conditions thus making them effective markers of muscle injury. An elevation in the enzyme levels is representative of cellular necrosis or tissue damage due to muscle injury. In addition to CK increase due to surgical procedures, myopathies and sports-related injuries, serum CK can also rise due to IM injections where the magnitude of CK increase is proportional to the volume of injection (Brancacchio et al., 2010).

The normal CK upper limit was determined from healthy rats to be 678μ/L (SD ≤ 1.99, n=3) which is in agreement with the study by Marshall and co-workers (2010) who reported the normal range of CK in Sprague Dawley rats to be 87-784μ/L.

The placebo group showed normal levels of CK at 2 hours, thereafter CK increased at 2-4 hours and then decreased to values within the normal range. The test group showed increasing values above normal from 2-6 hours after which the values decreased to the normal range. These findings indicate that permanent damage was not present due to the ability of CK to return to baseline within 24 hours. Furthermore, an increase in enzyme activity can be attribute to the test preparation itself without constitutive muscle damage (Surber and Sucker, 1987). The test group had higher levels of CK than the placebo group. This indicates that the elevation can associated with the therapeutic agent (Brazeau and Fung, 1989). Figure 6.12 illustrates the CK levels of both groups.

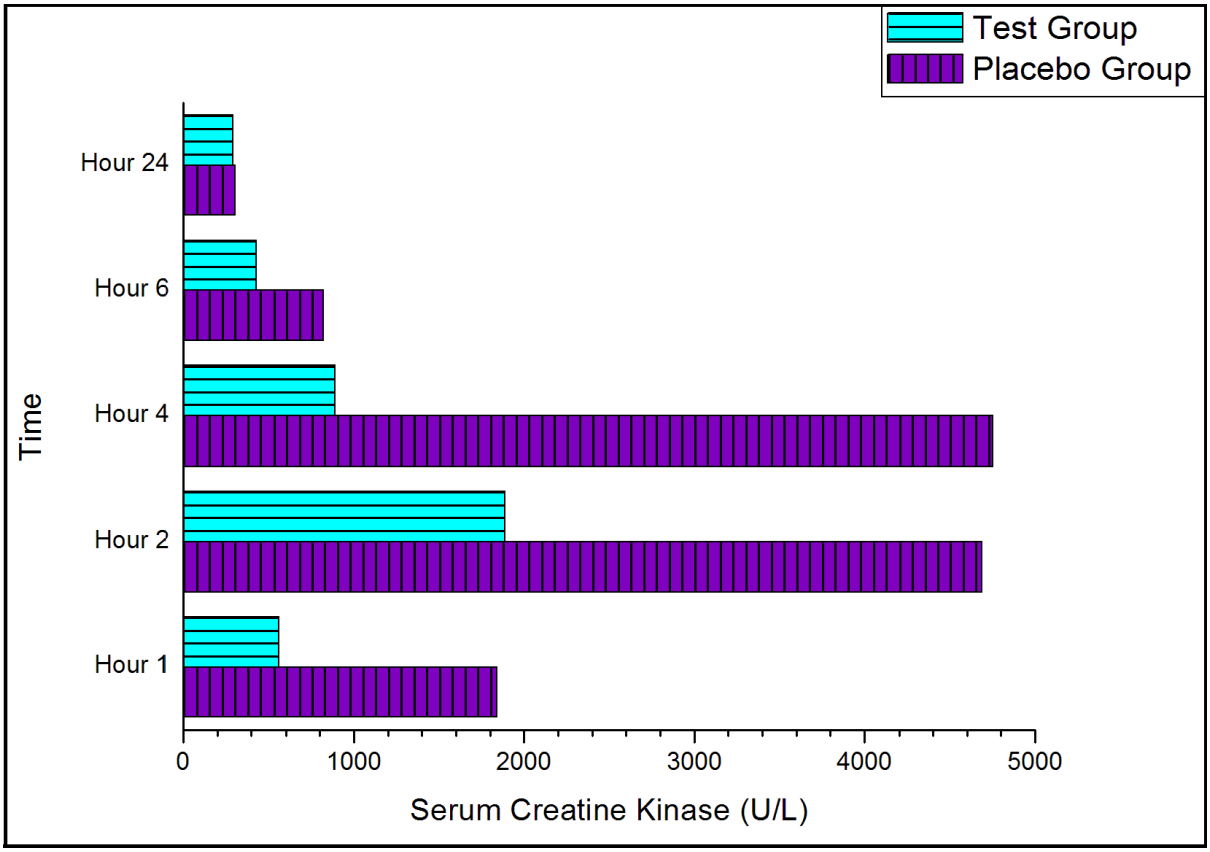

Figure 6.12: *In vivo* CK levels for the test group and placebo group.

The results obtained are in accordance with those reported by Brazeau and Fung (1989) and Rungseevijitprapa and co-workers (2008). Brazeau and Fung witnessed low CK release up to 2 hours and a marked increase within 2-4 hours. Rungseevijitprapa et al., observed that peak levels occurred around 2 hours and returned to normal 6 hours post-injection. After 6 hours there was no further increase in CK up to 24 hours.

Skeletal muscle has a close association with the nervous, vascular and immune systems which may be instrumental in the toxicity produced from IM preparations. By determining the myotoxicity *in vivo* these systems remain intact. Thus the *in vivo* study will provide a complete picture as these factors will be accounted for in the results (Rungseevijitprapa et al., 2008).

6.5.7 Histopathological evaluation of muscle tissue

In addition to elevated CK circulation levels, histological evaluation of muscle tissue can also be utilised to preclude myotoxicity. Results obtained from serological biomarkers must be accompanied by histopathologic evaluation in order to confirm the findings. This is necessary as markers may possess inadequate sensitivity and specificity especially in rats (Vassallo et al., 2009). The presence of considerable intrinsic fluctuations as well as

differences in CK at baseline and formulation and/or active induced levels can lead to in varied results. This categorises serological biomarkers as adjuncts to histopathology due to their limitation as accurate indicators of skeletal muscle toxicity (Vassallo et al., 2009). Histopathological changes at the site of injection are therefore crucial in establishing the safety of the delivery system.

Comparison of histopathology results from the test group and the placebo group yielded no significant differences thereby attesting to the fact that the active compound itself is not solely responsible for any histopathological changes present. The test group did not display any toxicity within the first hour. Histopathological alterations occurred from hour 2 to day 7 after which the levels dropped. The placebo group showed changes between day 1 and day 7 after which levels dropped.

At 1 hour no microscopic pathology was detected in the test group whilst in the placebo group minimal oedema and hyaline degeneration occurred and a mild increase in extravascular mast cells was seen. An infiltration of amorphous substance was also seen in the perimysium between muscle fibres.

At hour 2 the test group displayed minimal haemorrhage oedema, myofibre fragmentation and inflammation characterized by macrophages and neutrophils. The placebo group showed mild oedema in the perimysium and surrounding peripheral nerves and minimal hyaline degradation of scattered fibres.

At 4 hours mild haemorrhage and oedema was noted in the interstitium and perimysium of the test group along with a moderate inflammatory reaction. The placebo group displayed mild oedema and minimal neutrophil-inflammation along the perimysium. Hyaline degeneration was minimal.

At 6 hours no microscopic pathology was detected in the placebo group. The test group showed mild-moderate oedema with minimal fibrin deposition. Neutrophil and macrophage inflammation and myofibre fragmentation was moderate.

On day 1 oedema, fibrin deposition, fragmentation and inflammation were mild in the test group and in the placebo group.

On day 2 minimal oedema was noted with an increase in inflammation in the test group whilst in the placebo group oedema and inflammation were moderate.

On day 3 the test and placebo groups showed moderate fibrin deposition and mild oedema with increased inflammation. Myofibre degeneration was minimal in the test group and mild in the placebo group.

On day 7 moderate inflammation and oedema with minimal fibrosis and mild fragmentation was observed in the test group. The placebo group was the same except for the fibrosis, which was moderate, and the absence of fragmentation.

On day 14 no fragmentation occurred whilst inflammation remained moderate in the test group. Inflammation is moderately present in the placebo group. Both specimens showed a marked decrease in histopathological changes from day 7 to day 14.

On day 21 only minimal fibrosis and an area of mild macrophage infiltration was present in the test group. The placebo group showed moderate fibrosis and inflammation and minimal degeneration.

On day 28 inflammation, degeneration, fibrosis and fragmentation were mild in the test group whilst the placebo group remained the same as it was on day 21.

The decline in the severity of the histopathological lesions is indicative of acute toxicity and mild muscle tissue injury. Changes which were most evident include inflammation and fragmentation which are consistent with the changes expected for injury and repair in response to needle insertion into muscle tissue (Sluka et al., 2001). The minimal haemorrhage observed is attributed to administration technique as it is possible for slight bleeding to occur due to rapid administration of the formulation (Thuilliez et al., 2009). Histological images of a healthy muscle tissue and tissue with minimal, mild and moderate histopathological lesions are displayed in Figures 6.13a-6.13d.

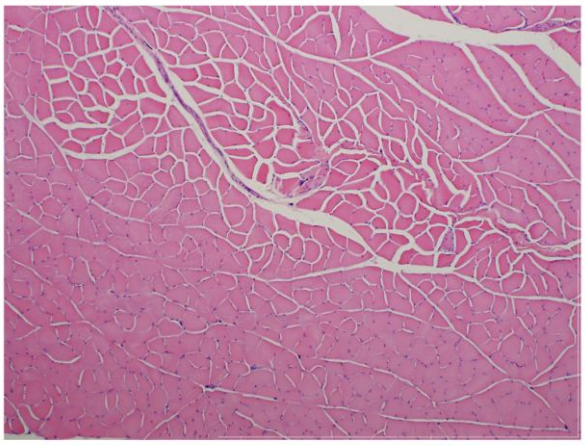

Figure 6.13a: Light microscopy histological image of healthy muscle tissue.

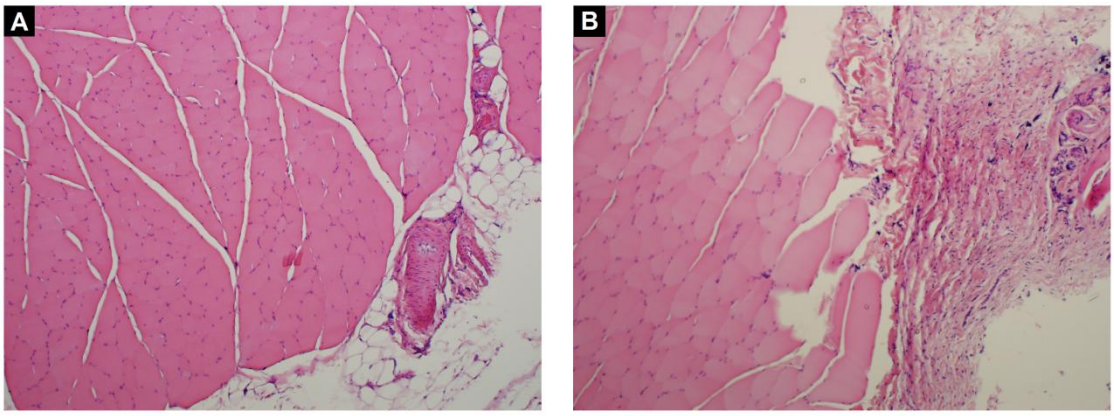

Figure 6.13b: Light microscopy histological image of muscle tissue with minimal histopathological lesions (A: test group, B: placebo group).

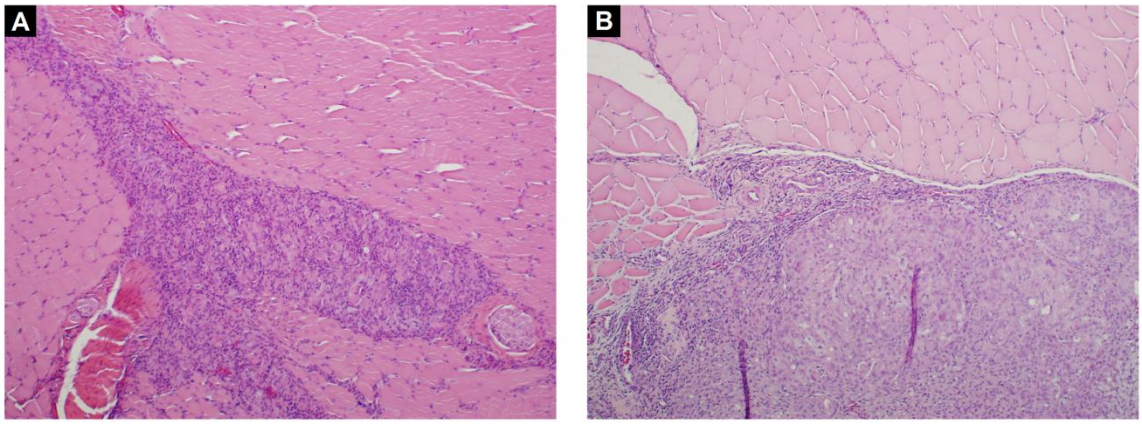

Figure 6.13c: Light microscopy histological image of muscle tissue with mild histopathological lesions (A: test group, B: placebo group).

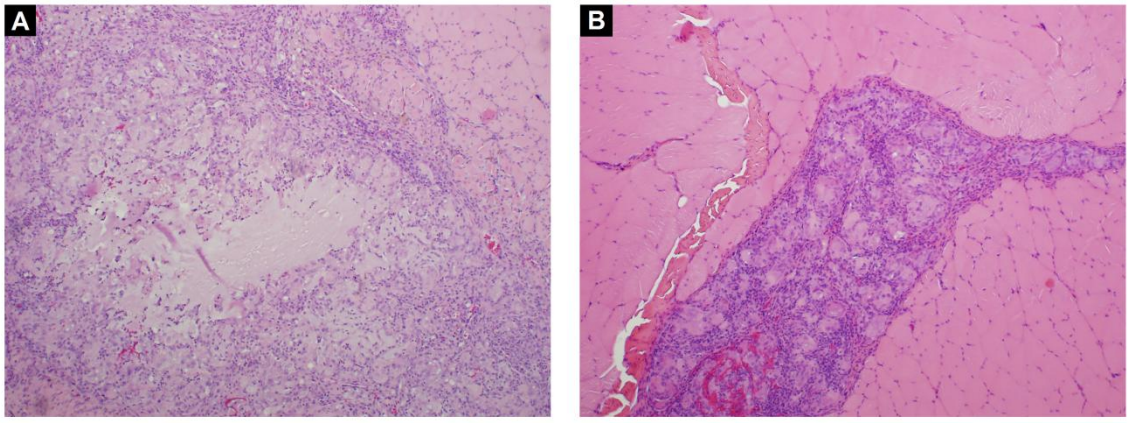

Figure 6.13d: Light microscopy histological image of muscle tissue with moderate histopathological lesions (A: test group, B: placebo group).

Components of the delivery system were sterilised prior to administration and needles and syringes employed were extracted from sterile, sealed packaging. Thus it is improbable that the results are on account of pathogenic contamination (Thuilliez et al., 2009). Factors that may be culpable of acute local damage include drug concentration, injected volume, vehicle type and pH (Thuilliez et al., 2009). The most likely explanation is the natural immune and inflammatory response due to the introduction of a significant volume of foreign matter into a small area.

Rats were monitored daily in order to ascertain the effect of the IM on their behaviour. A few rats from both groups were observed to have a slight limp for 24 hours post administration. This disappeared after 24 hours. All rats displayed signs of good health and no physical discomfort was noticed throughout the study.

All components have been used parenterally without any alarming reports. Vitamin E has been administered IM to humans (Feranchak et al., 1999) whilst TPGS has also been administered parenterally to mice with success (Baert et al., 2009). It also has a good safety profile as a dermal system (Aggarwal et al., 2012). Injectable formulations of GG were investigated by Oliviera et al., (2009, 2010) and results indicated a normal inflammatory response and good tissue intergration (Oliveira et al., 2009). Disulfiram has been used parenterally in humans and rats previously (Johnsen and Morlen, 1992; Sezgin et al., 2014). Additionally single and multiple IM injections of PF127 did not demonstrate any myotoxic potential (Liu et al., 2007).

6.6 Concluding Remarks

Part I of this chapter investigated the ability of the NEGC to release disulfiram into the excised muscle tissue and the myotoxicity of the NEGC *ex vivo*. The *ex vivo* drug release test proved that the NEGC is capable of releasing drug into the muscle whilst the myotoxicity test yielded negligible results. Part II, the *in vivo* examination, consisted of toxicity investigations, the efficacy of the NEGC to deliver disulfiram and the ability to detect disulfiram in plasma. The disease state (i.e. alcoholism/alcohol administration) was absent due to ethical considerations as well as for affirmation of the functionality of the NEGC which is to deliver disulfiram in a depot form and detect its presence in the plasma.

A UPLC method for the quantification of disulfiram in plasma was successfully developed. Disulfiram was detected in the plasma and the release profile matched that which is expected from a sustained release preparation. Although levels were lower from the NEGC compared to the oral group, the level was within the minimum therapeutic range. The determination of plasma concentrations has a double benefit. Not only does it confirm the effectual functioning of the delivery system and validation of the quantification method, it is also a recognised method of determining bioequivalence. A successful and widely used biomarker to determine bioequivalence is comparison of test and reference plasma profiles (Polli, 2008). This was also achieved in this study.

Ultra sound imaging comprised the confirmation of the formation of a solid gel depot that lasted for the entire 28 days of the study. Myotoxicity and histopathology results revealed mild toxicity and acute injury both of which are normal responses to intramuscular administration.

The *in vivo* analysis NEGC brings to light the therapeutic potential of this system. Fortuitously, the animal model utilised does display predictive validity. This implies that medications which are effective in the animal model are effective in humans too (Tabakoff and Hoffman, 2000). Thus it stands to reason that the results from the *in vivo* study can enable representational clinical forecasting.

CHAPTER 7
CONCLUSION AND RECOMMENDATIONS

7.1 Conclusion

Alcohol addiction is a chronic illness whereby the mind and body become dependent on alcohol. The recurrent usage of such substances affects the brain reward pathway as well as other related functions. This results in biological, psychological, social and financial repercussions. Due to the nature of this destructive condition, self-reliant treatment options can prove to be futile. In an alcoholic patient where cognitive function and behavioural control is impaired it is ignorant to assume that the patient can claim full responsibility for their pharmacological therapy even if the will to abstain is present. It is the duty of the health care professional to assist the patient by ensuring that the treatment regime is one that is easy to follow and simple to understand. In doing so the patients compliance will radically progress. This process can be assuaged by an emended drug delivery system. This system can be fabricated through judicious pharmaceutical manipulation.

Utilisation of a long-term sustained release delivery system is the quintessential solution as it enables automatic improvement of patient compliance even if the patient is at risk of surrendering to cravings and relapsing. This system, which will be administered under the guidance of the health care professional, eliminates the daunting task of placing overwhelming responsibility of achieving a successful therapeutic outcome in the hands of a patient that is suffering from a clinically recognised medical disorder. The system should be one that delivers a therapeutically effective agent in a safe, stable and functional system.

Such a delivery system has been extensively reported in this study. The FDA approved drug for alcoholism, disulfiram, was selected as the pharmacological agent of choice. Due to the profoundly hydrophobic nature of disulfiram, vitamin E TPGS was deliberately singled out as the polymer of choice. TPGS has the ability to encapsulate hydrophobic compounds as a result of its amphiphilic nature. Disulfiram-loaded nanomicelles with a uniformly small size, high drug loading percentage and sustained release properties were successfully formulated. The delivery vehicle chosen for the nanomicelles was a thermosensitive *in situ* gel comprising the biocompatible polymers PF127 and HAGG. This vehicle had the additional benefit and primary purpose of mitigating the few shortcomings noticed with the nanomicelle system. The gel maximised drug loading and delivery as well as stabilised the release of disulfiram. The gel had a favourable rheological profile and characterization and *in vitro* analysis of the two elements alone and in combination advocated for the development of the merged NEGC. Based on the outcome from the *in vitro* experiments, extensive *ex vivo*

and *in vivo* studies were conducted utilising the Sprague Dawley rat model. A model parenteral formulation is reliant on two factors; it should have minimal tissue damage while exhibiting suitable physicochemical and biopharmaceutical properties (Rungseevijitprapa et al., 2008). The NEGC system, which was administered to the rats via IM injection, allowed release of disulfiram over the 28 day test period demonstrating its viability as a sustained release system. The presence of the NEGC in the rat body was confirmed through high frequency ultra sound imaging. Myotoxicity and histopathology studies were conducted to verify the toxic potential of the system. Results obtained expressed acute outcomes typically expected due to IM administration. Thus the safety of the NEGC was certified. A model parenteral formulation is reliant on two factors; it should have minimal tissue damage while exhibiting suitable physicochemical and biopharmaceutical properties (Rungseevijitprapa et al., 2008). The NEGC system is based on this principle.

The fabrication of the NEGC was an uncomplicated process. It entailed the unification of simply four readily available, trusted, inexpensive materials to yield an effective dual-system. This system has significant promise as the foundation of combating alcohol addiction utilising a traditional, yet remarkable, active ingredient- disulfiram. Furthermore, the versatile nature of the system creates a broad spectrum of active-excipient applicability thereby expanding its usage across a multitude of disease fields. The outlined aims and objectives were achieved with a predominantly affirmative end-result.

7.2 Recommendations

7.2.1 Determination of the DER

The present study limited *in vivo* research to the detection of disulfiram in the blood. Successful determination of disulfiram-plasma levels leads on to the next research step which is to determine if the disulfiram level is ample enough to trigger a DER. As ethanol educes a carcinogenic effect in some animals including rats (Seitz and Stickel, 2007; Seitz et al., 1985) the effect of alcohol was not included in the study due to the institutes' ethics committee limitations.

However by adhering to ethical recommendations/guidelines/considerations, it would be a feasible notion to determine if the plasma levels of disulfiram are sufficient to trigger the DER. For determination of the DER to occur alcohol challenges will have to be conducted throughout the study. In an alcohol challenge a certain amount of alcohol is given to the test subject and the following responses measured: skin temperature, pulse rate, breath acetaldehyde levels, breath carbon disulfide levels (Phillips and Greenberg, 1992), aldehyde

dehydrogenase inhibition (Veverka et al., 1997) and blood acetaldehyde levels (Hellstrom et al., 1983).

The DER effect is highly variable and is dependent on multiple factors. The amount of disulfiram in the body, the amount of alcohol ingested as well as the time period between disulfiram administration and alcohol ingestion all play a vital role in the occurrence and severity of the DER. A worthwhile investigation would be to gauge the amounts/blood levels of each of these which are necessary to induce a DER without causing fatal consequences. Additionally it would be advisable to detect the daily dosage of parenteral disulfiram. This value is not known and it is uncertain if the 250-500mg of oral disulfiram is the same amount needed parenterally (Phillips and Gresser, 1984). To the best of our knowledge, such a study has not been reported with success.

7.2.2 Overcome the inconsistencies of disulfiram research

Although a lot of these potential research avenues have been explored in the past, there have been many difficulties and limitations in these prior attempts made with regards to the implementation of valid and reliable study design (Suh et al., 2006). Low treatment adherence, poor research methodology and confounding variables are accountable for the inconsistent findings. As such, disulfiram research is filled with disparate, inconclusive results. (Suh et al., 2006). However, with the advancement of pharmaceutical research and drug delivery technology, these options can be revisited and concrete, reliable results can be obtained. In this manner, incontestable and incontrovertible information on disulfiram can be compiled which can provide a solid platform from which to expand on the multitudinous pharmacological applications of this extraordinary albeit mysterious drug.

Another disparity associated with disulfiram encompasses great inter-individual discrepancies linked with disulfiram's side effects as well as its deterrent action (Tampier et al., 2008). Disulfiram has large variation in its pharmacokinetic properties and understanding of the its physicochemical aspects is minimal (Eneanya et al., 1981). A further distinctiveness in disulfiram therapy is the patient profile that can benefit from its usage. Patients who are older in age (>40 years old) with a longer history of drinking, socially stable with high motivation and Alcohol Anonymous attendance, possess the ability to sustain and dependent on therapy relationships and those with unimpaired cognitive function are the types of people that have displayed the most progression due to disulfiram therapy (Suh et al., 2006). Thorough pharmaceutical profiling with comprehensive data analysis can be implemented to minimise these variations.

The therapeutic effect of disulfiram is lies in its capacity to initiate an adverse effect with ethanol thus cataloguing it as an unparalleled/unconventional/puzzling/divergent/intriguing active ingredient (Phillips and Greenberg, 1992).

7.2.3 Pertinence of disulfiram to other diseases

Disulfiram has been expansively investigated for the treatment of conditions other than alcoholism such as cocaine addiction (Kosten et al., 2013; Carroll et al., 2016; Schottenfeld et al., 2014) and cancer (Zembko et al., 2014; Tawari et al., 2015; Liu et al., 2014; Bruning and Kast, 2014). This can be dually advantageous as co-occurrence of alcohol abuse and cocaine abuse is great and cancer is a prevalent occurrence due to chronic alcohol addiction. The mechanism of action of disulfiram in cocaine addiction is via a different neurobiological mechanism than its anti-alcohol effect (Suh et al., 2006). Combining disulfiram with other agents has also shown potential. When given together with an opiate antagonist it acts as an alcohol craving reducer by enabling psychological control over the urge to drink (Suh et al., 2006). Disulfiram also has a position in the treatment of latent HIV infection (Hochreiter et al., 2012). Shedler et al (2011) also documented that non-substance related addictions such as pathological gambling could be treated with disulfiram as a result of its inhibiting action/influence on dopamine-β-hydroxylase.

7.2.4 Refine *ex vivo* myotoxicity assessment

The *ex vivo* muscle tissue toxicity test could provide useful information by harvesting viable muscle tissue. Muscle tissue is most viable within a few hours of extraction and therefore the study should commence immediately without prior frozen storage of the tissue.

7.2.5 Applicability of alternative animal model

A different animal model, such as primates, may also be investigated in order to determine the behaviour of the NEGC in a larger animal model. The neurochemical, social and genetic similarities between humans and nonhuman primates classifies these animals as a suitable model to study alcoholism and alcohol abuse (Barr et al., 2004).

7.2.6 Correlation of tissue concentration with plasma concentration

The concentration of disulfiram remaining in the tissue could be determined by homogenising a portion of the muscle tissue and thereafter analysing the disulfiram content using UPLC. This would facilitate greater comprehension on the functioning of the NEGC as well as allow correspondence of the plasma disulfiram levels and the disulfiram remaining in the tissue at the injection site.

REFERENCES

1. Abandansari, H.S., Aghaghafari, E., Nabid, M.R., et al. (2013). Preparation of injectable and thermoresponsive hydrogel based on penta-block copolymer with improved sol stability and mechanical properties. *Polymer*, 54(4), 1329-1340.
2. Aggarwal, N., Goindi, S. and Mehta, S.D. (2012). Preparation and evaluation of dermal delivery system of griseofulvin containing vitamin E-TPGS as penetration enhancer. *AAPS PharmSciTech*, 13(1), 67-74.
3. Aggarwal, n., goindi, s., Mehta, sd., (2012). Preparation and evaluation of dermal delivery system of griseofulvin containing vitamin E-TPGS as penetration enhancer. *AAPS PharmSciTech* 13(1), 67-74.
4. Agnihotri, N., Mishra, R., Goda, C., et al. (2012). Microencapsulation- A Novel Approach in Drug Delivery: A Review. *Indo Global Journal of Pharmaceutical Sciences,* 2(1), 1-20.
5. Ahn, J.S., Kim, K.M., Ko, C.Y. et al. (2011). Absorption enhancer and polymer (Vitamin E TPGS and PVP K29) by solid dispersion improve dissolution and bioavailability of eprosartan mesylate. *Bulletin of Korean Chemical Society*, 32(5), 1587-1592.
6. Akala, E.O., Wiriyacoonkasem, P. and Pan, G. (2011). Studies on in vitro availability, degradation, and thermal properties of naltrexone-loaded biodegradable microspheres. *Drug Development and Industrial Pharmacy*, 37(6), 673-684.
7. Akash, M.S.H., Rehman, K. and Chen, S. (2014). Pluronic F127-based thermosensitive gels for delivery of therapeutic proteins and peptides. *Polymer Reviews*, 54(4), 573-597.
8. Alagusandaram, M., Madhu, C., Umashankari, K., et al. (2009). Microspheres as a Novel Drug Delivery System. *International Journal of ChemTech Research*, 1(3), 526-534.
9. Albertinia, B., Passerinia, N., Di Sabatinoa, M., et al. (2010). Poloxamer 407 microspheres for orotransmucosal drug delivery. Part I: Formulation, manufacturing and characterization. *International Journal of Pharmaceutics*, 399, 71–79.
10. Alemáan, C.L., Más, R.M., Rodeiro, I., et al. (1998). Reference database of the main physiological parameters in Sprague-Dawley rats from 6 to 32 months. *Laboratory animals*, 32(4), 457-466.
11. Alexis, F., Pridgen, E., Molnar, L.K., et al. (2008). Factors affecting the clearance and biodistribution of polymeric nanoparticles, *Molecular Pharmaceutics*, 5(4), 505–515.

12. Andersen, M.P. (1992). Lack of bioequivalence between disulfiram formulations: exemplified by a tablet/effervescent tablet study. *Acta Psychiatrica Scandanavica*, 86, 31-35.
13. Animal Welfare Branch. ARRP Guideline 20: Guidelines for the Housing of Rats in Scientific Institutions. [online] [viewed 15 May 2013]. Available from: http://www.animalethics.org.au/policies-and-guidelines/animal-care
14. Arici, M., Ersöz, N.B., Toker, Ö.S., et al. (2014). Microbiological, steady, and dynamic rheological characterization of boza samples: temperature sweep tests and applicability of the Cox-Merz rule. *Turkish Journal of Agriculture and Forestry*, 38(3), 377-387.
15. Asadi, H., Rostamizadeh, K., Salari, D., et al. (2011). Preparation and characterization of tri-block poly(lactide)–poly(ethylene glycol)–poly(lactide) nanogels for controlled release of naltrexone. *International Journal of Pharmaceutics*, 416, 356– 364.
16. Avachat, A.M. and Kapure, S.S. (2014). Asenapine maleate in situ forming biodegradable implant: An approach to enhance bioavailability. *International journal of Pharmaceutics*, 477(1), 64-72.
17. Baert, L., van't Klooster, G., Dries, W., et al. (2009). Development of a long-acting injectable formulation with nanoparticles of rilpivirine (TMC278) for HIV treatment. *European Journal of Pharmaceutics and Biopharmaceutics*, 72(3), 502-508.
18. Baffoe, C.S., Nguyen, N., Boyd, P. et al. (2015). Disulfiram-loaded immediate and extended release vaginal tablets for the localised treatment of cervical cancer. *Journal of Pharmacy and Pharmacology*, 67(2), 189-198.
19. Bajaj, I.B., Survase, S.A., Saudagar, P.S., et al. (2007). Gellan gum: fermentative production, downstream processing and applications. *Food Technology and Biotechnology*, 45(4), 341.
20. Balakrishnan, P., Park, E.K., Song, C.K., et al. (2015). Carbopol-Incorporated Thermoreversible Gel for Intranasal Drug Delivery. *Molecules*, 20(3), 4124-4135.
21. Barnes, H. A. (2000). A handbook of elementary rheology.
22. Barr, C.S., Schwandt, M.L., Newman, T.K. et al. (2004). The use of adolescent nonhuman primates to model human alcohol intake: neurobiological, genetic, and psychological variables. *Annals of the New York Academy of Sciences*, 1021, 221.
23. Benoit, J-P., Faisant, N., Vernier-Julienne, M-C., et al. (2000). Development of Microspheres for Neurological Disorders: from Basics to Clinical Applications. *Journal of Controlled Release*, 65, 285-296.

24. Bevins, R.A., Wilkinson, J.L. and Sanderson, S.D. (2008). Vaccines to Combat Smoking. *Expert Opinion on Biological Therapy*, 8(4), 379-383.
25. Bezerra, M.A., Santelli, R.E., Oliviera, E.P. et al. (2008). Response surface methodology as a tool for optimization in analytical chemistry. *Talanta*, 76(5), 965-977.
26. Bhatt, N., Bhatt, G. and Kothiyal, P. (2013). Drug delivery to the brain using polymeric nanoparticles: a review. *International Journal of Pharmaceutical and Life Sciences*, 2(3), 107-132.
27. Black, D. (1979). An allergic reaction to disulfiram implant. *British Journal of Addiction*, 74, 88-90.
28. Blasi, P., Giovagnoli, S., Schoubben, A., et al. (2007). Solid lipid nanoparticles for targeted brain drug delivery. *Advanced Drug Delivery Reviews*, 59, 454-77.
29. Bonoiu, A.C., Mahajan, S.D., Ding, H., et al. (2009). Nanotechnology approach for drug addiction therapy: gene silencing using delivery of gold nanorod-siRNA nanoplex in dopaminergic neurons. *Proceedings of the National Academy of Sciences of the United States of America*, 106(14), 5546-5550.
30. Bose, S., Ravis, W.R., Lin, Y-J., et al. (2001). Electrically-assisted transdermal delivery of buprenorphine. *Journal of Controlled Release*, 73, 197-203.
31. Bradbeer, J.F., Hancocks, R., Spyropoulos, F., et al.. (2014). Self-structuring foods based on acid-sensitive low and high acyl mixed gellan systems to impact on satiety. *Food Hydrocolloids*, 35, 522-530.
32. Brancaccio, P., Lippi, G. and Maffulli, N. (2010). Biochemical markers of muscular damage. *Clinical Chemistry and Laboratory Medicine*, 48(6), 757-767.
33. Brayden, D.J. and Martinez, M.N. (2007). Prediction of therapeutic and drug delivery outcomes using animal models. *Advanced Drug Delivery Reviews*, 59(11), 1071-1072.
34. Brazeau, G.A. and Fung, H.L. (1989). An in vitro model to evaluate muscle damage following intramuscular injections. *Pharmaceutical Research*, 6(2), 167-170.
35. Brazeau, G.A. and Fung, H.L. (1989). Use of an in vitro model for the assessment of muscle damage from intramuscular injections: in vitro-in vivo correlation and predictability with mixed solvent systems. *Pharmaceutical Research*, 6(9), 766-771.
36. Brazeau, G.A., Attia, S., Poxon, S. et al. (1998). In vitro myotoxicity of selected cationic macromolecules used in non-viral gene delivery. *Pharmaceutical Research*, 15(5), 680-684.
37. Brüning, A. and Kast, R.E. (2014). Oxidizing to death: disulfiram for cancer cell killing. *Cell Cycle*, 13(10), 1513-1514.

38. Buckiova, D., Ranjan, S., Newman, T., et al (2012). Minimally invasive drug delivery to the cochlea through application of nanoparticles to the round window membrane. *Nanomedicine*, 7(9), 1339-54.
39. Butt, A.M., Amin, M.C.I.M., Katas, H., et al. (2012). In vitro characterization of pluronic F127 and D-α-tocopheryl polyethylene glycol 1000 succinate mixed micelles as nanocarriers for targeted anticancer-drug delivery. *Journal of Nanomaterials*, 112.
40. Canal, F., Sanchis, J., and Vicent, M.J. (2011). Polymer-drug conjugates as nano-sized medicines. *Current Opinion in Biotechnology*, 22, 894-900.
41. Carotenuto, C., and Grizzuti, N. (2006). Thermoreversible gelation of hydroxypropylcellulose aqueous solutions. *Rheologica Acta*, 45(4), 468-473.
42. Carreño, M.J. and Mella Gajardo, F.P., (2011). Universidad De Concepcion, Laboratorios Andromaco Ss And Abl Pharma Colombia Sa. Pharmaceutical Compositions Containing An Inclusion Complex Formed By Disulfiram And A Cyclodextrine, Which Can Be Used In The Treatment Of Alcohol And Cocaine Dependence. U.S. Patent 20,110,021,458.
43. Carroll, K.M. Nich, C., Ball, S.A., et al. (1998). Treatment of cocaine and alcohol dependence with psychotherapy and disulfiram. *Addiction*, 93, 713–728.
44. Carroll, K.M., Fenton, L.R., Ball, S.A., et al. (2004). Efficacy of disulfiram and cognitive behavior therapy in cocaine-dependent outpatients: a randomized placebo controlled trial. *Archives of General Psychiatry*, 61, 264–272.
45. Carroll, K.M., Nich, C., Petry, N.M., et al. (2016). A Randomized Factorial Trial of Disulfiram and Contingency Management to Enhance Cognitive Behavioral Therapy for Cocaine Dependence. *Drug and Alcohol Dependence*.
46. Cassimjee, D.M.H. (2012). A Place for Antabuse. *South African Family Practice*, 12(6).
47. Cdc.gov. (2016). CDC - Fact Sheets-Alcohol Use And Health - Alcohol. [online] Available at http://www.cdc.gov/alcohol/fact-sheets/alcohol-use.htm [Accessed 23 Mar. 2016].
48. Center for Substance Abuse Treatment. (2009). Incorporating Alcohol Pharmacotherapies into Medical Practice. Treatment Improvement Protocol (TIP) Series 49. HHS Publication No. (SMA) 09-4380. Rockville, MD: Substance Abuse and Mental Health Services Administration.
49. Centers for Disease Control and Prevention (CDC). Alcohol and public health: Alcohol-related disease impact (ARDI). Available at: http://nccd.cdc.gov/DPH_ARDI/Default/Report.aspx?T=AAM&P=f6d7eda7-036e-4553-9968-9b17ffad620e&R=d7a9b303-48e9-4440-bf47-

070a4827e1fd&M=AD96A9C1-285A-44D2-B76D-BA2AE037FC56&F=&D= [Accessed 23 March 2016].

50. Centers for Disease Control and Prevention (CDC). Alcohol-Related Disease Impact (ARDI). Atlanta, GA: CDC.
51. Chan, V. and Perlas, A. (2011). Basics of ultrasound imaging. In *Atlas of ultrasound-guided procedures in interventional pain management* (pp. 13-19). Springer New York.
52. Checa-Casalengua, P., Jiang, C., Bravo-Osuna, I., et al. (2011). Retinal ganglion cells survival in a glaucoma model by GDNF/Vit E PLGA microspheres prepared according to a novel microencapsulation procedure. *Journal of Controlled Release*, 156, 92–100.
53. Chen, X., Zhang, L., Hu, X., et al. (2015). Formulation and preparation of a stable intravenous disulfiram-loaded lipid emulsion. *European Journal of Lipid Science and Technology*, 117(6), 869-878.
54. Chenite, A.M., Buschmann, D., Wang, C., et al. (2001). Rheological characterization of thermogelling chitosan/glycerol-phosphate solutions. *Carbohydrate Polymers*, 46(1), 39-47.
55. Chiang, C.N. and Hawks, R.L. (2003). Pharmacokinetics of the combination tablet of buprenorphine and naloxone. *Drug and Alcohol Dependence*, 70(2), 539-547.
56. Cho, S.S. (Ed.). (2001). *Handbook of dietary fiber* (Vol. 113). CRC Press.
57. Cho, Y. and Borgens, R.B. (2012). Polymer and nano-technology applications for repair and reconstruction of the central nervous system. *Experimental Neurology*, 233,126–144.
58. Choonara, Y.E., Pillay, V., Ndesendo, V.M.K., et al. (2011). Polymeric emulsion and crosslink-mediated synthesis of super-stable nanoparticles as sustained-release anti-tuberculosis drug carriers. *Colloids and Surfaces B: Biointerfaces*, 87, 243-254.
59. Cid, E., Cid Jr, E., Feuerhake, O., et al. (1991). Plasma Concentration of Disulfiram After Injection of Suspended Micropellets into Alcoholic Subjects. *Biopharmaceutics & Drug Disposition*, 2, 163-169.
60. Cohen, S., Lobel, E., Trevgoda, A., et al. (1997). A novel in situ-forming ophthalmic drug delivery system from alginates undergoing gelation in the eye. *Journal of Controlled Release*, 44(2), 201-208.
61. Cornaz, A-L., De Ascentis, A., Colombo, P., et al. (1996). In vitro characteristics of nicotine microspheres for transnasal delivery. *International Journal of Pharmaceutics*, 129, 175-183.

62. Costantino, L. and Boraschi, D. (2012). Is there a clinical future for polymeric nanoparticles as brain-targeting drug delivery agents? *Drug Discovery Today*, 17(718).
63. Coutinho, D.F., Sant, S.V., Shin, H et al. (2010). Modified Gellan Gum hydrogels with tunable physical and mechanical properties. *Biomaterials*,31(29), 7494-7502.
64. Cryan, J.F., Gasparini, F., van Heeke, G., et al. (2003). Non-nicotinic neuropharmacological strategies for nicotine dependence: beyond bupropion. *Drug Discovery Today*, 8(22).
65. Cunha-Filho, M.S., Alvarez-Lorenzo, C., Martínez-Pacheco, R., et al. (2012). Temperature-Sensitive Gels for Intratumoral Delivery of β-Lapachone: Effect of Cyclodextrins and Ethanol. *The Scientific World Journal*, 2012.
66. de Melo-Diogo, D., Gaspar, V.M., Costa, E.C., et al. (2014). Combinatorial delivery of Crizotinib–Palbociclib–Sildenafil using TPGS-PLA micelles for improved cancer treatment. *European Journal of Pharmaceutics and Biopharmaceutics*, 88(3), 718-729.
67. De Sousa, A. and De Sousa, A. (2004). A one-year pragmatic trial of naltrexone versus disulfiram in the treatment of alcohol dependence. *Alcohol and Alcoholism*, 39(6), 528-531.
68. Delgado, A., E´vora, C. and Llabre´s, M. (1996). Optimization of 7-day release (in vitro) from DL-PLA methadone microspheres. *International Journal of Pharmaceutics*, 134, 203– 211.
69. Dey, N.S., Majumdar, S. and Rao, M.E.B. (2008). Multiparticulate Drug Delivery Systems for Controlled Release. *Tropical Journal of Pharmaceutical Research*, 7(3), 1067-1075.
70. Dhuria, S.V., Hanson, L.R. and Frey, W.H. (2010). Intranasal Delivery to the Central Nervous System: Mechanisms and Experimental Considerations. *Journal of Pharmaceutical Sciences*, 99(4).
71. Diehl, A., Ulmer, L., Mutschler, J., et al. (2010). Why is disulfiram superior to acamprosate in the routine clinical setting? A retrospective long-term study in 353 alcohol-dependent patients. *Alcohol and Alcoholism*, 45(3), 271-277.
72. Dinarvand, R., Moghadam, S.H., Mohammadyari-Fard, L., et al. (2003). Preparation of Biodegradable Microspheres and Matrix Devices Containing Naltrexone. *AAPS PharmSciTech*, 4(3).
73. Diogo, L.N., Faustino, I.V., Afonso, R.A., et al. (2014). Voluntary Oral Administration of Losartan in Rats. *Journal of the American Association for Laboratory Animal Science*, 54(5), 549-556.

74. Dixit, R., Verma, A., Singh, U.P., et al. (2011). Preparation and characterization of gellan-chitosan polyelectrolyte complex beads. *Latin American Journal of Pharmacy*, 30(6), 1186-1195.
75. Dou, J., Zhang, H., Liu, X., et al. (2014). Preparation and evaluation in vitro and in vivo of docetaxel loaded mixed micelles for oral administration. *Colloids and Surfaces B: Biointerfaces*, 114, 20-27.
76. Duan X, Xiao J, Yin Q, et al. (2013). Smart pH-sensitive and temporal-controlled polymeric micelles for effective combination therapy of doxorubicin and disulfiram. *ACS Nano*, 7 (7): 5858-5869.
77. Duan, X., Xiao, J., Yin, Q., et al. (2014). Multi-targeted inhibition of tumor growth and lung metastasis by redox-sensitive shell crosslinked micelles loading disulfiram. *Nanotechnology*, 25(12), 125102.
78. Duffy, J.J., Hill, A., Walton, A. et al. (2011). Suspension stability: Why particle size, zeta potential and rheology are important. *Proceedings of Particulate Systems Analysis.*
79. Duhem, N., Danhier, F. and Préat , V. (2014). Vitamin E-based nanomedicines for anti cancer drug delivery. *Journal of Controlled Release*, 182,33–44.
80. Dumortier, G., Grossiord, J.L., Agnely, F. et al. (2006). A review of poloxamer 407 pharmaceutical and pharmacological characteristics. *Pharmaceutical Research*, 23(12), 2709-2728.
81. Eastman Chemical Company. (2005). Eastman Vitamin E TPGS NF Applications and Properties [Brochure] N.p.: Author.
82. EFSA Publication. (2007). *Opinion of the Scientific Panel on Food Additives, Flavourings, Processing Aids and Materials in Contact with Food on a request from the Commission related to D-alpha-tocopheryl polyethylene glycol 1000 succinate (TPGS) in use for food for particular nutritional purposes: Question No EFSA Q-2003-126*. European Food Safety Authority. *The EFSA Journal*, 490.
83. El-Kamel, A.H. (2002). In vitro and in vivo evaluation of Pluronic F127-based ocular delivery system for timolol maleate. *International Journal of Pharmaceutics*, 241(1), 47-55.
84. Eneanya, D.I., Bianchine, J.R., Duran, D.O. et al. (1981). The actions and metabolic fate of disulfiram. *Annual Review of Pharmacology and Toxicology*, 21(1), 575-596.
85. Escobar-Chávez, J.J., López-Cervantes, M., Naik, A., et al. (2006). Applications of thermo-reversible pluronic F-127 gels in pharmaceutical formulations. *Journal of Pharmacy and Pharmaceutical Sciences*, 9(3), 339-358.
86. Fahim, R.E.F., Kessler, P.D. and Kalnik, M. (2013). Therapeutic vaccines against tobacco addiction. *Expert Review of Vaccines*, 12(3).

87. Faiman, M.D., Artman, L. and Haya, K. (1980). Disulfiram Distribution and Elimination in the Rat After Oral and Intraperitoneal Administration. *Alcoholism: Clinical and Experimental Research,* 4(4).
88. Faiman, M.D., Jensen, J.C. and Lacoursiere, R.B. (1984). Elimination kinetics of disulfiram in alcoholics after single and repeated doses. *The Journal of Clinical Pharmacology.*
89. Falk, R., Randolph, T.W., Meyer, J.D., et al. (1997). Controlled release of ionic compounds from poly (L-lactide) microspheres produced by precipitation with a compressed antisolvent. *Journal of Controlled Release*, 44, 77-85.
90. Fan, Z., Chen, C., Pang, X., et al. (2015). Adding Vitamin E-TPGS to the Formulation of Genexol-PM: Specially Mixed Micelles Improve Drug-Loading Ability and Cytotoxicity against Multidrug-Resistant Tumors Significantly. *PLoS ONE*, 10(4),120-129.
91. Farokhzad, O.C. and Langer, R. (2009). Impact of nanotechnology on drug delivery. *ACS Nano*, 3(1), 16–20.
92. Fathy, M., and El-Badry, M. (2003). Preparation and evaluation of piroxicam - pluronic solid dispersions. *Bulletin of Pharmaceutical Sciences,* 26(2), 97-108.
93. Feranchak, A.P., Sontag, M.K., Wagener, J.S., et al. (1999). Prospective, long-term study of fat-soluble vitamin status in children with cystic fibrosis identified by newborn screen. *The Journal of Paediatrics*, 135(5), 601-610.
94. Fischer, A. (2013). New Abuse-Resistant Pharmaceutical Composition for the Treatment of Opioid Dependence. US Patent 20130071477.
95. Florence, A.T. and Attwood, D. (2015). Physicochemical Principles of Pharmacy: In Manufacture, Formulation and Clinical Use. *Pharmaceutical Press*.
96. Flores-Huicochea, E., Rodríguez-Hernández, A.I., Espinosa-Solares, T., et al. (2013). Sol-gel transition temperatures of high acyl gellan with monovalent and divalent cations from rheological measurements. *Food Hydrocolloids*, 31(2), 299-305.
97. Food and Drug Administration. (2004). Review and evaluation of the clinical data. (NDA 21-431). Meeting of the Psychopharmacologic Drugs Advisory Committee FDA White Oak Campus, 10903 New Hampshire Ave, Bldg. 31, Conference Center, Silver Spring, MD: Center for Drug Evaluation and Research.
98. Food and Drug Administration. (2010). Clinical Pharmacology of Vivitrol. (NDA 21-897). Meeting of the Psychopharmacologic Drugs Advisory Committee FDA White Oak Campus, 10903 New Hampshire Ave, Bldg. 31, Conference Center, Silver Spring, MD: Center for Drug Evaluation and Research.

99. Frijlink, H.W. (2003). Benefits of different drug formulations in psychopharmacology. *European Neuropsychopharmacology*, 13, 577-584.
100. Gao, L., Liu, G., Ma, J., et al. (2012). Drug nanocrystals: in vivo performances. *Journal of Controlled Release*.
101. Gao, Y., Li, L.B. and Zhai, G. (2008). Preparation and characterization of Pluronic/TPGS mixed micelles for solubilization of camptothecin. *Colloids and Surfaces B: Biointerfaces,* 64(2),194-199.
102. Garbutt, J.C., Kranzler, H.R., O'Malley, S.S., et al. (2005). Efficacy and Tolerability of Long-Acting Injectable Naltrexone for Alcohol Dependence. *Journal of the American Medical Association*, 293 (13).
103. García, M.C., Alfaro, M.C., Calero, N. et al. (2011). Influence of gellan gum concentration on the dynamic viscoelasticity and transient flow of fluid gels. *Biochemical Engineering Journal*, 55(2), 73-81.
104. Gaspar, R. and Duncan, R. (2009). Polymeric carriers: preclinical safety and the regulatory implications for design and development of polymer therapeutics. *Advanced Drug Delivery Reviews*, 61, 1220–1231.
105. George, T.P., Chawarski, M.C., Pakes, J. et al. (2000). Disulfiram versus placebo for cocaine dependence in buprenorphine-maintained subjects: a preliminary trial. *Biological Psychiatry*.
106. Ghadavi, A.G., Patel, B.N., Patel, D.M., et al. (2011). Medicated Chewing Gum- A 21st Century Drug Delivery System. *International Journal of Pharmaceutical Sciences and Research*, 2(8), 1961-1974.
107. Ghosh, K., Shu, X. Z., Mou, R., et al. (2005). Rheological characterization of in situ cross-linkable hyaluronan hydrogels. *Biomacromolecules*, 6(5), 2857-2865.
108. Gibis, M., Rahn, N. and Weiss, J. (2013). Physical and oxidative stability of uncoated and chitosan-coated liposomes containing grape seed extract. *Pharmaceutics*, 5(3), 421-433.
109. Gil-Alegre, M.E., Barone, M.L. and Torres-Suárez, A.I. (2005). Extraction and determination by liquid chromatography and spectrophotometry of naloxone in microparticles for drug-addiction treatment. *Journal of Separation Science*, 28(16), 2086-2093.
110. Global Information System on Alcohol and Health (GISAH). (2005). World Health Organisation [online] Available at: <http://www.who.int/gho/alcohol/en/ > [Accessed 30 January 2012].
111. Goddeeris, C., Willems, T. and Van den Mooter, G. (2008). Formulation of fast disintegrating tablets of ternary solid dispersions consisting of TPGS 1000 and

HPMC 2910 or PVPVA 64 to improve the dissolution of the anti-HIV drug UC 781. *European Journal of Pharmaceutical Sciences*, 34, 293–302.

112. Godin, B. and Touitou, E. (2007). Transdermal skin delivery: predictions for humans from in vivo, ex vivo and animal models. *Advanced Drug Delivery Reviews*, 59(11),1152-1161.
113. Goh, K.K., Haisman, D.R. and Singh, H. (2006). Characterization of a high acyl gellan polysaccharide using light scattering and rheological techniques. *Food Hydrocolloids*, 20(2), 176-183.
114. Gohel, M.C., Parikh, R.K., Nagori, S.A., et al. (2009). Preparation and evaluation of soft gellan gum gel containing paracetamol. *Indian Journal of Pharmaceutical Sciences*, 71(2), 120.
115. Goicoechea, M., Cia, F., San Jose, C., et al. (2008). Minimizing creatine kinase variability in rats for neuromuscular research purposes. *Laboratory Animals,* 42(1), 19-25.
116. Goldberg, M., Langer, R. and Jia, X. (2007). Nanostructured materials for applications in drug delivery and tissue engineering. *Journal of Biomaterials Science, Polymer Edition*, 18(3), 241-268.
117. Gradinaru, L.M., Ciobanu, C., Vlad, S., et al. (2012). Synthesis and rheology of thermoreversible polyurethane hydrogels. *Central European Journal of Chemistry*, 10(6), 1859-1866.
118. Green-Sadan, T., Kuttner, Y., Lublin-Tennenbaum, T., et al. (2005). Glial cell line-derived neurotrophic factor-conjugated nanoparticles suppress acquisition of cocaine self-administration in rats. *Experimental Neurology*, 194, 97-105.
119. Grillet, A.M., Gloe, L.M., and Wyatt, N.B. (2012). Polymer gel rheology and adhesion. *INTECH Open Access Publisher*.
120. Gross, A., Jacobs, E.A., Petry, N.M., et al (2001). Limits to buprenorphine dosing: a comparison between quintuple and sextuple the maintenance dose every 5 days. *Drug and Alcohol Dependence*, 64, 111-116.
121. Gu, P.F., Xu, H., Sui, B.W., et al. (2012). Polymeric micelles based on poly (ethylene glycol) block poly (racemic amino acids) hybrid polypeptides: conformation-facilitated drug-loading behavior and potential application as effective anticancer drug carriers. *International Journal of Nanomedicine*, 7, 109-22.
122. Guo, Y., Chu, M., Tan, S., et al. (2013). Chitosan-g-TPGS nanoparticles for anticancer drug delivery and overcoming multidrug resistance. *Molecular Pharmaceutics*,11(1), 59-70.

123. Gupta, H., Aqil, M., Khar, R.Ket al. (2013). Nanoparticles laden in situ gel for sustained ocular drug delivery. *Journal of Pharmacy And Bioallied Sciences*, 5(2), 162.
124. Gustow, E., Ryde, T. and Cooper, E.R. (2008). Nanoparticulate Topiramate Formulations. US Patent 7390505B2.
125. Haley, TJ., 1979. Disulfiram (tetraethylthioperoxydicarbonic diamide): a reappraisal of its toxicity and therapeutic application. Drug Metabolism Reviews, 9, 319–35.
126. Hamidi, M. (2015). Method and system for synthesizing nanocarrier based long acting drug delivery system for methadone. US Patent 20150024035.
127. Hamidi, M. (2015). Method and system for synthesizing nanocarrier based long acting drug delivery system for buprenorphine. US Patent 20150024033.
128. Hao, T., Chen, D., Liu, K., et al. (2015). Micelles of d-α-tocopheryl polyethylene glycol 2000 succinate (TPGS 2K) for doxorubicin delivery with reversal of multidrug resistance. *ACS Applied Materials & Interfaces*, 7(32), 18064-18075.
129. Heemskerk, A.A., van Haandel, L., Woods, J.M., et al. (2011). LC-MS/MS method for the determination of carbamathione in human plasma. *Journal of Pharmaceutical and Biomedical Analysis*, 54(4), 799-806.
130. Heidbreder, C. (2005). Novel pharmacotherapeutic targets for the management of drug addiction. *European Journal of Pharmacology*, 526,101–112.
131. Helander, A. and Tottmar, O. (1987). Assay of human blood aldehyde dehydrogenase activity by high-performance liquid chromatography. *Alcohol*, 4(2), 121-125.
132. Hellstrom, E. and Tottmar, O. (1980). Implantation of Disulfiram in Rats. *Pharmacology Biochemistry and Behaviour*, 13(1), 73-82.
133. Hellstrom, E. and Tottmar, O. (1982). Acute Effects of Ethanol and Acetaldehyde on Blood Pressure and Heart Rate in Disulfiram- treated and Control Rats. *Pharmacology Biochemistry and Behaviour*, 17, 1103-1109.
134. Hellström, E. and Tottmar, O. (1982). Acute effects of ethanol and acetaldehyde on blood pressure and heart rate in disulfiram-treated and control rats. *Pharmacology Biochemistry and Behavior*, 17(6), 1103-1109.
135. Hellstrom, E., Tottmar, O. and Widerlöv, E. (1983). Effects of oral administration or implantation of disulfiram on aldehyde dehydrogenase activity in human blood. *Alcoholism: Clinical and Experimental Research*,7(2), 231-236.
136. Herrmann, S., Winter, G., Mohl, S., et al. (2007). Mechanisms controlling protein release from lipidic implants: Effects of PEG addition. *Journal of Controlled Release*, 118, 161-168.

137. Hingson, R. and Kenkel, D. (2003). Social and Health Consequences of Underage Drinking. In press. As quoted in Institute of Medicine National Research Council of the National Academies. Bonnie, Richard J. and Mary Ellen O'Connell, eds. Reducing Underage Drinking: A Collective Responsibility. Washington, DC: The National Academies Press.
138. Hochreiter, J., McCance-Katz, E.F., Lapham, J., et al. (2012). Disulfiram metabolite S-methyl-N, N-diethylthiocarbamate quantisation in human plasma with reverse phase ultra performance liquid chromatography and mass spectrometry. *Journal of Chromatography B*, 897, 80-84.
139. Hoda, M., Sufi, S.A., Shakya, G., et al. (2015). Influence of stabilizers on the production of disulfiram-loaded poly (lactic-co-glycolic acid) nanoparticles and their anticancer potential. *Therapeutic Delivery*, 6(1), 17-25.
140. Hogan, M. E., Kikuta, A. and Taddio, A. (2010). A systematic review of measures for reducing injection pain during adult immunization. *Vaccin*e, 28, 1514-1521.
141. Hoichreiter, J., McCance-Katz, E.F., Lapham, J., et al. (2012). Disulfiram metabolite S-methyl-N,N-diethylthiocarbamate quantitation in human plasma with reverse phase ultra performance liquid chromatography and mass spectrometry. *Journal of Chromatography. B, Analytical technologies in the biomedical and life sciences,* 897, 80-84.
142. Homayoun, P., Mandal, T., Landry, D., et al. (2003). Controlled Release of Anti-Cocaine Catalytic Antibody from Biodegradable Polymeric Microspheres. *Journal of Pharmacy and Pharmacology*, 55, 933-938.
http://www.who.int/substance_abuse/publications/global_alcohol_report/msb_gsr_2014_1.pdf?ua=1 [Accessed 23 March 2016].
143. Hu, Y., Zheng, H., Huang, W., et al. (2014). A novel and efficient nicotine vaccine using nano-lipoplex as a delivery vehicle. *Human Vaccines and Immunotherapeutics*, 10(1), 64-72.
144. Hugerth, A., Nicklasson, F., Lindell, K., Thyressan, K. (2010). Multi-Portion Intra-Oral Dosage Form with Organoleptic Properties. US Patent 20100247586A1.
145. Hughes, J.C. and Cook, C.C. (1997). The efficacy of disulfiram: a review of outcome studies. *Addiction*, 92, 381–395.
146. Jaeger, M. and Rossler, W. (2010). Attitudes towards long-acting depot antipsychotics: A survey of patients, relatives and psychiatrists. *Psychiatry Research*, 175, 58–62.
147. Janssens, S., Nagels, S., de Armas, H.N.. et al. (2007). Formulation and characterization of ternary solid dispersions made up of Itraconazole and two excipients, TPGS 1000 and PVPVA 64, that were selected based on a

supersaturation screening study. *European Journal of Pharmaceutics and Biopharmaceutics.*

148. Jaspart, S., Bertholet, P., Piel, G., et al. (2007). Solid Lipid Microparticles as a Sustained Release System for Pulmonary Drug Delivery. *European Journal of Pharmaceutics and Biopharmaceutics*, 65, 47-56.
149. Jensen, J.C. and Faiman, M.D. (1980). Determination of disulfiram and metabolites from biological fluids by high-performance liquid chromatography. *Journal of Chromatography B: Biomedical Sciences and Applications*, 181(3), 407-416.
150. Jensen, J.C. and Faiman, M.D. (1984). Hypothermia as an index of the disulfiram-ethanol reaction in the rat. *Alcohol*, 1(2), 97-100.
151. Jeong, B., Kim, S.W., and Bae, Y.H. (2002). Thermosensitive sol–gel reversible hydrogels. *Advanced Drug Delivery Reviews,* 54, 37–51.
152. Jhaveri, A.M. and Torchilin, V.P. (2014). Multifunctional polymeric micelles for delivery of drugs and siRNA. *Frontiers in Pharmacology*, 5(77), 1-26.
153. Johansson, B. (1990). Plasma protein binding of disulfiram and its metabolite diethylthiocarbamic acid methyl ester. *Journal of Pharmacy and Pharmacology*, 42(11), 806-807.
154. Johnsen, J. and Mørland, J. (1991). Disulfiram implant: a double-blind placebo controlled follow-up on treatment outcome. *Alcoholism: Clinical and Experimental Research*, 15(3), 532–536.
155. Johnsen, J. and Mørland, J. (1992). Depot preparations of disulfiram: experimental and clinical results. *Acta Psychiatrica Scandinavica*, 86(S369), 27-30.
156. Juby, K.A., Dwivedi, C., Kumar, M., et al. (2012). Silver nanoparticle-loaded PVA/gum acacia hydrogel: Synthesis, characterization and antibacterial study. *Carbohydrate Polymers*, 89(3), 906-913.
157. Jung, H.J., Abou-Jaoude, M., Carbia, B.E. et al. (2013). Glaucoma therapy by extended release of timolol from nanoparticle loaded silicone-hydrogel contact lenses. *Journal of Controlled Release*,165(1), pp.82-89.
158. Junghanns, A.H. and Müller, R.H. (2008). Nanocrystal technology, drug delivery and clinical applications. *International Journal of Nanomedicine*, 3(3), 295–309.
159. Kapoor, D.N., Katare, O.P. and Dhawan, S. (2012). In situ forming implant for controlled delivery of an anti-HIV fusion inhibitor. *International Journal of Pharmaceutics*, 426(1),132-143.
160. Kasapis, S., Giannouli, P., Hember, M.W., et al. (1999). Structural aspects and phase behaviour in deacylated and high acyl gellan systems. *Carbohydrate Polymers*, 38(2), 145-154.

161. Kaur, J., Shalini, S. and Bansal, M.P. (2010). Influence of vitamin E on alcohol-induced changes in antioxidant defenses in mice liver. *Toxicology Mechanisms and Methods*, 20(2), 82-89.
162. Khan, S and Pace, G.W. (2002). Composition and method of preparing microparticles of water-insoluble substances, US Patent 6337092.
163. Kim, J.K., Kim, H.J., Chung, J.Y., et al. (2014). Natural and synthetic biomaterials for controlled drug delivery. *Archives of Pharmaceutical Research*, 37(1), 60-68.
164. Kim, K. and Pack, D. (2006). Microspheres for Drug Delivery. In: Ferrari, M., ed. *BIOMEMS and Biomedical Technology, Volume 1: Biological and Biomedical Nanotechnology*, Springer.
165. Kitchell, J.P., Muni, I.A. and Boyer, Y. (2995). Controlled Sustained Release Delivery System for Smoking Cessation. US Patent 5403595.
166. Kline, S.A. and Kingstone, E. (1977). Disulfiram implants: the right treatment but the wrong drug? *Canadian Medical Association Journal*, 116.
167. Koffi, A.A., Agnely, F., Ponchel, G., et al. (2006). Modulation of the rheological and mucoadhesive properties of thermosensitive poloxamer-based hydrogels intended for the rectal administration of quinine. *European Journal of Pharmaceutical Sciences,* 27, 328–335.
168. Kohane, D.S. (2006). Microparticles and Nanoparticles for Drug Delivery. *Biotechnology and Bioengineering*, 96(2).
169. Kojarunchitt, T., Hook, S., Rizwan, S., et al. (2011). Development and characterization of modified poloxamer 407 thermoresponsive depot systems containing cubosomes. *International Journal of Pharmaceutics*, 408(1), 20-26.
170. Koocheki, S., Madaeni, S.S. and Niroomandi, P. (2011). Development of an enhanced formulation for delivering sustained release buprenorphine hydrochloride. *Saudi Pharmaceutical Journal*, 29, 255-262.
171. Kopeček, J. (2013). Polymer–drug conjugates: Origins, progress to date and future directions *Advanced Drug Delivery Reviews*, 65, 49–59.
172. Kosten, T.R., Wu, G., Huang, W., et al. (2013). Pharmacogenetic randomized trial for cocaine abuse: disulfiram and dopamine β-hydroxylase. *Biological Psychiatry*, 73(3), 219-224.
173. Kranz, H., Brazeau, G.A., Napaporn, J., et al. (2001). Myotoxicity studies of injectable biodegradable in-situ forming drug delivery systems. *International Journal of Pharmaceutics*, 212(1), 11-18.
174. Kreuter, J. (2001). Nanoparticulate systems for brain delivery of drugs. *Advanced Drug Delivery Reviews,* 7, 65-81.

175. Kulhari, H., Pooja, D., Shrivastava, S., et al. (2015). Cyclic-RGDfK peptide conjugated succinoyl-TPGS nanomicelles for targeted delivery of docetaxel to integrin receptor over-expressing angiogenic tumours. *Nanomedicine: Nanotechnology, Biology and Medicine*, 11(6), 1511-1520.
176. Kumari, A., Yadav, S.K. and Yada, S.C. (2010). Biodegradable polymeric nanoparticle based drug delivery systems. *Colloids and Surfaces B: Biointerfaces*, 75, 1-18.
177. Lakshmana, P.S., Shirwaikar, A.A., Shirwaikar, A., et al. (2009). Formulation and evaluation of sustained release microspheres of rosin containing aceclofenac. *ARS Pharmaceutica*, 50(2), 51-62.
178. Larsen, J.C. and Mortensen, A. (2007). Opinion of the Scientific Panel on Food Additives, Flavourings, Processing Aids and Materials in Contact with Food on a request from the Commission related to D-alpha-tocopheryl polyethylene glycol 1000 succinate (TPGS) in use for food for particular nutritional purposes: Question number EFSA Q-2003-126. *European Food Safety Authority*.
179. Lautenschlager, H. and Elias, I. (2010). Nanoparticles containing nicotine and/or cotinine, dispersions, and use thereof. US Patent 20100247653A1.
180. Lee, H., Fisher, S., Kallos, M.S., et al. (2011). Optimizing gelling parameters of gellan gum for fibrocartilage tissue engineering. *Journal of Biomedical Materials Research Part B: Applied Biomaterials*, 98(2), 238-245.
181. Li, Y., Shi, T., Sun, Z., et al. (2006). Investigation of sol-gel transition in Pluronic F127/D2O solutions using a combination of small-angle neutron scattering and Monte Carlo simulation. *The Journal of Physical Chemistry B*, 110(51), 26424-26429.
182. Liao, J-B., Yong-Zhuo, L., Yun-Long, C., et al. (2015). Novel patchouli alcohol ternary solid dispersion pellets prepared by Poloxamers. *Iranian Journal of Pharmaceutical Research,* 14 (1): 15-26.
183. Lin, T-C., Chen, J-H., Chen, Y-Het al. (2013). Biodegradable micelles from a hyaluronan-poly-(ε-caprolactone) graft copolymer as nanocarriers for fibroblast growth factor 1. *Journal of Materials Chemistry B*, 1, 5977-5987.
184. Lipsky, J.J., Shen, M.L. and Naylor, S. (2001). In vivo inhibition of aldehyde dehydrogenase by disulfiram. *Chemico- Biological Interactions,* 130-132, 93-102.
185. Liu, L., Wang, B., Bai, T.C. et al. (2014). Thermal behavior and properties of chitosan fibers enhanced polysaccharide hydrogels *Thermochimica Acta*, 583, 8-14.
186. Liu, P., Kumar, I.S., Brown, S., et al. (2013). Disulfiram targets cancer stem-like cells and reverses resistance and cross-resistance in acquired paclitaxel-resistant triple-negative breast cancer cells. *British Journal of Cancer*, 109(7), 1876-1885.

187. Liu, Y., Lu, W.L., Wang, J.C., et al. (2007). Controlled delivery of recombinant hirudin based on thermo-sensitive Pluronic® F127 hydrogel for subcutaneous administration: in vitro and in vivo characterization. *Journal of Controlled Release,* 117(3), 387-395.
188. Liu, Y., Zhu, Y.Y., Wei, Get al. (2009). Effect of carrageenan on poloxamer-based in situ gel for vaginal use: Improved in vitro and in vivo sustained-release properties. *European Journal of Pharmaceutical Sciences*,37(3), 306-312.
189. Liversidge, G.G., Cundy, K.C., Bishop, J.F., et al. (1992).. Surface modified drug nanoparticles, United States Patent 5145,684.
190. Lorenzo, G., Zaritzky, N., and Califano, A. (2013). Rheological analysis of emulsion-filled gels based on high acyl gellan gum. *Food Hydrocolloids*, 30(2), 672-680.
191. Lu, J., Huang, Y., Zhao, W., et al. (2013). PEG-derivatized embelin as a nanomicellar carrier for delivery of paclitaxel to breast and prostate cancers. *Biomaterials*, 34(5), 1591-1600.
192. Madan, A. and Faiman, M.D. (1995). Characterization of diethyldithiocarbamate methyl ester sulfine as an intermediate in the bioactivation of disulfiram. *Journal of Pharmacology and Experimental Therapeutics*, 272(2), 775-780.
193. Madan, M., Bajaj, A., Lewis, S., et al. (2009). In situ forming polymeric drug delivery systems. *Indian Journal of Pharmaceutical Sciences*, 71(3), 242.
194. Mahajan, H.S., Gattani, S.G. (2009). Gellan Gum Based Microparticles of Metoclopromide Hydrochloride for Intranasal Delivery: Development and Evaluation. *Chemical and Pharmaceutical Bulletin* 57(4), 388—392.
195. Malvern Instruments. (2011). Zeta potential: An Introduction in 30 minutes. Zetasizer Nano Series Technical Note. MRK654-01.
196. Mandal, T.K. and Graves, R. (2014). Method of micro-encapsulation. US Patent 8628701.
197. Mangena, M. and Murty, B.R. (2005). Buprenorphine Microspheres. US Patent 20050048115A1.
198. Mao, R., Tang, J., and Swanson, B. G. (2000). Texture properties of high and low acyl mixed gellan gels. *Carbohydrate Polymers*, 41(4), 331-338.
199. Maravajhala, V., Papishetty, S. and Bandlapalli, S. (2012). Nanotechnology in development of drug delivery systems. *International Journal of Pharmaceutical Sciences and Research*, 3(1), 84-96.
200. Mariani, J.J., Pavlicova, M., Bisaga, A., Nunes et al. (2012). Extended Release Mixed Amphetamine Salts and Topiramate for Cocaine Dependence: A Randomized Control Trial. *Biological Psychiatry*, 72, 950-956.

201. Marques, M.R., Loebenberg, R. and Almukainzi, M. (2011). Simulated biological fluids with possible application in dissolution testing. *Dissolution Technologies*, 18(3), 15-28.
202. Marshall, M.V., Draney, D., Sevick-Muraca, E.M. et al. (2010). Single-dose intravenous toxicity study of IRDye 800CW in Sprague-Dawley rats. *Molecular Imaging and Biology*, 12(6), 583-594.
203. Matricardi, P., Cencetti, C., Ria, R., et al. (2009). Preparation and characterization of novel gellan gum hydrogels suitable for modified drug release. *Molecules*, 14(9), 3376-3391.
204. McCance-Katz, E.F., Kosten, T.R. and Jatlow, P. (1998). *Drug and Alcohol Dependence*, 52(27).
205. Mehnert, W. and Mäder K. (2001). Solid lipid nanoparticles: production, characterization and applications. *Advanced Drug Delivery Reviews*, 47, 165–196.
206. Melichar, J.K., Daglish, M.R.C. and Nutt, D.J. (2001). Addiction and withdrawal-current views. *Current Opinion in Pharmacology*, 1,84-90.
207. Menei, P., Croue, A., Daniel, V., et al. (1994). Fate and biocompatibility of three types of microspheres implanted into the brain. *Journal of Biomedical Materials Research*, 28, 1079–1085.
208. Mi, Y., Liu, Y. and Feng, S.S. (2011). Formulation of docetaxel by folic acid-conjugated d-α-tocopheryl polyethylene glycol succinate 2000 (Vitamin E TPGS 2k) micelles for targeted and synergistic chemotherapy. *Biomaterials*, 32(16), 4058-4066.
209. Mi, Y., Zhao, J. and Feng, S.S., 2012. Vitamin E TPGS prodrug micelles for hydrophilic drug delivery with neuroprotective effects. *International Journal of Pharmaceutics*, 438(1), 98-106.
210. Mishra, B., Patel, B.B., and Tiwari, S. (2010). Colloidal nanocarriers: a review on formulation technology, types and applications toward targeted drug delivery. *Nanomedicine*, 6, 9–24.
211. Miyazaki, S., Aoyama, H., Kawasaki, N., et al. (1999). In situ-gelling gellan formulations as vehicles for oral drug delivery. *Journal of Controlled Release*, 60(2), 287-295.
212. Miyoshi, E., Takaya, T., and Nishinari, K. (1996). Rheological and thermal studies of gel-sol transition in gellan gum aqueous solutions. *Carbohydrate Polymers*, 30(2), 109-119.
213. Mohamed, S., Parayath, N.N., Taurin, S. et al. (2014). Polymeric nano-micelles: versatile platform for targeted delivery in cancer. *Therapeutic Delivery,* 5(10), 1101-1121.

214. Moore, T., Croy, S., Mallapragada, S., et al. (2000). Experimental investigation and mathematical modeling of Pluronic® F127 gel dissolution: drug release in stirred systems. *Journal of Controlled Release*, 67(2), 191-202.
215. Moraes, I. C., Fasolin, L. H., Cunha, R. L., et al. (2011). Dynamic and steady: shear rheological properties of xanthan and guar gums dispersed in yellow passion fruit pulp (Passiflora edulis f. flavicarpa). *Brazilian Journal of Chemical Engineering*, 28(3), 483-494.
216. Moreira, H.R., Munarin, F., Gentilini, R., et al. (2014). Injectable pectin hydrogels produced by internal gelation: pH dependence of gelling and rheological properties. *Carbohydrate Polymers*, 103, 339-347.
217. Morris, E.R., Gothard, M.G.E., Hember, M.W.N., et al. (1996). Conformational and rheological transitions of welan, rhamsan and acylated gellan. *Carbohydrate Polymers*, 30(2), 165-175.
218. Morris, E.R., Nishinari, K., and Rinaudo, M. (2012). Gelation of gellan–a review. *Food Hydrocolloids*, 28(2), 373-411.
219. Mu, L., and Feng, S.S. (2002). Vitamin E TPGS used as emulsifier in the solvent evaporation/ extraction technique for fabrication of polymeric nanospheres for controlled release of paclitaxel. *Journal of Controlled Release*, 80, 129–144.
220. Mu, L., and Seow, P.H. (2006). Application of TPGS in polymeric nanoparticulate drug delivery system. *Colloids and Surfaces B: Biointerfaces,* 47, 90–97.
221. Mu, L., Elbayoumi, T.A. and Torchilin, V.P. (2005). Mixed micelles made of poly (ethylene glycol)–phosphatidylethanolamine conjugate and d-α-tocopheryl polyethylene glycol 1000 succinate as pharmaceutical nanocarriers for camptothecin. *International Journal of Pharmaceutics*, 306(1), 142-149.
222. Müller, R.H., Rühl, D., Runge, S., et al. (1997). Cytotoxicity of solid lipid nanoparticles as a function of the lipid matrix and the surfactant. *Pharmaceutical Research*, 14,, 458–462.
223. Musumeci, T., Ventura, C.A., Giannone, I., et al. (2006). PLA/PLGA nanoparticles for sustained release of docetaxel. *International Journal of Pharmaceutics*, 325, 172–179.
224. Muthu, M.S., Avinash K.S., Liu, Y. et al. (2012). Development of docetaxel-loaded vitamin E TPGS micelles: formulation optimization, effects on brain cancer cells and biodistribution in rats. *Nanomedicine*, 7(3), 353-364.
225. Nagai, N., Yoshioka, C., Mano, Y., et al. (2015). A nanoparticle formulation of disulfiram prolongs corneal residence time of the drug and reduces intraocular pressure. *Experimental Eye Research*, 132, 115-123.

226. National Institute on Drug Abuse Research Monographs Series. (1976). Narcotic Antagonists: The Search for Long-Acting Preparations. National Institute on Drug Abuse, Rockville, Maryland.
227. National Institute on Drug Abuse. Principles of Drug Addiction Treatment: A research-based guide, 2nd Ed. National Institute of Health. U.S Department of Health and Human Services.
228. Negrın, C.M., Delgado, A., Llabre´s, M., et al. (2001). In vivo-in vitro study of biodegradable methadone delivery systems. *Biomaterials*, 22, 563-570.
229. Negrın, C.M., Delgado, A., Llabre´s, M., et al. (2004). Methadone implants for methadone maintenance treatment. In vitro and in vivo animal studies. *Journal of Controlled Release*, 95, 413– 421.
230. Neiderhiser, D.H. and Fuller, R.K. (1980). The Metabolism of 14 C-Disulfiram by the Rat. *Alcoholism: Clinical and Experimental Research*, 4(3), 277-281.
231. Nicholas, A.P., McInnis, C., Gupta, K.B et al. (2002). The Fate of Biodegradable Microspheres Injected into Rat Brain. *Neuroscience Letters*, 323, 85-88.
232. Nishiyama, N., and Kataoka, K. (2006). Current state, achievements, and future prospects of polymeric micelles as nanocarriers for drug and gene delivery. *Pharmacology & Therapeutics,*112 , 630–648.
233. Noda, S., Funami, T., Nakauma, M., et al. (2008). Molecular structures of gellan gum imaged with atomic force microscopy in relation to the rheological behavior in aqueous systems. 1. Gellan gum with various acyl contents in the presence and absence of potassium. *Food Hydrocolloids*, 22(6), 1148-1159.
234. Novakova, L., Matysova, L. and Solich, P. (2006). Advantages of application of UPLC in pharmaceutical analysis. *Talanta*, 68(3), 908-918.
235. Office of Animal Care and Use, 1996. Guidelines for Endpoints in Animal Study Proposals [online] [viewed 15 May 2013]. Available from: http://oacu.od.nih.gov/ARAC/
236. Oliveira, J.T., Gardel, L.S., Rada, T. (2010). Injectable gellan gum hydrogels with autologous cells for the treatment of rabbit articular cartilage defects. *Journal of Orthopaedic Research*, 28(9), 1193-1199.
237. Oliveira, J.T., Santos, T.C., Martins, L., et al. (2009). Gellan gum injectable hydrogels for cartilage tissue engineering applications: in vitro studies and preliminary in vivo evaluation. *Tissue Engineering Part A*, 16(1), 343-353.
238. Oliveto, A., Poling, J., Mancino, M.J., et al. (2011). Drug and Alcohol Dependence, 113(184).
239. Orson, F.M., Kinsey, B.M., Singh, R.A.K., et al. (2008). Substance Abuse Vaccines. *Annals of the New York Academy of Sciences,* 1141, 257-269.

240. Osmałek, T., Froelich, A., and Tasarek, S. (2014). Application of gellan gum in pharmacy and medicine. *International Journal of Pharmaceutics*, 466(1), 328-340.
241. Packhaeuser, C.B., Schnieders, J., Oster, C.G., et al. (2004). In situ forming parenteral drug delivery systems: an overview. *European Journal of Pharmaceutics and Biopharmaceutics*, 58(2), 445-455.
242. Padalkar, A.N., Shahi, S. and Thube, M.W. (2011). Microparticles: An Approach for Betterment of Drug Delivery System. *International Journal of Pharma Research & Development*, 3(1).
243. Pagar, K.P. and Vavia, P.R. (2013). Naltrexone-loaded poly [La-(Glc-Leu)] polymeric microspheres for the treatment of alcohol dependence: in vitro characterization and in vivo biocompatibility assessment. *Pharmaceutical Development and Technology*, 19 (4), 385-394.
244. Pan, J. and Feng, S.S. (2008). Targeted delivery of paclitaxel using folate-decorated poly (lactide)–vitamin E TPGS nanoparticles. *Biomaterials*, 29(17), 2663-2672.
245. Pani, P.P., Trogu, E., Vacca, R., et al. (2010). Cochrane Database Syst. Rev., CD007024.
246. Parasuraman, S., Raveendran, R. and Kesavan, R. (2010). Blood sample collection in small laboratory animals. *Journal of Pharmacology and Pharmacotherapeutics* 1(2), 87–93.
247. Pardeike, J., Hommoss, A., Müller, R.H. (2009). Lipid nanoparticles (SLN, NLC) in cosmetic and pharmaceutical dermal products. *International Journal of Pharmaceutics*, 366, 170-184.
248. Parekh, P., Dey, J., Kumar, S., et al. (2014). Butanol solubilization in aqueous F127 solution: Investigating the enhanced micellar solvation and consequent improvement in gelation characteristics. *Colloids and Surfaces B: Biointerfaces*, 114, 386-391.
249. Park, E.K., and Song, K.W. (2010). Rheological evaluation of petroleum jelly as a base material in ointment and cream formulations: steady shear flow behavior. *Archives of Pharmaceutical Research*, 33(1), 141-150.
250. Park, H.O., Hong, J.S., Ahn, K.H., et al. (2005). Influence of preparation parameters on rheological behavior and microstructure of aqueous mixtures of hyaluronic acid/poly (vinyl alcohol). *Korea-Australia Rheology Journal*, 17(2), 79-85.
251. Parry, C. and Rehm, J. (2011). Addressing harmful use of alcohol is essential to realising the goals of the UN Resolution on non-communicable diseases (NCDs). *Global Alcohol Policy Alliance*.

252. Patel, K.H. (2009). Pharmacologic management of alcohol dependence. *U.S. Pharmacist* , 34(11), 1-4.
253. Paterson, N.E. (2011). Translational research in addiction: Toward a framework for the development of novel therapeutics. *Biochemical Pharmacology*, 81, 1388-1407.
254. Patil, S., Yeramwar, S., Sharma, P., et al. (2014). Review of recent studies on statistical optimization in drug delivery technologies. *Journal of Drug Delivery & Therapeutics,* 4(5), 58-68.
255. Petrakis, I.L., Carroll, K.M., Nich, C. et al. (2000). Disulfiram treatment for cocaine dependence in methadone-maintained opioid addicts. *Addiction*, 95 (219).
256. Pettinati HM, Rabinowitz AR. Recent advances in the treatment of alcoholism. Clin. Neurosci. Res. 2005;5:151-159.
257. Pettinati, H.M. and Rabinowitz, A.R. (2005). Recent advances in the treatment of alcoholism. *Clinical Neuroscience Research*, 5, 151-159.
258. Pettinati, H.M., Kampman, K.M., Lynch, K.G. et al. (2008). A double blind, placebo controlled trial that combines disulfiram and naltrexone for treating co-occurring cocaine and alcohol dependence. *Addiction Behavior* , 33, 651–657.
259. Phillips, M. and Greenberg, J. (1992). Dose-Ranging Study of Depot Disulfiram in Alcohol Abusers. *Alcoholism: Clinical and Experimental Research*, 16(5), 964-967.
260. Phillips, M. and Gresser, J.D. (1984). Sustained-release characteristics of a new implantable formulation of disulfiram. *Journal of Pharmaceutical Sciences*, 73(12), 1718-1720.
261. Phillips, S., and Cragg, B. (1983). Does consumption of alcohol in the presence of disulfiram cause brain damage? *Toxicology and Applied Pharmacology*, 69, 110-116.
262. Picout, D.R., and Ross-Murphy, S.B. (2003). Rheology of biopolymer solutions and gels. *The Scientific World Journal*, 3, 105-121.
263. Pitt, C.G., Marks, T.A. and Schindler, A. (1980). Biodegradable drug systems based on aliphatic polyesters: application to contraceptives and narcotic antagonists, in: R. Baker (Ed.), *Controlled Release of Bioactive Materials*, Academic, New York, pp. 19–43.
264. Polli, J.E. (2008). In vitro studies are sometimes better than conventional human pharmacokinetic in vivo studies in assessing bioequivalence of immediate-release solid oral dosage forms. *The AAPS Journal*, 10(2), 289-299.
265. Radnoti. (2015). Tissue Organ Bath Principles. [online] Available at: http://radnoti.com/resources/ [Accessed 23 September 2015].

266. Rao, D.A., Nguyen, D.X., Mishra, G.P., et al. (2015). Preparation and Characterization of Individual and Multi-drug Loaded Physically Entrapped Polymeric Micelles. *Journal of Visualized Experiments*, (102), e53047-e53047.
267. Rao, M.A. (2014). Flow and functional models for rheological properties of fluid foods. In *Rheology of Fluid, Semisolid, and Solid Foods* (pp. 27-61). Springer US.
268. Reinhardt, V. and Reinhardt A. (2002). Comfortable Quarters for Laboratory Animals. 9th ed. Washington DC: Animal Welfare Institute.
269. Ricci, E.J., Lunardi, L.O., Nanclares, D.M.A. et al. (2005). Sustained release of lidocaine from Poloxamer 407 gels. *International Journal of Pharmaceutics*, 288(2), 235-244.
270. Ricci, E.J., Lunardi, L.O., Nanclares, D.M.A., et al. (2005). Sustained release of lidocaine from Poloxamer 407 gels. *International Journal of Pharmaceutics*, 288(2), 235-244.
271. Riddick, T.M. (1968). Control of colloid stability through zeta potential: with a closing chapter on its relationship to cardiovascular disease (Vol. 1). Zeta-Meter, Incorporated.
272. Rogers, W.K., Wilson, K.M. and Becker, C.E. (1978). Methods for detecting disulfiram in biologic fluids: Application in studies of compliance and effect of divalent cations on bioavailability. *Alcoholism: Clinical and Experimental Research*, 2(4), pp.375-380.
273. Rudolph, N. and Osswald, T.A. (2014). *Polymer Rheology: Fundamentals and Applications*. Carl Hanser Verlag GmbH Co KG.
274. Ruel-Gariépy, E., and Leroux, J. C. (2004). In situ-forming hydrogels—review of temperature-sensitive systems. *European Journal of Pharmaceutics and Biopharmaceutics*, 58(2), 409-426.
275. Rungseevijitprapa, W., Brazeau, G.A., Simkins, J.W. et al. (2008). Myotoxicity studies of O/W-in situ forming microparticle systems. *European Journal of Pharmaceutics and Biopharmaceutics*, 69(1), 126-133.
276. Sabadini, R.C., Martins, V.C.A., and Pawlicka, A. (2015). Synthesis and characterization of gellan gum: chitosan biohydrogels for soil humidity control and fertilizer release. *Cellulose,* 22, 2045–2054.
277. Sadat, T., Kashi, J., Eskandarion, S., et al. (2012). Improved drug loading and antibacterial activity of minocycline-loaded PLGA nanoparticles prepared by solid/oil/water ion pairing method. *International Journal of Nanomedicine*, 7, 221-234.

278. Sahu, A., Kasoju, N., Goswami, P., et al. (2011). Encapsulation of Curcumin in Pluronic Block Copolymer Micelles for Drug Delivery Applications. *Journal Of Biomaterials Applications*, 25.
279. Salehi, R., Nowruzi, K., Salehi, S., et al. (2013). Smart Poly (N-Isopropylacrylamide)-block-Poly (L-lactide) Nanoparticles for Prolonged Release of Naltrexone. *International Journal of Polymeric Biomaterials*, 62, 686-694.
280. Sanchis, J., Canal, F., Lucas, R., et al. (2010). Polymer–drug conjugates for novel molecular targets. *Nanomedicine*, 5, 915–935.
281. Sander, C., Nielson, H.S., Søgaard, S.R., et al. (2013). Process development for spray drying of sticky pharmaceuticals; case study of bioadhesive nicotine microparticles for compressed medicated chewing gum. *International Journal of Pharmaceutics.*
282. Saracino, M.A., Marcheselli, C., Somaini, L., et al. (2010). Simultaneous determination of disulfiram and bupropion in human plasma of alcohol and nicotine abusers. *Analytical and Bioanalytical Chemistry*, 398(5), 2155-2161.
283. Saxena, V. and Hussain, M.D. (2012). Poloxamer 407/TPGS mixed micelles for delivery of gambogic acid to breast and multidrug-resistant cancer. *International Journal of Nanomedicine*, 7, 713-721.
284. Schottenfeld, R.S., Chawarski, M.C., Cubells, J.F. et al. (2014). Randomized clinical trial of disulfiram for cocaine dependence or abuse during buprenorphine treatment. *Drug and Alcohol Dependence*, 136, 36-42.
285. Schottenfeld, R.S., Chawarski, M.C., Cubells, J.F., et al. (2014). Randomized clinical trial of disulfiram for cocaine dependence or abuse during buprenorphine treatment. *Drug and Alcohol Dependence*, 1(136), 36-42.
286. Seitz, H.K. and Stickel, F. (2007). Molecular mechanisms of alcohol-mediated carcinogenesis. *Nature Reviews Cancer*, 7(8), 599-612.
287. Seitz, H.K., Czygan, P., Waldherr, R., et al. (1985). Ethanol and intestinal carcinogenesis in the rat. *Alcohol*, 2(3), 491-494.
288. Sethia, S., and Squillante, E. (2004). Solid dispersion of carbamazepine in PVP K30 by conventional solvent evaporation and supercritical methods, *International Journal of Pharmaceutics*, 272, 1–10.
289. Sezgin, B., Sibar, S., Bulam, H., et al. (2014). Disulfiram Implantation for the Treatment of Alcoholism: Clinical Experiences from the Plastic Surgeon's Point of View. *Archives of Plastic Surgery*, 41(5), 571-575.
290. Shanbhag, P. and Pandhare, P. (2016). In situ gelling polymeric drug delivery system. [online] Available at:

http://archivepharma.financialexpress.com/sections/res/2115insitugellingpolymericdrugdeliverysystem [Accessed 29 Mar. 2016].

291. Sharma, H.S. and Kiyatkin, E.A. (2009). Rapid morphological brain abnormalities during acute methamphetamine intoxication in the rat: an experimental study using light and electron microscopy. *Journal of Chemical Neuroanatomy*, 37(1), 18−32.
292. Shedler, J., Beck, A.T., Fonagy, P., et al. (2011). Disulfiram: An Anticraving Substance?. *American Journal of Psychiatry*, 168(1).
293. Shen, Y., Li, Q., Tu, J., Zhu, J., 2009, 'Synthesis and characterization of low molecular weight hyaluronic acid-based cationic micelles for efficient siRNA delivery', Carbohydrate Polymers 77, 95-104.
294. Shenoy, D.B. and Amiji, M.M. (2005). Poly(ethylene oxide)-modified poly (ε-caprolactone) nanoparticles for targeted delivery of tamoxifen in breast cancer. *International Journal of Pharmaceutics*, 293, 261-270.
295. Shin, G.H., Li, J., Cho, J.H., et al. (2016). Enhancement of Curcumin Solubility by Phase Change from Crystalline to Amorphous in Cur-TPGS Nanosuspension. *Journal of Food Science.*
296. Shin, S.C. and Kim, J. (2003). Physicochemical characterization of solid dispersion of furosemide with TPGS. *International Journal of Pharmaceutics*, 251(1), pp.79-84.
297. Shukla, S.N., Gaur, P. and Rai, N. (2014). Complexes of tetraethylthiuram disulphide with group 12 metals: single-source precursor in metal sulphide nanoparticles' synthesis. *Applied Nanoscience*, 1-11.
298. Shung, K.K. (2009). High frequency ultrasonic imaging. *Journal of Medical Ultrasound*, 17(1), 25-30.
299. Singh, B., Kumar, R., and Ahuja, N.(2005). Optimizing drug delivery systems using systematic design of experiments. Part I: Fundamental Aspects. *Critical Reviews in Therapeutic Drug Carrier Systems*, 22: 27-105.
300. Sirithananchai, Y., Junyaprasert, V.B., Sakchaisri, K. (2015). Effect of hydrophobic nanoparticle cores on the characteristics of poly (ε-caprolactone)-co-d-α-tocopheryl polyethylene glycol 1000 succinate nanoparticles loaded with camptothecin. *Mahidol University Journal of Pharmaceutical Science*s, 42(4), 169-177.
301. Sluka, K.A., Kalra, A. and Moore, S.A. (2001). Unilateral intramuscular injections of acidic saline produce a bilateral, long-lasting hyperalgesia. *Muscle and Nerve*, 24, 37–46
302. Sonali, Agrawal, P., Singh, R.P., Rajesh, C.V., et al. (2015). Transferrin receptor-targeted vitamin E TPGS micelles for brain cancer therapy: preparation, characterization and brain distribution in rats. *Drug Delivery*, 1-11.

303. Sopade, P.A., Halley, P.J., D'arcy, B.R., et al. (2004). Dynamic And Steady-State Rheology Of Australian Honeys At Subzero Temperatures. *Journal of Food Process Engineering*, 27(4), 284-309.
304. Sosnik, A., Cohn, D., Román, J.S. et al. (2003). Crosslinkable PEO-PPO-PEO-based reverse thermo-responsive gels as potentially injectable materials. *Journal of Biomaterials Science, Polymer Edition*, 14(3), 227-239.
305. Spanagel, R. (2000). Recent Animal Models of Alcoholism. *Alcohol Research and Health*. 24(2).
306. Spivak, A.M., Andrade, A., Eisele, E., et al. (2013). A pilot study assessing the safety and latency-reversing activity of disulfiram in HIV-1–infected adults on antiretroviral therapy. *Clinical Infectious Diseases*, p.cit813.
307. Srivalli, K.M.R. and Mishra, B. (2015). Improved Aqueous Solubility and Antihypercholesterolemic Activity of Ezetimibe on Formulating with Hydroxypropyl-β-Cyclodextrin and Hydrophilic Auxiliary Substances. *AAPS PharmSciTech.*
308. Stahre, M., Roeber, J., Kanny, D., et al. (2014). Contribution of excessive alcohol consumption to deaths and years of potential life lost in the United States. *Preventing Chronic Disease*, 11, 130293.
309. Stephen, A.M. and Phillips, G.O. eds. (2006). *Food polysaccharides and their applications* (Vol. 160). CRC Press.
310. Stolerman, I. ed. (2010). *Encyclopedia of Psychopharmacology*. Springer Science & Business Media.
311. Strasinger, C.L., Scheff, N.N., Wu, J. (2009). Carbon Nanotube Membranes for use in the Transdermal Treatment of Nicotine Addiction and Opioid Withdrawal Symptoms. *Substance Abuse: Research and Treatment*, 3, 31-39.
312. Substance Abuse and Mental Health Services Administration (SAMHSA). 2014 National Survey on Drug Use and Health (NSDUH). Table 5.8A—Substance dependence or abuse in the past year among persons aged 18 or older, by demographic characteristics: Numbers in thousands, 2013 and 2014. Available at: http://www.samhsa.gov/data/sites/default/files/NSDUH-DetTabs2014/NSDUH-DetTabs2014.htm#tab5-8a [Accessed 23 March 2016].
313. Substance Abuse and Mental Health Services Administration (SAMHSA). 2014 National Survey on Drug Use and Health (NSDUH). Table 5.5A—Substance dependence or abuse in the past year among persons aged 12 to 17, by demographic characteristics: Numbers in thousands, 2013 and 2014. Available at: http://www.samhsa.gov/data/sites/default/files/NSDUH-DetTabs2014/NSDUH-DetTabs2014.htm#tab5-5a. [Accessed 23 March 2016].

314. Suh, J.J., Pettinati, H.M., Kampman, K.M et al. (2006). The status of disulfiram: a half of a century later. *Journal of Clinical Psychopharmacology*, 26(3), 290-302.
315. Suksiriworapong, J., Rungvimolsin, T., Atitaya, A., et al. (2014). Development and characterization of lyophilized diazepam-loaded polymeric micelles. *AAPS PharmSciTech,* 15(1), 52-64.
316. Surber, C. and Sucker, H. (1987). Tissue tolerance of intramuscular injectables and plasma enzyme activities in rats. *Pharmaceutical Research*, 4(6), 490-494.
317. Swartz, H., (2005). Seeing is believing—visualizing drug delivery in vitro and in vivo. *Advanced Drug Delivery Reviews*, 57(8), 1085-1086.
318. Swift, R.M. (1999). Drug therapy for alcohol dependence. *New England Journal of Medicine*, 340,1482-1490.
319. Tabakoff, B. and Hoffman, P.L., (2000). Animal models in alcohol research. *Alcohol Research and Health*, 24(2), 77-84.
320. Tampier, L., Quintanilla, M.E. and Israel, Y. (2008). Tolerance to disulfiram induced by chronic alcohol intake in the rat. *Alcoholism: Clinical and Experimental Research*, 32(6), 937-941.
321. Tang, X., Liang, Y., Feng, X. (2015). Co-delivery of docetaxel and Poloxamer 235 by PLGA–TPGS nanoparticles for breast cancer treatment. *Materials Science and Engineering: C*, 49, 348-355.
322. Tawari, E.P., Liu, P., Wang, Z. (2015). Pluronic micelle-encapsulated Disulfiram targets cancer stem-like cells and reverses pan-resistance in acquired resistant breast cancer cell lines. *Cancer Research*, 75(15 Supplement), 4067-4067.
323. The John Hopkins University Animal Care and Use Committee. Procedures: The Rat. [online] [viewed 15 May 2013] available from: http://web.jhu.edu/animalcare/procedures/rat.html
324. Thuilliez, C., Dorso, L., Howroyd, P., et al. (2009). Histopathological lesions following intramuscular administration of saline in laboratory rodents and rabbits. *Experimental and Toxicologic Pathology*, 61(1), 13-21.
325. Tice, T. (2004). Delivering with depot formulations. *Drug Development and Delivery* 4(1).
326. Tice, T.R., Staas, J.K., Ferrell, T.M., et al. (2009). Injectable Methadone, Methadone and Naltrexone, or Buprenorphine and Naltrexone Microparticle Compositions and Their Use in Reducing Consumption of Abused Substances. US Patent 7473431B2.
327. Tiyaboonchai, W. (2003). Chitosan Nanoparticles: A Promising System for Drug Delivery. *Naresuan University Journal*, 11(3), 51-66.

328. Tosi, G., Costantino, L., Ruozi, B. (2008). Polymeric nanoparticles for the drug delivery to the central nervous system. *Expert Opinion on Drug Delivery*, 5, 155–174.
329. Trivedi, R., and Kompella, U.B. (2010). Nanomicellar formulations for sustained drug delivery: strategies and underlying principles. *Nanomedicine (Lond)*, 5(3), 485–505.
330. Trong, L.C.P., Djabourov, M., and Ponton, A. (2008). Mechanisms of micellization and rheology of PEO–PPO–PEO triblock copolymers with various architectures. *Journal of Colloid and Interface Science*, 328(2), 278-287.
331. United Nations Office on Drugs and Crime. World Drug Report 2016. http://www.unodc.org/unodc/secured/wdr/wdr2013/World_Drug_Report_2016.pdf. accessed 20 December 2016.
332. van Hemelrijck, C., and Müller-Goymann, C.C. (2012). Rheological characterization and permeation behavior of poloxamer 407-based systems containing 5-aminolevulinic acid for potential application in photodynamic therapy. *International Journal of Pharmaceutics*, 437(1), 120-129.
333. Varshosaz, J., Tabbakhian, M., and Salmani, Z. (2008). Designing of a thermosensitive chitosan/poloxamer in situ gel for ocular delivery of ciprofloxacin. *Open Drug Delivery Journal*, 2, 61-70.
334. Varshosaz, J., Zaki, M.R., Minaiyan, M., et al. (2014). Preparation, Optimization and Screening, the Effect of Processing Variables on Agar Nanospheres Loaded with Bupropion HCl by a D-Optimal Design. *BioMed Research International*.
335. Vasir, J.K., Tambwekar, K., Garg, S. (2003). Bioadhesive Microspheres as a Controlled Drug Delivery System. *International Journal of Pharmaceutics*, 255, 13-32.
336. Vassallo, J.D., Janovitz, E.B., Wescott, D.M., et al. (2009). Biomarkers of drug-induced skeletal muscle injury in the rat: troponin I and myoglobin. *Toxicological Sciences*, p.kfp166.
337. Venkatesh, G.M. and Harmon, T.M. (2011). Taste masked topiramate composition and an orally disintegrating tablet comprising the same. US Patent 20110212171A1.
338. Veverka, K.A., Johnson, K.L., Mays, D.C., et al. (1997). Inhibition of aldehyde dehydrogenase by disulfiram and its metabolite methyl diethylthiocarbamoyl-sulfoxide. *Biochemical Pharmacology*, 53(4), 511-518.
339. Vijan, V., Kaity, S., Biswas, S., et al. (2012). Microwave assisted synthesis and characterization of acrylamide grafted gellan, application in drug delivery. *Carbohydrate Polymers*, 90, 496– 506.

340. Vilela, J.A.P., Cavallieri , a.L.F., da Cunha, R.L. (2011). The influence of gelation rate on the physical properties/structure of salt-induced gels of soy protein isolated gellan gum. *Food Hydrocolloids* 25,1710-1718.
341. Vilos, C. and Velasquez, L.A. (2012). Therapeutic Strategies Based on Polymeric Microparticles. *Journal of Biomedicine and Biotechnology*.
342. Vinogradov, S.V., Batrakova, E.V., and Kabanov, A.V. (2004). Nanogels for Oligonucleotide Delivery to the Brain .*Bioconjugate Chemistry*, 15, 50-60.
343. Vinogradov, S.V., Bronich, T.K., and Kabanov, A.V. (2002). Nano-sized cationic hydrogels for drug delivery: preparation, properties and interactions with cells. *Advanced Drug Delivery Reviews*, 54, 135–147.
344. Vuddanda, P.R., Rajamanickam, V.M., Yaspal, M., et al. (2014). Investigations on Agglomeration and Haemocompatibility of Vitamin E TPGS Surface Modified Berberine Chloride Nanoparticles. *BioMed Research International.*
345. Wall, M.E., Brine, D.R., and Perez-Reyes, M. (1981). Metabolism and disposition of naltrexone in man after oral and intravenous administration. *Drug Metabolism and Disposition*, 9, 370–375.
346. Wang, A.T., Liang, D.S., Liu, Y.J. et al. (2015). Roles of ligand and TPGS of micelles in regulating internalization, penetration and accumulation against sensitive or resistant tumor and therapy for multidrug resistant tumors. *Biomaterials*, 53, 160-172.
347. Wang, J-J., Liu, K-S., Sung, K.C., et al. (2009). Lipid nanoparticles with different oil/fatty ester ratios as carriers of buprenorphine and its prodrugs for injection. *European Journal of Pharmaceutical Sciences*, 38, 138-146.
348. Wieber, A., Selzer, S.T. and Kreuter, J. (2011). Characterization and stability studies of a hydrophilic decapeptide in different adjuvant drug delivery systems: A comparative study of PLGA nanoparticles versus chitosan-dextran sulphate microparticles versus DOTAP-liposomes. *International Journal of Pharmaceutics*, 421, 151– 159.
349. Williams, S.H. (2005). Medications for treating alcohol dependence. *American Family Physician*, 72(9).
350. Wills S. (2005). *Drugs of Abuse*. London; Chicago: Pharmaceutical Press.
351. Wilson A., Davidson, W.J., Blanchard. R., et al. (1978). Disulfiram implantation. A placebo-controlled trial with two-year follow-up. *Journal of Studies on Alcohol,* 39, 809–819.
352. Wilson, A., Blanchard, R., Davidson, W., et al. (1984). Disulfiram implantation: a dose response trial. *Journal of Clinical Psychiatry*, 45, 242–247.

353. Wilson, A., Davidson, W.J. and Blanchard, R. (1980). Disulfiram implantation. A trial using placebo implants and two types of controls. *Journal of Studies on Alcohol*, 41, 429–436.
354. Wilson, A., Davidson, W.J. and White J. (1976). Disulfiram implantation: placebo, psychological deterrent, and pharmacological deterrent effects. *British Journal of Psychiatry,* 129, 277–280.
355. Wong, H.L., Wu, X.Y. and Bendayan R. (2011). Nanotechnological advances for the delivery of CNS therapeutics. Advanced Drug Delivery Reviews.
356. World Health Organisation. (2011). Global Status Report on Alcohol and Health, WHO, Geneva.
357. World Health Organization (WHO). (2014). Global status report on alcohol and health, p. XIV. 2014 ed. Available at:
358. Xing, S., Bullen, C.K., Shroff, N.S. (2011). *Journal of Virology*, 85 (6060).
359. Xu, X., Li, B., Kennedy, J.F., et al. (2007). Characterization of konjac glucomannan–gellan gum blend films and their suitability for release of nisin incorporated therein. *Carbohydrate Polymers,* 70, 192–197.
360. Yahyavi-Firouz-Abadi, N, and See, R.E. (2009). Anti-relapse medications: preclinical models for drug addiction treatment. *Journal of Pharmacology and Experimental Therapeutics*, 124, 235-247.
361. Yang, F., Xia, S., Tan, C., et al. (2013). Preparation and evaluation of chitosan-calcium gellan gum beads for controlled release of protein. *European Food Research and Technology*, 237, 467–479.
362. Yao, H.J., Ju, R.J., Wang, X.X., et al. (2011). The antitumor efficacy of functional paclitaxel nanomicelles in treating resistant breast cancers by oral delivery. *Biomaterials*, 32(12), 3285-3302.
363. Yapar, E-A., Inal, Ö., Özkan, Y., et al. (2012). Injectable In Situ Forming Microparticles: A Novel Drug Delivery System. *Tropical Journal of Pharmaceutical Research*, 11(2), 307-318.
364. Yaşar, K., Kahyaoglu, T., and Şahan, N. (2009). Dynamic rheological characterization of salep glucomannan/galactomannan-based milk beverages. *Food Hydrocolloi*ds, 23(5), 1305-1311.
365. Yin, W., Akala, E.O., and Taylor, R.E. (2002). Design of naltrexone-loaded hydrolysable crosslinked nanoparticles. *International Journal of Pharmaceutics*, 244, 9-19.
366. Yoo, J-W., Doshi, N. and Mitragoti, S. (2011). Adaptive micro and nanoparticles: temporal control over carrier properties to facilitate drug delivery. *Advanced Drug Delivery Reviews*, 63, 1247-1256.

367. Yourick, J.J. and Faiman, M.D. (1989). Comparative aspects of disulfiram and its metabolites in the disulfiram-ethanol reaction in the rat. *Biochemical Pharmacology*, 38(3), 413-421.
368. Zembko, I., Ahmed, I., Farooq, A., et al. (2015). Development of Disulfiram-Loaded Poly(Lactic-co-Glycolic Acid) Wafers for the Localised Treatment of Glioblastoma Multiforme: A Comparison of Manufacturing Techniques. *Journal Of Pharmaceutical Sciences,* 104,1076–1086.
369. Zeng, X., Tao, W., Mei, L., et al. (2013). Cholic acid-functionalized nanoparticles of star-shaped PLGA-vitamin E TPGS copolymer for docetaxel delivery to cervical cancer. *Biomaterials*, 34(25), 6058-6067.
370. Zhang, H., and Ding, J. (2010). Frequency-and temperature-dependent rheological properties of an amphiphilic block co-polymer in water and including cell-culture media. *Journal of Biomaterials Science, Polymer Edition*, 21(2), 253-269.
371. Zhang, L., Gu, F.X., Chan, J.M., et al. (2008). Nanoparticles in medicine: therapeutic applications and developments. *Clinical Pharmacology and Therapeutics*, 83, 761–769.
372. Zhang, L., Jiang, Y., Jing, G., et al. (2013). A novel UPLC–ESI-MS/MS method for the quantitation of disulfiram, its role in stabilized plasma and its application. *Journal of Chromatography B*, 937, 54-59.
373. Zhang, Z., Tan, S., Feng, S-S. 2012. Vitamin E TPGS as a molecular biomaterial for drug delivery. *Biomaterials*, 33(2012), 4889-4906.
374. Zhao, J., Mi, Y., Liu, Y. et al. (2012). Quantitative control of targeting effect of anticancer drugs formulated by ligand-conjugated nanoparticles of biodegradable copolymer blend. *Biomaterials*, 33(6), 1948-1958.
375. Ziegler, C.B. and Johnson, B.A. (2006). Composition and Methods for Intranasal, Buccal, Sublingual and Pulmonary Delivery of Varenicline. US Patent 20060084656A1.

APPENDICES

APPENDIX A

A Review of the Trends and Advances in Drug Delivery Technologies for the Treatment of Substance Abuse and Drug Addiction

Fatema Mia, Yahya E. Choonara, Charu Tyagi, Lomas Kumar Tomar, Lisa C. du Toit, Pradeep Kumar and Viness Pillay*

Wits Advanced Drug Delivery Platform Research Unit, Department of Pharmacy and Pharmacology, School of Therapeutic Sciences, Faculty of Health Sciences, University of the Witwatersrand, Johannesburg, 7 York Road, Parktown, 2193, South Africa

*Corresponding Author:
Professor Viness Pillay
Tel: +27-11-717-2274
Fax: +27-11-642-4355
Fax2Email: +27-86-553-4733
Email: viness.pillay@wits.ac.za

Abstract- Substance abuse and addiction is a recognised psychiatric illness with severe psychological, physiological, social and financial repercussions. Due to the complexity of the illness, the pharmacological treatment plans tend to be complicated and tedious resulting in poor adherence. This negatively impacts on patient compliance which ultimately leads to relapse. Therefore an easily maintained long-term treatment option is a prerequisite for complete abstinence. Multiparticulate delivery technologies such as nano- and microsystems can considerably meet these requirements and could therefore be employed to ensure an optimal therapeutic outcome. This review discusses these traits, the preparation methods of an existing range of nano- and microsystems as well as the challenges posed by these novel carrier systems. The fundamental differences between these systems and their implications on drug delivery in substance abuse are highlighted. The choice of excipients determines the properties of the delivery system and is particularly important in CNS disorders wherein delivery across the Blood-Brain Barrier is essential for a therapeutic effect. Manipulation of excipients, which allows researchers to obtain a specific desired effect, also forms a part of this review. The actives that have been researched include those approved for addiction treatment as well as those that are not but have shown a degree of clinical efficacy. The findings of these studies have been summarised in this review that reflects promising potential of multiparticulates in the treatment of addiction and suggests that further studies could greatly benefit in fighting the scourge of addiction and drug abuse through formulation manipulation.

APPENDIX B

Design fabrication, statistical optimization and in vitro characterization of disulfiram-loaded D-α-tocopheryl polyethylene glycol 1000 succinate nanomicelles

Fatema Mia, Yahya E. Choonara, Pradeep Kumar, Lisa C. du Toit, Viness Pillay[1*]

[1]Wits Advanced Drug Delivery Platform Research Unit, Department of Pharmacy and Pharmacology, School of Therapeutic Sciences, Faculty of Health Sciences, University of the Witwatersrand, Johannesburg, 7 York Road, Parktown, 2193, South Africa

***Corresponding Author:**
Professor Viness Pillay
Tel: +27-11-717-2274
Fax: +27-11-642-4355
Fax2Email: +27-86-553-4733
Email: viness.pillay@wits.ac.za

Abstract - Purpose. The aim of the study was to fabricate nanomicelles for the delivery of disulfiram. The objective of the delivery system is to develop a suitable carrier for sustained release of disulfiram. D-α-tocopheryl polyethylene glycol 1000 succinate was selected for nanomicelle synthesis due to its compatibility with highly hydrophobic drugs and its ability to form self-assembling nanomicelles.

Methods. The nanomicelles were fabricated using solvent casting method. Statistical optimization was undertaken using a Central Composite design of experiments consisting of 13 formulations based on two independent variables. Design responses included particle size, drug entrapment and drug release. The effect of the respective variables on the design responses was investigated utilizing analysis of variance protocols prior to the optimal formulation being obtained. Advanced *in vitro* physicochemical and physicomechanical analyses were performed on the optimised formulation in addition to structural, thermal and morphological characterisation.

Results. The optimized nanomicelle system demonstrated a high drug loading (33.66%) exceeding that reported in the literature and an entrapment efficiency (50.98%) in line with literature. Sustained release of 65% of disulfiram was achieved over 28 days. The nanomicelles were small in size (21.61nm). The nanomicelles had a zeta potential of -252.0mV and a CMC of 0.02%w/v indicative of good stability. The presence of disulfiram in the nanomicelles is confirmed through FTIR, DSC and XRD which also verify that the structural integrity of the system was maintained without any chemical interactions.

Conclusion. The incorporation of disulfiram into tpgs nanomicelles was successfully achieved. The utilization of a Design of Experiments was useful in obtaining an optimized formulation with desirable entrapment efficiency, drug loading efficiency and drug release as well as advantageous physicochemical characteristics.

APPENDIX C

The influence of the degree of gellan gum acetylation on the rheological properties of Pluronic F127-gellan gum gels

Fatema Mia, Yahya E. Choonara, Pradeep Kumar, Lisa C. du Toit, Pierre P.D. Kondiah, Viness Pillay[1]*

[1]Wits Advanced Drug Delivery Platform Research Unit, Department of Pharmacy and Pharmacology, School of Therapeutic Sciences, Faculty of Health Sciences, University of the Witwatersrand, Johannesburg, 7 York Road, Parktown, 2193, South Africa

***Corresponding Author:**
Professor Viness Pillay
Tel: +27-11-717-2274
Fax: +27-11-642-4355
Fax2Email: +27-86-553-4733

Email: viness.pillay@wits.ac.za

ABSTRACT. In this study two sets of gels were formulated: High Acyl Gellan Gum (HAGG) with Pluronic F127 (PF127) and Low Acyl Gellan Gum (LAGG) with PF127. Rheological characterization was conducted to determine the effect of degree of gellan gum (GG) acetylation on the properties of the gels formed as well as to determine which gel is ideal for the application of a depot delivery system. The gels were prepared by dispersing varying concentrations of PF127 with varying concentrations of gellan gum (high acyl and low acyl) in deionized water and stirred and then cooled until dissolved. Temperature sweep, frequency sweep, time sweep and flow curve tests were carried out on the gels. All gels displayed a physical change in response to increasing temperature. HAGG gels were predominantly thermosensitive whilst LAGG gels were predominantly thermoreversible. Frequency sweep confirmed the formation of true gels differing only in the degree of strength. The HAGG gels had a faster gelation time than the LAGG gels. Flow curve analysis revealed applicability of two models depending on the concentration of PF127, concentration of GG and temperature being tested. The two common models were the Cross model and Herschel-Bulkley models. The concentration of GG, concentration of PF127 and the strain of GG used all have significant influence on the rheological properties of PF127-GG gels. Overall, HAGG displayed a discernable structured trend compared to LAGG which can be attributed to the acetyl constituents present. The combination of PF127 and HAGG resulted in gels with improved strength. This occurrence, exclusive to HAGG, is controlled by the synergistic reaction of PF127 and HAGG at specific concentrations. HAGG is preferred for the use in a depot due to the increased strength, a structured response to rising temperature, fast gelation time and favorable flow behavior.

A disulfiram-loaded nano-enclatherated-gel-composite for the treatment of alcohol abuse and addiction: physicochemical characterization and *in vitro*, *in vivo* studies

Fatema Mia, Yahya E. Choonara, Pradeep Kumar, Lisa C. du Toit, Viness Pillay[1]*

[1]Wits Advanced Drug Delivery Platform Research Unit, Department of Pharmacy and Pharmacology, School of Therapeutic Sciences, Faculty of Health Sciences, University of the Witwatersrand, Johannesburg, 7 York Road, Parktown, 2193, South Africa

***Corresponding Author:**
Professor Viness Pillay
Tel: +27-11-717-2274
Fax: +27-11-642-4355
Fax2Email: +27-86-553-4733
Email: viness.pillay@wits.ac.za

Purpose
Substance abuse and addiction is highly prevalent in society with many South Africans affected by this psychological condition. Successful rehabilitation amongst drug users is poor due to the irrepressible cravings experienced by the patient which ultimately results in relapse. The key to a positive therapeutic outcome may lie in the development of a drug delivery system that can enhance compliance whilst minimising the risk of relapse. This can be achieved through the design of an intramuscular preparation that possesses the ability to release an active agent consistently over a one month period, maintaining therapeutic drug levels. This study therefore provides for the formulation of a sustained release intramuscular system for the treatment of substance abuse and addiction by entrapping the active component, disulfiram, within a nanomicelle system which is then combined with a thermosensitive gel.

Methods
Disulfiram-loaded nanomicelles were prepared with D-α-tocopheryl polyethylene glycol 1000 succinate (TPGS) using a solvent casting method. The gel component comprised 15% Pluronic F127 with 0.3% High Acyl Gellan Gum. The nanomicelles and free disulfiram were both dispersed within the gel matrix to produce the final Nano-Enclatherated-Gel-Composite (NEGC). The NEGC, and variations of this, were evaluated for *in vitro* drug release. The formulations were also evaluated rheologically to determine the effect on gelation time, flow properties and response to changing temperature. Structural variation, thermal characteristics, degree of crystallinity and surface morphology of the NEGC and various combinations were evaluated. The release of disulfiram from the NEGC and myotoxicity thereof was analysed *ex vivo* using rat muscle tissue. The *in vivo* biodistribution, plasma levels, histopathology and myotoxicity following oral disulfiram administration and intramuscular NEGC administration were also assessed in rats.

Key Findings
The NEGC and variations displayed sustained release over 28 days. Rheological aspects of the NEGC were favourable with an appropriate gelation temperature, fast gelation time and desirable flow properties. High frequency ultra sound imaging confirmed the presence of NEGC in muscle over 28 days whilst toxicity studies indicated reversible and mildly acute muscle injury. Plasma levels of oral disulfiram were higher than that of the NEGC although NEGC levels were within the therapeutic range reported in the literature. The in vivo plasma profile of the NEGC confirmed sustained release with peak plasma levels being reached at 21 days.

Conclusions
Results obtained in this study were promising, indicating that the designed delivery system has the potential to successfully treat drug addiction and substance abuse contributing to a healthier and safer society.

STRICTLY CONFIDENTIAL

ANIMAL ETHICS SCREENING COMMITTEE (AESC)

CLEARANCE CERTIFICATE NO. 2014/43/C

APPLICANT: Ms F Mia

SCHOOL: Pharmacy & Pharmacology

LOCATION: Faculty of Health Sciences

PROJECT TITLE: *Intramascular delivery and in vivo evaluation of disulfiram depot injection in Sprague-Dawley rats*

Number and Species

75 Sprague-Dawley Rats

Approval was given for to the use of animals for the project described above at an AESC meeting held on 26 August 2014 . This approval remains valid until 25 August 2016.

The use of these animals is subject to AESC guidelines for the use and care of animals, is limited to the procedures described in the application form and is subject to any additional conditions listed below:

None.

Signed: _____ Date: 12th SEPT. 2014
(Chairperson, AESC)

I am satisfied that the persons listed in this application are competent to perform the procedures therein, in terms of Section 23 (1) (c) of the Veterinary and Para-Veterinary Professions Act (19 of 1982)

Signed: _____ Date: 11th September 2014
(Registered Veterinarian)

cc: Supervisor: Prof V Pillay
Director: CAS

Works 2000/Iain0015/AESCCert.wps